



ANNUAL REPORT 2020-21



**WADIA INSTITUTE OF HIMALAYAN GEOLOGY
DEHRADUN**

(An Autonomous Institute of Dept. of Science & Technology, Govt. of India)

Cover Photo: Downstream and upstream view of the devastated site of the National Thermal Power Corporation (NTPC) hydro-electric project (HEP) over Dhauliganga River near Tapovan, after the Chamoli disaster in February 2021.

(Courtesy: Drs. Amit Kumar and Akshaya Verma)

ANNUAL REPORT 2020-21



WADIA INSTITUTE OF HIMALAYAN GEOLOGY

(An Autonomous Institute of Department of Science & Technology, Government of India)

33, General Mahadeo Singh Road, Dehra Dun - 248 001

EPABX : 0135-2525100

EPABX : 0135-2525100; Fax: 0135-2625212

Email: dir.off@wihg.res.in; Web: <http://www.wihg.res.in>

Contact :

The Director,
Wadia Institute of Himalayan Geology
33, General Mahadeo Singh Road, Dehra Dun - 248 001
Phone : 0135-2525103, Fax : 0135-2625212 / 2525200
Email : director@wihg.res.in
Web: <http://www.wihg.res.in>

CONTENTS

	Page Nos.
1. Executive Summary	i
2. Activities	
Activity-1A: Geodynamics of Indo-Eurasian collisional zone and crystalline thrust sheets: crustal evolution, carbon sequestration, and economic mineralization	1
Activity-1B: Mantle upwelling fluid circulation and metasomatic processes in the Himalaya: Implications on fluid-rock interaction	6
Activity-2A: Subsurface Characterization of Main Himalayan Thrust (MHT) across the Sub-Himalaya	8
Activity-2B: Geometry and rheological assessment of the Main Himalayan Thrust and their implications toward seismogenesis and lithospheric flexuring	8
Activity-2C: Monitoring of earthquakes for seismological, seismotectonic, and subsurface related processes: evaluation of seismic hazard in the Himalaya	14
Activity-3: Biotic and abiotic investigations of Cenozoic successions of NW and NE Himalaya with reference to paleo-environment, global bio-events, and paleoclimate reconstructions	21
Activity-4A: Climate variability and landscape responses in the selected transects in the NE and NW Himalaya	25
Activity-4B: Ecology and climate dynamics of the Himalaya: Cenozoic to present	30
Activity-5: Geological and Geomorphic controls on Landslide for risk assessment and zonation in the Himalaya	31
Activity-6A: Glacial Dynamics, Glacier Hydrology, Mountain Meteorology, and Hazard	39
Activity-6B: Hydrogeology-Himalayan Fluvial Systems and Ground waters	45
Activity-7: Quantification of strain accumulation and strain release rate along the Main Himalayan Thrust (MHT) at different time scales	47
3. Sponsored Research Projects	53
4. Research Publications	81
5. Seminar/Symposia/Workshop organized	88
6. Awards and Honours	92
7. Ph.D. Theses	93
8. Participation in Seminars/Symposia/Meetings	95
9. Lectures delivered / Invited Talk by Institute Scientists	96
10. Membership	99
11. Publication and Documentation	100
11. Library	100
13. S.P. Nautiyal Museum	101
14. Technical Services	102
15. Celebrations	104
16. Status of implementation of Hindi	108
17. Miscellaneous Items	109
18. Staff of the Institute	110
19. Members of Governing Body / Research Advisory Committee / Finance Committee / Building Committee	112
20. Statement of Accounts	115

WIHG ORGANISATIONAL SET-UP

GOVERNING BODY

Ashok Sahni
Secretary to the GOI or his/her nominee
Talat Ahmad
V.M. Tiwari
Harilal B. Menon
G.V.R. Prasad
Rasik Ravindra
Deepak Srivastava
Pramod K. Verma
S.K. Dubey
Financial Adviser or his/her nominee
Director, WIHG
Pankaj Kumar

RESEARCH ADVISORY COMMITTEE

Shailesh Nayak
Talat Ahmad
D.C. Srivastava
O.N. Bhargava
K.J. Ramesh
P.P. Chakraborty
N.V. Chalapathi Rao
Thamban Meloth
O.P. Mishra
Prakash Chauhan
Biswajit Mishra
Avinash Chandra Pandey
Ajoy Bhowmik
Vandana Prasad
Prantik Mandal
Anil V. Kulkarni
Kalachand Sain
Rajesh Sharma

FINANCE COMMITTEE

Vishvajit Sahay
Rasik Ravindra
Kalachand Sain
Pankaj Kumar
Rahul Sharma

BUILDING COMMITTEE

Kalachand Sain
Vishvajit Sahay or his/her nominee
H.K. Sachan
Representative of Survey of India
Hathibarkala, Dehradun
D.K. Tyagi
Prashant Singh
Poonam Gupta
Pankaj Kumar
C.B. Sharma

RESEARCH ACTIVITIES

UNITS ANCILLARY TO RESEARCH

ADMINISTRATION

Research Groups

- Structure & Tectonics
- Petrology & Geochemistry
- Biostratigraphy
- Geomorphology Env. & Eng. Geology
- Sedimentology & Quaternary Geology
- Geophysics
- Glaciology & Hydrology

Activities

- 1A: Geodynamics of Indo-Eurasian collisional zone and crystalline thrust sheets: crustal evolution, carbon sequestration, and economic mineralization
- 1B: Mantle upwelling fluid circulation and metasomatic processes in the Himalaya: Implications on fluid-rock interaction
- 2A: Subsurface Characterization of Main Himalayan Thrust (MHT) across the Sub-Himalaya
- 2B: Geometry and rheological assessment of the Main Himalayan Thrust and their implications toward seismogenesis and lithospheric flexuring
- 2C: Monitoring of earthquakes for seismological, seismotectonic, and subsurface related processes: evaluation of seismic hazard in the Himalaya
- 3: Biotic and abiotic investigations of Cenozoic successions of NW and NE Himalaya with reference to paleo-environment, global bio-events, and paleoclimate reconstructions
- 4A: Climate variability and landscape responses in the selected transects in the NE and NW Himalaya
- 4B: Cenozoic to present: Ecology and climate dynamics of the Himalaya
- 5: Geological and Geomorphic controls on Landslide for risk assessment and zonation in the Himalaya
- 6A: Glacial Dynamics, Glacier Hydrology, Mountain Meteorology, and Hazard
- 6B: Hydrogeology-Himalayan Fluvial Systems and Ground waters
- 7: Quantification of strain accumulation and strain release rate along the Main Himalayan Thrust (MHT) at different time scales

TCPME

- Publication & Documentation
- Library
- Museum
- Analytical Services
- Sample Preparation
- Consultancy

Registrar's Office

- Finance & Accounts
- Establishment
- Stores & Purchase
- Computer and Networking
- Works, Building & Maintenance
- Transport
- Guest House

EXECUTIVE SUMMARY



Wadia Institute of Himalayan Geology is a premier Geological institute involved in both basic and applied research to unravel the Geodynamics of the Mighty Himalaya, which covers a wide spectrum of Geoscientific disciplines: petrology, geochemistry, structural geology, geophysics, sedimentology, biostratigraphy, earthquake geology, geomorphology, environment & engineering geology, quaternary geology, hydrology, glaciology, etc. The state-of-the-art sophisticated analytical laboratories strongly substantiate the field data for understanding the geodynamic evolution of the Himalaya, seismogenesis of the region, studying landslides and avalanches, characterization and mitigation of geohazards related to earthquakes, landslides, snow/ice avalanche, glacier lakes outbursts, exploration of natural resources (minerals/ore bodies, hydrocarbons, springs, geothermal etc.), comprehending glacier dynamics and fluvial systems etc. Additionally, sub-surface features such as crustal heterogeneities, accumulation of elastic strain and convergence rate, crust-mantle interaction, mantle anisotropy, and shallow/deep earth processes are also being probed continuously by geophysical instrumentation and modern analytical techniques. Besides adding significantly to the knowledge base on the surface and subsurface orogenic processes, the Institute provides geoscience support to other government agencies/bodies in understanding and mitigating several hazards-related programs like landslides, earthquakes, and floods in the Himalaya. It also serves as a National reference center for Himalayan Geology, and provides consultancy services to geoengineering projects, groundwater surveys, hydrocarbon exploration, and natural hazards. The Institute houses a beautiful geological museum within its campus. The ongoing primary mission of our research is the “Characterization and Assessment of Surface and Sub-surface Processes in Himalaya (CAP-Himalaya): Implications on Geodynamics, Seismogenesis, Bio-Events, Paleo-climates, Natural Hazards and Natural resources for Sustainable Development”. The research program is grouped into following broad Activities:

- Activity-1A: Geodynamics of Indo-Eurasian collisional zone and crystalline thrust sheets: crustal evolution, carbon sequestration, and economic mineralization
- Activity-1B: Mantle upwelling, fluid circulation and metasomatic processes in the Himalaya: Implications on fluid-rock interaction
- Activity-2A: Subsurface Characterization of Main Himalayan Thrust (MHT) across the Sub-Himalaya
- Activity-2B: Geometry and rheological assessment of the MHT and their implications toward seismogenesis and lithospheric flexuring
- Activity-2C: Monitoring of earthquakes for seismological, seismotectonic, and subsurface processes: evaluation of seismic hazard in the Himalaya
- Activity-3: Biotic and abiotic investigations of Cenozoic successions of NW and NE Himalaya with reference to paleo-environment, global bio-events, and paleoclimate reconstructions
- Activity-4A: Climate variability and landscape responses in the selected transects of the NE and NW Himalaya
- Activity-4B: Ecology and climate dynamics of the Himalaya: Cenozoic to present
- Activity-5: Geological and Geomorphic controls on Landslide for risk assessment and zonation in the Himalaya
- Activity-6A: Glacial Dynamics, Glacier Hydrology, Mountain Meteorology, and Hazard
- Activity-6B: Hydrogeology - Himalayan Fluvial Systems and Ground waters
- Activity-7: Quantification of strain accumulation and strain release rate along the Main Himalayan Thrust (MHT) at different time scales

An overview of the ongoing research activities shows that the year witnessed all-around progress and has yielded interesting and useful outcome. The different themes of activities mentioned above are supplemented by sponsored research projects focusing on various issues within the ambit of the Institute's mandate. An executive summary of the significant contributions, made by each activity, is highlighted below:

Geodynamics of Indo-Eurasian collisional zone and crystalline thrust sheets: crustal evolution, carbon sequestration and economic mineralization

- The geochronological and geochemical data of the Jutogh Thrust sheet, Himachal Pradesh has been integrated with published data to define the regional tectonic evolution and present-day Himalayan structural architecture. This has provided information related to the origin, deposition, and development of Neoproterozoic-Cambrian rocks of Jutogh Group. An effort has been made to propose crustal evolutionary model of the northern Indian margin during the Proterozoic to Cambrian (ca. ~1.9 - 0.8 Ga).
- The U-Pb (zircon) geochronological ages of meta-sedimentary rocks of the Chail Formation and granitic gneisses of the Jutogh Thrust sheet suggest a maximum depositional age of ~880 Ma for Chail Formation and ~680 Ma for the Jutogh Thrust sheet.
- The detrital zircons of the Jutogh group have yielded a cluster of ca. 1250-800 Ma and few grains with 2500-2300 Ma and 1750-1300 Ma, suggesting that prominent zircons of Neoproterozoic age were derived from the adjacent continent during the assembly of Rodonia supercontinent.
- Ophi-calcite of peridotites from western Himalayan Ophiolites (Indus Suture Zone) and their strontium isotope ratio of 0.711-0.712 show crustal signature at the fluid-rock interaction during ophiolite emplacement demonstrating the remnant signature of Cretaceous seawater mixed with continental crust-derived fluid during Neo-Tethys closure. The presence of micron size exsolution and base metal sulphides, from another ophiolite suite, shows a genetic link between metals deposit and ilmenite mineral in the same rock. The mineral phase study shows that the exsolved ilmenites were sourced from > 300 km depth, and has brought out an important bearing in the model reconstruction.
- The study on ophiolites of Tuting-Tidding Suture Zone (TTSZ) suggests ophiolites formation in two different phases. In the first stage, highly depleted peridotites were derived from interactions of a residual forearc mantle with high-temperature boninitic melts in a nascent forearc that was followed by generation of mafic intrusives during continued forearc spreading. Finally, the rocks

underwent through low-temperature metamorphism resulting from fluid-rock interactions that are evident from the numerous metamorphic minerals.

- Fluid inclusion study on the low to medium grade metasedimentary rocks as well as on the mineralized quartz veins in and around the Larji-Rampur tectonic window, Himachal Himalaya shows that majority of the fluid inclusions are saline aqueous-carbonic. Type 1 inclusions are primary H₂O-CO₂ inclusions with CO₂ phase varying from 10 to 60 volume%. Fluid inclusions with the high filling ratio of CO₂, associated with Type 2 aqueous as well as nearly pure carbonic Type 3 inclusions, are abundant in the healed microfractures and along the grain boundaries.

Mantle upwelling, fluid circulation and metasomatic processes in the Himalaya: Implications on fluid-rock interaction

- The peak P-T conditions of migmatization in the Leo Pargil Dome have been constrained at 9.2-11.0 kbar, 810-825 °C for the amphibole+biotitemigmatite and 700-745 °C, 7.2-7.9 kbar for the sillimanite+muscovitemigmatite using the thermodynamic modeling.
- Peak P-T conditions are followed by an early isothermal decompression, with final melt crystallization occurring at 785-790 °C, 7.0-7.2 kbar for the amphibole+biotitemigmatite and at 675 °C, 5.6-5.8 kbar for the sillimanite+muscovitemigmatite.
- The partial melting processes, responsible for the formation of migmatites, involves both water-fluxed melting (amphibole+biotitemigmatite) and muscovite dehydration melting (sillimanite+muscovitemigmatite).
- Primary CO₂ and CO₂-H₂O fluid inclusions, as well as secondary CO₂ fluid inclusions, are observed in quartz. The study infers that the primary carbonic-aqueous (V_{CO₂} - L_{H₂O}) fluid inclusions were initially trapped in the system, later H₂O content was lost during the exhumation, leading to the formation of pure CO₂ fluid inclusions. The source of CO₂ fluid may be from the prograde decarbonation of carbonate-bearing protoliths.
- The Ladakh granite has been studied for Trace, REE, Sr, and Nd isotopes. The study infers that

metasomatization of lithospheric mantle wedge occurred at Mesoproterozoic (1.34 and 1.08 Ga) by exhumation melting of the UHP Indian crustal rocks after decoupling of oceanic crust by Kohistan-Ladakh asthenospheric mantle melting.

Subsurface Characterization of Main Himalayan Thrust (MHT) across the Sub-Himalaya

- An attempt has been made to explore the NE and NW Himalaya to characterize subsurface structures (geometry and subsurface disposition) for understanding geotectonics of the related areas, and petrophysical properties for the exploration of hydrocarbons.
- High-resolution 2D/3D reflection seismic and well data have been procured from the National Data Repository-Directorate General of Hydrocarbons (NDR-DGH) Govt. of India for these research purposes.
- Data loading and initial quality check have been completed. A detailed investigation is being carried out using the available seismic reflection and well data.
- Different seismic experiments using an open-source database have been performed before adventuring into this research activity.

Geometry and rheological assessment of the MHT and their implications toward seismogenesis and lithospheric flexuring

- The site effect and attenuation studies, carried out in the Kinnaur region of northwest Himalaya, reveals that the Tethyan Himalaya has a higher seismic hazard compared to the adjoining part of the High Himalayan Crystalline of the Kinnaur Himalaya.
- The ambient noise and surface wave data have characterized the sediment thickness of the Indo-Gangetic Plain and Tarim Basin. A low velocity in the middle and lower crust beneath the Tibetan Plateau has been inferred.
- The receiver function study in the Siang Window of the Arunachal Himalaya has brought out crustal thickness in the range of 45-50 km with average V_p/V_s ratio of 1.69-1.90.
- A shallow mantle discontinuity (Hales discontinuity) has been identified and characterized

beneath the eastern Ladakh-Karakoram zone based on receiver function modeling.

- Magnetotelluric studies reveal a low-angle NE dipping intra-crustal high conducting layer (IC-HCL) at 8-15 km depth beneath the Lohit Valley, Arunachal Himalaya.
- The MT impedances at eight sites along the Rohtak-Delhi profile have been modeled. Mahendargarh - Dehradun fault zone has appeared as a conductive feature implying the role of fluids in seismogenesis along this fault.
- Magmatic and metamorphic evolution of crystallines from the Himalayan metamorphic core of the Bhagirathi Valley has been investigated based on mesoscopic, microstructural, mineral chemistry, and U-Pb geochronology of zircons. The study shows that the uppermost part of the Greater Himalayan Sequence (GHS) and the lower part of the GHS including the Main Central Thrust (MCT) zone are two distinct tectonic slices with different metamorphic evolution.
- The GHS in the Dhauliganga valley (Garhwal Himalaya) displays inverted Barrovian metamorphism. The study of allanite and monazite in the Dhauliganga valley further suggests that the allanite-out reaction is the result of prograde metamorphism that occurred at $\sim 660^\circ\text{C}$ temperature and 9.5 kbar pressure.

Monitoring of earthquakes for seismological, seismotectonic, and subsurface processes: evaluation of seismic hazard in the Himalaya

- Upper mantle anisotropy beneath the western segment of NW Himalaya has been investigated using shear wave splitting of core-refracted (S(K)KS) phases. The study reveals that the anisotropy is primarily caused due to strain-induced deformation in the top ~ 200 km owing to the India-Asia collision with some contribution from the mantle flow in the direction of the Indian plate motion.
- The seismic structure of the crust and upper mantle beneath the Doda-Kishtwar region in NW Himalaya has been explored by using the receiver functions (RFs) technique. The study reports 47-57 km thick crust and delineation of upper crustal Low-velocity Layer (LVL), coinciding with the local

seismicity and suggesting fluid-seismicity linkage. The 410 and 660 global mantle discontinuities are observed deeper due to the effect of low temperature.

- Different geophysical parameters viz. the seismicity, plate velocity, and attenuation have been computed for both the Garhwal and Kumaun region of NW Himalaya, and the study shows that the Kumaun region is highly heterogeneous and tectonically active as compared to the Garhwal region.
- A site response study, for the Kumaun-Garhwal region at different frequencies corresponding to single-story, double-story, and 3-4 story and high-rise buildings, shows that the spectral amplification decreases from south to north, as the general trend of soil condition changes from soft alluvium at Deoband (Indo-Gangetic plains) to hard rock in Kotkhai in the higher Himalaya. The spectral amplifications for the stations of the Kumaun Himalaya are found to be higher than those of the Garhwal Himalaya.
- The Focal Mechanism Solution has been computed for the April 23, 2019, Mechuka earthquake (Mw 5.9) that occurred in the Siang Valley of the Arunachal Himalaya. The results of moment tensor solution (i.e. Strike $\Phi=208^\circ$, dip $\delta=12^\circ$, and rake $\lambda=33^\circ$) suggests a low angle thrust faulting associated with the MCT located at the western limb of the Siang Window, which is seismically active down to a depth of 40 km.

Biotic and abiotic investigations of Cenozoic successions of NW and NE Himalaya with reference to paleo-environment, global bio-events, and paleoclimate reconstructions

- Identification of a new micro-fossil assemblage from the Lower Siwalik (middle Miocene) succession of the Ramnagar area, (Jammu and Kashmir) is very significant, as it represents fossil tree shrews and hedgehogs, which were poorly known from the Siwaliks. These micro-mammals were tentatively identified as belonging to *Tupaia* sp. and *Galerixrutlandae*. *Tupaia* sp. from the present locality now represents the oldest record of fossil tupaiids in the Siwaliks and extends their time range in the region by ~2.5-4 million years.
- The newly identified materials of *Nalamerx* confirm previously observed morphological features allowing to test the phylogenetical position of this genus within a cladistics analysis oriented on Paleogene ruminants. Isotopic analyses highlight the complex ecology of the small ruminants in the context of the Himalayan orogeny.
- Forty-four species attributable to twenty-eight genera have been reported. Based on the new reported foraminiferal assemblages, a refinement in age between the upper-middle Eocene to upper Eocene and paleoenvironmental interpretations for the Upper Disang Formation was possible.
- The data from Bednikund Lake suggests that increased Indian summer monsoon (ISM) precipitations were found during ~5930-3950 (mid-Holocene climate optimum), ~3380-2830 (Minoan Warm Period), ~2610-1860 (Roman Warm Period), ~1050-760 (Medieval Climate Anomaly), and ~320 calyr BP to Present (Current Warm Period). The decreased ISM strengths were found during ~3950-3380, ~2830 e2610, ~1860e1050 (Dark Ages Cold Period), ~760-580, and ~500-320 calyr BP (Little Ice Age).

Climate variability and landscape responses in the selected transects in NW and NE Himalaya

- The flood deposits of the Indus and Zaskar catchments of Ladakh UT provide evidence of the presence of humans in the drier Himalaya throughout the past 15 ka. The study suggests the occurrence of large floods during phases of strengthened ISM when the monsoon penetrated into the arid Ladakh.
- Based on the comprehensive investigation and stable isotopic studies of Sclerochronology of the deltaic sequence of Pangong Tso, four phases of climatic changes have been identified since the last 2ka.
- Based on fault gouge, tilted paleolake deposits, and the chronology of deformed fluvial gravels constrained by OSL dating, the Ladakh Himalaya provides evidence for the tectonic activity along the ISZ between 78 and 58 ka.
- The study on a speleothem from the Umsyrng cave, Meghalaya shows wet conditions in northeastern India between ~ 15.4 and 12.9 kyr BP, and ~ 11.3

to 10.1 kyr BP, punctuated by a dry phase between ~ 12.9 and 11.3 kyr BP including the Younger Dryas (YD) cold interval.

- A relatively high concentration of Equivalent Black Carbon (EBC) (up to $2.23 \pm 0.57 \mu\text{gm}^{-3}$) was recorded at Gangotri during the peak tourist season i.e., May-June and Oct-Nov every year. A high EBC (up to $1.27 \pm 0.57 \mu\text{gm}^{-3}$) is also recorded at Tapovan.

Ecology and Climate Dynamics of the Himalaya: Cenozoic to Present

- The study of $\delta^{13}\text{C}_{\text{org}}$ and TOC in the Middle Bhuban formation (Early Miocene-Middle Miocene siliciclastic sequence) in the NE Himalaya shows productivity variation during the Early Miocene-Middle Miocene, especially the $\delta^{13}\text{C}_{\text{org}}$ record shows carbon isotope negative excursions -26.39‰ (min -23.32‰). The CIA, CIW, PIA, and A-CN-K proxy records reveal that the source rock of the Middle Bhuban formation is a proficient felsic source and in moderate chemical weathering. The results of climate value (C-value) ranges from 0.69 to 1.06 suggest the semi-moist to moist climatic conditions during the Early to Middle Miocene.
- Tree growth-climate relationship shows that *A. Pindrow* in the region is adversely affected by high-temperature conditions, whereas cool and wet conditions are ideal for its growth. Further, 231 years long (1785-2015 CE) temperature (October-June and March-June) record has been reconstructed for Din Gad valley, Uttarkashi, Uttarakhand using *A. Pindrow* ring-width chronology.

Geological and Geomorphic controls on Landslide for risk assessment and zonation in the Himalaya

- A total of 56 landslides have been delineated in the Mussoorie township and its surrounding area, 54 landslides have been classified as planner debris slides, and 2 as rock-cum-debris slides. The landslide susceptibility mapping (LSM) reveals that ~44% of the study area falls under very high, high, and moderate landslide susceptible zones and ~56% in the low and very low landslide susceptible zones. The dominant part of the area falling under high and moderate landslide hazard zones lies in the area covered by highly fractured Krol limestone.
- Seven unstable zones along the entire Mansa Devi hill bypass (MDHB) road were identified which are

prone to landslides. A GPR survey carried out at five different locations of MDHB road suggests that the road is constructed on loose soil and hard rock is not visible up to a depth of 12 m.

- A total of 57 landslides are observed in the Yamuna valley, Garhwal Himalaya, of which 33 are classified as debris slides and 24 as rock falls. Along a stretch of 16 km in the Higher Himalaya, 25 landslides are observed, while 32 landslides are noted along a length of 59 km in the Lesser Himalaya. It is observed that the majority of the landslides (72%) are concentrated in the vicinity of the MCT in the Higher Himalaya.
- The study reports 390 glaciers in the Subansiri basin in the Brahmaputra catchment, where 191 glaciers are hanging in nature, 59 ice aprons, 52 cirques, 40 niches, 37 valley glaciers, dominantly north facing, 9 icecaps, and 2 outlet glaciers. Total 52 glacial lakes were observed with a cumulative area of 3.358 km^2 .

Glacial Dynamics, Glacier Hydrology, Mountain Meteorology and Hazard

- The glaciers in Suru Basin have fluctuated greatly throughout the Marine Isotope Stage (MIS) 3 and 2 to Little Ice Age (LIA). The data provide a record of six glacial advances of decreasing magnitude since MIS 3 till the present day. Further, the depression of equilibrium-line altitude (ELA) was ~538 m upward from the oldest glacial advance (Suru-I) to the present day, followed by four other events (Suru-II, III, IV, and V) with ELA depressions of ~522, ~399, ~243, and 215 m, respectively. Suru Basin has lost ~502 km^2 glaciated area and ~163 km^3 ice volume from Suru-I to the present day.
- Reconstructing the recent changes in the mass balance (2016-2019) along with the Little Ice Age (LIA) extent of the Pensilungpa Glacier (PG) shows that the PG was joined by the five tributary glaciers during the LIA having an area of ~18 km^2 and extended ~3 km downstream from its present-day snout located at $4470 \pm 1 \text{ m.a.s.l.}$ Since the LIA, the PG have retreated ~2941 $\pm 75 \text{ m}$, at an average rate of $5.6 \pm 0.15 \text{ m a}^{-1}$.
- The average net annual mass balance of PG is estimated to be $\sim -3.67 \times 10^6 \text{ m}^3 \text{ w.e. a}^{-1}$ with the $-0.36 \text{ m w.e. a}^{-1}$ specific balance between 2016 and

2019. During the period 2016-2019, the PG has lost $\sim 11.03 \times 10^6 \text{ m}^3$ w.e. ice volume.

- Assessed and documented the Rishi Ganga flash flood as due to The breaking of rock mass and overlying hanging glacier from Raunthi peak (5600 m asl) to Raunthi stream (3600 m asl). This created slurry materials that dammed the Rishigangariver at ~ 2300 m asl. The slurry further entrained a large quantity of sediment, wood debris, ice block, and water, and caused devastation to Rishiganga and Tapovan Hydro Electric Power Plants along with roads and bridges downstream.
- The study focuses on the evaluation of Physico-chemical and isotopic compositions to trace the changes in the water quality in the UGB during the COVID-19 induced lockdown (May, and June-2020). The carbonate and silicate weathering processes, carried out at variable scales, results in the heterogeneity and composition of river water.

Hydrogeology - Himalayan Fluvial Systems and Ground waters

- The uplift of the Himalaya contributes to CO_2 mediated silicate weathering through the Ganga-Brahmaputra (G-B) River systems and hence it regulates the long-term changes in the global climate.
- In the Doon Valley, karst occurs in the form of dissected ridges, which suggests that ridges are highly karstified, with karstification degrees range between 20 to 40 kd. The karst springs show a highly fluctuating pattern during the monitoring period with discharge ranging from $0.28\text{-}0.45 \text{ m}^3 \text{ S}^{-1}$.

Quantification of strain accumulation and strain release rate along the MHT at different time scales

- A first mega trench was excavated at Himebasti village, Arunachal Pradesh, to develop paeoearthquake catalog using modern geological techniques. The study includes twenty-one radiocarbon dates to limit the timing of displacement after 1445 CE, suggesting that the area was devastated in the 1697 CE event, known as the Sadiya Earthquake, with a dip-slip displacement of 15.3 ± 4.6 m. Intensity prediction equations and scaling laws for earthquake rupture size allow us to constrain a magnitude of $M_w 7.7\text{-}8.1$ and a minimum rupture length of ~ 100 km for the 1697 CE earthquake.

- The study of interseismic geodetic strain-rate pattern in the Garhwal-Kumaun Himalaya suggests that locked portions of the MHT within the Outer Lesser Himalaya and the Sub-Himalaya are characterized by low strain rates. As expected, the high compressional strain and predominant deformation are happening in the Himalayan Seismic Belt.
- Doon valley shows a horizontal movement of 1.62 ± 0.1 mm/yr toward the southwest direction and it is uplifting at a rate of 0.39 ± 0.2 mm/yr. By analyzing the vertical motion of stations in the north and south of the Himalayan Frontal Thrust (HFT) (TSW1 and BIHA), the results indicate that the HFT is uplifting at a geodetic rate of 8.58 ± 0.7 mm/yr and the rate of uplift is in near correlation with the geological uplift rates of the HFT ($6.9\text{-}1.8$ mm/yr). From the study, it is clear that the HFT is active and the recent earthquake ($M 3.9$) that occurred NW of Haridwar also supports the active nature of the HFT in the study area.
- Thirty-eight new apatite and zircon fission-track ages have been determined from twenty-six bedrock samples, which vary from 2.0 ± 0.3 to 12.1 ± 1.2 Ma, and 3.3 ± 0.3 and 13.2 ± 0.7 Ma, respectively along three transects of the Kurung, Subansiri, and Siyom Rivers, that flow across the major structures of the Arunachal Himalaya.

Other Research Highlights

Geosciences play a very important role in the socio-economic development of a country like ours. Seismic is the most suited Geophysical tool that provides quite accurate information on subsurface geological features from surface measurement, which are widely used for the (i) identification of *Mineralized zones*, (ii) exploration of Hydrocarbons, (iii) delineation of Ground water contamination, (iv) understanding the *Basin evolution and Geo-tectonics*, and (v) comprehending *Earthquake Processes*.

Seismic data keeps on increasing in volume, making the data processing computationally intensive and interpretation tedious. So, the question is - Can we automate the process of interpretation with a reduced intervention of a human analyst?

To address this challenge, WIHG has initiated neural-based new approaches for automatic delineation of subsurface geologic features and properties from

voluminous 3D seismic data at its Artificial Intelligence Center of Excellence for Geosciences (AICEG) and Seismic Interpretation Laboratory (SIL). The approach is based on Artificial Intelligence consisting of several steps: special filtering and processing of 3D seismic data to improve the signal; computation of several attributes, specific to a geologic target; fusing the attributes into a single attribute, called the meta-attribute, through training and testing over a small volume of data; validating the process, and finally running the trained system over the entire volume of data. This will automatically pick up the geometry of subsurface geologic feature/target based on characteristics of meta-attribute, and aid in the quick and advanced interpretation of 3D seismic data. Oil industries have expressed interest in this endeavor. The approach would also be extended based on several other neural algorithms and applied to various geoscientific data for addressing issues related to the landslides, earthquakes and glaciers, etc.

High-resolution 2D/3D seismic data at the foothills of NW and NE Himalaya have been procured from the available sources and/or oil industries. These data would be subjected to advanced processing and modeling for the delimitation of fine-scale structures, geometry and disposition of decollement (i.e. the boundary between the underlying Indian plate and overriding Eurasian plate), ramp limiting the ruptures, thrust geometry of the Himalaya, the configuration of other faults, etc. with a view to understanding the seismogenesis and geodynamic evolution of the Himalaya and adjoining regions. The SIL would also deliver the geomorphological features at different subsurface depths - useful inputs for understanding geo-hazards, configuration of channel-levee, hydrocarbon accumulation, geothermal, architecture of intrusive, flow kinetics, sedimentation, paleo-environment, modulated sedimentary structures, basin evolution, etc.

Subsequent to the disaster in the Rishiganga-Dhauliganga that took place on February 07, 2021, WIHG immediately sent a team of scientists to understand the reasons behind the disaster. From the ground-based and heliborne observations, the entire incident has been explained by three important sequences (Sain et al., JGSI, 2021):

- Breaking of a sizeable rock mass along with overlying hanging glacier from Raunthi (bank) glacier upper catchment from an altitude of 5600 m asl to Raunthi stream below at an altitude of 3600 m asl.

- The impact over the remnant saturated debris and sediments lead to the formation of a complex admixture of snow, glacier ice, rock fragments, morainic debris, and sediments, defined as slurry, which dammed the Rishiganga River at its confluence of ~2300 m asl.
- The slurry further entrained a large quantity of sediment, wood debris, ice block, and water, and caused devastation to Rishiganga and Tapovan hydroelectric projects along with roads and bridges downstream.

Such natural events cannot be prevented but their impact on properties, lives, and livestock can be reduced through a Real-time Monitoring, Setting up an Early Warning System (EWS), and Alerting through a Standard Operating System (SOP). An attempt is being made for the development of an Monitoring and EWS for mitigation of glacial disaster, which requires basic information on the topography, geology, geomorphology, and structure of a basin under investigation based on remote sensing and GIS data for selecting potential sites in establishing the network of hydrological, meteorological and seismological observatories.

Academic Pursuits

During 2020, a total of 116 research papers were published in peer-reviewed journals of national and international repute. Total 13 research scholars were awarded the Ph.D. degree and 8 theses were submitted by scholars for the award of Ph.D. degree. The laboratories and research facilities are providing the analytical database to the scientists and scholars of the Institute. Moreover, these facilities are also used for the benefit of scientists, academicians, and research scholars across our country. Institute provided summer and winter training to a large number of Master's students representing the whole country. As a part of outreach, the institute has organized earthquake mitigation drills and demonstrations in several schools and colleges of Uttarakhand. The museum and library of the Institute were visited by some guests, though students and local visitors didn't get chance to visit due to COVID-19 and Lockdown. The Institute has organized the (i) 4th National Geo-Research Scholars Meet during 23-24, June 2020, which was attended by a total number of about 200 research scholars from different organizations, including research institutes, Universities, IITs, and IISERs, (ii) International

Workshop on “Assessment and Mitigation of Landslides in the Himalaya” during October 28-29, 2020, and (iii) e-workshop on “Luminescence dating technique and new applications” during 25-27 November 2020.

Institute scientists were recognized by awards and felicitations at various platforms. The Director was elected as the Vice President of the Indian Geophysical Union (2020-2023) during 2020. He was also honoured with the Fellowships by the Indian National Science Academy, New Delhi, and Indian Academy of Sciences, Bangalore. Dr. H.K. Sachan received the MR Srinivas Rao Award-2020 by the Geological Society of India for excellent contribution in the field of Petrology. Dr. R.J. Perumal was conferred the Anni Talwani Memorial Prize by the Indian Geophysical Union- 2020.

Other Highlights

"Himalayan Geology", is a biannual (January and July) flagship scholarly journal of the Wadia Institute of Himalayan Geology. The impact factor of the journal has been significantly increased to 1.293 in 2021 (Source: Clarivate -Journal Citation Report).

The Institute strictly followed the Rajbhasha guidelines and published circulars and various office orders in bilingual modes. The Institute publishes annually a Hindi Magazine 'Ashmika'. Volume 26 of 'Ashmika' has been published during 2020-2021. Hindi Pakhwara was celebrated with due fervor. All national festivals were celebrated with great enthusiasm and various government programs like the Swachh Bharat Abhiyan were supported in the utmost manner.

Padma Shri Prof. K. Vijay Raghavan, Principal Scientific Adviser to the Government of India delivered the "National Science Day Lecture- 2021" on virtual platform. In his lecture, he emphasized that increased opportunity of knowledge generation and decreasing the gap between knowledge and the society as well as increased usage of Artificial Intelligence in analyzing the large volume of data can make India a world leader in Science, Innovation, and Technology. Prof. Ashutosh Sharma, Secretary DST was the chief guest and patron in the 4th National Geo-research Scholars Meet (NGRSM) held during June 23-24, 2020, and delivered his inaugural address.

Kalachand Sain
Director

ACTIVITIES

Activity: 1A

Geodynamics of Indo-Eurasian collisional zone and crystalline thrust sheets: crustal evolution, carbon sequestration and economic mineralization

(Rajesh Sharma, A.K. Singh, Barun K. Mukherjee, Paramjeet Singh, Pratap Chandra Sethy and M. Rajnikant Singh)

Detrital zircon Geochronology and Geochemistry of Jutogh Thrust sheet, Himachal Pradesh

During the Cenozoic evolution of the Himalayan orogeny (ca. ~55 Ma ago), four main litho units were tectonically juxtaposed from south to north (Fig. 1). The progression of continental collision between the India and Eurasia plates resulted in southward propagation of the crumpled part of the Higher Himalayan Sequence (HHS) along the MCT. The far-traveled thrust sheet (HHS) is thrust over the Lesser Himalayan Sequence (LHS) zone, such as Jutogh Group thrust over the LHS (Chail Formation) in eastern Himachal Pradesh, Lansdown, Almora, Baijnath, and Askotklippen thrust over the LHS in Kumaun-Garhwal region. In the last few decades, the detrital zircon U-Pb geochronology analysis has been widely used to study the provenance history and crustal evolution. The geochronological and Geochemical data has been integrated with published data to (a) define the regional tectonic evolution and present-day Himalayan structural architecture, (b) origin, deposition, and development Neoproterozoic-Cambrian rocks of Jutogh Group, (c) and to proposed crustal evolution model of northern Indian margin during the Proterozoic to Cambrian (ca. ~1.9 - 0.8 Ga). The new U-Pb (zircon) geochronological ages of two meta-sedimentary rocks (one quartzite of Chail Formation) and two granitic gneisses of Jutogh Thrust sheet are obtained. Based on detrital zircon U-Pb age data generated from the (P1 and P4) sample locations, plots shown in figure 2 (a-b), maximum depositional age of ~880 Ma for Chail Formation and ~680 Ma for the Jutogh Thrust sheet is suggested.

In addition, Detrital zircon from Chail Formation quartzite (P1) exhibits a well-defined peak around ca. 1860Ma, with small peaks of ca. 1150Ma, 1210Ma, 1380Ma, and 1730Ma, respectively. Both the older zircons (~2500Ma) and a few zircon recording youngest age with maximum depositional ages ~880Ma are noticed. It is suggested that sediments were deposited in the base of the Lesser Himalayan basin during the

different time intervals and also sourced from the different tectonic settings present to the northern and southern sides. Most of the zircon of Paleoproterozoic age were sourced from the southern Aravalli Craton and northern Paleoproterozoic margin (Wagtu Gneisses Body). Additionally, the zircons of the Neoproterozoic age were also sourced from southern Aravalli-Delhi supergroups and Neoproterozoic HHS present in the northern margin of the Indian Plate. Therefore, it is evident from the above data sets that the early Mesoproterozoic sedimentary basins were developed in the north Indian continental margin and are named as the Lesser Himalayan Sedimentary Belt. The concordant U-Pb (zircon) ages of sample locations (P5, P6, and P7) of different granite and granitic gneiss are mainly from the Jutogh Thrust sheet and the mean ages are ~868Ma, ~830Ma, and ~825Ma respectively. Similarly, Detrital zircons from the Jutogh Thrust sheet (Fig. 2b), sample P4, is a thin-bedded mica-schist that provides the 115 euhedral zircon grains. The U-Pb crystallization age populations are with the main cluster of ca. 1250-800Ma and few grains with 2500-2300 Ma, 1750-1300Ma, and a small peak of ~650Ma. Maximum depositional age of ~650Ma is assigned. Based on our data, we suggest that the most prominent zircons of Neoproterozoic age were derived from the adjacent continent that comes together during assembly of the Rodinia supercontinent and also have intrusive Cambrian-ordovician (~500-600 Ma) age. The Geochemical datasets are obtained from XRF and ICPMS labs of WIHG. The AFM diagram suggests the calc-alkaline composition of all the samples (Fig. 2c). The primitive mantle-normalized trace element plot of all the samples suggests the depletion of Nb, Sr, P, and Ti indicating that all the sediments were source from a magmatic arc type and provide the hydrous -oxidizing tectonic environment (Fig. 2d). The trace element data of all samples plotted in tectonic discrimination diagram showing the syn-collisional or magmatic arc related source of samples figure 2 (e-f).

Field-based Geology and Structural study along Mandi-Kataula-Bajura-Manikaran-Tos section, Himachal Pradesh

In February 2021, the geological field investigation was conducted in the Mandi-Kataula-Bajura-Manikaran-Tos section, Himachal Pradesh along the Parashar-Parvati river valleys from the Main Boundary Thrust

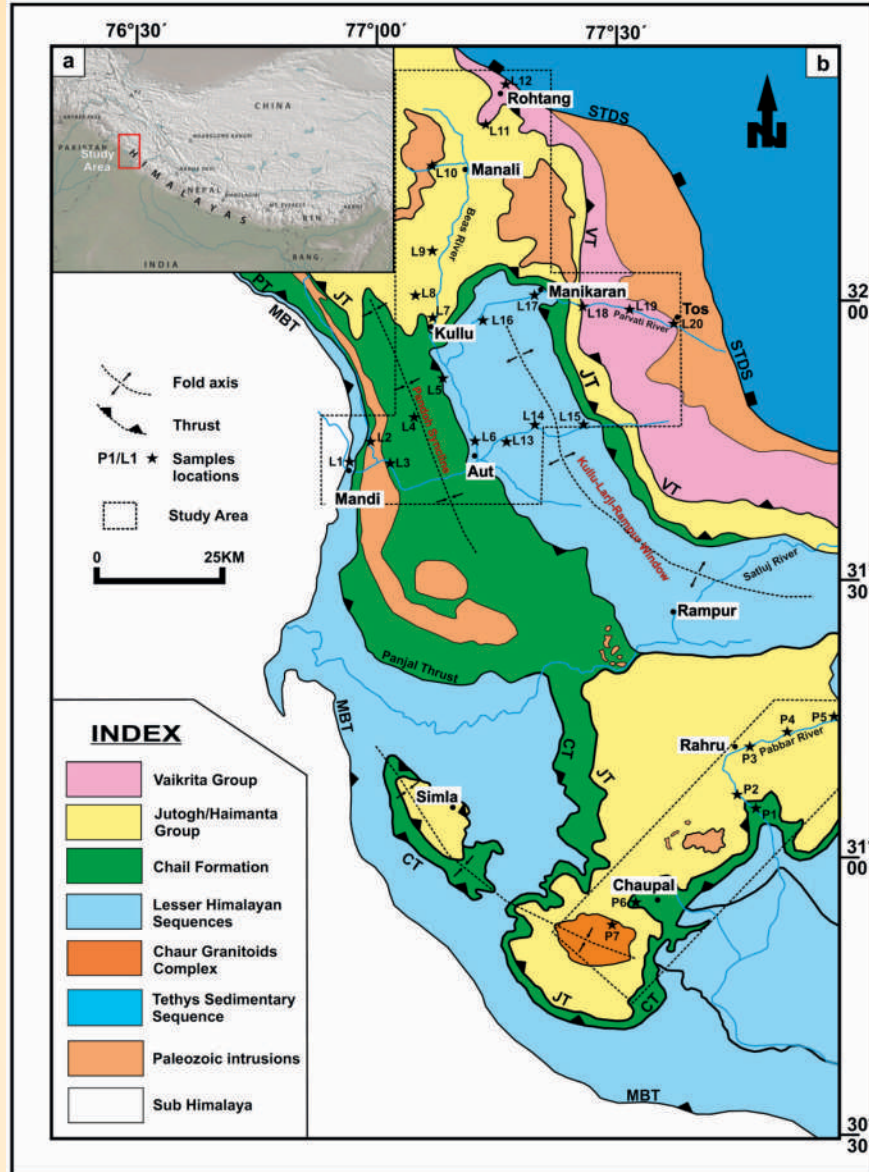


Fig. 1: (a) Topography based on the GTOPO30 digital elevation model, (U.S. Geological Survey) of the Himalaya. (b) Geology cum Tectonics map of the Himachal Himalaya (Modified after Thakur, 1992; Pandey et al., 2003; Srikantia and Bhargava, 1998; Bhargava and Srikantia, 2014) black-dotted box indicates the study area and black stars shows the locations. MBT: Main Boundary Thrust; CT: Chail Thrust; JT: Jutogh Thrust; PT/MCT: Panjal Thrust/Main Central Thrust; VT: Vaikrita Thrust and STDS: South Tibetan Detachment System.

(MBT) to the South Tibetan Detachment System (STDS). This dip-section revealed the structural imprints of the MBT, Panjal/Chail Thrust, Vaikrita Thrust, and the position of STDS (Fig. 1a-b). Some specific locations are shown in figure 1 as L1, L2, ...L20. Clear exposure of MBT (Fig. 3a), between upper Dharamshala Formation sandstone of grey colour in the footwall and meta-basics of Mandi-Darla volcanic in the hanging wall, is seen near Mandi town. To the north of meta-volcanics near Katindhi village, the white colour quartzite is thrust over the Mandi-Darla

meta-volcanics along the Mandi Thrust. Distinct Chail Thrust is seen along the Ur river near the north campus of IIT Mandi (Fig. 3b). The low-grade green schist is exposed near the bridge over Ur river on Mandi-Bajura road. Similarly, the exposure of the Window and its contact with the Chail Formation are observed north of Chhaini village on Mandi-Bajura road and to the north of Manikaran town after the bridge (Fig. 3c-d). Suitable samples for geochemical and thermochronological studies were collected.

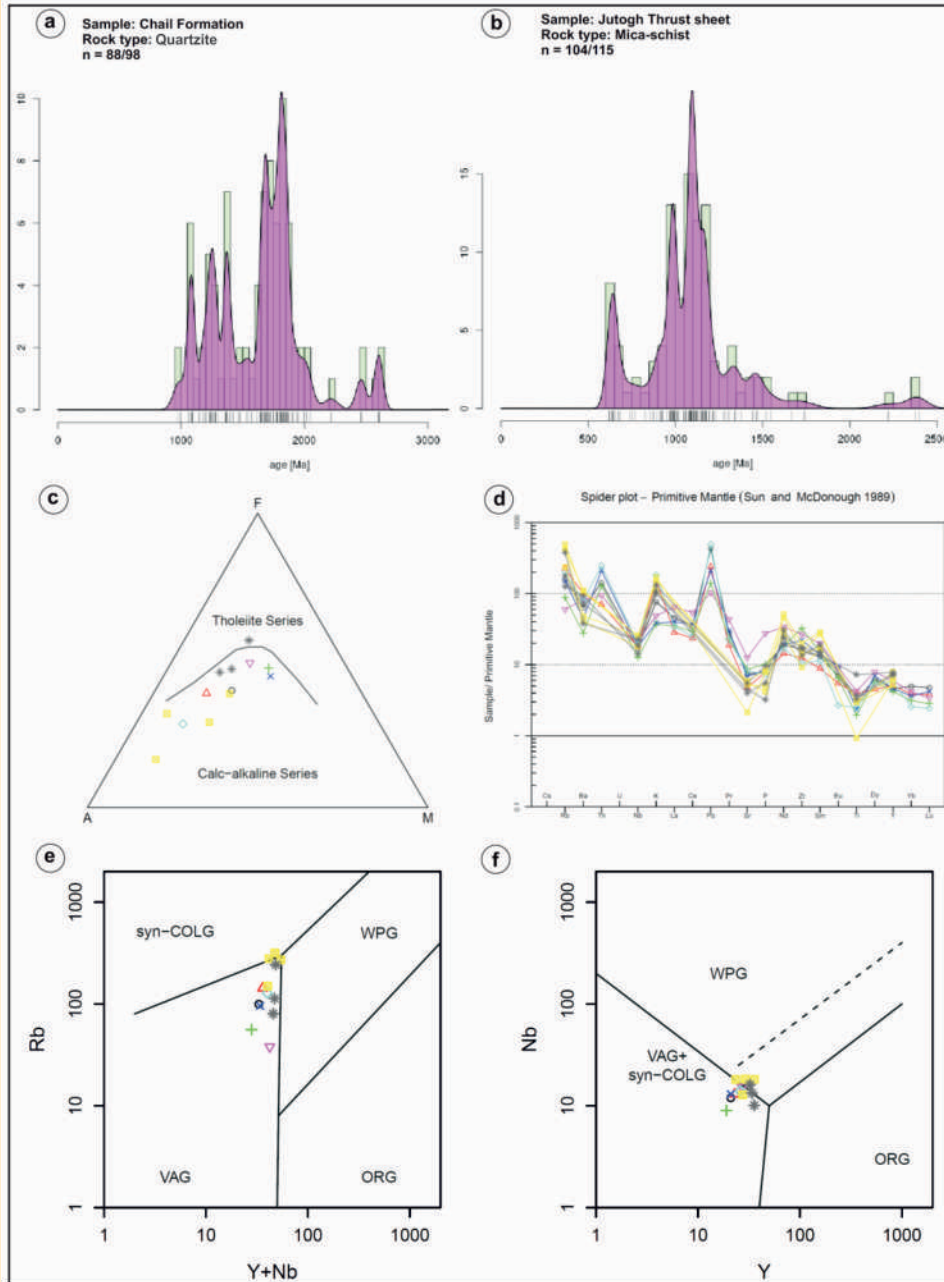


Fig. 2: (a-b) Detrital zircon U-Pb age data generated from the (P1 and P4) sample locations, (c) The AFM diagram suggest the calc-alkaline composition of all the samples, (d) The primitive mantle-normalized trace element plot, (e-f) The tectonic discrimination diagram showing the syncollisional or magmatic arc related source of the samples.

The newly generated FT ages from the section range between 1.9 ± 0.2 and 4.9 ± 0.9 Ma. Based upon the AFT age obtained for the proximity of the MCT hanging wall, the initial results suggest the reactivation of MCT at ~ 3 Ma. The AFT ages obtained farthestmost to the MCT are older (>5 Ma). This suggests the last tectonic activity along the MCT during the Plio-Quaternary periods.

Study of the Ophiolite Suites

Ophiolite slices are constituted of oceanic crust and underlying upper mantle that has been obducted above sea level and often emplaced onto crustal rocks of the continental plate. In the ISZ Himalaya, finding and characterization of ophiolite-associated peridotite advances in understanding how deep mineral phases and fluid re-cycling are transferred into the mantle than

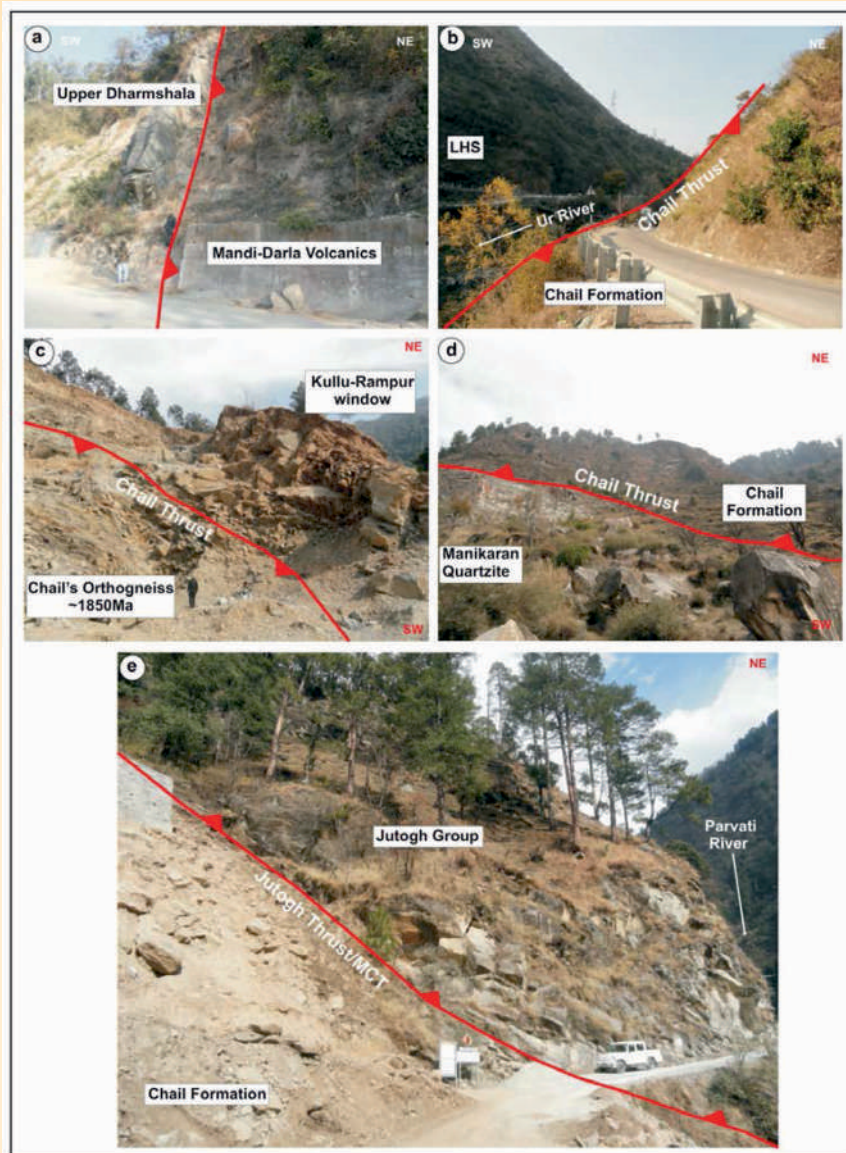


Fig. 3: (a-e): The field photographs showing the contact zone of various thrust along the Mandi-Bajura-Manikaran-Tos section of Himachal Pradesh.

to the surface. From ophi-calcite of peridotite rock, strontium isotope ratio of 0.711-0.712 show crustal signature, which participated at the fluid-rock interaction either on the ocean floor or during ophiolite emplacement. The occurrence of opicalcite veins hosted by ultramafic rocks of the Indus Ophiolite, Nidar Valley, Ladakh Himalaya, is interpreted within the context of serpentinization of the allochthonous Cretaceous upper mantle section during the uplift of the Himalaya orogeny (Chemical Geology, 2020). Remanent occurrences of micron size exsolution structures and base metal sulphides from the Himalayan peridotite, envisioned the possible genetic link between metals deposit and Iron-Titanium mineral phase in the

same rock, exposed along the western Ladakh segment of Indus suture zone. For the study of metals and fluids transportation mechanism in the subduction process, this sample could be more effective in the model reconstruction and are considered as primary Fe-Ti carriers from the deep lithosphere > 300km to the shallow depth but because of their relative instability against pressure (P) and temperature (T), such phases were generally associated with the mineral of shallow origin.

Ophiolites of Tuting-Tidding Suture Zone (TTSZ)

A comprehensive geochemical data set of whole-rock geochemistry and mineral phases from the mantle

peridotites and mafic intrusives of the Lohit ophiolite section and Dibang ophiolite section are also studied. The areas are part of the Tuting-Tidding Suture Zone (TTSZ) ophiolites, eastern Himalaya, north-east India. The TTSZ, which runs east of the Siang antiform, and has been considered as the south-eastern extension of the Indus-Tsangpo Suture Zone. It further extends south to the Indo-Myanmar Orogenic Belt and the Andaman-Nicobar Island Arc. The lithology for the Lohit ophiolite section consists of meta-volcanics and chloritized schist along with serpentized peridotite (at places intruded by mafic dykes), foliated volcano-sedimentary sequences, and a band of grey- to white-coloured limestone. The mafic rocks, in both the Lohit and Dibang valley sections, occur as small meter-scale dykes in the host peridotites (Fig. 4a,b). The limestone band occurs on both the upstream (towards the east) and downstream (towards the west) of the Lohit section. The complete ophiolite section is about 7 km thick with the ultramafic part stretching only for about 500 m and the rest being metabasics and carbonates. There is a sudden change of lithology from metabasalt to granodiorite in this section near Paya. This change can be considered as the contact between the rocks of the suture zone and the LPC, and might be the position of the Lohit Thrust. In the Dibang river valley, dismembered bodies of mafic and peridotites, which are considered to be a part of the

ophiolite sequence are exposed starting from about 40 km north-east from Roingupto 22 km upstream of Mayodia towards Hunli. In this section, a number of outcrops of well-exposed peridotite and gabbro are observed (Fig. 4c,d). The mafic rocks (intrusives as well as basalts) have completely chloritized and metamorphosed into amphibolites. The occurrence of a hornblendite dyke is also noted. The ophiolite section is interlayered with slivers of garnetiferous sillimanite schist, which might either be a part of the Greater Himalayan Sequence a part of the metamorphic sole of the ophiolite sequence.

Combining all the available data of mineral and elemental chemistry in conjunction with the petrology and field evidence, it is proposed that the TTSZ ophiolites represent fragments of oceanic lithosphere and mainly comprise partially to completely serpentized peridotites associated with mafic intrusives along with metabasalts, amphibolites, and a minor amount of carbonates. The petrography, whole-rock geochemistry (low norm clinopyroxene, low Al_2O_3 , and CaO and TiO_2 values, trough-shaped REE patterns, enrichments observed in HFSE), and mineral chemistry (Cr-spinel compositions, high forsterite of primary olivines, Al_2O_3 in the source melt) of the TTSZ peridotites indicate that a spinel facies N-MORB mantle

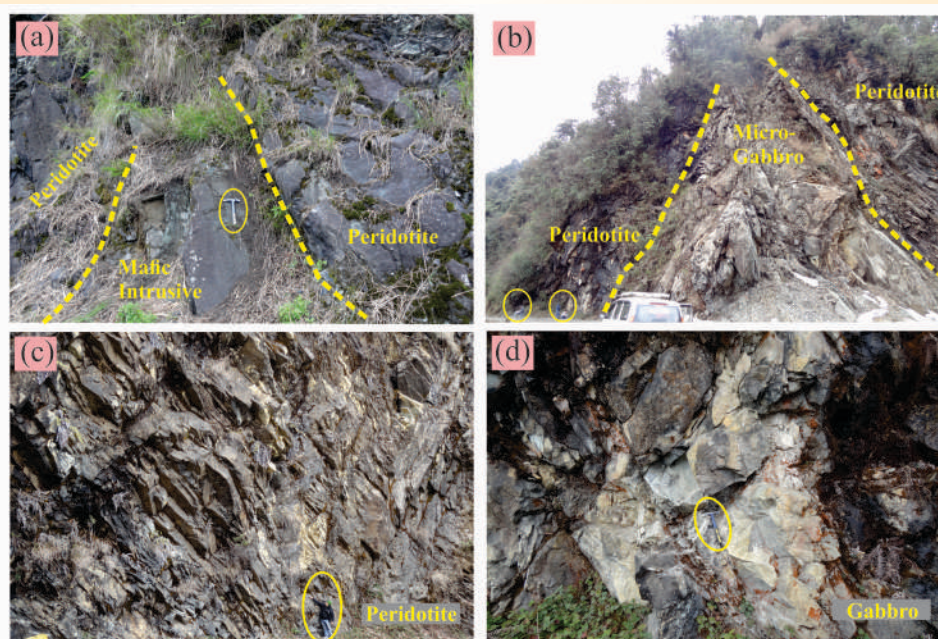


Fig. 4: Field photographs showing different lithological units of the Tuting-Tidding Suture Zone (TTSZ) ophiolites along the Lohit and Dibang ophiolite sections of Eastern Himalaya (a) Peridotite host body in the Lohit section with the intrusion of a mafic dyke and (b) Micro-gabbro intrusive in the Dibang section. Well-exposed outcrops of (c) peridotite and (d) gabbro in the Dibang section. Yellow dashed lines indicate lithological contacts while the yellow circles mark the scales.

underwent moderate to a high degree of partial melting to form refractory peridotites. These peridotites later became part of the SSZ and experienced another episode of partial melting which generated high-temperature boninitic melts in the nascent forearc. The overall petrological and geochemical features of mafic intrusives are comparable to those of MORB. Their incompatible element ratios and REE patterns suggest that they have formed due to a low to moderate degree of partial melting of a less depleted deeper N-MORB mantle source. This deeper source rose to shallower depths due to continued intra-arc rifting and underwent decompression melting followed by interactions with subduction-derived fluids to form the mafic intrusives. Either during the late phase of subduction (mature subduction zone) or exhumation of the ophiolites, the rocks underwent low-temperature metamorphism due to fluid-rock interactions which are evident from the numerous metamorphic minerals like Cr-chlorite and tremolite in the peridotites and albite, tschermakite, phlogopite, and in the mafic intrusives. A detailed evaluation of petrological and geochemical characteristics suggests that the TTSZ ophiolites were formed in two different phases. During the first stage, highly depleted peridotites were derived from interactions of a residual forearc mantle with high-temperature boninitic melts in a nascent forearc that was followed by generation of mafic intrusives during continued forearc spreading. A third stage can be identified where the complete unit underwent low-temperature metamorphism during exhumation to finally form the TTSZ ophiolite sequence. Further, comparisons drawn with the other Neo-Tethyan ophiolites help in inferring that the TTSZ ophiolites might also be a part of the subduction process which formed the Indus-Tsangpo Suture Zone ophiolites.

Study of ore mineralization

The ore mineralization in the Rangpo, Sikkim is represented by copper-lead-zinc bearing ores hosted within the metasediments with intercalations of quartz veins. The ores are hosted within the Gorubathan Formation comprising of meta-sediments and metabasics, mostly quartz-chlorite schist/phyllites, quartzites, and quartz-chlorite-sericite schists. Reflected light microscopy study shows that the ore minerals are enriched in metabasics, whereas, the metasedimentary rocks show minor sulphide minerals. The pyrrhotite, chalcopyrite, sphalerite, galena, arsenopyrite, cobaltite, and pyrite are observed as major primary ore mineral phases, whereas the covellite, azurite, limonite, and malachite are present as secondary ore minerals. Quartz forms the ubiquitous

gangue. The textural relationship and back-scattered imaging of the minerals suggest at least two stages of ore mineralization. Several line scans using SEM ESX were carried out, in order to understand the elemental variation through the minerals. Scans along galena indicate a significant concentration of trace elements like bismuth and molybdenum. Chalcopyrite, galena, and pyrite show stoichiometric composition, without significant compositional variation. A fluid inclusion study has been carried out on the low to medium-grade metasedimentary rocks as well as on the mineralized quartz veins. The majority of the fluid inclusions are saline aqueous-carbonic. Type 1 inclusions are primary H₂O-CO₂ inclusions with CO₂ phase varying from 10 to 60 volume %. Fluid inclusions with the high filling ratio of CO₂, and associated with Type 2 aqueous as well as nearly pure carbonic Type 3 inclusions are abundant in the healed microfractures and along the grain boundaries. The work was also focused on the natural graphitic carbonaceous material distributed in metasedimentary and crystalline rocks in and around Larji - Rampur tectonic window, Himachal Himalaya. The GCM, at places, shows affiliation with the ore mineralization. The micro Raman spectroscopy of representative samples confirms that this GCM is mostly poorly ordered. The carbon isotope compositions reflect the source of carbon in GCM at various locations, which infer a diversity in carbon source and mixing of carbon reservoirs.

Activity: 1B

Mantle upwelling fluid circulation and metasomatic processes in the Himalaya: Implications on fluid-rock interaction

(H.K. Sachan, Aditya Kharya, Saurabh Singhal and Perumal Samy)

The peak P-T conditions of migmatization, in the Leo Pargil Dome, have been constrained at 9.2-11.0 kbar, 810-825°C for the amphibole+biotitemigmatite and 700-745°C, 7.2-7.9 kbar for the sillimanite + muscovitemigmatite using the thermodynamic modeling. Peak P-T conditions are followed by an early isothermal decompression, with final melt crystallization occurring at 785-790 °C, 7.0-7.2kbar for the amphibole+biotitemigmatite and at 675°C, 5.6-5.8 kbar for the sillimanite+muscovitemigmatite. The partial melting processes responsible for the formation of migmatites involved both water-fluxed melting (amphibole+biotitemigmatite) and muscovite dehydration melting (sillimanite + muscovitemigmatite). Primary CO₂ and CO₂-H₂O fluid

inclusions, as well as secondary CO₂ fluid inclusions, are observed in quartz. This study suggests that the primary carbonic-aqueous (V_{CO₂} - L_{H₂O}) fluid inclusions were initially trapped in the system later H₂O content was lost during exhumation, leading to the formation of pure CO₂ fluid inclusions. The source of CO₂ fluid may be from the prograde decarbonation of carbonate-bearing protoliths.

The geochemistry of Shyokvolcanics, NW Himalaya is studied to understand its origin and explore the genetic relation with the nearby Khardungvolcanics. The total alkali-silica (TAS) diagram classifies the studied Shyokvolcanics into mafic (basalt), intermediate (basaltic andesite and andesite), and felsic (dacite and rhyolite) units. These volcanics are essentially calc-alkaline in nature similar to the Khardung volcanics.

Primitive mantle normalized multielement pattern (not shown here) exhibits conspicuous negative anomaly at P and Nb, a trait of subduction-related calc-alkaline volcanics. A depletion in Nb and elevated Th and Ba content in the Shyok volcanics also highlight their geochemical similarities to the arc-related volcanics. The Shyok volcanics are also characterized by an elevated Pb content rendering high Pb/Ce akin marine sediments and arc volcanics, which is also apparent from mild positive Pb anomaly on the primitive mantle normalized multielement pattern (not shown here). Tectonic discrimination diagrams for granitoids are used to infer the tectonic setting in which the felsic volcanics were generated. The studied dacites and rhyolites show geochemical affinity to the volcanic arc granitoids thus by, further supporting the continental arc-related origin of these volcanics similar to that

inferred for the Khardung volcanics.

The Ladakh granite has been studied in detail for Trace, REE, and Sr, and Nd isotope studies. The primitive normalized tracer elemental patterns (Fig. 5) for the two types of enclaves are richer in large ion lithophile elements (LILE) such as Rb, Ba, Th, U, Pb) and light rare earth elements (LREEs) and depleted in higher rare earth elements (HREEs) as well as strong depletion in high field strength elements (Nb, Ta, Zr, Hf) with SrI (0.705-0.708) suggesting that metasomatization of lithospheric mantle wedge at Mesoproterozoic (1.34 and 1.08 Ga) by exhumation melting of UHP Indian crustal rocks after decoupling of oceanic crust by Kohistan-Ladakh asthenospheric mantle melting. The Ladakh magmatic rocks are enriched LILE, LREE and depletion in HREE, HFSE with sharp positive K, Pb spike are similar to arc type magmas (Fig. 6) with low to high ⁸⁷Sr/⁸⁶Sr initial value (0.697-0.719) are similar to the UHP orthogneisses in the Indus suture zone. The values range from -3.74 to -12.01 for Ladakh magmatic rocks, which yield two types of mixing (hyperbola line) with Archean (2.81-3.11 Ga), Paleoproterozoic (1.70-2.41 Ga), and Mesoproterozoic (1.31-1.34 Ga) juvenile arc crust by crustal and mantle interaction (reworking and assimilation) takes place during the exhumation of deeply subducted continental crust (Fig. 7). The decompression melting of continental crustal rocks metasomatizes the overlying mantle wedge, eventually the arc mafic magmas generation. The mafic magma reacts with a lower arc crust formed metaluminous mafic enclave. The magmatic differentiation and fractional crystallization of mafic magmas generate intermediate to felsic.

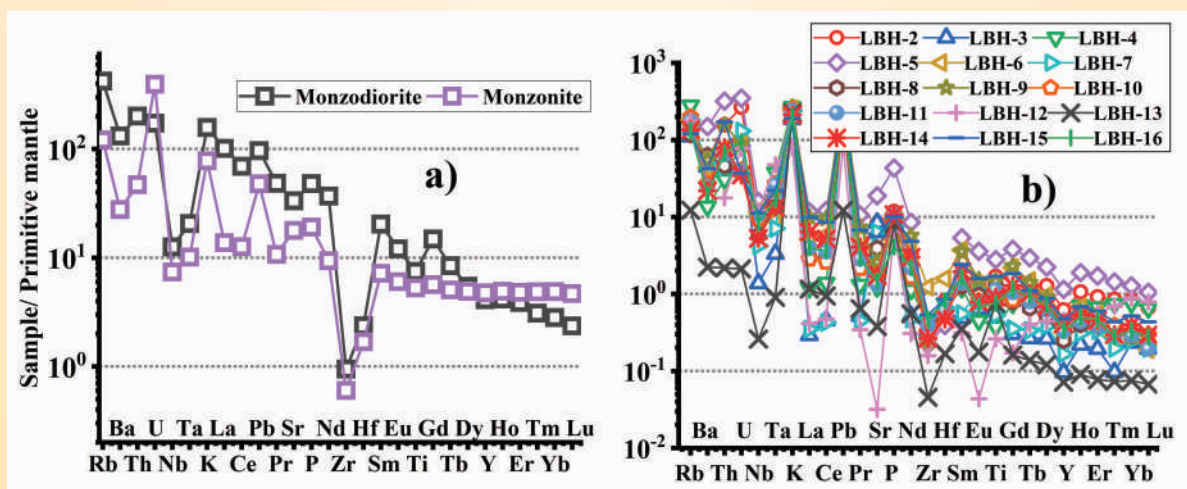


Fig. 5: Primitive mantle normalized diagram, a) mafic enclave, ii) Ladakh granitoids.

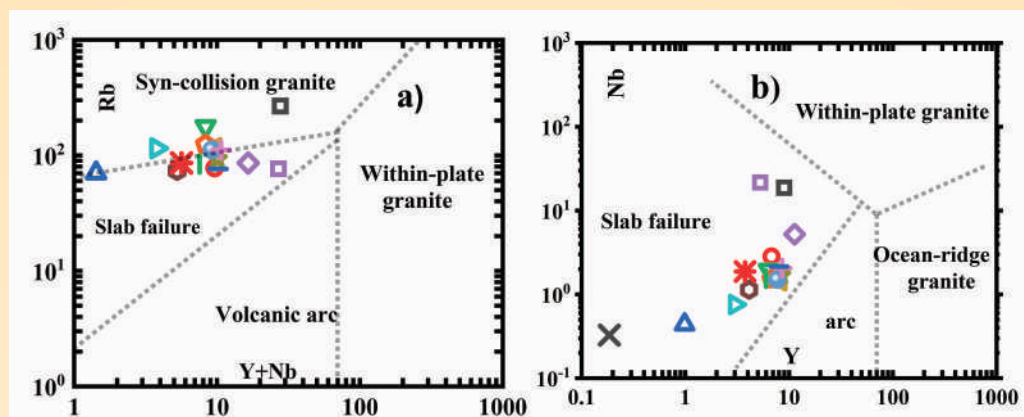


Fig. 6: Tectonic discrimination diagram, a) Y+Nb vs Rb, b) Y vs Nb.

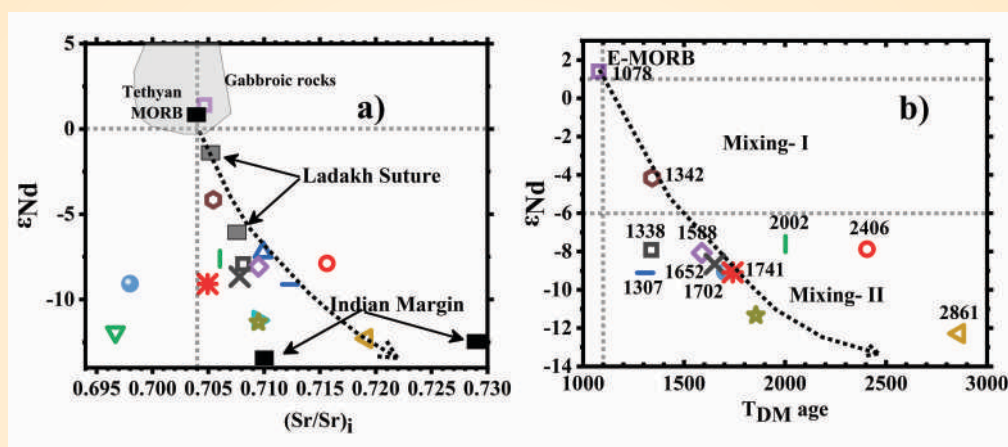


Fig. 7: Epsilon Nd versus (Sr)I and modal age diagram for mafic enclave and Ladakh granitoids.

Activity: 2A

Subsurface Characterization of Main Himalayan Thrust (MHT) across the Sub-Himalaya

(Kalachand Sain, Priyadarshi Chinmoy Kumar and Pankaj Chauhan)

Shallow structures and advanced interpretation

An attempt has been made to explore the NE and NW Himalayas to characterize the subsurface structures (geometry and subsurface disposition) and petrophysical properties. High-resolution 2D/3D reflection seismic and well data has been procured from National Data Repository (NDR), Directorate General of Hydrocarbons (DGH), New Delhi for this research to delimit subsurface fine-scale structures, decollement zones, ramp limiting ruptures, and geometry of fault systems prevailing in the Himalayan terrain. Data loading and initial quality check have been completed. The team is now making a detailed investigation of the available seismic reflection and well data. Different seismic experiments using an open-source database have been performed before adventuring into this

seismic research activity. Several new seismic meta-attributes have been computed using the artificial neural approaches to augment the interpretation of seismic data. The research outputs of the activity have been put to publications in several journals of international repute. Besides these works of CAP Himalaya, the team has also worked on (i) Assessment of geothermal energy resources in the NW Himalaya, (2) Understanding the causes of recent glaciological disasters in Rishiganga Dhauliganga catchment, (iii) Delineation and quantification of gas-hydrates.

Activity: 2B

Geometry and rheological assessment of the Main Himalayan Thrust and their implications toward seismogenesis and lithospheric flexuring

(Naresh Kumar, Devajit Hazarika, Gautam Rawat, Kousik Sen, and S.S. Thakur)

The work is performed based on the geological and geophysical data of the Himalaya, Tibet, and Indo-

Gangetic Plain (IGP) regions. The study reveals that Tethyan Himalaya has a higher seismic hazard compared to the adjoining part of the High Himalayan Crystalline (HHC) of the Kinnaur Himalaya. The ambient noise and surface wave data characterize the sediment thickness of the IGP and Tarim basin and suggesting low velocity in the middle and lower crust of Tibet. A shallow mantle discontinuity (Hales discontinuity) has been identified and characterized beneath the eastern Ladakh-Karakoram zone. Crustal thickness in the range of 45-50 km and V_p/V_s ratio of 1.69-1.90 is obtained in the Siang window of NE Himalaya. Magnetotelluric studies reveal a low-angle NE dipping intra-crustal high conducting layer (IC-HCL) at 8-15 km depth beneath the Lohit valley, Arunachal Himalaya. A similar study in the National Capital Region, New Delhi suggests the Mahendargarh-Dehradun fault zone is a conductive feature implying the role of fluids in seismo-genesis of recent moderate magnitude seismicity in the Capital and adjoining parts.

Magmatic and metamorphic evolution of crystallines from the Himalayan metamorphic core of Bhagirathi Valley is studied based on mesoscopic, microstructural, mineral chemistry, and U-Pb geochronology of zircon investigations. Evaluation of carbon dioxide entrapment, sulfide mineralization, and carbonate metasomatism in the shallow lithospheric mantle through microtextural, fluid inclusion, mineral chemistry, and Raman Spectroscopic analysis in the ultramafic and alkaline rocks of Sung Valley Meghalaya. The inverted metamorphic sequence display of the rocks of Greater Himalayan Sequence (GHS) in the Dhauliganga valley marks the kyanite grade metamorphism in the lower and middle structural levels and sillimanite grade metamorphism in the upper structural level. The P-T condition suggests that the GHS have undergone inverted Barrovian metamorphism. Metamorphic study of allanite and monazite in the Dhauliganga valley further suggests that the allanite-out reaction is the result of prograde metamorphism which occurred at the temperature of $\sim 660^\circ\text{C}$ and the pressure of 9.5 kbar. The detailed results are given below

Site effect and attenuation characteristics of the Kinnaur Himalaya

The site effect and attenuation studies are carried out for the Kinnaur region of northwest Himalaya, India. The region, to the north of the South Tibetan Detachment System (STDS), reports anomalous high seismicity of low magnitude earthquakes which is the only such region of northwest Himalaya. A total of 109 local earthquakes occurred in the Kinnaur region of

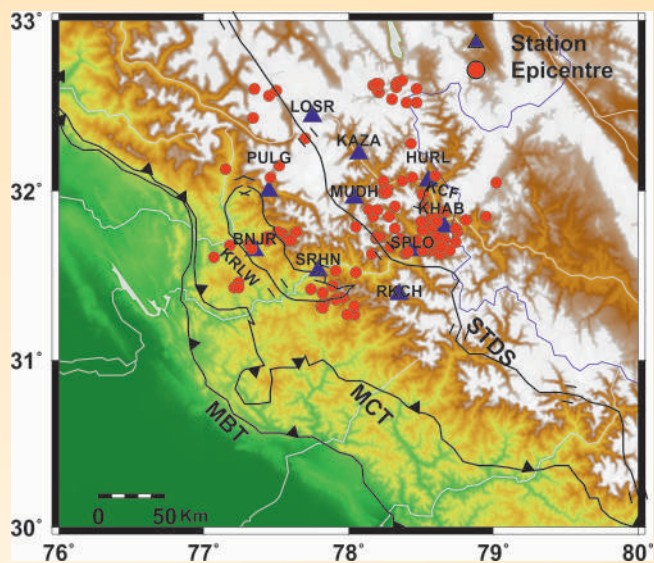


Fig. 8: Seismotectonic map of the study region of the Kinnaur Himalaya and adjoining parts. Blue triangles are the locations of the Broadband Seismographs of WIHG and red circles are the data recorded by this network used for the present study.

magnitude range 1.6-4.5 are utilized for the present work (Fig. 8). Seismic waves are influenced by the seismic station site effect depending on soft sediment thickness beneath the recording sites. Therefore, the work is performed to evaluate and correct the site effects (Fig. 9) to estimate quality factor (inverse of attenuation) for the P-wave (Q_p), S-wave (Q_s), and coda-wave (Q_c). The frequency-dependent attenuation relations obtained for $Q_p(f)$, $Q_s(s)$, and Q_c are free from site effects to utilize for further studies. The Kinnaur Himalaya mainly belongs to HHC and Tethyan Himalaya, where these two geological units are differentiated by the STDS. The resonance frequencies and attenuation characteristics are estimated for both regions. A comparison is made between the HHC and Tethyan Himalaya in the form of resonance frequencies and attenuation properties. The low-value resonance frequency and high rate of attenuation are observed to the northern side of the STDS compared to the HHC. These parameters of the Tethyan Himalaya support the presence of low-grade metasedimentary rocks. It suggests that the Tethyan Himalaya has a high seismic hazard potential zone compared to the HHC.

The work is achieved from a good amount of data by using a set of 661 waveform records obtained through a very dense BBS seismic network installed in the Kinnaur region. The waveform records corrected for site effects provide the regional attenuation relationship. The resonance frequency corresponding to maximum amplification is computed from the site

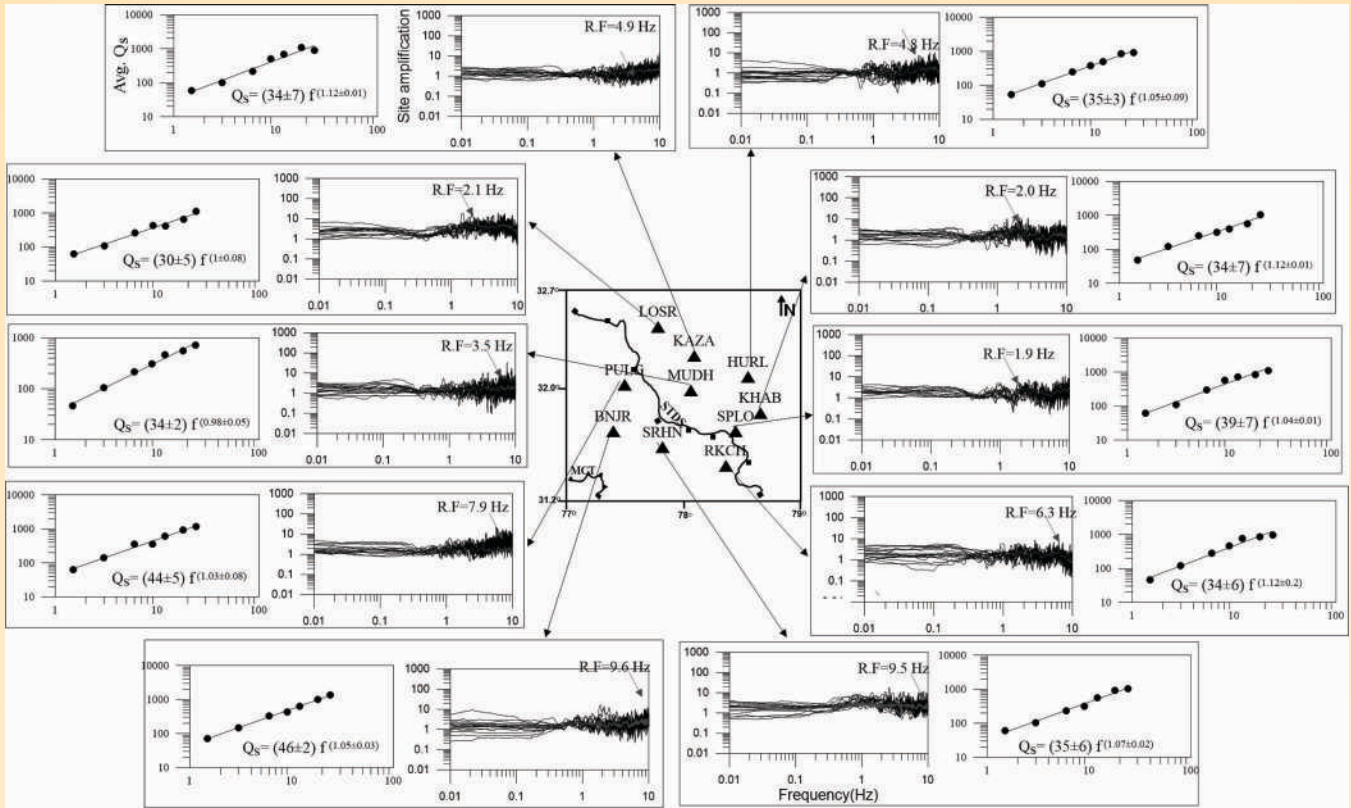


Fig. 9: The obtained site amplification curves and S-wave quality factor relationship at different stations. The black and grey color curves denote the site amplification curve for different events and the average of these curves, respectively. The R.F. represents the resonance frequency corresponds to maximum amplitude and the triangle represents the location of the recording station.

amplification curve, i.e., the resonance frequency is the frequency upon which earthquake waveform gets amplified. The resonance frequency varies from region to region as it turns out to be low with the increasing basement depth or for the regions that belong to younger alluvial deposits and vice versa. The stations that exist to the southern side of the STDS have high resonance frequency in the range of 6.3-9.6 Hz, while stations towards the northern side have low resonance frequency, i.e., 1.9-4.9 Hz (Fig. 10). It is noticed that resonance frequencies have a close resemblance with the geology of the study region. Comparison of obtained relations with other available relations for the Himalayan region validates the reliability of present results.

Crustal thickness and Poisson's ratio variations in the Siang Window of Eastern Himalaya

A seismological network comprised of 8 broadband seismological stations was established in the Siang Window of Arunachal Himalaya during December 2018 for investigation of seismotectonics and subsurface structure (Fig. 11). Each seismic station is equipped with a Trillium Compact-120 seismometer and Centaur

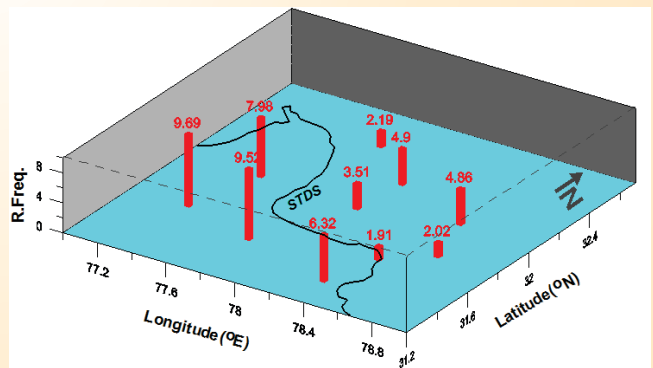


Fig. 10: The distribution of resonance frequency values at different Broadband stations.

datalogger (Nanometrics, Canada). Continuous data were recorded with a sampling rate of 100 samples per second (SPS). Time synchronization of the digitizer is done using Global Positioning Systems (GPS). The waveform data has been collected for the period from December 2018 to February 2021 from these remote seismological stations. The teleseismic earthquakes recorded by this network have been analyzed using the receiver function (RF) method to investigate crustal structure. The Iterative deconvolution method of

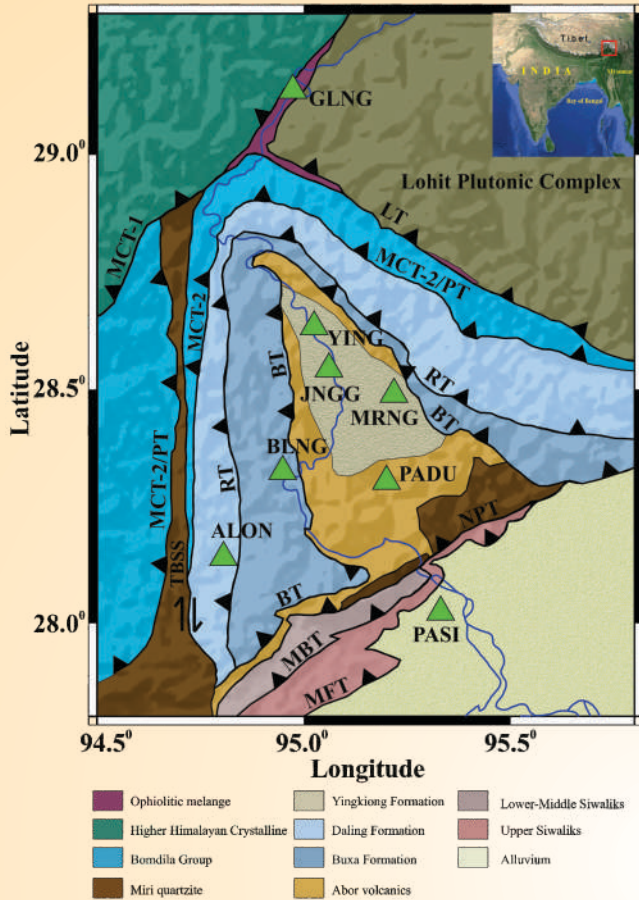


Fig. 11: Distribution of seismological stations of Siang Window, Arunachal Himalaya, plotted over the simplified tectonic map (Modified after Booth et al. 2009).

Ligorria and Ammon (1999) has been used for RF computation. The teleseismic earthquake data have been selected based on a high signal-to-noise ratio, $M \geq 5.5$, and epicentral distance: 30° - 90° . The network has recorded 480 teleseismic events out of which 370 teleseismic earthquakes passed the data selection criteria. The individual RFs have been plotted with respect to back azimuth to examine the azimuthal variation of crustal structure if any. The data used in this study are shown in figure 12. Examples of RFs at each station are shown in figure 13.

In continuation of the previous annual report, the average crustal thickness (H) and Poisson's ratio were estimated with the help of the H-k stacking analysis of receiver functions at all 8 stations. The estimated Poisson's ratios show significant variation from 0.23 to 0.328 in the window, suggesting the presence of heterogeneity in crustal composition. The Poisson's ratios are observed to be low at ALON (0.23), PASI

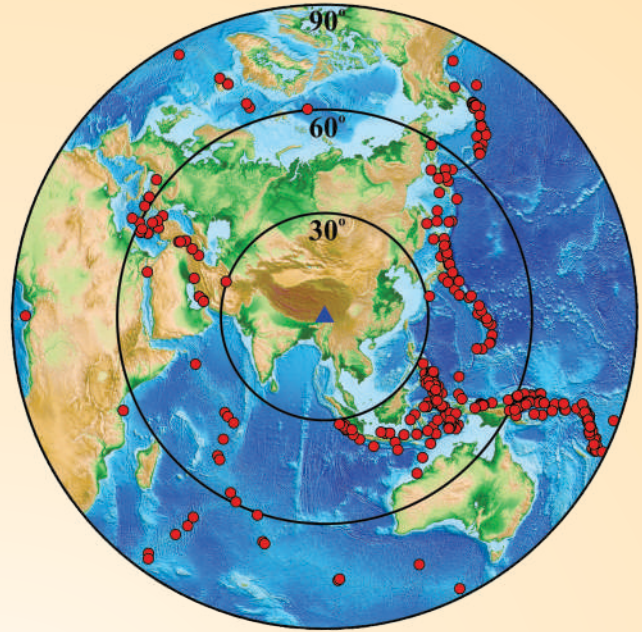


Fig. 12: An azimuthal projection showing the distribution of teleseismic earthquakes (red circles) of magnitude greater than 5.5. The blue triangle shows the network center.

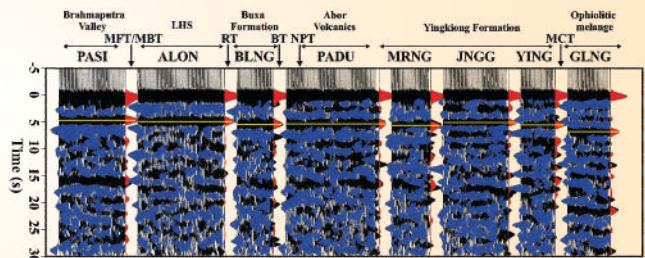


Fig. 13: Example of receiver function along the AB profile.

(0.244), and JNGG (0.24) stations; intermediate at MRNG (0.253) and PADU (0.269) stations. The high Poisson's ratio (0.287-0.328) is found at BLNG, YING, and GLNG. This wide range of variation in Poisson's ratio can be attributed to the local geology.

The RF inversion has been carried out at few stations. The RF inversion process is highly nonlinear and hence we preferred to use the NA inversion of Sambridge (1998). An example of RF inversion is shown in figure 14. The results from RF inversion and H-k stacking analysis show a variation of crustal thickness from ~40 km in the Pasighat area (PASI) to ~50 km at the northernmost station (GLNG, Fig. 11).

MT studies in Lohit Valley, Arunachal Pradesh, and around the National Capital Region New Delhi

Magnetotelluric derived electrical resistivity cross-section of the Lohit Valley in the Eastern Himalayan Syntaxial bend depicts the crustal structure in terms of

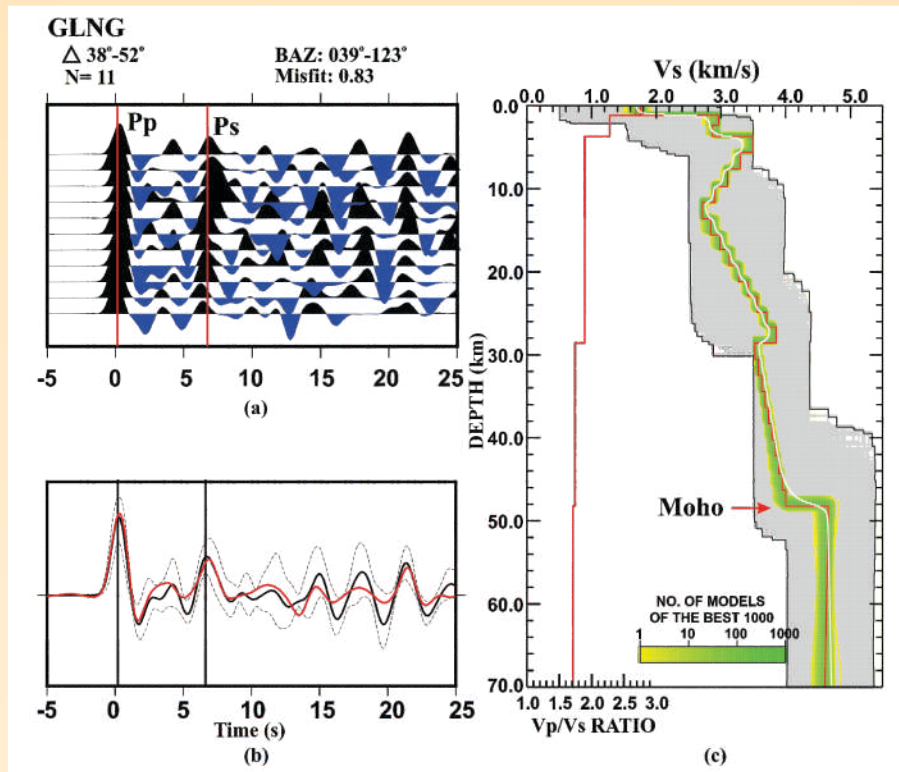


Fig. 14. Illustration of the inversion scheme using Neighborhood Algorithm (NA) considering receiver function data of GLNG station located in the Tuting Suture Zone. The RFs used for inversion are shown at the top left corner. The inverted models are shown in the right panel. The range of models (40 000 models) searched to find the best model are shown by grey area, and the best 1000 models are shown by a green area with a minimum error between observed and computed receiver functions. The red and white lines indicate the best-fitting and average models, respectively. The best-fitting V_p/V_s model (red line) is shown to the left of the shear wave velocity models. The Moho is marked by a red arrow. The comparison of stacked observed RF (red waveform) and synthetic RF (black waveform) obtained from the NA inversion is shown in the bottom left. The ± 1 standard deviation bounds are shown by black dashed lines.

resistivity. The resistivity cross-section is dominated by a low-angle northeast dipping IC-HCL. The layer is in a depth range of 8-15 km and present throughout the profile. The thrust and suture zone across the profile is imaged as dipping conducting layers which are merging to the intra-crustal high conducting layer. The Lesser Himalaya and the Lohit Plutonic Complex are imaged as resistive bodies where later is more resistive. The Tidding suture zone is imaged as a conductive zone between the Lesser Himalaya and the Lohit Plutonic Complex, where the Tidding Suture is dipping towards NE. The conductivity of the IC-HCL is lower in comparison with other sectors of the Himalaya implying a significant difference in the intensity of the tectonic processes in this part of the Himalaya.

Last year National Capital Region (NCR) has witnessed series of tremors, which originated at faults present around the region e.g. Mahendargarh-Dehradun fault, Delhi - Hardwar Ridge, etc. To have a quick understanding of subsurface structures and to examine plausible seismogenic structures around NCR, a team of

WIHG and NCS, MoEs carried out an MT survey in the region. Total 54 sites were occupied with 3-4 day occupancy at every site for magnetotellurics measurements along four profiles. The NCR and its surrounding region are dominantly occupied by several industries and motor-operated tube-wells for agricultural farming. Most of the survey period is also affected by low solar activity. Further, the measurements are heavily affected by cultural noise and require intensive time for its processing to yield significant impedance tensor elements for at least up to 1-10 sec.

The MT impedances at eight sites along the Rohtak-Delhi profile are modeled. Mahendargarh-Dehradun fault zone has appeared as a conductive feature implying the role of fluids in seismogenesis along this fault.

Magmatic and metamorphic evolution of crystallines from the Himalayan metamorphic core of Bhagirathi Valley

The Himalayan metamorphic core in the Bhagirathi

valley region of NW India consists of continuous exposures of Lesser Himalayan gneiss and metapelite to the south and the higher grade rocks of the GHS to the north. In this study, the juxtaposition of the Lesser Himalayan greenschist facies rock beneath the amphibolite grade rocks of the GHS is observed in a 2-3 km thick high strain zone identified as the MCT. Our study shows that the lower part of the GHS, the MCT zone, and its footwall show a moderate T high P inverted metamorphic sequence with pre- to syn-kinematic, inclusion-rich garnet. On the other hand, the uppermost part of the GHS shows high T moderate P prograde metamorphism with post tectonic inclusion free garnet and showing evidence of partial melting both in outcrop- and microscopic scales. We envisage that the uppermost part of the GHS and the lower part of the GHS including the MCT zone are two distinct tectonic slices with different metamorphic evolution. The protracted period of partial melting at the uppermost part of the GHS is more akin to a channel flow model. However, inverted metamorphism in the MCT zone, its exhumation, and propagation of deformation towards the foreland suggest accretion of new tectonic slices towards the south, for which an in sequence shearing model is more consistent with our data.

The Himalaya is characterized by the presence of both pre-Himalayan Paleozoic and syn-Himalayan Cenozoic granitic bodies, which can help unravel pre- to syn-collisional geodynamics of this Orogen. In the Bhagirathi Valley of Western Himalaya, such granites and the Tethyan Himalayan Sequence (THS) hosting them are bound to the south by the top-the-north extensional Jhala Normal Fault (JNF) and low-grade metapelite of the THS to its north. The THS is intruded by a set of leucocratic dykes concordant to JNF. Zircon U-Pb LA-MC-ICP-MS geochronology of the THS and one leucocratic dyke reveal that both of the rocks have a

strikingly similar age distribution with a common and most prominent age-peak at ~ 1000 Ma. To the north of the THS, lies Bhaironghati Granite, a Paleozoic two-mica granite, which shows a crystallization age of 512.28 ± 1.58 Ma. Our geochemical analysis indicates it to be a product of pre-Himalayan Paleozoic magmatism owing to extensional tectonics in a back-arc or rift setting following the assembly of Gondwana (500-530 Ma). The Cenozoic Gangotri Leucogranite lies to the north of Bhaironghati Granite and the U-Pb dating of zircon from this leucogranite gives a crystallization age of 21.73 ± 0.11 Ma. Our geochemical studies suggest that the Gangotri Leucogranite is a product of muscovite-dehydration melting of the lower crust owing to flexural bending in relation to steepening of the subducted Indian plate. The leucocratic dykes are highly refracted parts of the Gangotri Leucogranite that migrated and emplaced along extensional fault zones related to JNF and scavenged zircon from the host THS during crystallization.

Metamorphism and stability of allanite and monazite in the GHS rocks of the Dhauliganga Valley, Garhwal Himalaya

The Metamorphism vis a vis the occurrence and relative stability of metamorphic allanite and monazite in metapelites of the GHS in the Dhauliganga valley, Garhwal Himalaya have been studied in detail. The GHS is marked by kyanite grade metamorphism in the lower and middle structural levels and sillimanite grade metamorphism in the upper structural level. The rocks of the GHS of the Dhauliganga valley display an inverted metamorphic sequence. The P - T condition calculated for GHS samples suggests the peak metamorphic temperature in a range of 659° - 800° C and pressure in a range of 8.7 - 11.9 kbar (Table 1). The metamorphic temperature

Table 1: Mineral assemblages and P-T conditions of metamorphism (T in $^{\circ}$ C; P in kbar). Mineral abbreviations in the tables and text are from Kretz (1983).

Sample	Mineral assemblage	Metamorphic zone	Occurrence of allanite and monazite	T and P from Av. P-T method (P in bracket)
M25	ky-grt-bt-ms-pl-qtz-ilm-ap-aln	ky zone	Allanite occurs as inclusion in the garnet as well as in the matrix, Monazite is absent in the sample.	$708 \pm 30(11.9 \pm 1.4)^*$
HH52	ky-grt-bt-ms-pl-qtz-ilm-rt-ap-mnz	ky zone	Monazite occurs as a matrix phase. Allanite is absent in the sample.	$659 \pm 25(9.5 \pm 1.3)^*$
M6	grt-bt-ms-kfs-pl-qtz-ap-mnz	ky zone	Monazite occurs as a matrix phase. Allanite is absent in the sample.	$723 \pm 61(8.7 \pm 2.8)^{**}$
HH30	sil-grt-bt-kfs-pl-qtz-ilm-ap-mnz	sil-kfs zone	Monazite occurs as a matrix phase. Allanite is absent in the sample.	$800 \pm 45(10.4 \pm 2.0)^{**}$

*From Thakur et al., 2015

**From this study

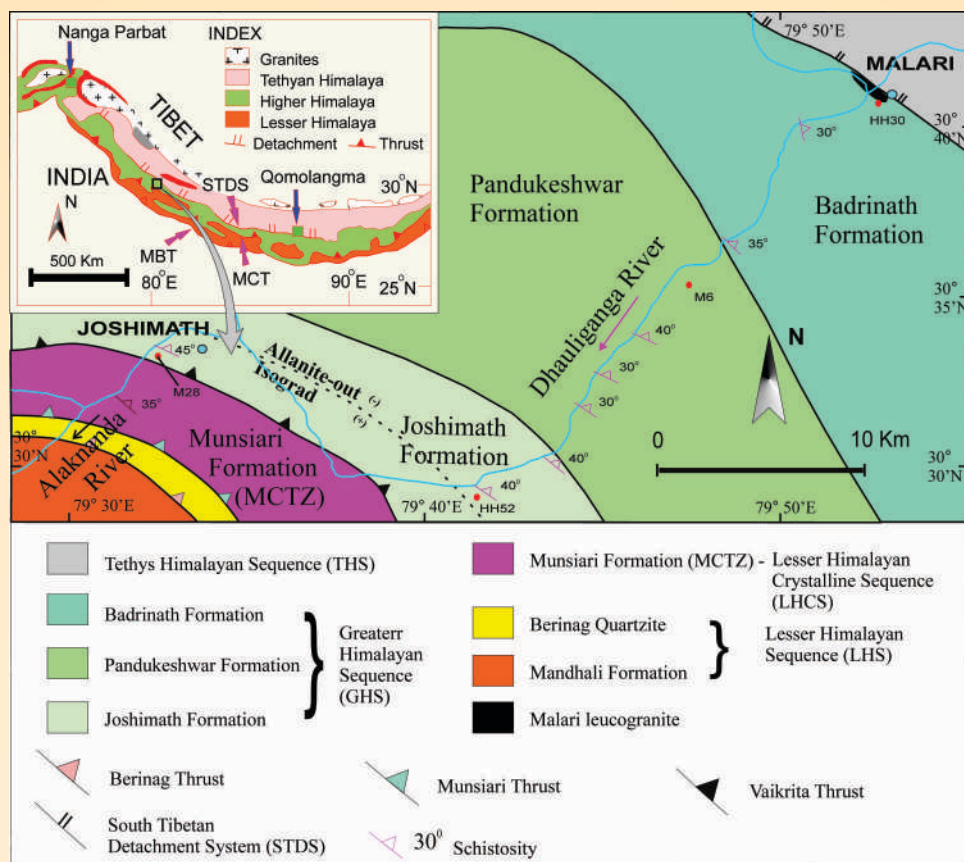


Fig. 15 Geological map of the Dhauliganga valley (modified after Valdiya et al. 1999; Spencer et al., 2012). Sample locations are marked by pink circles. Inset shows map of the Himalayan orogen. (abbreviation: MCTZ = Main Central Thrust Zone).

gradually increases from the lower structural level to the high level of GHS starting from the MCT to the STDS. The P - T condition of the studied samples suggests that the GHS of Dhauliganga valley (Garhwal Himalaya) have undergone inverted Barrovian metamorphism.

Study shows that the occurrence of allanite in the Dhauliganga valley is restricted to the lower structural level, while monazite occurs in all structural levels. Monazite is likely formed by the breakdown of the allanite. The allanite-out reaction is demarcated at the lower structural level of the GHS in the Dhauliganga Valley (Fig. 15). Metamorphic study of allanite and monazite in the Dhauliganga valley further suggests that the allanite-out reaction is the result of prograde metamorphism which occurred at the temperature of $\sim 660^\circ\text{C}$ and the pressure of 9.5 kbar.

Activity: 2C

Monitoring of earthquakes for seismological, seismotectonic, and subsurface related processes: evaluation of seismic hazard in the Himalaya

(Sushil Kumar, Ajay Paul, Dilip Kumar Yadav, Narendra Kumar, Praveen Kumar and Chinmoy Haldar)

Non-uniformity of the Himalaya foresees significantly large earthquake events. It is found that the Himalaya is not uniform and assume different physical and mechanical properties in different directions. The NW region of Himalaya, an area covering Garhwal and Himachal Pradesh, has been hit by four destructive moderate to great earthquakes since the beginning of the 20th century - the Kangra earthquake of 1905, the Kinnaur earthquake of 1975, the Uttarkashi earthquake of 1991, and the Chamoli earthquake of 1999. These seismic activities manifest large-scale subsurface deformation and weak zones, underlining the need for deeper insights into the ongoing deformation beneath

these tectonically unstable zones. The study using seismic waves from 167 earthquakes recorded by 20 broadband seismic stations deployed in the Western Himalaya suggested that the major contribution of the anisotropy is mainly because of the strain induced by the Indo-Eurasia collision since last 50 million years and deformation due to the collision is found to be larger in the crust than in the upper mantle. It has been recently published in 2020 in the Journal 'Lithosphere (GSA)'.

The inhomogeneity along the Himalayas influences the stressing rate is because of variation in the geometry of the MHT system, and it controls the rupture size during the earthquake. This lack of homogenous physical and mechanical properties of the Himalayas could help explore new perspectives about deformations taking place at the Himalaya-Tibet crustal belt involved in the formation of the Himalayan Mountains.

The study area is shown as a rectangle. Geological boundaries, in addition to those defined in figure 16, include BNS (Bangong-Nujiang suture zone), JRS (Jinsha-River suture), ATF (Altyn Tagh fault), KF (Karakoram fault), QBF (Qaidam Basin fault), IGP: Indo-Gangetic plain, SH: Siwalik Himalaya, LH: Lesser Himalaya, HH: Higher Himalaya, TH: Tethys Himalaya, LDH: Ladakh Himalaya, ISC: Indian sub-continent, DVP: Deccan volcanic province, EDC:

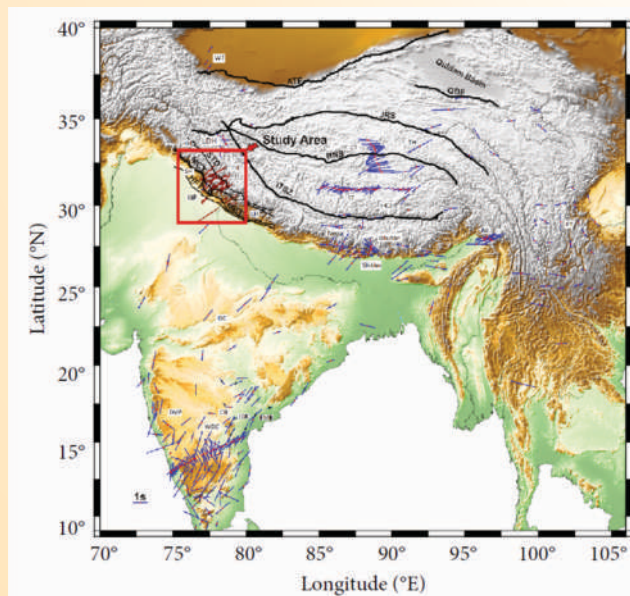


Fig. 16: Map showing the fast polarization azimuths (Φ) and delay times (δt) from previous studies with blue bars and red bars indicate the average shear-wave splitting results from this study. The previous splitting measurements are obtained from fr/DB.

Eastern Dharwar craton, WDC: Western Dharwar craton, CB: Cuddapah basin, EMB: Eastern-Ghat Mobile Belt, WT: Western Tibet, CT: Central Tibet, ET: Eastern Tibet, ST: Southern Tibet, HCZ: Himalayan collision zone, CA: Central Asia, NEI: North-East India. The solid-filled circle and the length of the bar represent the location of the stations and the delay time, respectively.

Seismic structure of the crust and upper mantle beneath the Kishtwar region, NW Himalaya, India using receiver function technique

The P-to-S converted wave data recorded at the Doda-Kishtwar region in the North-West Himalaya have been used to investigate the crust and upper mantle structure using the receiver functions (RFs) technique. This study provides a correlation between the upper crustal Low-velocity Layer (LVL) and local seismicity. Three-component waveforms of the teleseismic earthquakes, recorded by a network of 6 broad-band seismological stations that are operated by Wadia Institute of Himalayan Geology (WIHG), have been used for the inversion of the stack RFs show increase in crustal thickness from 47 km to 57 km from south to north. The MHT is observed beneath four stations out of six from an individual as well as stack receiver functions whose depth varies from 21 to 26 km. However, the LVL is observed below each station, which varies from 11.1 km to 13.3 km with a high value of V_p/V_s . The high value of V_p/V_s in the LVL of the upper crust may be due to shear heating within the ductile regime and/or decompression and cooling related to the exhumation indicating the presence of fluid/partial melt at depths between ~ 10 to 15 km. Out of 211 local events in the study region, 143 earthquakes occurred at depths of ≤ 15 km and the remaining 68 events occurred at depths of ~ 16 to 35 km. Interestingly, the LVL coincides with the occurrences of most of the crustal seismic activity, and thus we conclude that the upper crustal LVL, associated with the weak zone, is responsible for the generation of most of the local earthquakes. The arrival time difference between the T_{P660s} and T_{P410s} converted phases in the study region are larger than the normal 24 s (w.r.t. the standard time of IASP91) due to the effect of low temperature.

Variation of seismicity in HHC

An effort has been made to compare various geophysical parameters in the Garhwal and Kumaun regions of the North-West Himalaya. This exercise provides empirical evidence of the distinct nature of these two regions. Three different parameters viz. the seismicity, plate velocity, and attenuation are compared

in these two regions. For this purpose, a compilation of the earthquake data, Global Positioning System (GPS) data, and Quality factor data is made for Garhwal and Kumaun regions. The spatial distribution of 772 earthquakes in these regions indicates that the Kumaun

region is seismically more active than the Garhwal region specifically from the MCT to the STDS. The variation in velocity field as indicated by the GPS data also suggests a higher convergence rate for the Kumaun region than Garhwal. Moreover, the attenuation studies

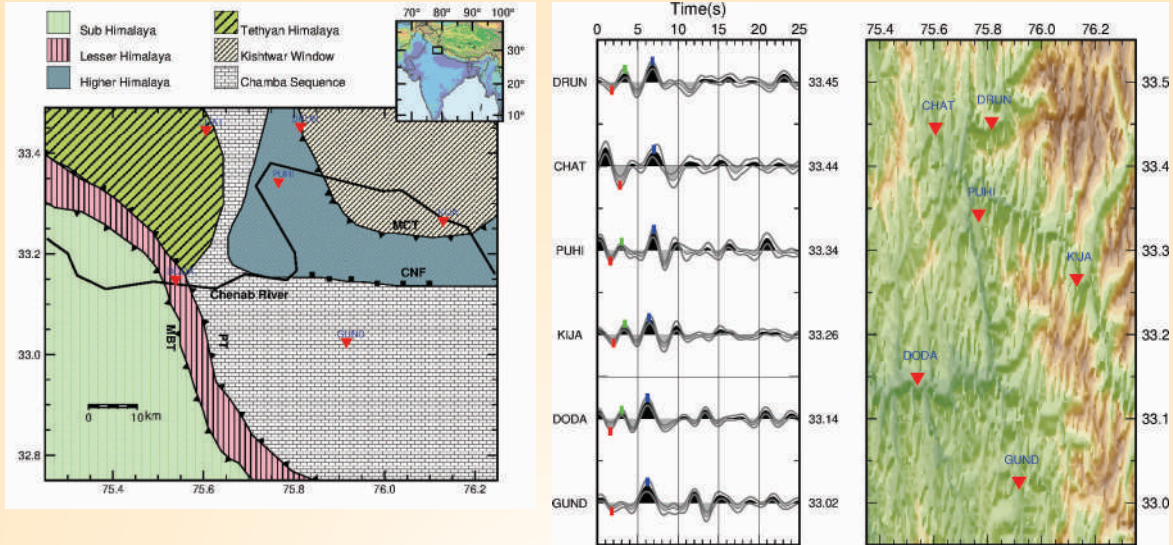


Fig. 17: Seismic coverage of broadband seismic stations (inverted red triangles) along with a geological map of the study region. The right figure shows the stack PRFs arranged with increasing order of latitude.

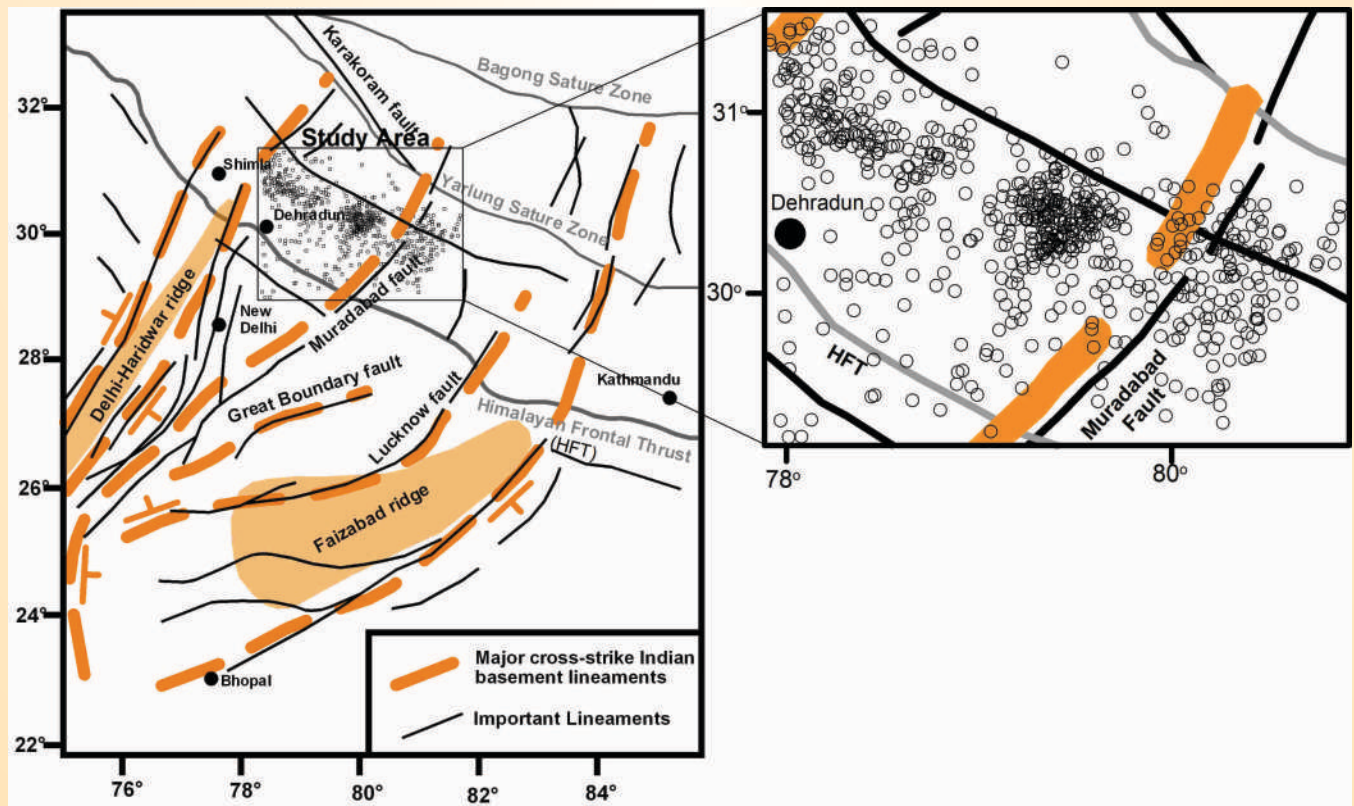


Fig. 18: Map showing major cross-strike Indian basement lineaments along with the seismicity in the Garhwal-Kumaun region, the circles represent the locations of epicenters (Modified after Godin, L., Harris, L.B., 2014).

by various researchers in these regions support the higher heterogeneous and tectonically active nature of Kumaun than the Garhwal region. The variation of seismicity in HHC is observed across the Pinder River, which separates Garhwal and Kumaun regions. This variability of seismicity is may be due to the structural discontinuity as shown in figure 18. It is monitored from figure 18 that seismicity is varying across the fault, which is the northward extension of the Muradabad transverse fault (Godin and Harris, 2014; Sastri et al., 1971). The possible reason for the variation of these parameters may be due to the presence of structural discontinuity on the fault between the Kumaun and Garhwal regions along the Pinder River i.e. Northward extension of the Muradabad fault.

Estimation of Site Response Functions for the Kumaun-Garhwal Himalaya

The spatial distributions of site spectral amplification levels at different frequencies corresponding to single-story, double-story, and 3-4 story tall, and high-rise buildings have been obtained for the Kumaun-Garhwal Himalaya. One Dimensional site response function has been estimated using 885 waveforms of 56 local earthquakes recorded at 14 sites using the Horizontal to Vertical (H/V) ratio Technique. The seismic spectral amplifications obtained at 10Hz (single-story building), 5Hz (Double story building), 2 Hz (3-4 story building), and 1Hz (Tall buildings) are shown in figures 19-22.

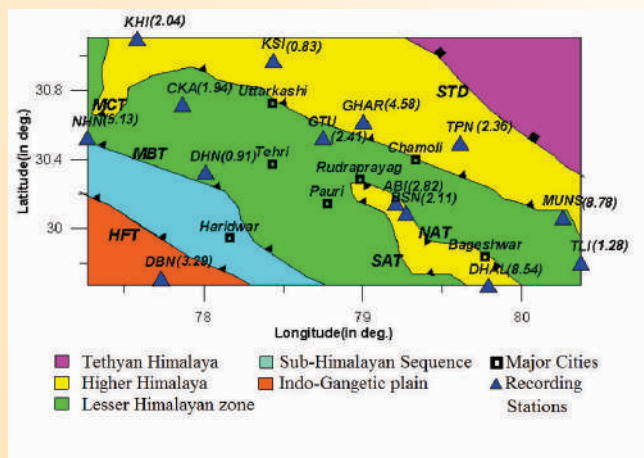


Fig. 19: Spatial distribution of spectral amplification values corresponding to a single-story building (at 10 Hz frequency). Blue triangles show recorded stations and numerical values in the brackets are showing the spectral amplification. Black square (blank center) shows major cities in the region. Dark black solid lines show the major thrusts situated in the region: MBT, MCT, HFT, SAT, NAT.

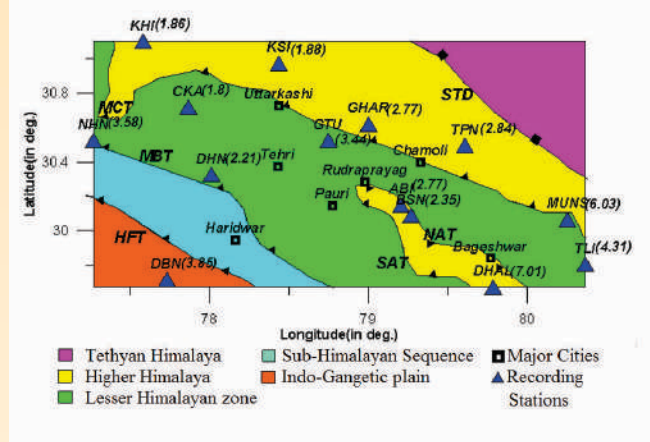


Fig. 20: Spatial distribution of spectral amplification values corresponding to a double-story building (at 5 Hz frequency). Blue triangles show recorded stations and numerical values in the brackets are showing the spectral amplification. Black square (blank center) shows major cities in the region. Dark black solid lines show the major thrusts situated in the region: MBT, MCT, HFT, SAT, NAT.

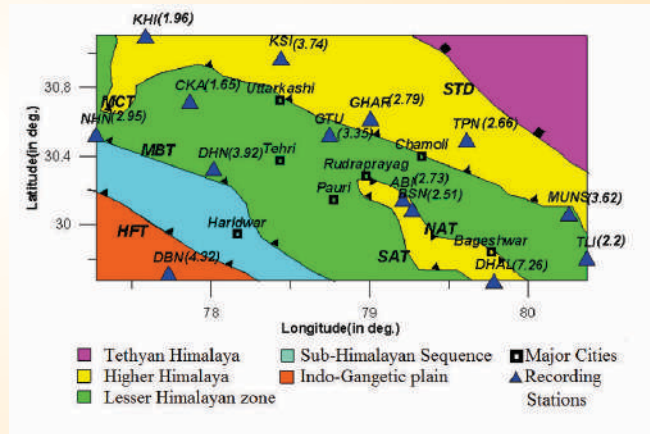


Fig. 21: Spatial distribution of spectral amplification values corresponding to the 3-4-story buildings (at 2 Hz frequency). Blue triangles show recorded stations and numerical values in the brackets are showing the spectral amplification. Black square (blank center) shows major cities in the region. Dark black solid lines show the major thrusts situated in the region: MBT, MCT, HFT, SAT, NAT.

It has been found that as we move from south to north in the Himalaya i.e. from Indo-Gangetic Plain, outer Himalaya to the Lesser Himalaya followed by the Higher Himalaya the spectral amplification decreases as the general trend of soil condition changes from soft alluvium at Deoband (Indo-Gangetic plain) to hardest rock in Kotkhai in the higher Himalaya. The spectral amplifications for the stations of the Kumaun Himalaya

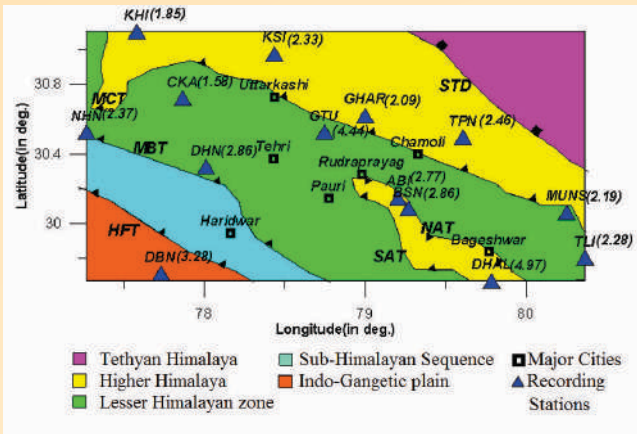


Fig. 22: Spatial distribution of spectral amplification values corresponding to the tall building (at 1 Hz frequency). Blue triangles show recorded stations and numerical values in the brackets are showing the spectral amplification. Black square (blank center) shows major cities in the region. Dark black solid lines show the major thrusts situated in the region: MBT, MCT, HFT, SAT, NAT.

are found to be higher than those of the Garhwal Himalaya.

These maps show that the site spectral amplification levels for the single-story buildings in the cities of Uttarkashi, Haridwar, Pauri, Chamoli, and Tehri in the region are not significant while it cannot be overlooked for the city of Bageshwar. The site spectral amplification levels for the tall buildings in the cities of Pauri, Tehri, and Bageshwar in the region are significant. The outcome of the present study is expected to be useful for the proper evaluation of seismic hazards in the region.

Reverse migratory behaviour of the earthquakes aftershock sequences along Himalayan Seismic Belt, Northwest Himalaya

The majority of the compression earthquakes that display upward seismicity migration typically occur along steep faults. However, in the context of the Himalayan seismicity, the opposite migratory behaviour of the aftershock sequence is observed even along the gentle dipping source faulting. The alteration in the effective strength of the rock mass which imply the variation in the crustal hydrostatic fluid pressure at shallow depth (0-15 km) have been studied and inferred that four major factors are responsible for the upward propagation of seismicity: i) Topography, ii) Prevailing tectonic principal orientations, iii) pore pressure exerted by the subsurface fluids and iv) Rheology of the upper seismogenic crust.

Focal Mechanism Solution (FPS) of Mechuka earthquake ($M_w=5.9$) and existing FPS with their P-axes Orientations in and around Siang Valley of Arunachal Himalaya, NE-India

The MT solution method of Sokos and Zahradnik, (2008) is used to determine the source mechanism of the Mechuka earthquake ($M 5.9$, April 23, 2019). The waveform inversion has been carried out using the computer software ISOLA. The inversion scheme of ISOLA follows the iterative deconvolution method for waveform inversion of local earthquakes. Moment tensor inversions involve complete waveform Green's function calculations and a grid search over a set of trial source positions and time shifts for obtaining the optimal centroid position in terms of absolute values of the correlation coefficient between the observed and synthetic waveforms. The best matching between observed and synthetic waveforms can be shown based on Variance reduction values (VR). The full-wave elastodynamic Green's functions have been computed for a given earth structure, source position, and station location. A local 1-D crustal velocity model from a previous study (Bhattacharya, et. al 2010) is used for Green's function calculation. The MT solutions and the waveform matching of the Mechuka event and its beachball presentation of the source mechanism are done.

The MT solution has a deviatoric and volumetric part. We focus on the deviatoric inversion. The Deviatoric tensor decomposition approach is applied to separate the double-couple (DC) part and the compensated linear vector dipole (CLVD) part. The DC percentage is estimated by the equation $DC\% = 100 \cdot (1 - 2n)$. The matching between the observed and synthetic data is quantified by variance reduction: $V_{\text{reduced}} = 1 - E/O$, where $E = \sum(O_i - S_i)^2$ and $O = \sum(O_i)^2$, where O and S stand for observed and synthetic data. Waveform data of 6 stations (PASI, BLNG, ALON, JNGG, MRNG, and PADU) were pre-processed and bandpass filtered within the low-frequency band 0.04 to 0.09 Hz. The best MT solution is grid searched considering five trial depths within the range 10-45 km in steps of 2 km and a temporal grid search between -3 and +3 s with respect to origin time keeping the source horizontal location fixed to the epicenter. The waveform inversion process was repeated for each depth. The Green's functions are estimated using the crustal velocity model of Bhattacharya et al. (2010). Comparison of observed (black) and synthetic (red) waveforms are shown in figure 23a. Due to the large misfit, we excluded the data of the PADU station from the inversion process. The DC percentage for the earthquake is 90%. The source position versus time shift is shown with respect to

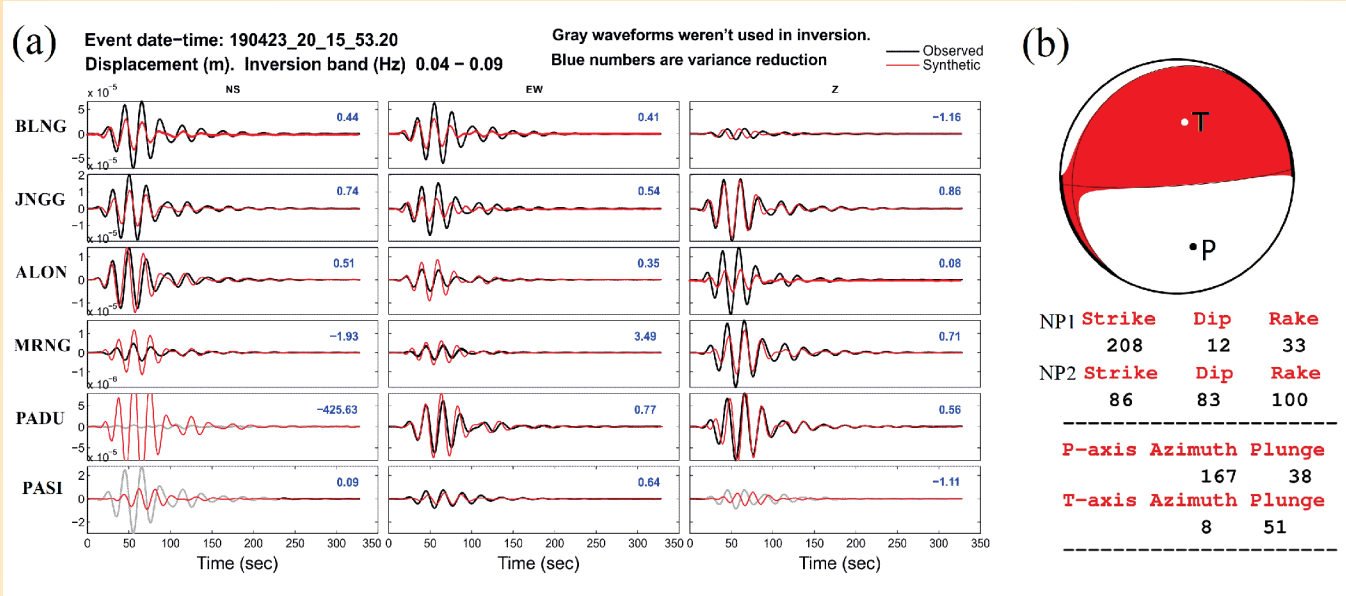


Fig. 23: (a) Comparison of observed (black) and synthetic (red) waveforms of the Mechuka earthquake Mw 5.9 using the ISOLA program. (b) Beachball presentation of the MT solution with parameters of nodal planes (NP1 and NP2).

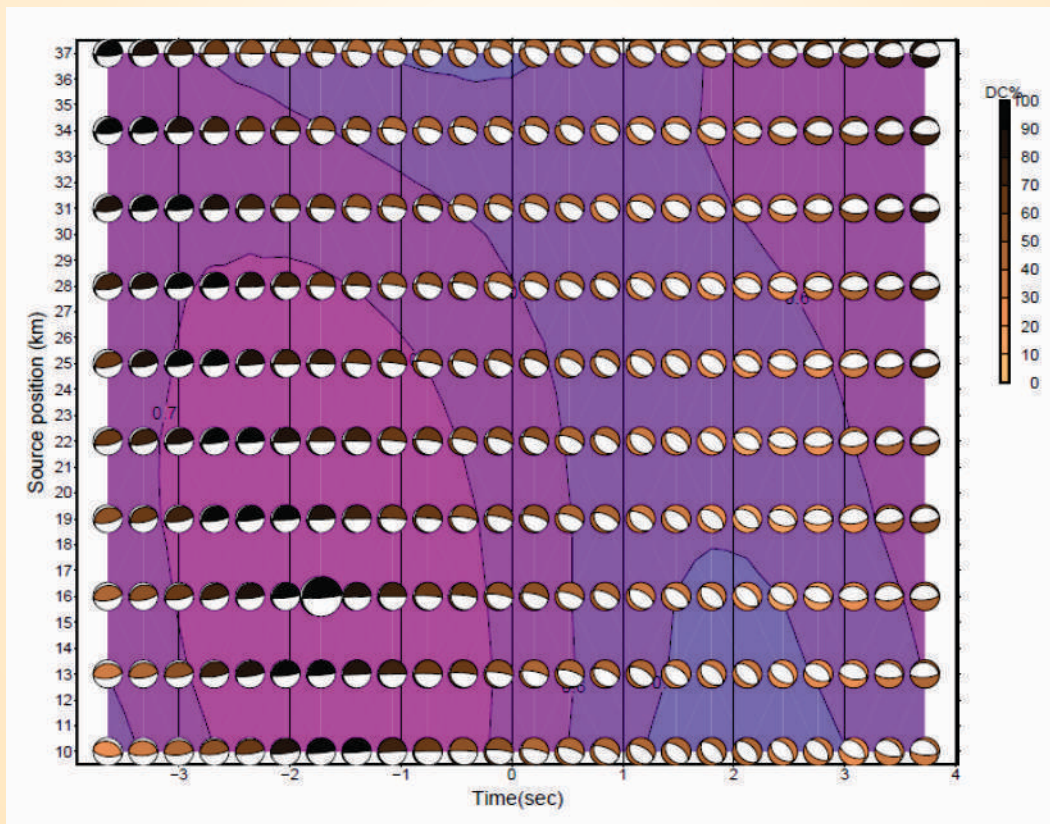


Fig. 24: Source position vs time shift correlation plot for event shown in figure 23. The largest correlation was obtained for source depth 16 km and the time shift was -0.18. The preferred solution with a 90% DC percentage is depicted by a larger beach ball with black colour.

correlation variation in figure 24. The bigger beachball shows the final solution corresponding to the focal depth of 16 km with a time shift of -0.18 s in the origin time. The best fit solution of the inversion provides two sets of strike (Φ), dip (δ), and rake (λ) values i.e. $\Phi=208^\circ$, $\delta=12^\circ$ and $\lambda=33^\circ$ for nodal plane-I and $\Phi=85^\circ$, $\delta=83^\circ$ and $\lambda=100^\circ$ for nodal plane-II (Fig. 23b). Based on the knowledge of local geology and tectonics of the region, the NE-SW trending nodal plane-I is considered as the inferred fault plane of the earthquake. This inferred fault plane can be correlated with the MCT with a low dip angle near the Mechuka region. The other nodal plane presents a high dip angle ($\delta=83^\circ$) and does not follow the local geological structure.

For a comprehensive study of seismotectonics of the study area, we considered the available data of International Seismological Center (ISC) and Global Centroid Moment Tensor (GCMT) solutions for 11 earthquakes of $M \geq 4.8$ in the study region and presented in figure 25. The FMS data show mostly thrust fault and thrust fault with the strike-slip component (an oblique mechanism). The FMS nos. 11, 8, and 5 lie on the western limb of Siang Antiform, and the inferred fault planes (NE-SW trending) follow the strike of the MCT with a low dip angle. Event no. 8 is close to the Mechuka earthquake and shows a similar mechanism (Fig. 25). The FMS with serial numbers 10, 4, and 1 are at the syntaxial bend of the Namcha Barwa. Event 10 and 4 shows pure thrust and thrust with strike-slip component whereas event 1 shows normal faulting with a minor strike-slip component. The FMS 6 and 7 are showing strike-slip solutions, whose NW-SE trending nodal plane follows the strike of the Jiali fault zone. The FMS no. 3 is correlatable with the eastern part of the Namche Barwa syntaxis bend. The FMS 9 is of pure thrust faulting nature following the strike of the eastern limb of Siang Antiform, with a dip towards NE. The fault plane no. 2 is a strike-slip type faulting which shows its association with the trend of Lohit thrust fault which is trending in the NW-SE direction. The depth distribution of the earthquakes has been observed along the EF section. A clear trend of depth distribution is observed. Seismicity is deeper in the Siang window compared to the Namche Barwa region and the region to its south. The pressure axis (P-axis) orientations of 11 earthquakes (Fig. 25) show the north-east trend suggesting the direction of maximum compressive force owing to the India-Asia collision in this part of the Himalaya.

Seismotectonic and stress pattern of Chandigarh-Ambala (CHD-AMB) ridge region

Digital waveform data are collected from the broadband

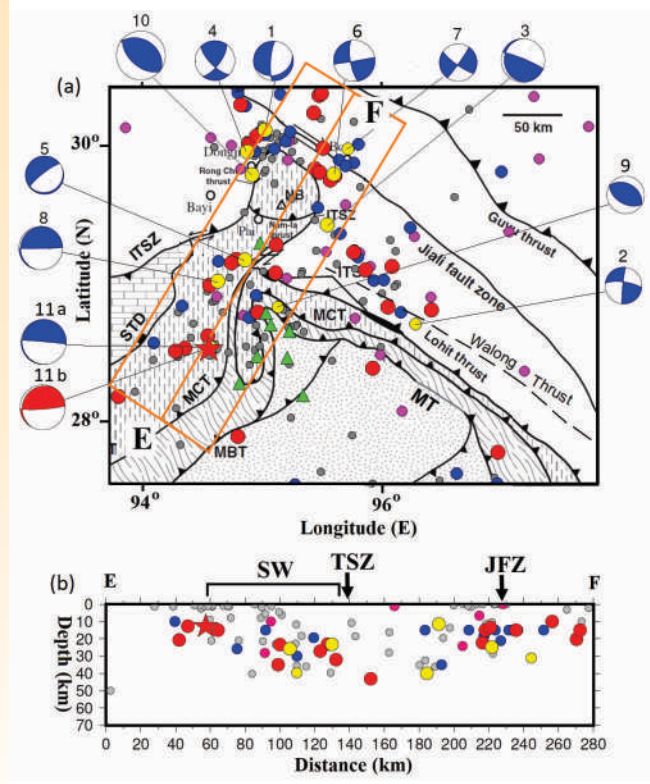


Fig. 25: (a) Seismicity of the study region with 11 fault plane solutions. (b) Seismic cross-sections along E-F, across the study region. The earthquakes of $M < 4.0$ are recorded by the local seismological stations whereas earthquakes with $M > 4.0$ are obtained from the ISC-EHB catalog. The tectonic features MBT: Main Boundary Thrust, MCT: Main Central Thrust, STD: South Tibetan Detachment, and ITSZ: Indus-Tsangpo Suture Zone are marked in the map as well as in the depth sections. SW=Siang Window, TSZ = Tidding Suture Zone, JFZ = Jiali Fault Zone.

seismic (BBS) network of the CHD-AMB region for the period November 2019 to February 2021. Local and regional earthquake events are extracted from the continuous record for the period 2019 to 2020 and are compiled with the events of other BBS networks existing in this region of northwest Himalaya to obtain precise hypocentral parameters. The FMSs are determined for local events with magnitudes ≥ 3.0 using P-wave first motion polarity as well as waveform inversion (ISOLA). Most of the earthquakes of this network are aligned along the north-south trending Mahendragarh-Dehradun fault, the FPS of the events determined along this fault is showing the strike-slip type of faulting with a small amount of thrust component. One of the nodal planes (NP-I) is trending in NNE-SSW directions. A felt earthquake of magnitude

~4.1 occurred in and around the Hardwar region on 1st December 2020 at 09 hrs 41min. The waveform record of this event was extracted from the continuous records of the CHD-AMB network (WIHG) and three BBS stations of the Indian Institute of Remote Sensing, Dehradun (IIRS-DDN) in and around the epicentral area to get better azimuthal coverage. The preliminary hypocentral parameters of the event are as: Lat:30.078°N, Long: 77.909°E, Depth: 45 km and the Magnitude is 4.1.

Activity: 3

Biotic and abiotic investigations of Cenozoic successions of NW and NE Himalaya with reference to paleo-environment, global bio-events, and paleoclimate reconstructions

(R.K. Sehgal, Kapesa Lokho and Suman Lata Srivastava)

In the north-western Himalaya belt, a new micro-fossil assemblage was identified from the Lower Siwalik (middle Miocene) succession of the Ramnagar area, (Jammu and Kashmir). The assemblage was recovered through bulk screen wash of nearly 300 kg. of the sediments through maceration. The new fossil discovery is very significant as it represents fossil tree shrews and hedgehogs which are very poorly known from the Siwaliks. These micro-mammals were tentatively identified as belonging to *Tupaia* sp. and *Galerix rutlandae*. *Tupaia* sp. from the present locality now represents the oldest record of fossil tupaiids in the Siwaliks and extends their time range in the region by ~2.5-4 million years. Furthermore, the occurrence of *Galerix rutlandae* is the first erinaceid documented from the Indian Siwaliks. The biogeographic presence of *Galerix rutlandae* across India, Pakistan, and Thailand may also indicate similar climatic affinities during the middle Miocene. Besides *Tupaia* sp. and *Galerix rutlandae*, rodents such as *Democricetodon kohatensis*, *Kanisamys indicus*, *Sayimys sivalensis*, and *Antemus chinjiensis* from Dehari and Tarmin Peak localities, lying in the vicinity of Ramnagar, can be used to provide an age estimate for Ramnagar equivalent to the Chinji Formation in Pakistan.

Fossil ruminants (Mammalia) were recovered from the Cenozoic Ladakh Molasse Group in the past field works. These fossils were attributed to *Nalameryx savagei*. A phylogenetic study of the *Nalameryx* was attempted in collaboration with researchers from Panjab University, Chandigarh. It was observed that the newly identified materials of *Nalameryx* confirm previously observed morphological features allowing to test the phylogenetical position of this genus within a cladistics

analysis oriented on Paleogene ruminants. Isotopic analyses highlight the complex ecology of the small ruminants in the context of the Himalayan orogeny. These results are the first quantitative paleoecological study directly observed on an Asiatic Paleogene ruminant.

To reconstruct the paleoenvironment of a part of the Siwalik section exposed along the Katilu Khad, Dunera area in Pathankot District of Punjab, sampling of nodules from the paleosol was carried out. Of the nearly 2000 m thick section, sampling from basal 400 m was done in February 2021 (Fig. 26). The samples were treated for laboratory analysis. Well preserved ichnofossils were also encountered from several beds in the succession. Two horizons showing micro-fossil potential were also identified and bulk samples for screen wash (nearly 400 kg) were collected in the field. The presence of significant micro-fossils was noticed in these samples and the identification of the fossils is in progress.

A broad review of the biostratigraphic analysis of the mammalian fauna from the Siwalik Group of the Indian subcontinent was attempted. It was noticed that lithology in the several sections of Siwaliks, in the Indian part, is time transgressive and the faunal contacts are also transitional. A revision of the micro-mammals, particularly rodents was undertaken and recent findings of Primates were synthesized. Upgradation of the faunal lists for the different formations of the Siwalik Group



Fig. 26. Field photograph: A sampling of nodules from paleosols in the Siwalik succession was exposed in KatiluKhad, Dunera, Pathankot.

was carried out. It was also noticed that the Siwalik foreland basin extends further south, as Siwalik age fossils are now reported from several localities lying south of Himalaya, such as Sulaiman and Marwat

ranges, and Bugti Basin of Pakistan, Irrawady valley, Myanmar, and some localities lying in peninsular India, including Kutch and Perim Island, western India and Baripada Beds in Odisha.

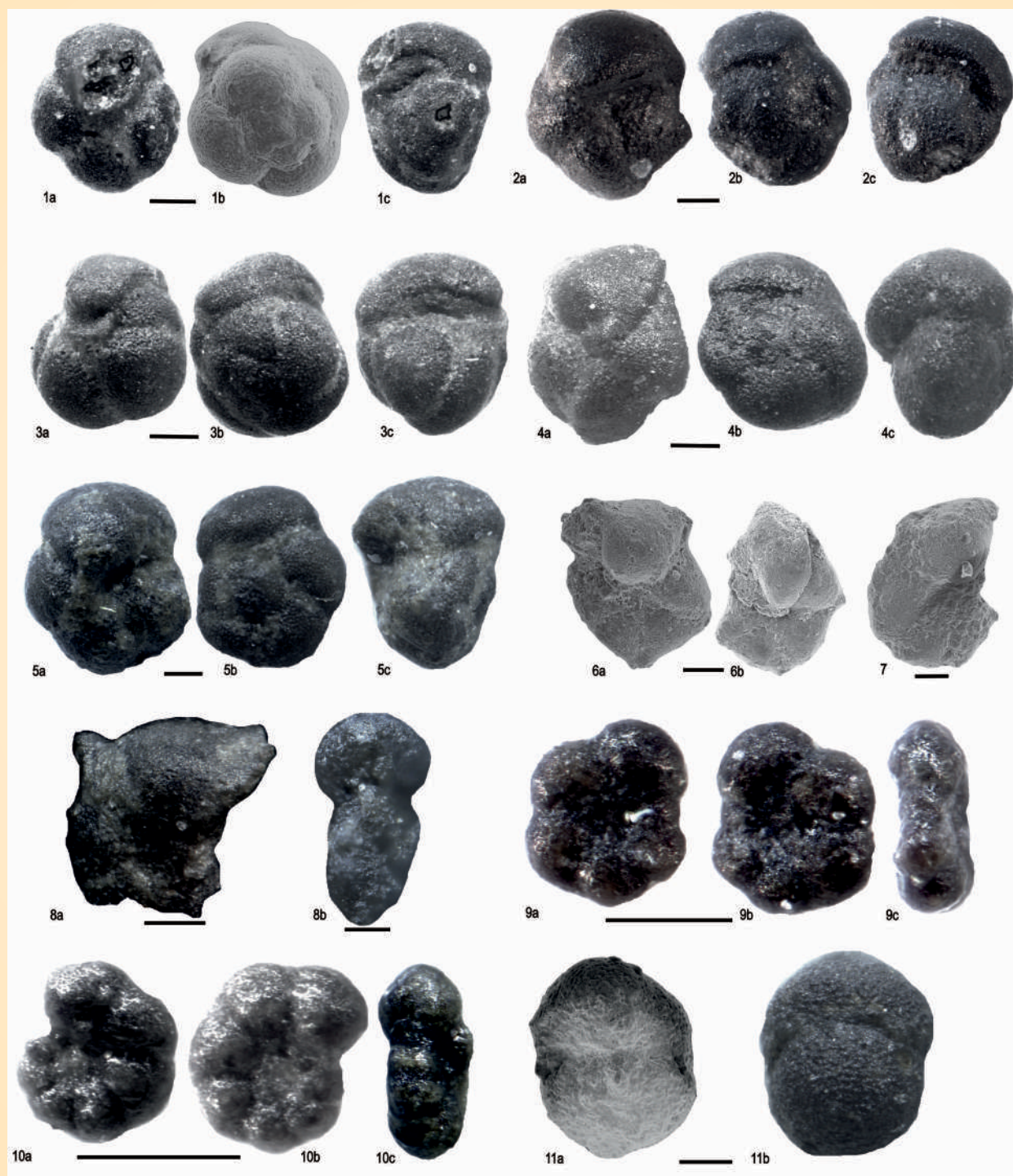


Fig. 27. 1(a-c) *Turborotaliacerroazulensis*; 2(a-c) *T. increbescens*; 3(a-c) *T. pomeroli*; 4(a-c) *T. cocoaensis*; 5(a-c) *T. ampliapertura*; 6(a-b) *Hantkeninananggulanensis*; 7. *H. primitive*; 8(a-b) *H. alabamensis*; 9(a-c) *Pseudohastigerinamicra*; 10(a-c) *P. naguwichiensis*; 11(a-b) *Globigerinathekatorialis*. Scale bar = 100 μ m. (Lokho et al., 2020).

Further in the North-eastern part of India, the study of Paleogene and Neogene fossil investigations from the Indo-Myanmar Range and Mikir Hills of Assam were carried out, for their biostratigraphic significance, and paleoenvironment and tectonic implications. The Naga Hills are NNE-SSW trending, westward over-folded set of mountains that form the northern-most segment of the IMR. The eastern syntaxis of the Himalayan belt marks a sharp turn in the trend of regional structures around Namche Barwa into Arunachal Pradesh and the Naga thrust belt. Structures continue southward into the IMR and further south into the Andaman-Sumatra subduction zone of the Java Trench where it transitions from continental collision to oceanic subduction. The IMR is juxtaposed to the west

against the Shillong-Mikir massif, which represents the NE extension of the Indian shield. The Disang Group incorporates the oldest Cenozoic clastic sedimentary rocks that crop out in a series of NNE-SSW trending ridges and valleys throughout much of the Naga Hills. The stratigraphic position of this unit is not well constrained due to a paucity of definitively recognizable, *in situ* fossils. The Formation is disrupted by west-vergent thrusts that have developed as the India-Myanmar collision progresses with the uplift of the IMR. The timing of deposition of the Disang Group is not fully understood, and its internal stratigraphic succession has not been well defined. The stratigraphic subdivisions amongst the sedimentary facies within the Cenozoic sequences in the region are based almost

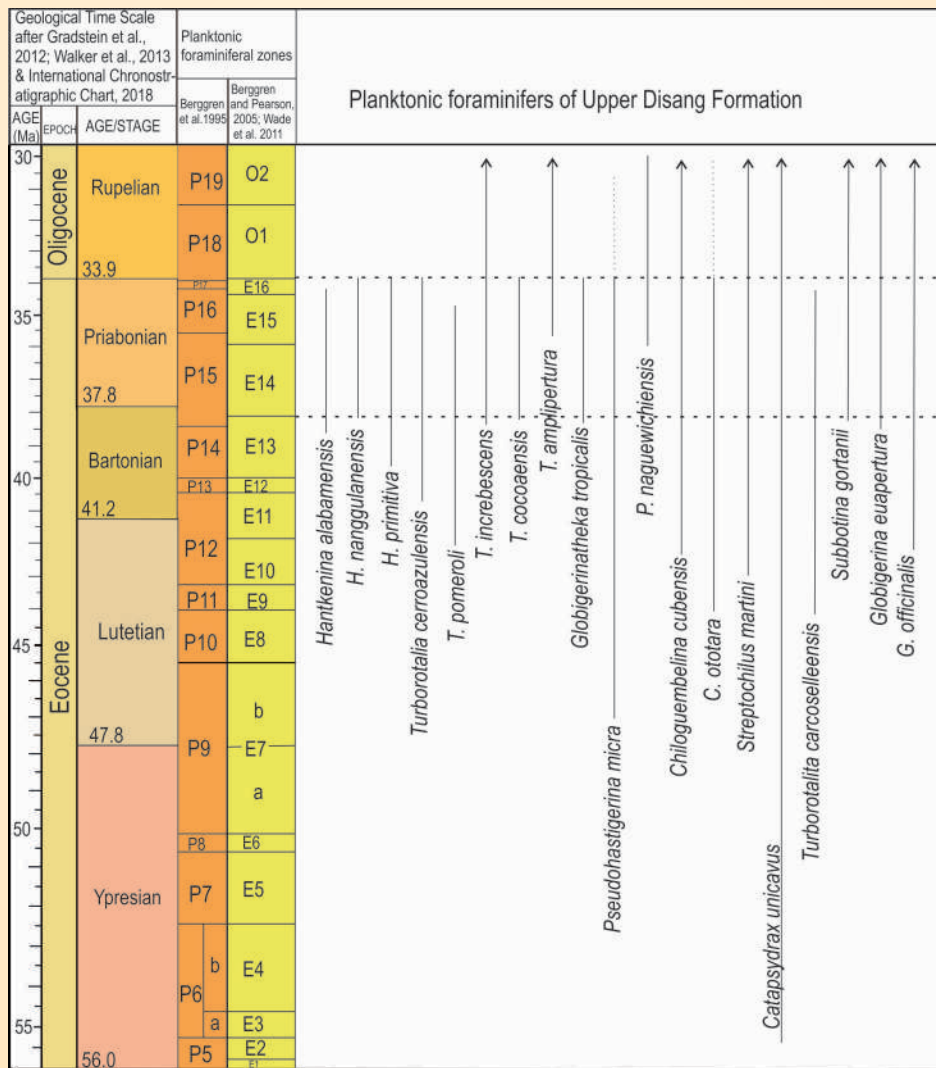


Fig. 28. Planktonic foraminiferal range chart based on Berggren et al. (1995), Pearson et al., 2006 and Wade et al. (2011). The Geologic Time Scale by Gradstein et al. (2008; 2012), Walker et al. (2013), and the International Chronostratigraphic Chart 2018 by Cohen et al., (2003, updated) for the UDF of Manipur.

entirely on the lithological comparison, with little paleontological control. Previous workers have regarded the Disang Group as either sparsely fossiliferous or barren. Although a study of the geology of this region started more than a century ago, still many basic questions remain unanswered. Difference of opinion exists in respect of the depositional environment of the Disang sediments from a shallow marine deltaic setting to a deep, rapidly deepening basinal setting different to that of coeval shelfal sediments of the Sylhet and Kopilli. The age of the Upper Disang Formation is ambiguous as different ages have been inferred by various workers based on sporadic occurrences of fossils across the region. Considerable diligence and perseverance are required to locate fossiliferous localities as the region is highly tectonised, structurally disrupted, and commonly covered with thick vegetation. This work was undertaken to make a detailed study of the Eocene foraminifers from the Upper Disang Formation in the Naga Hills of Manipur in order to infer its biostratigraphic age and examine its paleoenvironmental significance within the Neo-Tethyan realm in the Indo-Myanmar orogenic zone. Forty-four species attributable to twenty-eight genera are reported. Based on the new reported foraminiferal assemblages (Fig. 27), a refinement in age and paleoenvironmental interpretations for the Upper Disang Formation was carried out. We recognize Planktonic Foraminiferal Zones E14-16 correlative to upper-middle Eocene to upper Eocene (Fig. 28) in the

Upper Disang Formation within the Naga Hills. A basin model (Fig. 29) for this lithological unit involving an upper bathyal bathymetry, rapidly shallowing in a restricted basin with slump deposits where anoxic conditions prevailed is proposed based on field observations, foraminiferal assemblages, and published data.

The Mikir Hills in Assam and the Shillong Plateau in Meghalaya constitute the northeastern extension of the Precambrian Shield of the Indian peninsula in northeast India. The Mikir Hills lie in the East Karbi Anglong district of Assam and are separated from the Shillong Plateau by the NW-SE trending Kopili Fault. Larger foraminiferal studies integrated with lithofacies and stable carbon isotope analyses are carried out in the Sylhet Limestone of Karbi Anglong District, Assam to delineate foraminiferal biostratigraphy, depositional history, and paleogeography of the Sylhet Limestone of the Mikir Hills of Assam, NE India on implications for an open Tethys.

Another important component of Activity 3 is to understand the impact of climate variability on cultural changes in the Indian subcontinent. To achieve the desired results, a high-resolution centennial to millennial-scale middle Holocene Indian summer monsoon (ISM) variability was reconstructed from Bednikund Lake, located in an alpine meadow of the Pindar basin, Central Himalaya. Increased ISM precipitations were found during ~5930-3950 (mid-Holocene climate optimum), ~3380-2830 (Minoan Warm Period), ~2610-1860 (Roman Warm Period), ~1050-760 (Medieval Climate Anomaly), and ~320 calyr BP to Present (Current Warm Period). The decreased ISM strengths were found during ~3950-3380, ~2830 e2610, ~1860e1050 (Dark Ages Cold Period), ~760-580, and ~500-320 calyr BP (Little Ice Age). The covariance between our records of precipitation change and total solar irradiance for the middle to late Holocene and with Northern hemisphere (NH) temperature for the past two millennia suggested solar insolation as a primary forcing mechanism of ISM variability. The reconstructed paleoclimate combined with archaeology and historical records indicated that ancient Indian civilizations e.g., the Indus Valley (~5200-3300 calyr BP) and Vedic (~3400-2400 calyr BP) had established and thrived during periods of strengthened ISM precipitation, whereas their collapse closely corresponded to the decreased strength in ISM. From ~2400 to 200 calyr BP, the Indian subcontinent witnessed the rise and fall of various Kingdoms/dynasties. This period saw an exponential

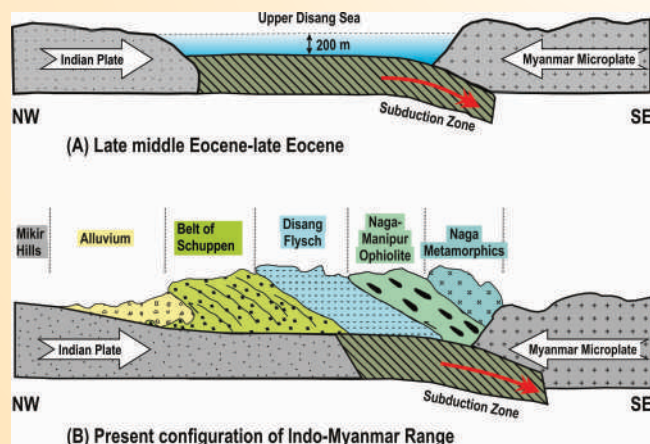


Fig. 29. (A) Model of the paleo bathymetry and tectonic setting of Upper Disang Sea during the late middle Eocene-late Eocene in the Naga Hills of Manipur. (B) Schematic cross-section of the present configuration of the Indo-Myanmar Range (Adapted from Mitchell et al., 1981; Bhattacharjee, 1991).

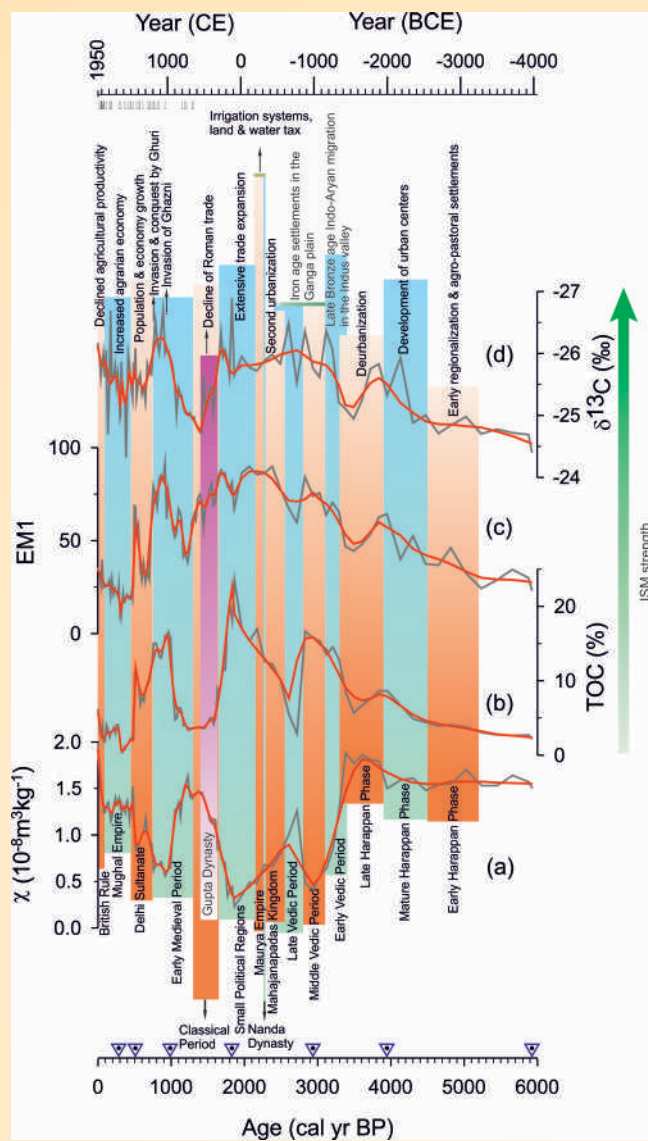


Fig. 30. Climate and cultural relationship over the past ~6000 years in the Indian subcontinent. The small triangles at the top side of the figure mark historical records of droughts and famines. (Rawat et al., 2021, QSR).

expansion/growth in agriculture, economy, population, languages, architecture, and religions in the Indian subcontinent. The agrarian-based economy showed little or no impact of monsoon weakening after ~2400 calyr BP possibly due to development and reforms in administrative policies, construction of irrigation systems such as dams, lakes, and canals, use of technology for irrigation such as waterwheel, knowledge of double cropping, production of cash crops. The ancient civilizations of India were directly impacted by the strengthening and weakening of ISM, whereas for the later periods, civilizations were able to adapt to climate change (Fig. 30).

Activity: 4A

Climate variability and landscape responses in the selected transects in the NE and NW Himalaya

(Pradeep Srivastava, Anil Kumar, Som Dutt, Pinkey Bisht, Chhavi Pandey, Suresh, N., Subhojit Saha, and P.S. Negi)

Flood records from Ladakh

Catastrophic flood records in the upper Indus catchment in Ladakh were studied using slack water deposits (SWDs) preserved along the Indus and Zaskar Rivers. SWDs are composed of stacks of sand-silt couplets deposited rapidly during large flooding events in areas where a sharp reduction of flow velocity is caused by local geomorphic conditions. Each couplet represents a flood, the age of which is constrained using Optically Stimulated Luminescence for sand and AMS ^{14}C for charcoal specks from hearths. The hearth is characterized by the presence of red-baked sediment (Fig. 31), flaked stones are cobble size and charred. Hearths found in many of the flood sediment sections indicate previously undocumented cultural activities (presence of dung cake; Fig. 31) on the flood deposits of the Indus and Zaskar catchments of Ladakh. The results provide evidence of the presence of humans in the drier Himalaya throughout the past 15 ka. The study suggests the occurrence of large floods during phases of strengthened ISM when the monsoon penetrated arid Ladakh. Comparison with flood records of rivers draining other regions of the Himalayas and those influenced by the East Asian Summer Monsoon (EASM) indicates asynchronicity with the Western Himalaya that confirms the existing anti-phase relationship of the ISM-EASM occurred in the Holocene. Detrital zircon provenance analysis indicates that sediment transportation along the Zaskar River is more efficient than in the main Indus channel. Post LGM human migration, during warm and wet climatic conditions, into the arid upper Indus catchment is revealed from hearths found within the SWDs (Sharma et al., *Bulletin*, accepted).

Sclerochronology of a deltaic sequence of Pangong Tso

Sedimentological, geomorphological, and paleo-biotic concentration investigation on eight selected sections from the periphery of the Pangong Tso was conducted to understand the fluctuations of lake levels as a function of climate variability in Ladakh Himalaya. Based on the sedimentological studies that include the lithology and sedimentary structures, two major facies were identified in the studied sections that are deltaic deposits and fluvial deposits. The deltaic sequences show the

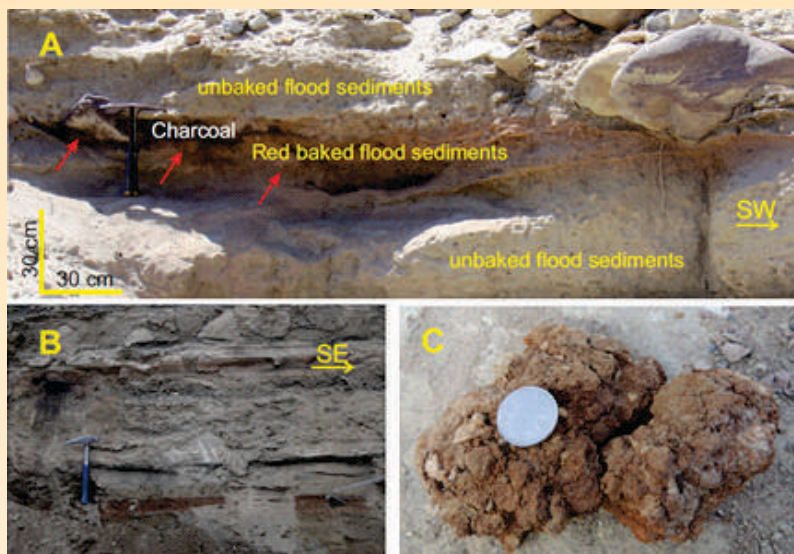


Fig. 31: (A). Hearth located in the SWDs lower Zaskar. (B). Hearth in an SWDs section located in the upper Zaskar. (C). Dung cake is found inside a hearth along the Indus River.

deposition of a wedge-shaped body of sediments, comprising of relatively flat-lying top-set, and long, steeply dipping forests, which prograde from the channel and lake interaction, and relatively thinner, flat-lying bottom-set. The mollusc shells collected from the different sections are recognized as the *Radix brevicauda*, *Radix lagotis*, *Valvatapiscinalis*, and *Gyraulus* species of freshwater origin gastropods. Fluvial facies is subdivided into two sub-facies (1) channelized and (2) non-channelized. The channelized facies are characterized by rounded gravels and cross-bedded sand. However, the non-channelized facies have sub-angular gravels with erosional basal contact.

Based on the comprehensive investigation and stable isotopic studies, we identified four phases of climatic changes since the last 2ka. During ~1.8 ka lake level was relatively higher and the appearance of freshwater gastropod shells is observed which implies that the shell growth temperature and summer salinity was 9-10°C and 4 ppt, respectively which as compared to modern climate was warm and wetter. This is followed by a dry phase from 1.8 to 1.3 ka identified by the progradation of the deltaic lobes due to lake-level fall. A warm phase is marked by the appearance of freshwater gastropod shells by freshwater input to the lake and retrogradation of deltaic sequences during 1.3 to 1 ka. The lake water salinity was approx. 4 ppt at 1.3 ka was further diluted to 2 ppt and the shell growth temperature was quantified near about 10-12°C during this period. The 4th phase is identified as the rapid fall in the lake level in the last 1ka of approx. 8m which was also identified by Srivastava et al. (2020). Regionally this rapid dry period is identified all along the Tibetan

plateau. The present-day salinity of Pangong Tso is approx. 7.2±1.8 ppt" (Chaudhari et al., 2020), which gives evidence of rapid lake-level fell since 2ka in arrears to the high evaporation rate.

Landscape responses to tectonic of Ladakh Himalaya

Although the tectonic evolution of the southern Himalaya has been extensively studied, relatively few studies have focused on potential neo-tectonic activity in the most hinterland part of Himalaya, north of the region that separates the southern edge of the Tibetan plateau from the peaks of the Higher Himalayan Range. Here we use a combination of new structural and geomorphic field data, Optically Stimulated Luminescence (OSL) chronology, as well as previously published seismicity and denudation rate dataset, to suggest that the Trans-Himalaya within the region of the Indus Suture Zone (ISZ) is neo-tectonically active. Based on fault gouge, tilted paleolake deposits, and the chronology of deformed fluvial gravels constrained by OSL dating, the present study provides evidence for the tectonic activity along the ISZ between 78 and 58 ka.

It is envisaged that the fault and fold systems in the Ladakh region such as the Upshi-Bazgo thrust originated due to (1) acceleration in the northward movement of the Indian plate relative to the Eurasian plate, and (2) post-collisional shortening parallel to plate convergence. On account of this, the Eocene to Miocene post-collisional sedimentary sequences, such as the Indus Molasse, rode over the now-extinct Ladakh Arc, as it acted as a rigid body, and formed a system of back thrusts, which are neo-tectonically active. (Kumar et al., 2020C, *Tectonophysics*).

Climate variability as recorded in a speleothem

- i) A speleothem record from the Mawmluh cave, northeast India indicate moderate Indian summer monsoon (ISM) conditions prevailed during ~212 BCE to 400 CE punctuated with weak intervals, strong ISM during 400 & 500 CE, and from 640 to 1060 CE, whereas weak ISM conditions prevailed during 520-540 CE, 820-850 CE and 940-980 CE and after 1060 CE. Rainfall reduced substantially in the 2nd millennium CE than that of the 1st millennium showing a centennial-scale North Atlantic forcing. (Dutt et al., 2021a; Fig 32).
- ii) A review study shows distinct Spatio-temporal variability in ISM precipitation during Northgrippian to Meghalayan transition. A dry phase lasting ~1000 yrs was observed ~4.2 ka BP in southern and

northwestern India whereas a 200-300 yrs event occurred in northeastern parts. (Dutt et al., 2021b).

- iii) Around 750 sub-samples of speleothem carbonates have been analyzed for oxygen and carbon isotopes analysis. 320 sub-samples were extracted from speleothems using a hand-held drill. Eight speleothems are sent for the U-Th dating at the University of Heidelberg. Speleothem petrography work is under progress for reconstructing more robust paleoclimate records suggesting the regional hydrological conditions.
- iv) Collaborative work on a speleothem from the Umsyrng cave, Meghalaya shows wet conditions in northeastern India between ~ 15.4 and 12.9 kyr BP, and ~ 11.3 to 10.1 kyr BP, punctuated by a dry phase between ~ 12.9 and 11.3 kyr BP including

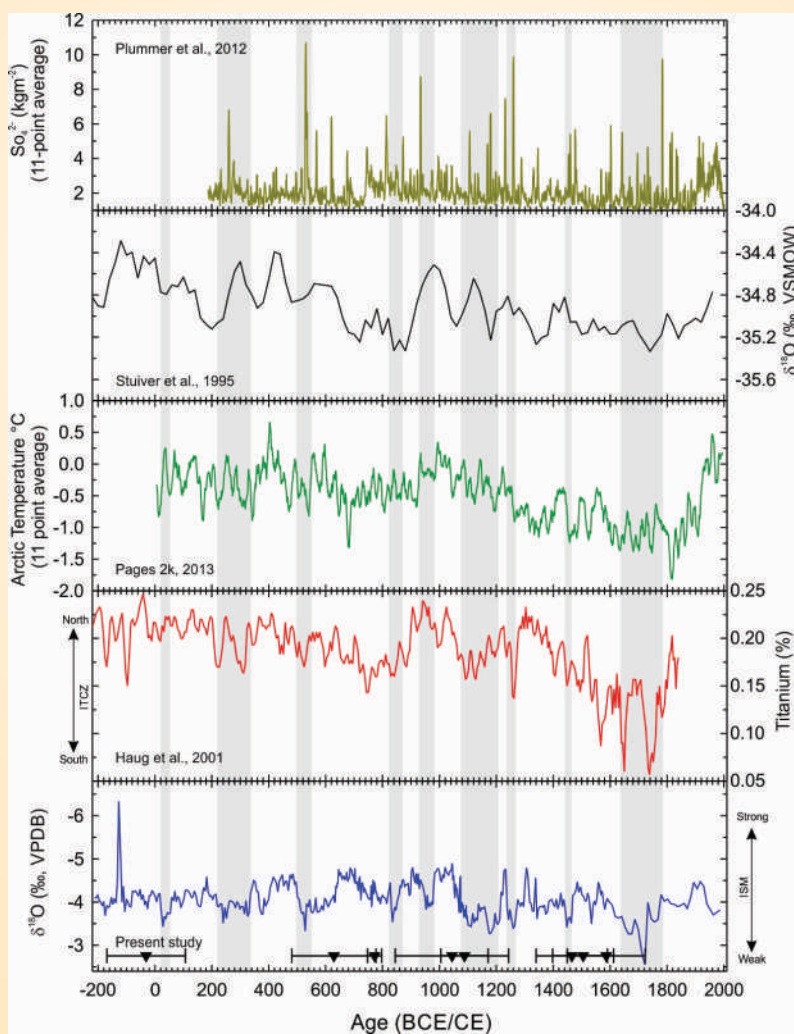


Fig. 32: $\delta^{18}\text{O}$ record of ISM variability from the Mawmluh cave (this study) for the interval 212 BCE to 1986 CE compared with Ti (%) record of ITCZ migration from ODP Site 1002, Cariaco Basin (Haug et al., 2001), Arctic temperature data, 11 points averaged (PAGES 2k, 2013), $\delta^{18}\text{O}$ record from Greenland Ice Sheet Project (GISP) (Stuiver et al., 1995), and Volcanic sulphur loading to the atmosphere, 11-point averaged (Plummer et al., 2012).

the Younger Dryas (YD) cold interval. A southward positioning of the Intertropical Convergence Zone in addition to weak Atlantic Meridional Overturning Circulation during the YD event suggested as a causative factor for weak Indian summer monsoon conditions during the YD.

Black Carbon aerosols, its Optical & Physico-Chemical Characterization

Six days of fieldwork have been carried out to conduct a ground survey besides a collection of black carbon (BC) data from observation stations located in Gangotri Glacier Valley. Five different locations of different microenvironments at different altitudes with different anthropogenic influences along 24 km long Gangotri Glacier Valley viz. Gangotri (~3200 m amsl), Chirbasa (~3600 m amsl), Bhojbasa (~3800 m amsl), Gaumukh (~4000 m amsl), and Tapovan (~4400 m amsl) (Fig. 33). After incorporating the previous year's random recording of equivalent black carbon (EBC) aerosols, the first multiyear (2015-2020) investigation from pristine localities along Gangotri Glacier Valley has been performed. For the estimation of the mass concentration of EBC aerosols in the ambient air, MicroAeth AE 51 monitor was used, which is based on the principle of optical attenuation method.

A relatively high concentration of EBC (up to $2.23 \pm 0.57 \mu\text{gm}^{-3}$) was recorded at Gangotri which is a famous Indian pilgrimage center and remains highly crowded during the peak tourist season i.e., May-June and Oct-Nov every year. Surprisingly, we also recorded high EBC (up to $1.27 \pm 0.57 \mu\text{gm}^{-3}$) at Tapovan, which is surrounded by high ice-snow peaks. HYSPLIT cluster trajectory and CALIPSO data images suggest

that besides local anthropogenic activities, polluted air mass-produced due to burning of forest and agriculture biomass and fossil fuels, etc. transported from Indo Gangetic Basin might be playing a potential role in ambient BC concentration in the study area.

To understand the relative change in EBC emissions during different stages of the Covid-19 lockdown period, real-time measurement of equivalent black carbon (EBC) measurements were performed in an urban area (WIHG campus) of Doon valley. The monthly average mass concentration for the study site is $2.21 \pm 1.41 \mu\text{gm}^{-3}$, $2.58 \pm 1.46 \mu\text{gm}^{-3}$, $2.74 \pm 1.49 \mu\text{gm}^{-3}$ and $2.12 \pm 1.32 \mu\text{gm}^{-3}$ for April, May, June, and July, respectively. The typical diurnal variations of surface EBC aerosols with prominent two peaks (one in the morning and another in the late evening) as well as a relatively flat pattern during noon for the month of April-July 2020 are depicted in figure 34. These critical patterns/phenomena are directly related to the boundary layer dynamics of the region. In general, morning EBC peak occurs mainly due to the combined effect of radiative cooling at the surface, low height of planetary boundary layer, and local level of EBC pollutant. During noon hours, boundary layer height increases (as air expands with surface heating by solar radiation intensity) which in turn results in proper mixing of pollutants.

To identify the elemental composition of ambient aerosol (from Doon Valley), the electron micrographs coupled with EDX-spectra were analyzed. C, O, Na, F, Al, Si, K, Ca, and Ti elements were also identified. The maximum contribution to particulate matter belonged to Carbon and Oxygen is more than 90 %. Contribution percentage of rest of the elements recorded in our sample are $\text{Si} > \text{Na} > \text{Ca} > \text{K} > \text{Al} > \text{Ti}$, respectively.

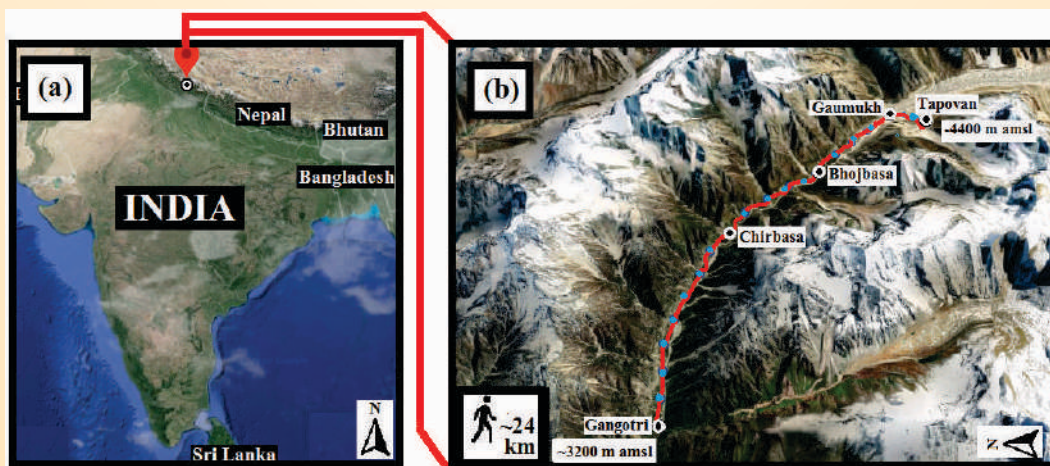


Fig. 33: (a) Location of the study site (Gangotri Glacier Valley) in south Asia. (b) Expedition site: Gangotri (site 1) - Chirbasa (site 2) - Bhojbasa (site 3) - Gaumukh (site 4) - Tapovan (site 4).

Lesser Himalayan Sedimentary Basin

Deoban and Mandhali Formations of the Tejam Group, Lesser Himalaya was examined to understand the depositional environment and basin dynamics. Deoban Formation is mainly carbonate-dominated, whereas the overlying Mandhali Formation is mixed carbonate-siliciclastic in origin. Based on detailed field and laboratory studies 'molar-tooth structures' (MTS) and 'hybrid event beds' (HEBs) have been identified and characterized from the Deoban and Mandhali Formations, respectively.

Molar-tooth Structures from Deoban Formation: Molar tooth structures (MTS) are microcrystalline calcite-filled randomly oriented fissures, cracks, voids, and globules that mostly occur in Proterozoic marine carbonates. On outcrop scale, these are generally deformed millimeter to centimeter thick ribbons and microscopic observations suggest these are internally composed of ~ 5 to 15 μm equant calcite crystals. Lack of any detrital infill, uniform crystal size, and gradational contact with host limestone indicate rapid calcite precipitation in fluid-filled cracks. Reworking of MT as intraclast, folding and offset of MT ribbons support for early formation before significant lithification. Moderate TOC (0.1 to 0.9) is possibly due to organic matter preservation under sub-oxic to slightly anoxic/ dysoxic conditions. Storm-generated bedforms indicate deposition in between fair weather- and storm wave bases in a sub-tidal setting. Average

1.4‰ depletion of $\delta^{13}\text{C}$ in MT relative to host limestone, presence of relict microbial lamina along the margin of the MT cracks, and storm-generated bed forms at outcrop scale indicates that the cracks might have formed by the combined effect of degassing of CO_2 generated during the microbial oxidation of organic matter and wave loading by storm. Precipitation of microcrystalline calcite within the cracks may have been triggered by alkalinity generated by the mixing of the outflowing CO_2 with seawater.

Hybrid event beds (HEBs) from Mandhali Formation

The classical 'Bouma sequence' seldom fails to explain the origin of co-occurring sediment gravity flow and transitional flow deposits within many turbidite systems. These types of deposits are variably mud rich, encountered in the marginal parts of the shallow to deep water systems, and variably named as slurry flows, cogenetic turbidite-debrite beds, linked debrite, matrix rich beds, and hybrid event beds. The ideal succession of HEBs reflects changes in flow rheology and comprises five major divisions (from base to top) i.e., H1 (massive clean sandstone; a product of high-density turbidity current), H2 (Banded Sandstone; deposited in transitional flow condition), H3 (debris flow), H4 (Sand-mud couplet; resulted from low-density turbidity current) and H5 (Mud; Suspension Fallout). Outcrop and petrographic studies from sediment gravity flow deposits of the Mandhali Formation, Lesser Himalaya

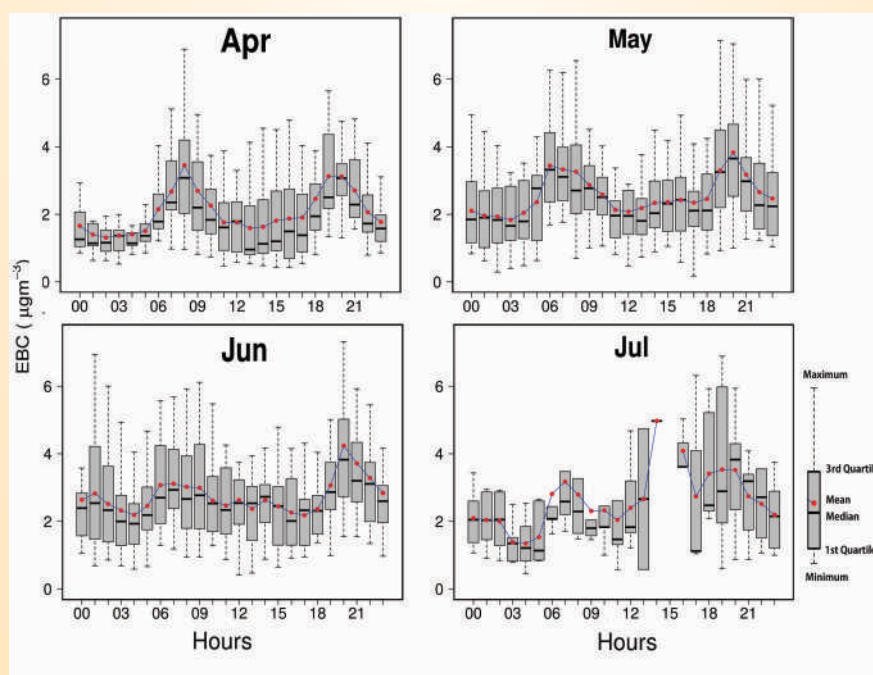


Fig. 34: Diurnal variation of EBC from WIHG campus during lockdown time April-July 2020.

identified that the H1, H3, H4, and H5 divisions are mostly preserved. However, H2 division is not preserved. The HEBs of the Mandhali Formation are the result of either run-out of a debris flow following partial transformation to a fore-running turbidity current or segregation of sand from suspension before the onset of cohesion and en-masse deposition of sands and clay.

Paleoglaciaticion and associated landforms

Garbyang lake, situated ~35 km downstream, is studied to understand the relation between paleo-glaciation and its formation. The lake extends up to Gunji from the Garbyang covering a distance of ~14 km (Heim and Gansser, 1939). The distal part of the Garbyanglake is situated in Gunji at an altitude of ~3200 m asl where the Yankti river joins the Kali river. In Gunji, four levels of terraces are present which may be related to the deglaciation history of the glaciers in the valley. Juyal et al. (2004) by dating top ~28 m lake sequences using OSL dating suggested that the Garbyang has evolved before the LGM and was formed by moraine damming the Kali River at Chiyalekh during MIS-3/4 glaciations (communicated to Quaternary Science Reviews).

Further extending this, 180 sediment samples at the 2 cm resolution from the top 3.6 m of the deltaic part of the lake present at Gunji were collected. Four OSL samples from the fine to medium sand layers of the lake and one OSL sample from each terrace were collected for chronology. All the samples are in process for different analysis like grain size, magnetic susceptibility, pollen analysis, oxygen isotope, and dating. The result of these analyses will provide a clear picture of the interaction between Garbyang lake, outwash terraces, and glaciation in the whole valley.

Activity: 4B

Ecology and climate dynamics of the Himalaya: Cenozoic to present

(Narendra Kumar Meena, Jayendra Singh, Sudipta Sarkar and Prakasam M.)

Climate variability and ecological linkage in the Himalayan region: a multi-archival and multi-proxy approach

A reconnaissance field trip was conducted in the Alaknanda river valley, Gangotri area (Bhagirathi valley), and the Chopta area (Rudraprayag). During this fieldwork, more than 200 samples were collected for paleoclimatic, fluvial geomorphological, and other studies. The higher altitude areas of the Himalayan

(Bugyals) and other meadows will be new sites to understand the variability of climate and its impact on sensitive biodiversity. The vis-à-vis relation of paleoclimatic variability with River valley and its fluvial system will be understood.

Successful bacterial culture from the 'moon milk water' of Sahastradhara Cave, Dehradun provides the first-ever clue of the bio-mediated calcium carbonate precipitation; the data will be significant to understand the cave ecology and also correction in speleothem based paleo-thermometry.

The quantification of the Biological Proxies, such as diatom, is the new area of science that will enable to qualify the climatic variation from various lacustrine and aquatic deposits. To quantify the climatic data, the living diatoms were cultured from various rivers such as Ganga (Rishikesh), Soung (Dehradun), and Roberts Cave (Dehradun). Various stress experiments have been done on the living diatoms to understand their lower and upper tolerance limits in various environments.

Sedimentary section: Stable isotope and elemental geochemistry signatures of the sedimentary rocks of the Middle Bhuban formation (Early Miocene-Middle Miocene siliciclastic sequence), NE Himalaya has been studied for the paleoclimate, weathering, source rock types, and depositional environment. The marine sequences, exposed along the road cuts at Dartlang area, Mizoram, north-east India were sampled. A total of 24 sandstone/shale samples were collected and analyzed for the stable isotope of $\delta^{13}\text{C}_{\text{org}}$.

Total Organic Carbon (TOC) and geochemical parameters such as major oxides, trace elements, and rare earth elements. We have used elemental data to calculate the Chemical Index of Alteration (CIA), Chemical Index of Weathering (CIW), Plagioclase Index of Alteration (PIA), and climate value (C-value). The $\delta^{13}\text{C}_{\text{org}}$ and TOC records reveal productivity variation during the Early Miocene-Middle Miocene, especially the $\delta^{13}\text{C}_{\text{org}}$ record shows carbon isotope negative excursions -26.39 ‰ (min -23.32 ‰). The CIA, CIW, PIA, and A-CN-K proxy records reveal that the source rock of the Middle Bhuban formation is a proficient felsic source and in moderate chemical weathering. The results of climate value (C-value) ranges from 0.69 to 1.06, suggesting the semi-moist to moist climatic conditions during the Early to Middle Miocene.

Sea sediment core: The Arabian Sea sediment core samples (~400) have been processed for geochemical analysis, which will be utilized for climate and

Himalayan weathering reconstruction during the Late Quaternary.

Paleolake/active lake sediments: Late-Quaternary paleoclimatic studies using multiproxy records from lacustrine archives have been initiated. The sedimentary diatom records of Renuka Lake and its link with recent global warming and climate change have been reported during the current year. The age-depth model and multiproxy data of the Chitkul (Baspa valley), Kotikanasar (Chakrata), and ITBP camp (Sangla) have also been generated. The diatom and other biological proxies are under analysis.

Samples have also been prepared and processed for diatom from the Rewalsar Lake, Lesser Himalaya. The analysis for siliceous microfossil diatoms is being performed. Samples from Rewalsar lake, H.P. were analyzed for major and trace elements using XRF. The geochemical data reveals the last 2000 years' climatic and cultural variations.

Dendrochronology: Tree ring-width chronology (1656-2015 CE) of Himalayan fir (*Abies pindrow*) was developed from Din Gad valley, Dokriani glacier region, Uttarkashi, Uttarakhand. Tree growth-climate relationship revealed that *A. pindrow* in the region is adversely affected by high-temperature conditions, whereas cool and wet conditions are ideal for its growth. Further, reconstructed 231 years long (1785-2015 CE) temperature (Oct-June and March-June) record for Din Gad valley, Uttarkashi, Uttarakhand using *A. pindrow* ring-width chronology. Reconstructed temperature series captured coherency with other tree-ring-based temperature reconstructions from the western Himalaya, central Himalaya, and the Tibetan plateau, indicating the relevance of the reconstruction in understanding climate variability at a regional scale. The reconstruction also captured a linkage with the Dokriani glacier winter mass balance (November-April) which provides a valuable database to delineate periods of mass loss and mass gain with respect to temperature in the past 231 years.

Activity: 5

Geological and Geomorphic controls on Landslide for risk assessment and zonation in the Himalaya

(Vikram Gupta, K. Luirei and Swapnamita C. Vaideswaran)

Himalayan Landslide Risk Assessment and Zonation map

Landslide is a dynamic system and due to changes in either natural or anthropogenic factors or both, the

incidences of landslides in a particular area increase. It has been noted that ~400 causalities occur in the Himalayan region every year due to these phenomena. Further, the frequency and magnitude of the landslides increase every year, particularly in the hilly townships, mainly because there is a lot of developmental activities in the region. This demands the large-scale landslide hazard, and risk assessment of the region be carried out. During the reporting year, our study mainly focused on the states of Himachal Pradesh and Uttarakhand, and a hazard zonation map of the Mussoorie township and the surroundings has been prepared (Fig. 35). These are briefly described hereunder:-

Landslide Hazard Zonation in the Mussoorie township and its surroundings (Uttarakhand)

Mussoorie township and its surrounding areas located in the Lesser Himalaya experience frequent landslides in the monsoon season. It is therefore important to understand the landslide hazards in the area and to divide the area into different landslide hazard potential zones. This will help to do planning for further development in the area. In view of this, landslide susceptibility mapping (LSM) of the area between longitude 77°59'59"E and 78°07'46"E and latitude 30°25'58" N and 30°29'08" N has been carried out (Fig. 35). It covers an area of ~ 85 km² and is located in the Survey of India 1:50,000-scale toposheet no. 53J/3. The study area has several ridges with elevations varying between 900m and 2290m above mean sea level (msl). The Mussoorie hill trends east-west and is the water divide between the Yamuna basin and Ganga basin. The maximum elevation of the study area is at Lal Tibba point with an elevation of 2290 m above msl. Aglar river, a tributary of the Yamuna river, flows west and has an elevation of ~ 800 m. The study area falls in zone IV of the seismic zonation map of India. There are many methods for the LSM, but in the present work bivariate statistical Yule Coefficient (YC) method has been chosen to utilize GIS and high-resolution satellite imageries. In this method, the binary association between landslides and their various possible causative factors like lithology, land use-landcover (LULC), slope, aspect, curvature, elevation, road-cut, drainage, and lineament were calculated.

A total of 56 landslides have been delineated in the area, 54 landslides have been classified as planner debris slides, and 2 as rock-cum-debris slides. These landslides are active mostly during the rainy season and their dimensions increase every year. Further, about 80% of landslides have > 100m² aerial coverage and are

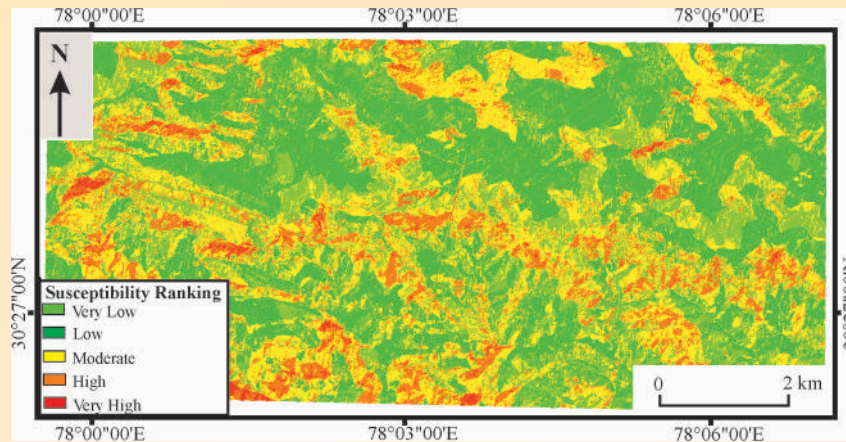


Fig. 35: Landslide susceptibility map of the Mussoorie and its surrounding region.

shallow. 40 landslides were randomly selected for the preparation of the LSM and the remaining 16 were used for the validation of the map. The results indicate that ~44% of the study area falls under very high, high, and moderate landslide susceptible zones and ~56% in the low and very low landslide susceptible zones. The dominant part of the area falling under high and moderate landslide hazard zones lies in the area covered by highly fractured Krol limestone exhibiting slopes ranging between 65° and 77° .

To assess the accuracy of the prepared landslide susceptibility map, validation of the map was carried out using the success rate curve (SRC) and the prediction rate curve (PRC). Both these curves have been drawn using the cumulative percentage of the study area and the cumulative percentage of landslides, and indicate the accuracy and the predictive value of the landslide susceptibility map (LSM), respectively. The AUC value of the prediction rate curve for the model was found to be 0.70 indicating good agreement between the LSM and the occurrences of landslides.

Engineering geological studies along the Mansa Devi hill-bypass (MDHB) Road, Haridwar, Uttarakhand

Engineering geological studies, including geotechnical and ground penetration radar (GPR) surveys, were carried out along the Mansa Devi hill bypass (MDHB) road between longitude $78^{\circ}10'9.6''E$ & $78^{\circ}10'4.7''E$ and latitude $29^{\circ}58'17.1''N$ & $29^{\circ}57'32.5''N$, located in the Haridwar township, Uttarakhand. The aim was to assess the slope instability conditions along the road that was built in 1958 to negotiate the overwhelming traffic in the township. The road was completely closed after 1998 due to increasing landslide activity in the area. Several frequent small-scale landslides and rock fall activities

are reported along MDHB road almost every year during monsoons.

Detailed geological mapping depicts that the area is composed of mudstone and sandstone with thick overburden constituting sandy soil. The geotechnical tests in the laboratory reveal low geo-mechanical strength and high permeability of the material constituting the slope. The laboratory tests on sandstone reveal that fresh sandstone exhibits an exceptionally higher value of unconfined compressive strength (>100 MPa) than the weathered sandstone (< 35 MPa). The mudstone is non-durable and contains a considerable amount of expanded clay minerals which has a tendency to expand in the presence of water. It can weather easily and facilitate instability at shallow depth. A ground-penetrating radar (GPR) survey confirmed that the road is unstable particularly on those spots where the road either lying over mudstone beds or over thick non-cohesive sandy soil.

Seven unstable zones along the entire MDHB road were identified which are prone to landslides. To assess the subsurface conditions of the slope below the MDHB road, a GPR survey at five different locations has been carried out using the GPR fieldfox unit having a frequency range between 2MHz and 100 GHz. The profile at location 1 deciphers the presence of a subsurface water channel (Fig. 36: GPR-2). The road is constructed on loose soil and hard rock is not visible up to a depth of 12 m (Fig. 36: GPR-1). The soil is moist and therefore signal below 6 m depth attenuates. The profiling at location 2 indicates that the road is constructed over sandy soil, and there is high attenuation of radar waves. The profiling at location 3 indicates pebble-rich soil deposits along a high angle channel connected to the road (Fig. 36: GPR-3). The rest part of the road is constructed over sandstone (Fig.

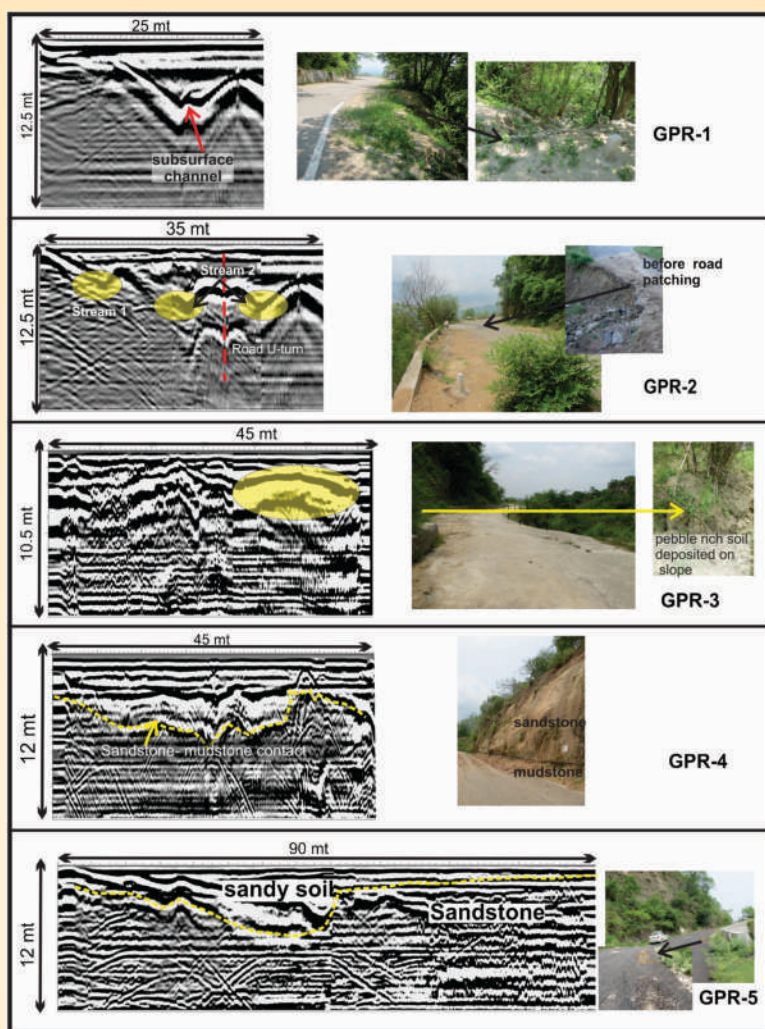


Fig. 36: GPR profiling at various locations along the MDHB road.

36: GPR-4) and hence the area seems stable. The profile at location 4 depicts that the road is constructed on mudstone beds whose thickness varies from 3-4 m. Sandstone is present beneath the mudstone. GPR profile at location 5 depicts that the road is constructed over the hard sandstone and only a small portion of the road is located over unconsolidated material i.e. sandy soil (Fig. 36: GPR-5).

Summing up, it has been concluded that the (i) the instability in this area is mainly caused by the alternate layering of competent sandstone and incompetent mudstone (ii) The mudstones consist of a considerable proportion of smectite minerals which has the property to expand-shrink with the water activity and hence deteriorate rapidly during monsoons. (iii) A part of the MDHB road was constructed over mudstone and thus unstable during monsoon because of mudflow activities although shallow in nature. (iv) The rest part of the MDHB road was constructed over sandy soil which

causes instability as it is non-cohesive, has higher permeability, and higher water filtration rate. (v) Heavy retaining walls have been constructed over non-cohesive sandy soil without proper placement procedure. Therefore in absence of proper surface and subsurface drainage, ingress of water into underlying sandy soil has resulted in instability.

Landslide studies in the Yamuna valley, Garhwal Himalaya: Litho-tectonic and precipitation implications

In this study, analyses of the relation between geomorphic indices, lithology, and structure of 57 active landslides have been done along a stretch of 75 km following the Yamuna River between 78°01'01"E - 78°26'46"E longitudes and 30°38'54"N-30°59'59"N latitudes. A quantitative analysis of the stream profile to determine the tectonic regime of the region was resorted to, from the various geomorphic indices such as stream

length gradient, topographic swath profile, channel steepness index, and the ratio of valley floor width to valley height.

Analysis of the longitudinal profile helped in identifying knick points along the river channel, which was further substantiated by the stream length gradient index. The high stream length gradient index values coincide with knick points and lithologic boundaries. The topographic swath profile helped in understanding the overall relief pattern such as the transition zone from Lesser Himalaya to Higher Himalaya, as indicated by the abrupt increase in relief. However, this relation is mainly justifiable in the Higher Himalaya Crystallines rather than in the Lesser Himalaya, which seem quite faint. A high stream length gradient index value of 1425m in the Wazri region, where the Main Central Thrust passes, is indicative of certain activity in its domain. To verify the channel response to the tectonics of the region, indices such as the ratio of valley floor width to valley height and steepness index were used. The low valley height values, reflecting the down-cutting of the V-shaped valleys in response to active uplift, corresponding with the high steepness index (high uplift) signifies active tectonics in the Higher Himalaya.

A total of 57 landslides are observed in the study area, of which 33 are classified as debris slides and 24 as rockfalls. Along a stretch of 16 km in the Higher Himalaya (HH), 25 landslides are observed, while 32 landslides are noted along a length of 59 km in the Lesser Himalaya. The spatial distribution of landslides was correlated with lithology and various geomorphic indices (SL index, topographic swath profile, V_f ratio, and K_s) to understand the relative contribution of these factors on the hillslopes and hence landslides.

It is observed that the majority of the landslides (72%) are concentrated in the vicinity of the MCT in the Higher Himalaya. The density of landslides is greater within the MCT zone, which decreases with distance, further downstream from the MCT. The landslides bear a close relationship with the geomorphic parameters. The landslides in the area are mostly found in regions exhibiting high stream length gradient index and channel steepness index, and low valley floor width to height ratio, implying that landslides are prone in regions with narrow, V-shaped valleys where the slopes are relatively steep, with lithologic variations such as the transition from resistant to weaker rocks. This indicates a close relationship of landslides with the tectonic structures of the region.

The river profile in the area, in general, exhibits a

concave-up shape with some convexities along its path, which might be related to active tectonics and lithological contacts. It is observed that, except for knick points K-3 and K-8, all other knick points in the area exhibit lithological contacts (Fig. 37). Knickpoint K-3 coincides close to the proximity of the Hanuman Ganga-Yamuna River confluence and a fault plane runs close to it, while K-8 corresponds with the Barni Gad Fault. Knickpoints K-1 and K-2 coincide with the fault planes. The pronounced knick point at K-4 is related to the MCT while that at K-6, with the NAT. Hence, the knick points (K-1, 2, 4, 5, 6, 7) coinciding with lithological contrast may also be attributed to tectonic influence. The relation of channel gradient with lithology and the tectonic regime has been further verified using other morphometric indices such as stream length gradient and topographic swath profile.

The topographic profile also clearly demonstrates the abrupt rise in topography from the Lesser Himalaya (LH) to the HH. A pronounced rise in topography is also observed in the region between Naugaon and Barni Gad in the LH. This may be attributed due to the Barni Gad fault. Higher values of SL, in the Syanachatti-Wazri region and downstream of Naugaon, may be attributed to the confluence of streams with the Yamuna River. The Syanachatti-Wazri region also demarcates the contact of the LH with the HH. All the geomorphic indices in this region such as prominent knick points, higher SL, remarkable increase in topography, etc. are indicative of tectonic influence in the area. The NAT, which passes through Gangani village, does not show abnormally high SL values, though there is a knick point in the region. However, surface impressions as evident from field observation indicate a possible neotectonic activity in the form of strath terraces.

Landslides in the Yamuna Valley are notably a function of lithology and various geomorphic parameters. The distribution of landslides with respect to lithology, K_s , SL, and V_f indicate that the landslides are more concentrated in regions with high K_s , SL, and low V_f values, which in general, coincide with lithologic contacts, particularly in the HH region, i.e., upstream of Wazri, whereas in the LH, the distribution of landslides is quite inconsistent. Summing up, the majority of the landslides in the study area are located in areas of lithological change and bearing high values of SL and K_s , and low V_f . Further, most of these landslides are found concentrated around knick points, particularly in the HH. However, not much interrelationship could be drawn in the LH, with the anthropogenic intervention being one of the reasons.

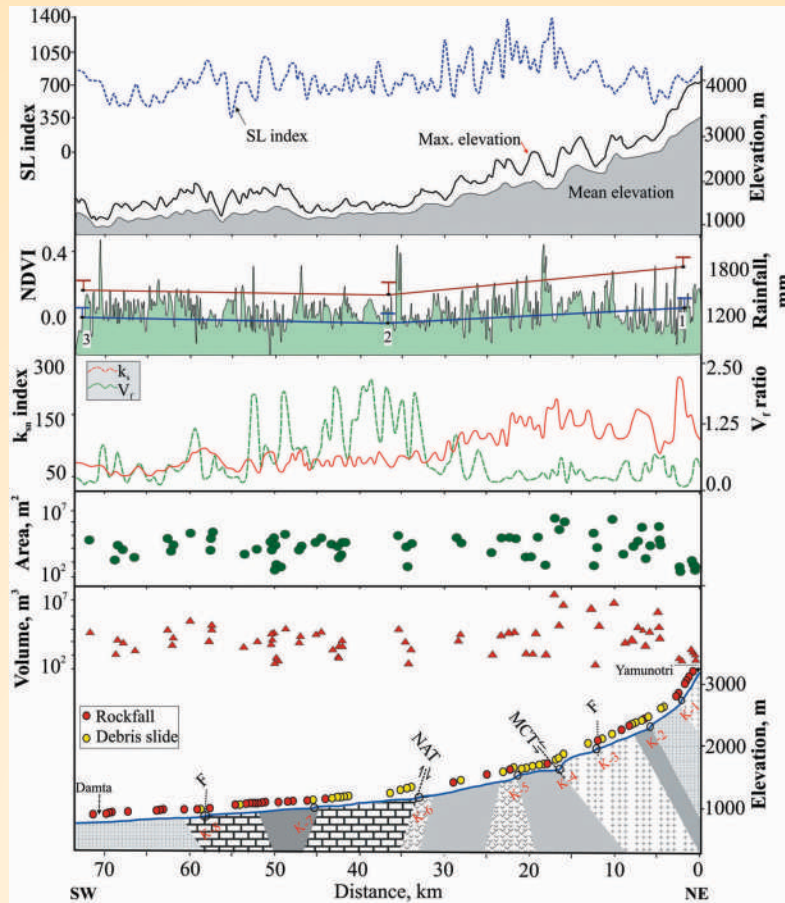


Fig. 37: Litho-tectonic and precipitation regimes. Spatial variability of stream length gradient index (SL), topographic swath profile, NDVI, rainfall, steepness index (Ks), valley floor width to valley floor height (Vf), and area and volume of individual landslides along the river longitudinal (L) profile. K-1 to K-8 denote knick points. F denotes fault, MCT and NAT refer to the Main Central Thrust and the North Almora Thrust, respectively. 1, 2, and 3 represent TRMM rainfall data locations, which are Yamunotri, Barkot, and Damta, respectively.

Morphotectonic evolution of major and minor faults leading to landslide hazard and risk assessment

The frontal part of the Himalaya in the Tanakpur area in the eastern part of Kumaun Himalaya suggests high instability of the slopes as the region is dotted by numerous landslide debris fans (Fig. 38). In the Ladhiya valley, almost all the debris fan deposits are observed on the left bank of the Ladhiya River. At Kathol huge landslide debris fan is observed which has been laid down by Kagota Khola, almost 50m thick debris section is observed along Ladhiya river. Uprakot is nestled on a large debris fan of more than 120m thick at the height of 587m asl laid down Jafaldhonga Gad. At Kukanda and Ajron high levels of debris fan deposits are observed at 510 m asl and 447m asl, respectively. The terraces of the Chuka and Khaldhunga are overlain by the huge thickness of debris. Jariakhal area constitutes an apron of large debris fan laid down by Shukur Khola and Gaoji

Gad. Between Thuligaon and Bastia, numerous debris fan deposits are observed. Valdiya et al. (1992) has classified the debris fans into Uchaulikot Fan and Bastia Fan. Bastia fan is best observed along Hathi khor where a distinct break in sedimentation is observed towards the apex of the fan deposit are overlain by 0.3m thick sheet flow deposit comprising mainly of medium to coarse-grained sand. The numerous fans are basically landslides debris that has been laid down by the streams and points towards the instability of the south-facing Siwalik Hills and were deposited in numerous phases. The latest debris fan was deposited by Batna Gad during the monsoon of 2010 where massive debris was generated by landslides taking place in the Siwalik Hills, prior to 2010 continuous debris deposition is also evident from Google Earth image of 2004. Exposed sections of the fans comprised mainly clasts of sandstones in a matrix of coarse rock fragments and around 60m of the Babat Gad fan is exposed along the

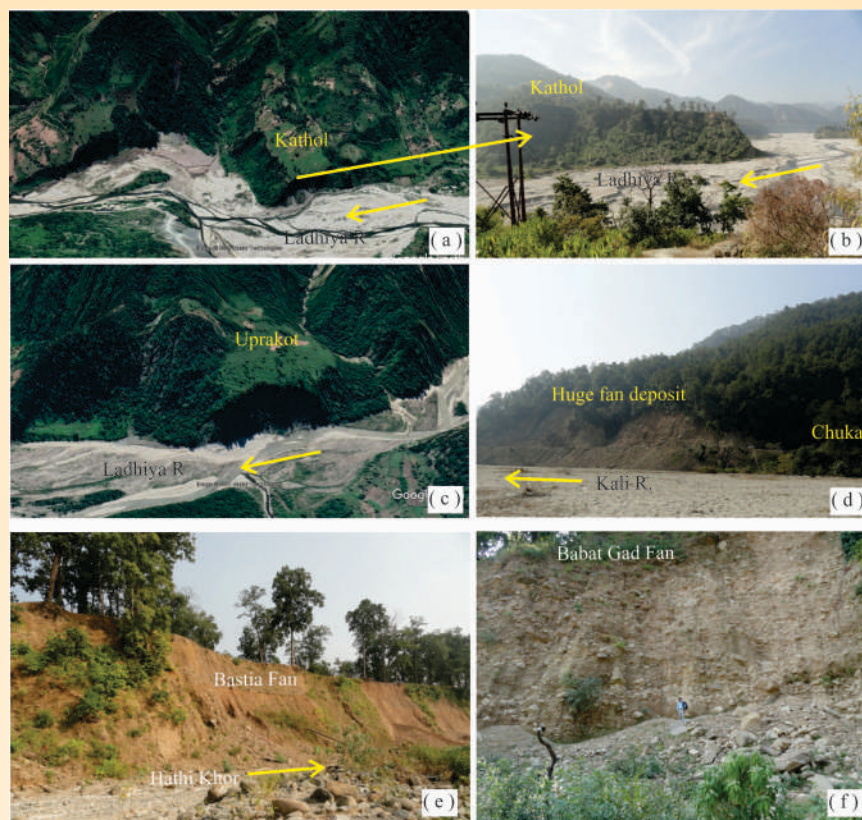


Fig. 38: Numerous landslide debris fan deposits are observed along the Ladhiya and Kali valleys and the frontal part of the Kumaun sub-Himalaya, in some cases exposed section measures more than 50m in height as observed at Kathol (a) and (b), Uprakot (c) and at Chuka (d). The debris fans in the frontal part are highly incised by streams and more than 25m fan deposits are exposed along Hathi Khor (e) and Thuligad.

Kali River which suggests multiple phases of deposition.

Fluvial terraces are well developed along Ladhiya and Kali river valleys (Fig. 39). A stretch of river sections between Bilaspur and Shim in Ladhiya River valley and between Shim and Tanakpur in Kali River valley has been considered for aggradational landforms. Ladhiya valley becomes very wide from Dugbaur just upstream of Bilaspur, at Bilaspur-Bilkhet two levels of aggradational landforms are developed. T_1 is at 627 m asl while the present river bed is at 625 m asl, and is made up of clast mainly of the rocks belonging to Ramgarh and Almora groups. At Shantok, 2 km downstream of Bilaspur six levels of fluvial terraces are developed T_6 at 672 m asl while the present river bed at 608m asl; here also the highest fluvial terrace is capped by debris fan deposit. Downstream at Kathol, three levels of terraces are developed, T_3 is developed only in path while the lower terraces are more widely developed. T_3 is at 620m asl, T_2 at 610m asl, and T_1 at 602 m asl, at Chalthi a single level of terrace is developed at 592m asl. Further downstream at Phukijal opposite of Uprakot one level of the paired terrace at

468m asl is observed on either side of Balapipal Gadhera. At Bilkhet and Sera one level of paired terrace is observed, at Ban and Shim one level of terraces is developed. At the confluence of the Kali river and Ladhiya rivers at Chuka two levels of terraces are developed, T_2 is widely developed and is heterogeneous in the composition of medium-sized clast and exposed section of the terrace tread is about 10 m, while T_1 is not well developed. Khaldhunga (India) and Parigaon (Nepal) section of the Kali river valley represents the widest section of the Kali river valley where the width measures about 3 km. In this section unpaired levels of terraces are developed on the Indian section at Khaldhunga, three levels of terraces are developed while on the Nepalese section two levels of terraces are developed. At Khaldhunga T_3 is at 385m asl, T_2 is at 352m asl, and T_1 at 330m asl; terraces at Parigaon T_2 is at 334m asl and T_1 is at 324m asl. T_3 of Khaldhunga is exposed along the road section and composed of thick sand deposits overlain by mud and debris. Further 1.5 km downstream from Khaldhunga thick mud deposit is observed. Between Khaldhunga and Jariakhal alternation of debris flow

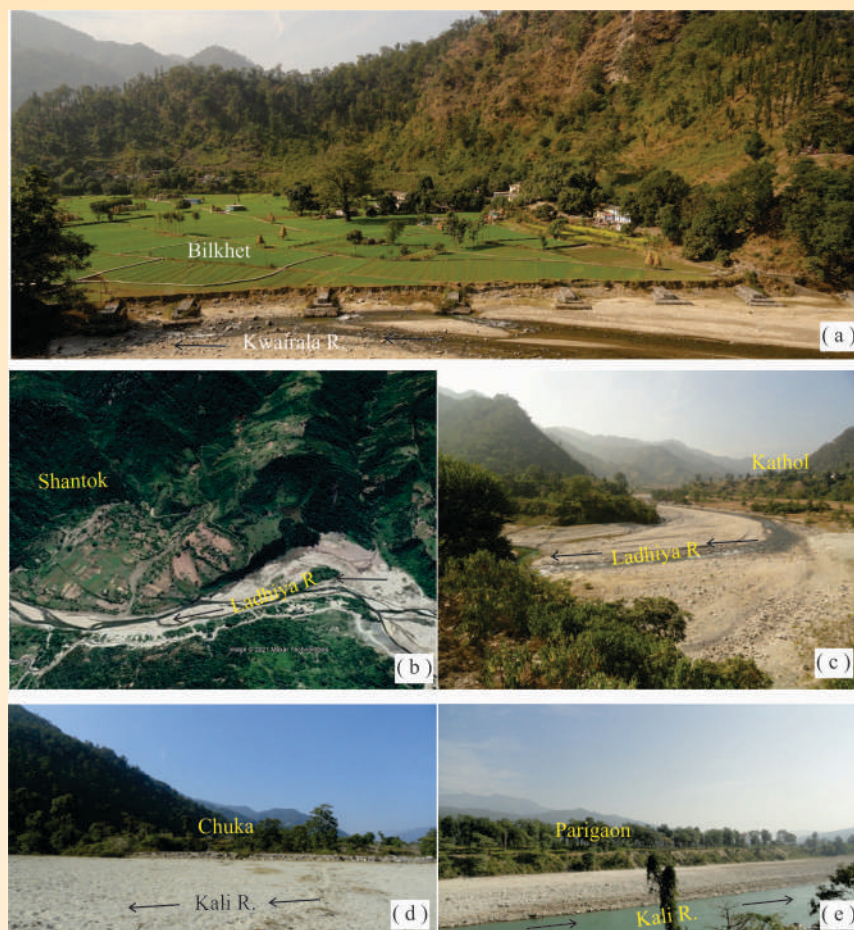


Fig. 39: Field photographs and Google Earth Image showing the development of terraces at various sections of Ladhiya River valley and Kali River valley (a) Wide terrace at Bilkhet in the Ramgarh Thrust zone. (b) Six levels of terraces developed at Shantok, the terraces are overlain by thick landslide debris. (c) At Kathol unpaired levels of terraces are observed on the right bank two levels of terraces are formed while on the left bank three levels of terraces are developed. (d) and (e). At Chuka and Parigaon the width of Kali Valley becomes very wide with wide terraces.

deposit and thick sand deposits are observed. The alternation of sand and mud deposits is tilted by 5° towards SW. At Tanakpur two levels of terraces are developed and the T_2 section can be best observed along the Dhana Gad section at Khorpa Tal, while T_1 is best exposed along Uchalikot.

The drainage pattern of the present study area is dendritic; structural control on drainage network and pattern is observed in some sections of faults. Structural control on the Kali River flow pattern is observed along the Thuligad Fault and almost E-W trending lineament running parallel to the MBT and Ramgarh Thrust. The south-flowing Kali River in the immediate hanging wall of the MBT took almost U-turn along this lineament and flows NW for about 5 km before returning to its original flow direction. Khethi Gad also flows along the trend of this lineament and flows in the ESE direction and the confluence with

Kali River which also follows this lineament. Northeast of Tanakpur Kali River flows along Thuligad Fault having E-W trend for about 5km just before exiting into the Gangetic plain. The Ladhiya River shows structural control along the Jhamarcheru Fault in the upper reaches and along the Uprakot Fault downstream. The Jhamarcheru Fault has an NNW-SSE trend and the Ladhiya river flow along this fault for about 23km and flows towards SE; while along Uprakot Fault which trend almost E-W the Ladhiya river flows along the fault in the eastward direction. West of Sukhidhang Patkholi Nadi a tributary of Kali River flows parallel to the strike of the bedrock for about 10km in east direction before flowing across the sub-Himalaya and exiting into the Gangetic plain. Saj Gad and Chaha Khola tributaries of Kalaunia River follow the trend of the bedrock in WSW. The Rangun Khola flows west almost straight along the strike of the bedrocks/lineaments for about 21km and the confluence

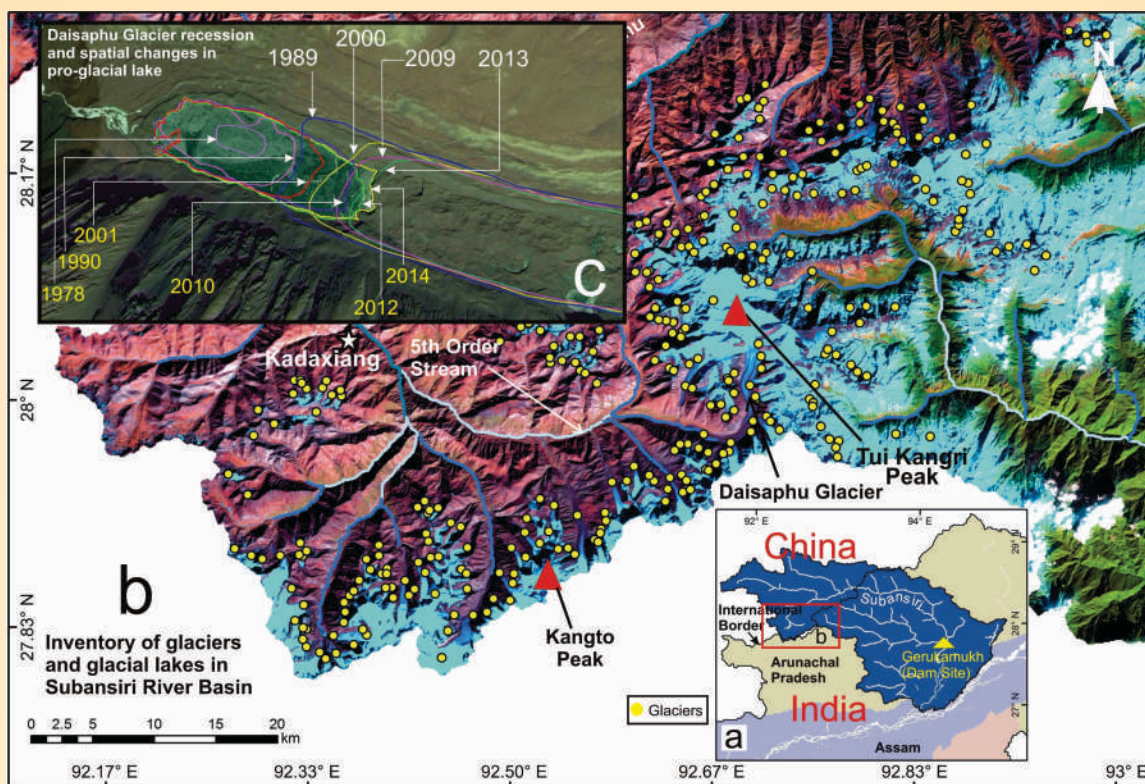


Fig. 40: The Subansiri Basin showing locations of important streams and the glacier inventory located east of the basin.

with the Kali River at Khaldhunga. The Puntura Gad, a tributary of Rangun Khola, also flows along the strike of the Siwalik bedrock and is slightly oblique to the Rangun Khola. In the upper catchment area of Hathi Khor the main trunk of this stream also follows the Sukhidhang Fault. Along the active fault of the MBT zone in Nepal, structural control on 1st and 2nd order streams is observed.

Development of inventory for landslide and glacial lake outburst flood

The Subansiri River is the largest tributary of the Brahmaputra River. The lower catchment of the river is also prone to flash floods in the monsoon season. This river has attracted attention owing to the under-construction 2000 MW Lower Subansiri hydropower project at Gerukamukh. This 116 m high gravity dam has raised concerns about the socio-economic and environmental impacts on the rich biodiversity of the region.

After the recent past disasters like the Mandakini Valley in June 2013 devastating the temple town of Kedarnath, the recent Rishi Ganga-Dhauliganga Valley in February 2021, and very close to the Subansiri Basin, in the Great Bend region on the

Yarlung Tsangpo River in March 2021, the need to continuously monitor mountain lakes and landslide susceptible zones have become most necessary. While a lot of inventory work has been done for the western Himalaya, a major lack of data for the eastern Himalaya exists. Especially because most of the glaciated and snow-covered region in this basin lies across the border in China, while a greater-sized population is dependent on agriculture in its flood plain in the lower catchment in India.

Therefore, as a first step, a complete, validated glacier and lake inventory, using Landsat Operational Land Imager (OLI) data, for the years between 1978 and 2014, was created for the Subansiri Basin. In the absence of instrumental climate data for the area, Gridded temperature and precipitation data were used from Climate Research Unit (CRU) Time-Series 4.03 (TS 4.01) having a spatial extent of 0.5° X 0.5° latitudinal and longitudinal grids for years between 1901 to 2019. The data shows a continuous increase in temperature for 117 years. A slight decrease in summer precipitation is seen. The mean monthly minimum temperature (2.7°C) is observed in January, and the average minimum monthly precipitation (4 mm) is seen in January and December. This study reports 390 glaciers where 191 are hanging glaciers,

59 ice aprons, 52 cirques, 40 niches, 37 valley glaciers, dominantly north facing, 9 icecaps, and 2 outlet glaciers (Fig. 40). The snow-covered region occupies 0.96% of the total basin area. There are 52 glacial lakes with a cumulative area of 3.358 km². The Daisaphu Proglacial-lake shows a growth of 0.471 km² in area, and an increase of 0.0833 km³ in water volume between 1978 and 2014.

Activity: 6A

Glacial Dynamics, Glacier Hydrology, Mountain Meteorology and Hazard

(Kalachand Sain, Manish Mehta, Vinit Kumar and Sameer K. Tiwari)

Status of Glacier Surface Changes in Doda and Suru River basins; Past and current status, priorities and future prospects

The late Quaternary glacial history of Suru Basin and its associated tributary valleys in the western Himalaya

(i.e., Achambur, Kangriz, Shafat, Rangdum, and Pensilugnpa) have been reconstructed (Fig. 41) based on the data collected from field surveys (2015-2019), satellite images, and Optically Stimulated Luminescence (OSL) dating. The results suggest that the glaciers in Suru Basin have fluctuated greatly throughout the Marine Isotope Stage (MIS) 3 and 2 to Little Ice Age (LIA). The data provide a record of six glacial advances of decreasing magnitude since MIS 3 till the present day. Further, the depression of equilibrium-line altitude (ELA) was ~538 m upward from the oldest glacial advance (Suru-I) to the present day, followed by four other events (Suru-II, III, IV, and V) with ELA depressions of ~522, ~399, ~243, and 215 m, respectively. Suru Basin has lost ~502 km² glaciated area and ~163 km³ ice volume from Suru-I to the present day. The magnitude of glacier extent decreased from the MIS 3 and 2, early to late-Holocene, and LIA in synchronous with the Northern Hemisphere pattern.

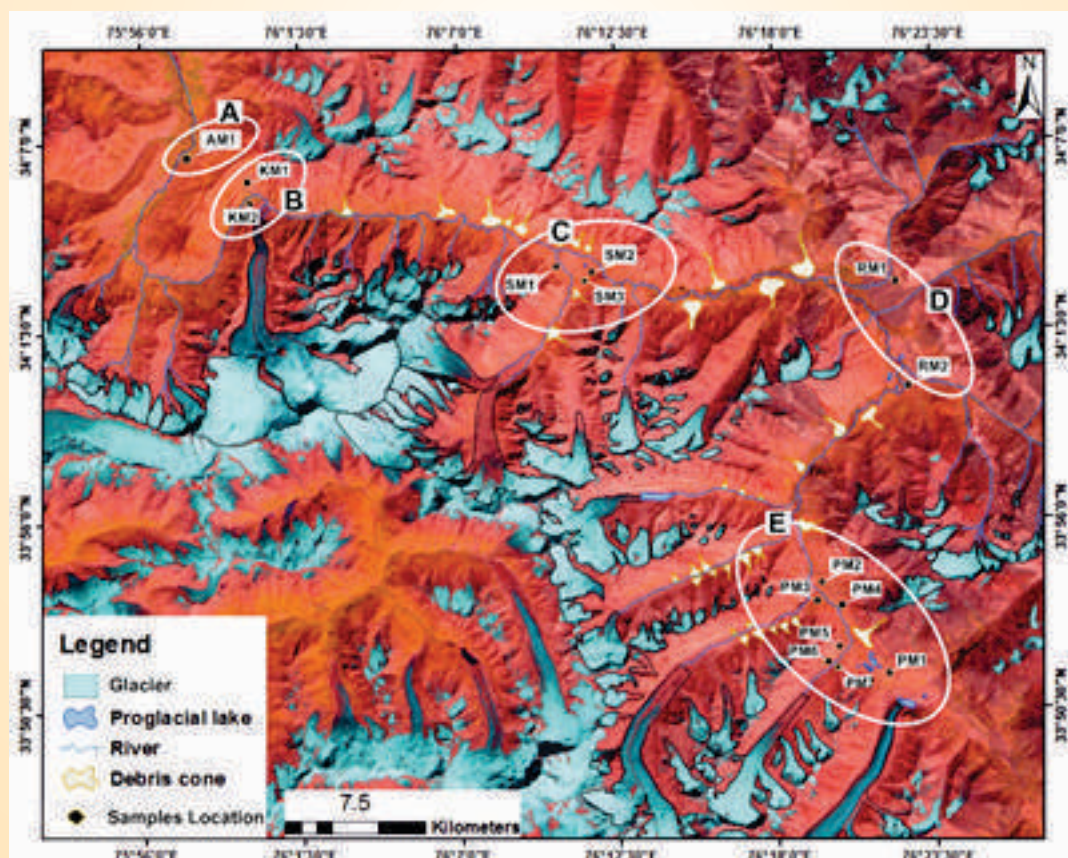


Fig. 41: Studied sections (white circles) and samples collection site. (A) Achambur Moraine (AM1), (B) Kangriz Moraine (KM1 & 2), (C) Shafat Moraine (SM1, 2 & 3), (D) Rangdum Moraine (RM1 & 2), and (E) Pensilugnpa Moraine (PM1 to PM7). The background image is False Colour Composite (FCC) of Sentinel-2A (2017) showing glaciers in Suru Basin.

We have studied the impact of climate change with regard to the past and present response of the Pensilungpa Glacier (Fig. 42), Suru Basin, Zaskar Himalaya. Reconstructing the recent changes in the mass balance (2016-2019) along with the Little Ice Age (LIA) extent of the PG shows that the PG was joined by the five tributary glaciers during the LIA having an area of $\sim 18 \text{ km}^2$ and extended $\sim 3 \text{ km}$ downstream from its present-day snout located at $4470 \pm 1 \text{ m.a.s.l.}$ Since the LIA, the PG has retreated $\sim 2941 \pm 75 \text{ m}$, at an average rate of $5.6 \pm 0.15 \text{ m a}^{-1}$. Field observations for the last 4 years (2015-2019) show that the glacier now is retreating by $\sim 27 \pm 11 \text{ m}$ at an average rate of $6.7 \pm 3 \text{ m a}^{-1}$, which is similar to the one since the LIA. The ablation data reveal the significant influence of debris cover on the mass balance and terminus retreat of the PG. Furthermore, the mass balance data for the last 3 years (2016-2019) show a negative trend with a small accumulation area ratio (AAR) (43%). The average net

annual mass balance is estimated to be $\sim -3.67 \times 10^6 \text{ m}^3 \text{ w.e. a}^{-1}$ with the $-0.36 \text{ m w.e. a}^{-1}$ specific balance between 2016 and 2019. During the period 2016-2019, the PG has lost $\sim 11.03 \times 10^6 \text{ m}^3 \text{ w.e. ice volume}$.

In-situ hydro-meteorological records in conjunction with stable isotope systematics to understand the hydrological processes in Glaciers of Garhwal Himalaya, India

Glaciers in the Indian Himalayan Region (IHR) are sensitive to climatic changes. Rivers originating from the Himalaya have higher water yields in the ablation season due to large inputs from the melting of snow and glaciers, which is critical for sustaining downstream ecosystems, agricultural practices, hydroelectric power generation, and urban water supplies. Integrated investigations are frequently unavailable at a regional scale over a longer period, which is hampered due to the non-availability of data caused by harsh weather conditions, difficult terrain, as well as difficulty in maintaining the instruments at such high altitudes ($> 3000 \text{ m asl}$). The hydrological understanding of melting processes from glacierized basins requires a network of reliable meteorological and hydrological observations. In absence of such reliable meteorological data, most of the hydrological simulation studies are forced to extrapolate air temperature from nearby basins, lower elevations, or consider satellite-based observations, which often deviate or differ from the actual ground conditions and lead to large uncertainty in model outputs. Therefore, an integrated approach for collecting hydrological and meteorological data along with other data like snow-cover, suspended sediment transfer and stable isotopic signatures of different components of the hydrograph were conceptualized for glacierized river basins in Garhwal Himalaya (Bhagirathi and Alaknanda). Our results suggest that the annual distribution of temperature lapse rates (TLR) exhibits a bimodal pattern and the TLR's are significantly lower than the adiabatic lapse rate. The major components of the streamflow are derived from snow and glacier melt, while rainfall contributes little during the Indian Summer Monsoon (ISM). Westerlies significantly feed the glacier with snow, while rainfall is dominant during the Indian Summer Monsoon (ISM). Precipitation and temperature are the dominant meteorological factors controlling melting processes and sediment delivery. Climate and topography control the distribution of seasonal snow cover/ snowline in the region. Extreme events like heavy rainfall, flash floods, glacial lake outbursts floods, etc. can be traced using hydrometeorological and isotopic data at high altitude stations. Therefore, in light of the challenges and

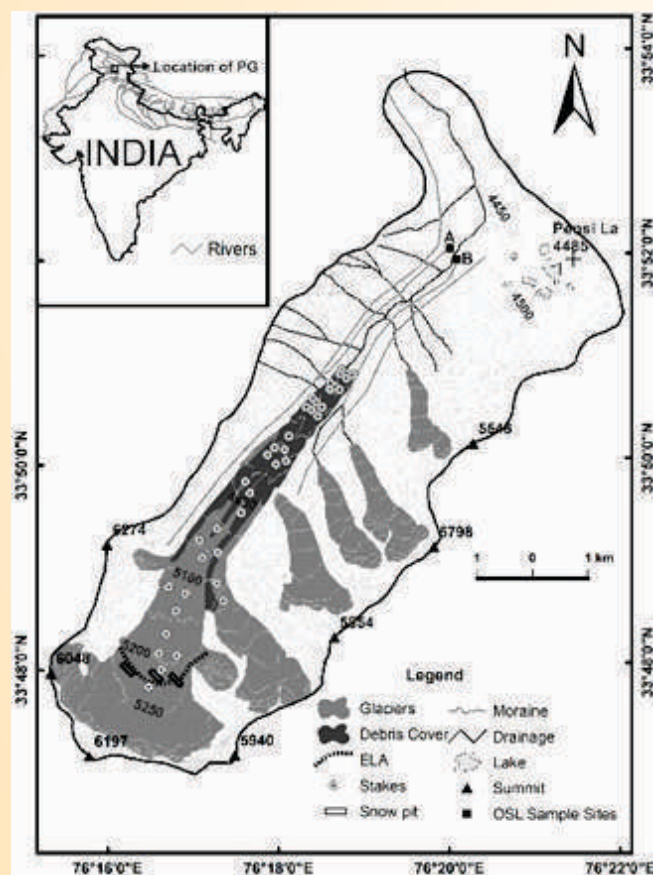


Fig. 42: Location of the Pensilungpa Glacier showing the geomorphological overview and lateral moraines of the LIA extent with the installed stakes network for accumulation/ablation measurement. Stakes are shown in white circles, and black rectangle are snow pits locations.

potential research gaps, the study produces actionable knowledge in the Garhwal Himalaya for better understanding and modeling of glacio-hydrological processes by incorporating ground-based observations.

Integrated long-term hydro-meteorological investigations are not frequently available in Indian Himalaya Region (IHR), especially near the glacier terminus. Collection and analysis of integrated hydro-meteorological observations help in understanding the weather conditions, glacier melting patterns, and other flow-generation processes. Changes in local precipitation, snow cover pattern, and glacier storage are likely to affect discharge in terms of volume and its variability. Hence, there is a need to establish a linkage between glacio-hydrological processes with the climate. The time series analysis has been utilized for determining correlations and Auto-correlation (ACF). The analysis suggests a very high discharge auto-correlation for each year and the combined data series of individual glaciers. The substantial storage of meltwater in the glacier body and its delayed response to the runoff is attributed to the high dependency of a particular day's discharge on its previous day's discharge. Variations in the physical features of the glacier, weather conditions, precipitation, and its distribution over the time on the basin account for changes in correlations. A comparison of correlations between discharge and temperature, and discharge and rain shows that temperature has a better correlation with discharge for all the years. In the early stages of the ablation period, poor drainage networks and stronger storage characteristics are observed in the glaciers due to the presence of seasonal snow cover. The impact of such meltwater storage and delaying characteristics of glaciers on hydropower projects being planned and/or developed on glacier-fed streams in Garhwal Himalaya are highlighted.

- 1) Regular monitoring, hydro-meteorological observations, and sample collection at Gangotri, Dokriani, Chorabari, Dunagiri-Bangni glaciers were continued for the summer period (May-October).
- 2) A team of scientists conducted a ground-based and heliborne survey immediately after the disaster that took place on 7th February 2021 in the Chamoli district of Uttarakhand. Based on these observations and freely available Google Earth imagery, they arrived at plausible causes of this catastrophe as due to detachment of a sizeable rock mass and overlying hanging glacier in the Raunthi catchment that dammed the Rishiganga River and led to the devastation of roads, bridges, and hydropower projects in downstream.

- 3) Various instruments like CH₄, CO₂, H₂O gas analyzer, automatic water level recorder (AWLR), fluorometer, snow fork, etc. would be utilized for environmental monitoring, automated water level observations, tracer studies, snow pack studies.

Tree-ring isotope-derived seasonal atmospheric moisture dynamics and greening effect on the central Himalayan glaciers

Accelerated glacier mass loss is primarily attributed to greenhouse-induced warming, but land-climate interaction has increasingly been recognized as an important forcing at the regional-local scale. However, the related effects on the Himalayan glaciers are less explored but believed to be an important factor regulating spatial heterogeneity. We present a multi-decadal approximation on hydroclimate and glacier interaction over the western central Himalaya (WCH). Three highly coherent, multi-species, tree-ring $\delta^{18}\text{O}$ site-chronologies from WCH were used to derive regional changes in atmospheric humidity (atmospheric moisture content: AMC: Fig. 43) over the last four centuries.

Coherency analyses between AMC and glacier mass balance (GMB: tree-ring $\delta^{13}\text{C}$ -derived) indicate an abrupt phase shift since the 1960s within a common record of 273 years. To ascertain the cause of phase-shift, annual AMC was disintegrated into seasonal-scale, utilizing $\delta^{18}\text{O}$ record of deciduous species. Seasonal (winter: October-March; & summer-accumulation season: April-September) decomposition results reveal that winter-westerlies rather than summer precipitation from Indian summer monsoon (ISM) govern the ice-mass variability in WCH. Decadal coherency between summer-season AMC and GMB remained relatively stable since the mid-20th century, despite a decline in central Himalayan summer precipitation (tree-ring $\delta^{18}\text{O}$ records). We hypothesize that excess water vapor brought to the atmosphere through an increase in pre-monsoon precipitation and a greening-mediated increase in evapotranspiration might have been recycled through the summer season to compensate for the ISM part of precipitation. However, isotope-enabled ecophysiological models and measurements would be able to strengthen this hypothesis. In addition, high-resolution radiative forcing and glacier valley-scale vegetation trend analyses point towards a probable influence of greening on GMB. Results indicate that attribution of ice mass to large-scale dynamics is likely to be modulated by local vegetation changes. We contend that glacier-climate models fed with these feedback processes could reliably improve the projections.

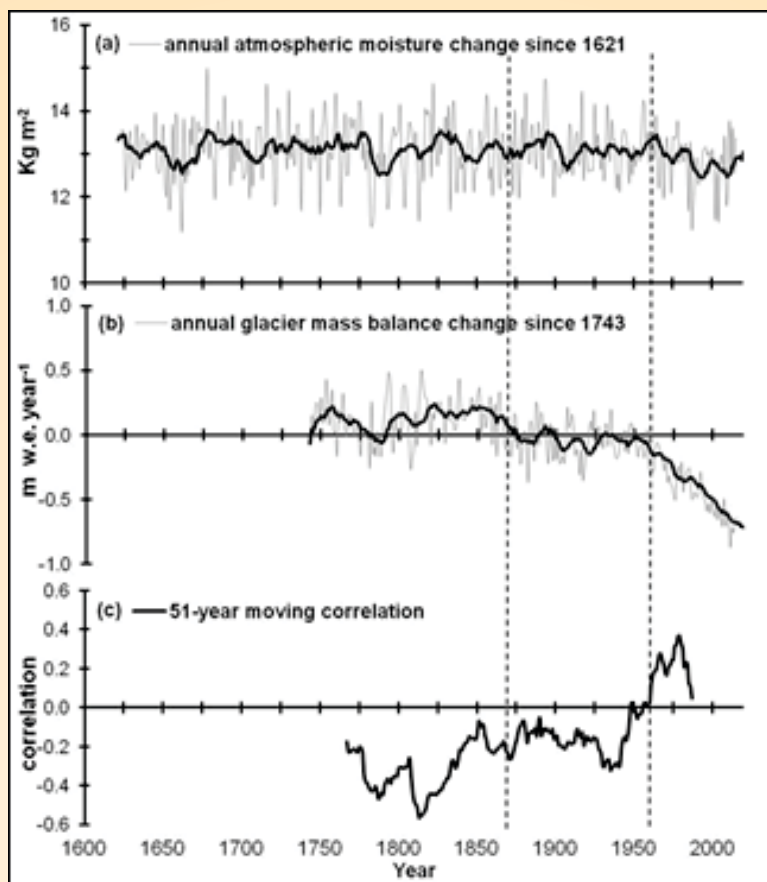


Fig. 43: (a) Annual atmospheric moisture reconstruction derived from regional conifer $\delta^{18}\text{O}$ chronologies, (b) 273-years of glacier mass balance variability reconstructed utilizing regional tree-ring cellulose $\delta^{13}\text{C}$ records, and (c) Low-frequency temporal correlations (51-year moving correlations) between atmospheric moisture and glacier mass balance. A sharp phase shift since the 1960s may be noted. Dark lines denote an 11-year moving average. Vertical dashed lines are the results of the break-point analysis.

Impact of COVID-19 induced lockdown on river water quality: An assessment from Upper Ganga Basin (UGB) Uttarakhand, India

The work was carried out in the headwaters of the Ganga and Yamuna river systems of the India Himalayan region, covering $77^{\circ}50'\text{N} - 78^{\circ}50'\text{N}$ latitudes and $29^{\circ}50' - 30^{\circ}50'\text{E}$ longitudes (Fig. 44). It extends from about 10 km upstream of Alaknanda river at Mulya, and 25 km upstream of Bhagirathi river at (Koteshwar Dam), down to Devprayag at their confluence to become Ganga, and further down till the Haridwar city. In the upper reaches of the Yamuna river, sampling covers the Yamuna river at Barkot to down to Dakpathar at the Vikas Nagar.

The study focuses on the evaluation of Physico-chemical and isotopic compositions to trace the changes in the water quality in the UGB during the COVID-19 induced lockdown (May, and June-2020). We have also calculated the WPI of earlier studies carried out in the

same basin and compared these with the present study to quantify the improvement in the water quality during the lockdown. Since the Rivers carry the continental weathered products to oceans and play a major role in global sea-water evolution. Further, Carbonate and silicate weathering processes are mainly carried out at variable scales resulting in the heterogeneity and composition of river water. Therefore, This study insight into the processes of chemical (Carbonate/silicate) weathering in the upper Ganga basin.

A perspective on Rishiganga-Dhauliganga flash flood in the Garhwal Himalaya, India

Uttarakhand has witnessed several disasters such as GLOF, debris flows, and flash floods which include Kedarnath, 2013 (Bhambri et al., 2016), Gangotri, 2017 (Kumar et al., 2018), and Rishiganga-Dhauliganga, 2021 (This study: Fig. 45). Breaking of rock mass and overlying hanging glacier from Raunthi peak (5600 m asl) to Raunthi stream (3600 m asl) created slurry

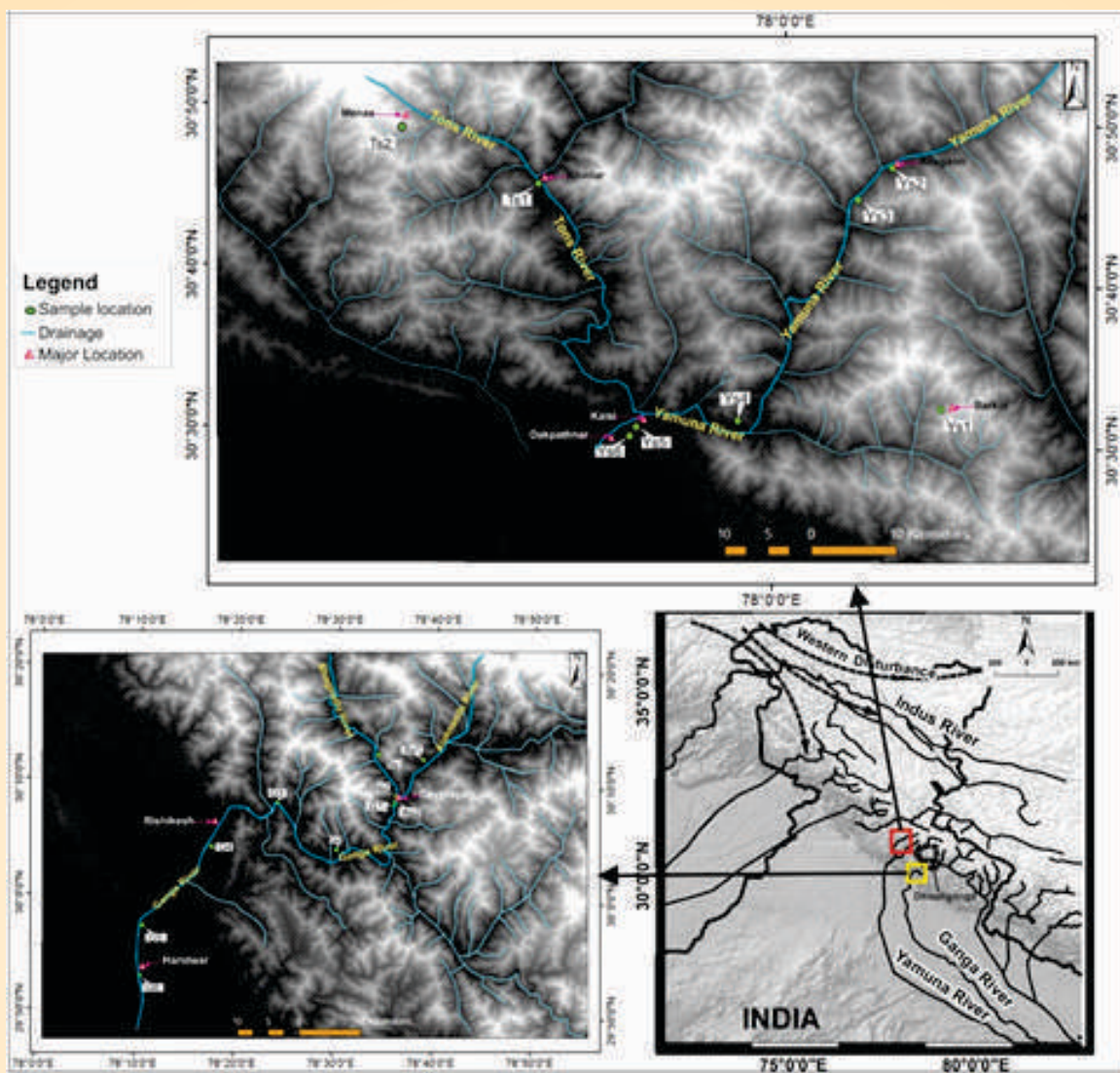


Fig. 44: Location map of Study area.

materials that dammed the Rishiganga river at ~ 2300 msl. The slurry further entrained a large quantity of sediment, wood debris, ice block, and water, and caused devastation to Rishiganga and Tapovan Hydro Electric Power Plants along with the roads and bridges downstream. Therefore, continuous long-term monitoring of glaciers and glaciated regions in the Himalayas should be of utmost importance. The data collected through long-term monitoring can be beneficial for developing early warning systems. Further, the local communities must be educated and sensitized to such hazards, which will help reduce the loss of lives, livestock and properties. The awareness in the local people could have saved some lives, if not all, as the time lag between the Rishiganga and Tapovan HEP was ~ 16 minutes.

Assessment of geothermal reservoirs temperature using dissolved silica geothermometry: A case study from Garhwal Northwest Himalaya, India

The growth in population and their reliance on modern technology stress more and more on energy, which is dwindling in India. Mostly, the energy demand is met by fossil fuels that produce CO_2 - a greenhouse gas and is responsible for global warming. Again, we produce only 30% of our energy requirement indigenously and spend huge money for importing the remaining. This necessitates an alternate source of energy for sustainable development with a reduced impact on climate change or global warming. Under this scenario, it is envisaged to tap renewable and unconventional green energy reserves. The geothermal fields in the northwest (NW) Himalaya offer renewable energy



Fig. 45: Field photograph of Rishiganga-Dhauliganga flash flood.

resources that have great potential for generating electricity and heating/cooling purposes. The present work aims for estimating the subsurface reservoir's temperature based on dissolved silica geothermometry to harness this energy that can meet the local requirements in the Himalaya and adjoining regions. For this, we have investigated the silica-water reactions in low to moderate (30°C to 93°C) surface temperatures at 20 active geothermal springs in the Garhwal

Himalaya. The results of modified silica-quartz with no steam loss and silica chalcedony methods show an average minimum reservoir temperature of 81°C at Matli and the highest temperature of 146°C at Jankichatti sites. The estimated reservoir temperatures of geothermal springs are likely to be the minimum temperature. The average reservoir temperature is estimated to be 125±10°C, indicating that the geothermal fields in the Garhwal (Uttarakhand)

Himalaya possess low to medium enthalpy resources. Since no major variation in geochemistry has been found during the last fifty years (1970-2020), the geothermal resources are active, as manifested by hot springs and encrustations around the springs. It has been planned for exploitation of geothermal energy into electricity at Tapoban in the Garhwal Himalaya. The geothermal fields can be monitored on regular basis by observing variation in hydro-chemistry of discharges.

Activity: 6B
Hydrogeology - Himalayan Fluvial Systems and Ground waters

(Santosh K Rai and Rouf A. Shah)

Hydrogeological studies of groundwater in karst settings of the Indian Himalayas

Two field campaigns were conducted to Doon Valley

(Fig. 46), central Himalaya, India. Collecting appropriate samples from the catchment water and Identification of Karstified litho-units remain the most important work component of these two field campaigns. Water samples (n=84) were taken from streams (n=19), groundwater (n=26) and event-based precipitation (n=29) for water isotopes and for ionic constituents. The samples were collected in HDPE bottles of different volumes, implementing the IAEA standard sampling procedures. Besides, Seven precipitation stations (n=7) were set up at various locations like Mussoorie, Dehradun, Sahastradhara, Roorkee, Tapkeishwar, and Ponta Sahib. Carbonate lithology in the region provides a good general view of Exo and endokarst geomorphic imprint in the form of Karren fields of varied dimensions, caves (both as pheratic and relict), springs, demonstrating the importance of this formation as a productive

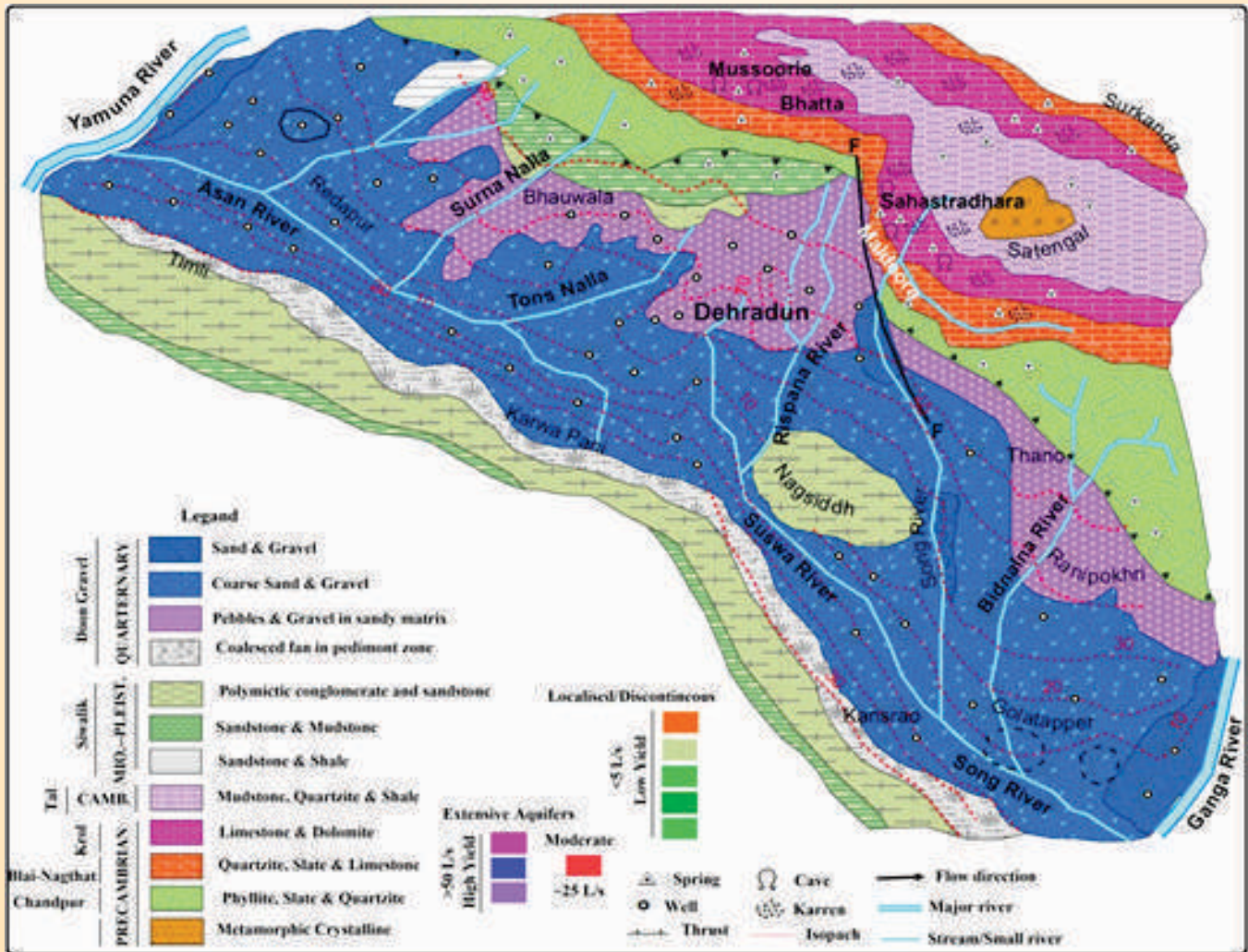


Fig. 46: Hydrogeological map of the Doon Valley (Modified after Bartarya, 1995).

groundwater reservoir. In the Doon Valley, karst occurs in the form of dissected ridges, and are well distributed at Shahastradhara, Maussooree, Donaulti, Robbers, etc. The dissolution of carbonate rocks and subsequent development of pools and parks at Shahastradhara and at Robbers, feature these areas as popular holiday destinations. To understand the karst aquifer functioning and dynamics, discharge of all major karst springs was measured using continuity equations. The preliminary results (geomorphic and discharge data) suggest that ridges are highly karstified, with karstification degrees range between 20 to 40 kd. The karst springs show a highly fluctuating pattern during the monitoring period with discharge ranging from 0.28 -0.45 m³ S⁻¹. Moreover, the conceptual sketch of monsoon circulation within the region is illustrated in figure 47.

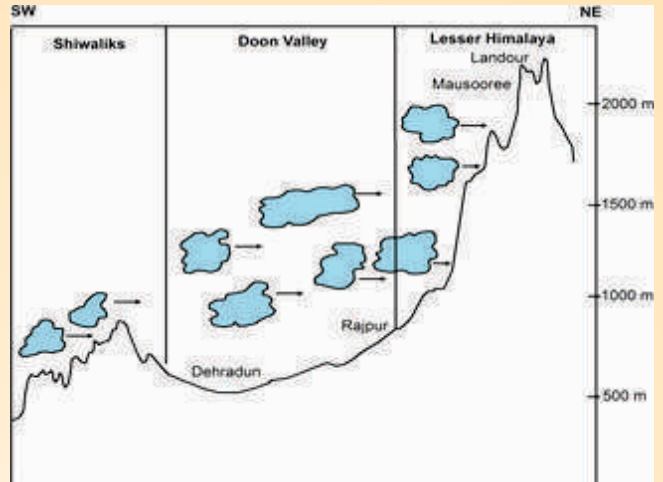


Fig. 47: Conceptual Map of the Monsoon circulation for the Doon Valley.

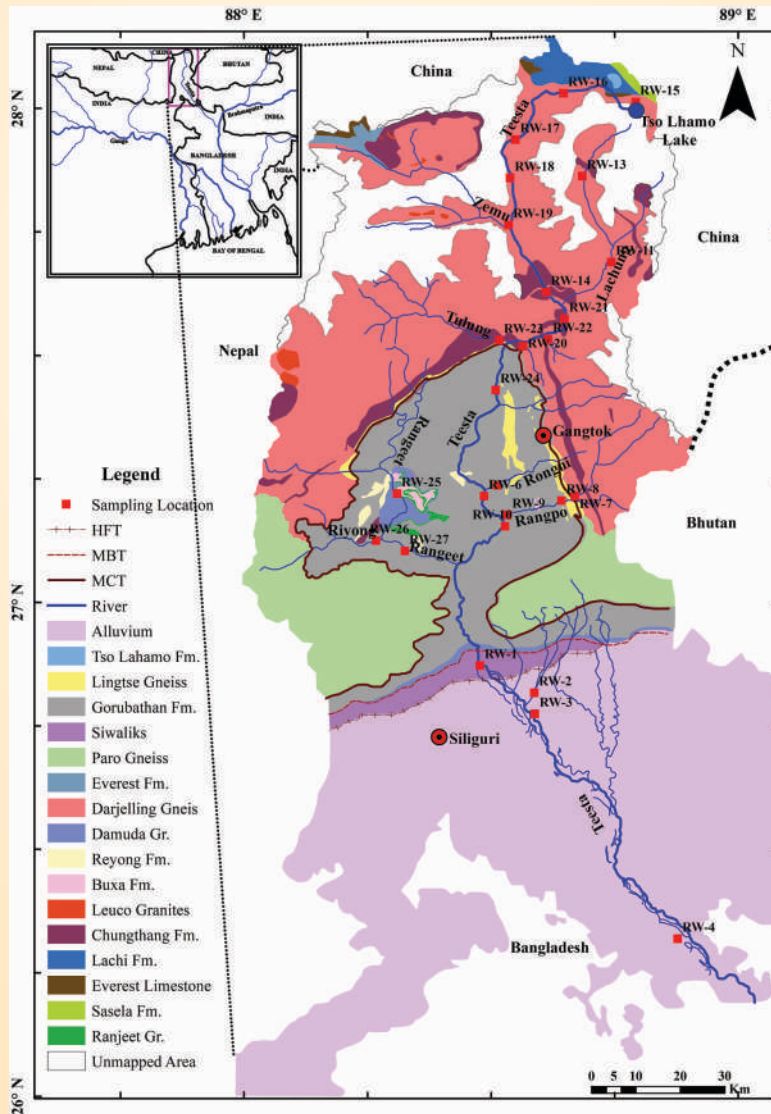


Fig. 48: Geological map of the Teesta river basin.

The role of Sulfuric Acid in continental weathering

Chemical denudation of the continental rocks serves as a major pathway for the cycling of elements in rivers, oceans, atmosphere, soils, and sediments. Weathering of silicate rocks has significant control as it draws CO_2 from the atmosphere and hence influences the climate on longer time scales under greenhouse conditions. In this context, the uplift of the Himalaya contributes to CO_2 mediated silicate weathering through the Ganga-Brahmaputra (G-B) River systems and hence it regulates the long-term changes in the global climate. However, the alternative mechanism of silicate weathering is also possible if it is mediated through H_2SO_4 , which consumes no CO_2 from the atmosphere. Geochemical results obtained for the Teesta River system (Fig. 48) were used to infer the role of Sulfuric Acid in continental weathering. The major findings of the work is that (1) Sulfate concentrations of the Teesta are higher than that of regional rainwater (2) About half of the cations are supplied through H_2SO_4 -mediated weathering (3) At outflow, the CO_2 uptake (silicate weathering) and release (H_2SO_4 - carbonate weathering) rates are in balance.

Activity: 7

Quantification of strain accumulation and strain release rate along the Main Himalayan Thrust (MHT) at different time scales

(R.J. Perumal, S. Rajesh, PKR Gautam and Vikas Adlakha)

The primary aim of this activity is to study the accumulation and release rate of strain at varied spatio-temporal scales across the Himalayan convergent zone using paleoseismological, thermochronological, and geodetic methods. Historical archives document massive destruction in the eastern Himalaya during closely time-spaced earthquakes in the Late-Medieval times (Iyengar et al., 1999). These earthquakes sometimes ruptured the Himalayan Frontal Thrust (HFT) at the surface, or remained blind, like the 2015 Gorkha earthquake. However, blind events rupture the down-dip segment of the MHT and thus transfer stress to the locked up-dip portion of this megathrust, which eventually breaks in subsequent, great earthquakes. Despite an increasing number of paleoseismological studies in the central Himalaya during the last decade (Jayangondaperumal et al., 2018), only a few investigations have been conducted along the eastern Himalayan front, and the studied trench sites are rather sparsely spaced at ~ 50 to ~ 200 km apart. The area includes the Bhutan-Arunachal Pradesh segment of the

Himalaya, which lies in the mesoseismal zone of the 1950 CE great earthquake (Fig. 49). Large spacing amongst the sites causes uncertainties associated with locations, surface rupture extents, chronologies, and magnitudes of historical earthquakes. Therefore, assessing seismic hazards associated with earthquakes on the HFT and determining its seismic behaviour in the eastern Himalaya has proven difficult. To better understand the seismogenic potential of the east Himalayan front, we conducted a palaeoseismological investigation between the Subansiri and Siang river valleys at Himebasti village in Arunachal Pradesh, India (Figs. 50 and 51).

A first mega trench was excavated at Himebasti village, Arunachal Pradesh, India, to develop paleoearthquake catalog using modern geological techniques (Fig. 52). The study includes twenty-one radiocarbon dates to limit the timing of displacement after 1445 CE, suggesting that the area was devastated in the 1697 CE event, known as the Sadiya Earthquake, with a dip-slip displacement of 15.3 ± 4.6 m. Intensity prediction equations and scaling laws for earthquake rupture size allow us to constraints a magnitude of Mw 7.7-8.1 and a minimum rupture length of ~ 100 km for the 1697 CE earthquake.

The interseismic geodetic strain-rate pattern in the Garhwal-Kumaun Himalaya

Understand the crustal deformation and strain accumulation in the Garhwal-Kumaun region, which lies in the Central Seismic Gap of the Northwest Himalaya, is one of the objectives under Activity-7. Surface strain rates are a proxy for the identification of potential earthquake zones in an active convergent regime like the Himalaya. Using GPS measured interseismic crustal velocities the surface strain rates in the region have been estimated. Continuous observations of GPS data from 37 stations including Wadia Institute local network, IGS (International GNSS Service), and from other published data for 8 years were used in this study, and the estimated strain-rate pattern in the study region is shown in figure 53. The data were processed using the GAMIT/GLOBK software. Local strain rates at each grid node are estimated using the modified least square approach and a weight function is used for the error reduction. The principal strain components are estimated along with the second invariant of strain rates to aid the interpretation of available structural data.

Results show that the locked portion of the MHT within the Outer Lesser Himalaya and the Sub-Himalaya are characterized by low strain rates (LSZ).

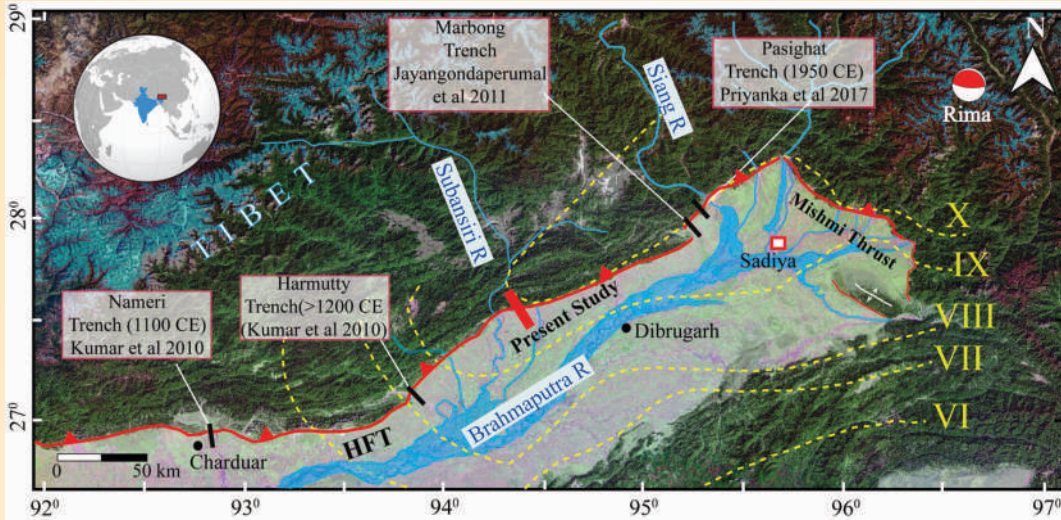


Fig. 49: A simplified map showing the location of a trench along the eastern Himalayan Frontal thrust. A beach ball shows the epicenter location and mechanism of the 1950 Assam-Tibet earthquake (Pandey et al., 2021).

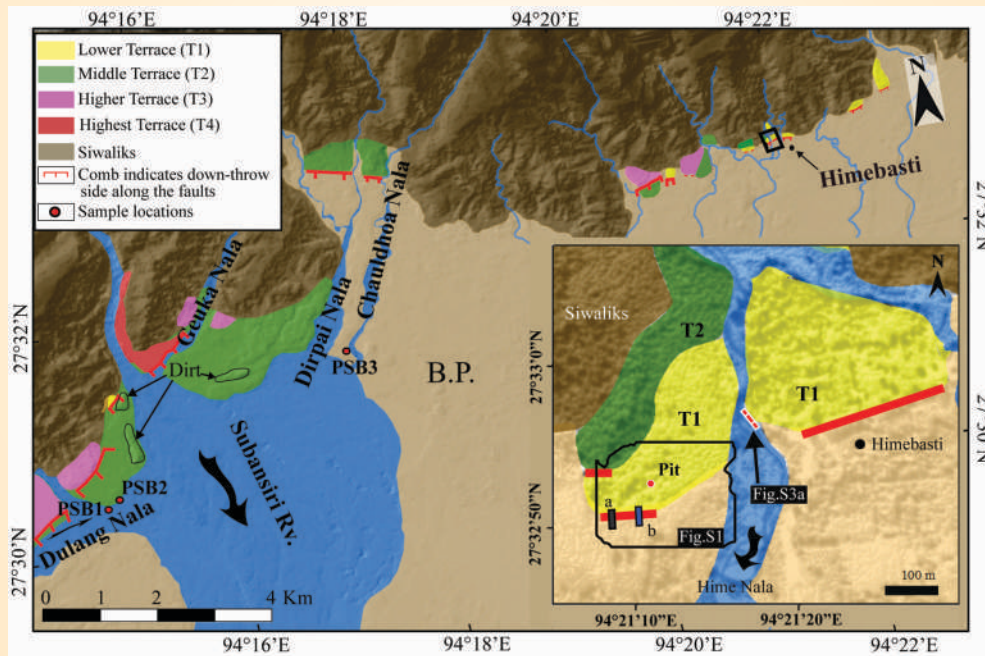


Fig. 50: Tectono-geomorphic map of Subansiri valley. Inset shows a detailed deformed terrace along the active fault at Himebasti trench site (after Pandey et al. 2021). The present study trench site is shown in the inset as 'b'.

As expected, the high compressional strain (HCZ) and the predominant deformation are happening in the Himalayan Seismic Belt. However, a curvilinear strain-rate pattern (encircled area in figure 53) is observed in the Inner Lesser Himalaya which continued towards the Chamoli earthquake cluster, where the shear deformation of the upper crust is mainly aided by the presence of mid-crustal fluids. Surface strain observations show that the Ton thrust and the North Almora thrust act as a structural barrier between the low

strain rate and the high strain-rate zones. There are two low strain-rate (LSZ) corridors in the Garhwal-Kumaun region; namely the Ramganga-Baijro and the Nainital-Almora in the Sub and the Outer Lesser Himalaya as potential zones, where no Major or Great earthquakes had occurred for the last 200 years. Interestingly, a purely extensional deformation zone (EDZ) exists in the Kumaun frontal Himalaya, where the strain transfer along the MHT diffuses and may lead to the active deformation of the Himalayan frontal thrust systems.

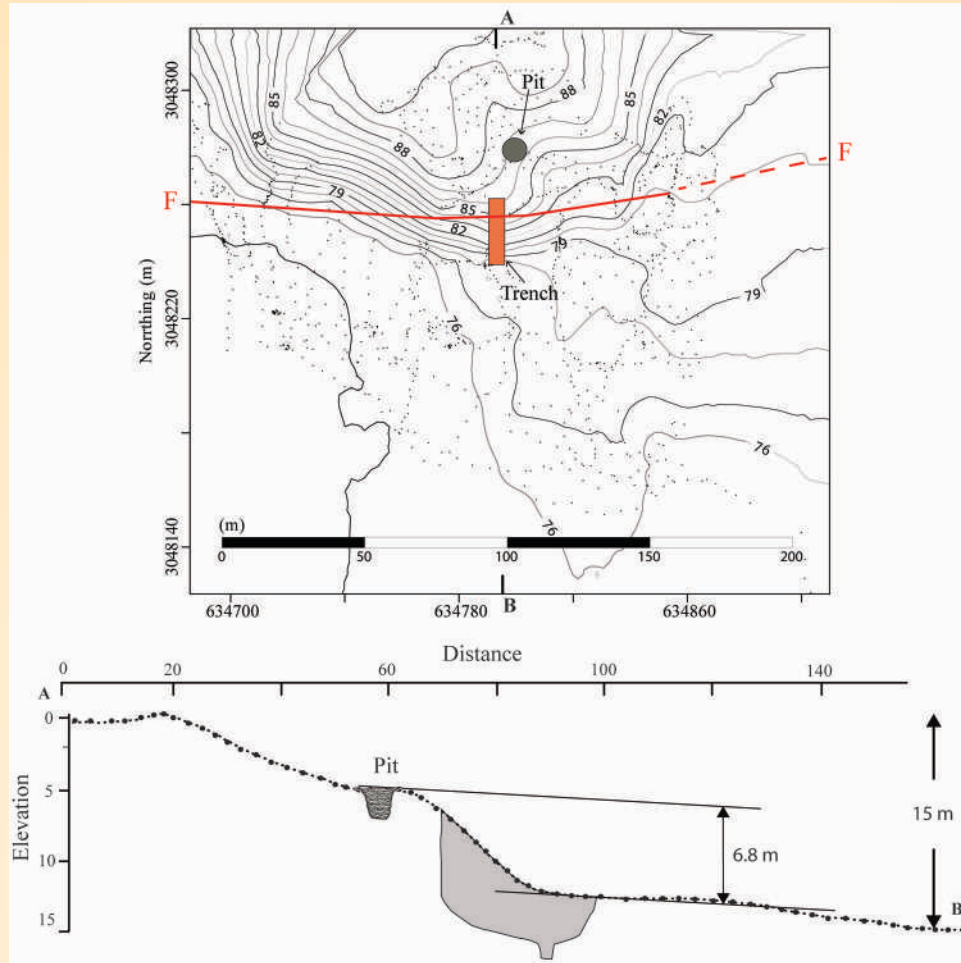


Fig. 51: Topo-profile across the trenched fault scarp.

Present-day kinematics of the HFT and the adjoining Ganga Tear Fault (GTF)

The long-term geological deformation as uplifts or subsidence rates were observed at the Himalayan frontal thrust systems in the proximity of GTF through Paleoseismological investigations. This evinces interest to know whether the HFT is active during the inter-seismic short-term geodetic time scale, and what is the nature of deformation of the connected systems like GTF in the midst of overall plate level kinematics? To study the present-day kinematics of the HFT and the adjoining GTF, we took repeated GPS measurements and estimated the crustal velocities along with the permanent GPS measurements in the study area, and shown in figure 54.

Figure 54 elucidates the regional picture of the velocities in the frontal Himalaya and the adjoining GTF, particularly at the Chandi and Mansi hills in the Haridwar region. Velocity estimation from 5 GPS stations (3 CORS and 2 Campaign) are plotted in figure

54. Where the red arrows indicate the resultant horizontal velocities of the sites in the Indian reference frame and the blue arrows represent the vertical movement. Stations situated at the east of the Ganga tear fault CHDI and HARI at the north and south of the HFT; respectively, show northwest movement. Whereas the Western stations of the GTF; namely, MNSI and the BIHA situated at the north and the south of the HFT show southeast movement. This shows that both the blocks at the west and the east of the GTF show opposite movements in tandem with the along the arc movement of the HFT. Thus the present-day kinematics of the HFT is dominated by the arc parallel movement; whence the much-anticipated along the strike-slip movement of the Ganga Tear is abysmally low. This implies the inactive nature of the tear kinematics of GTF.

We also observed that stations, except HARI, situated in the Ganga basin show uplift in their vertical component and it can relate with the activity of the HFT. TSWI station in the alluvial-filled Doon valley shows a horizontal movement of 1.62 ± 0.1 mm/yr toward the

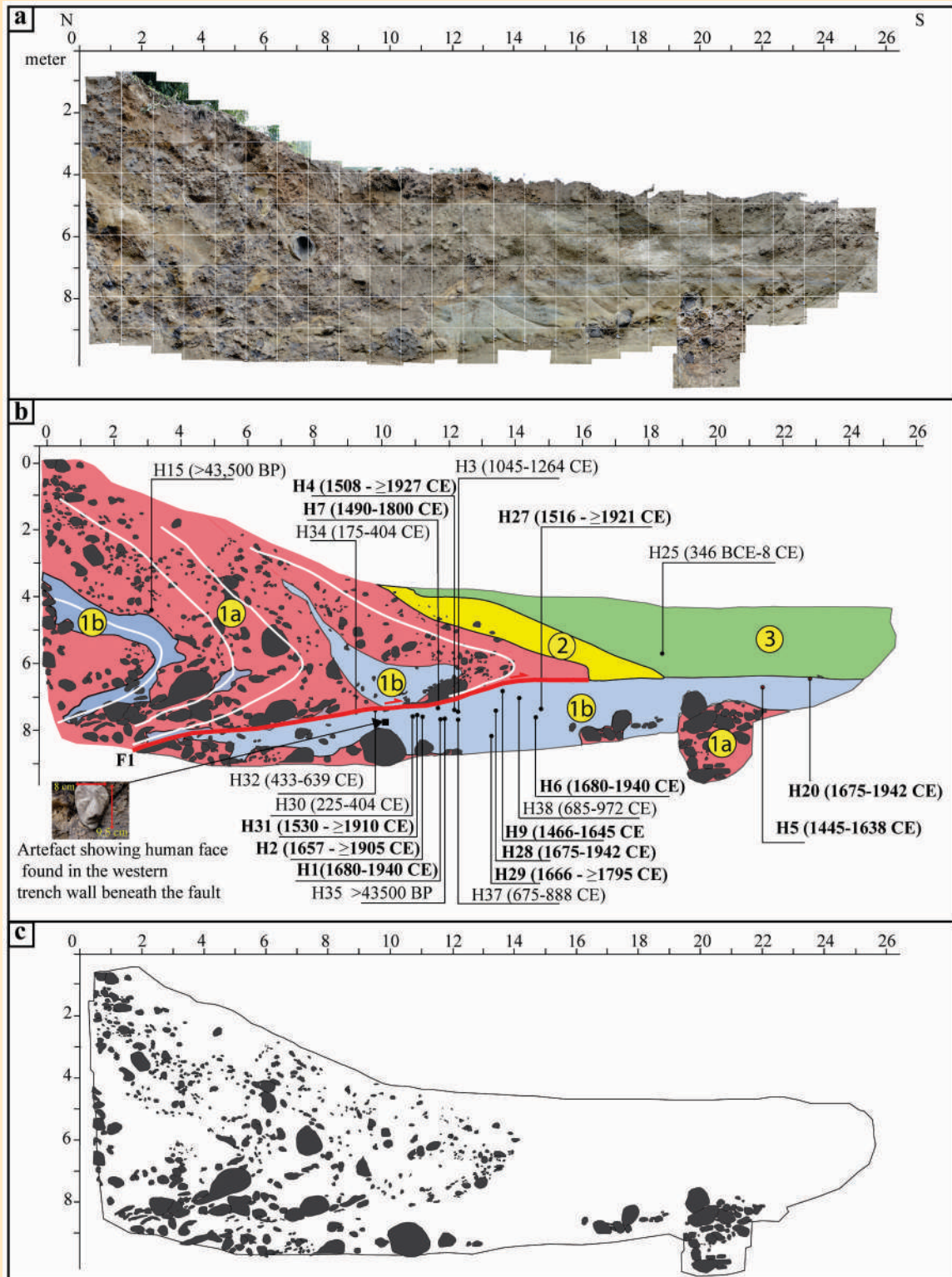


Fig. 52. Photomosaic of the excavated trench exposures at Himebasti, (middle) Interpreted log, and (bottom) deformed fabric showing south verging fold.

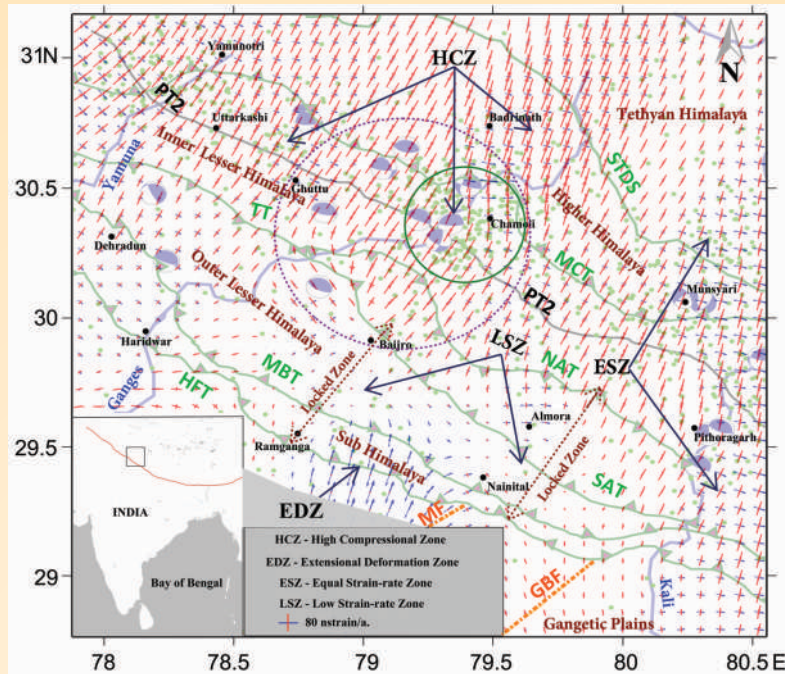


Fig. 53: Estimated surface strain-rate pattern in the Garhwal-Kumaun Himalaya from GPS crustal velocities. The dotted encircled area represents the observed curvilinear strain-rate pattern around the Chamoli Earthquake cluster. The solid green circle area represents the Chamoli Earthquake cluster.

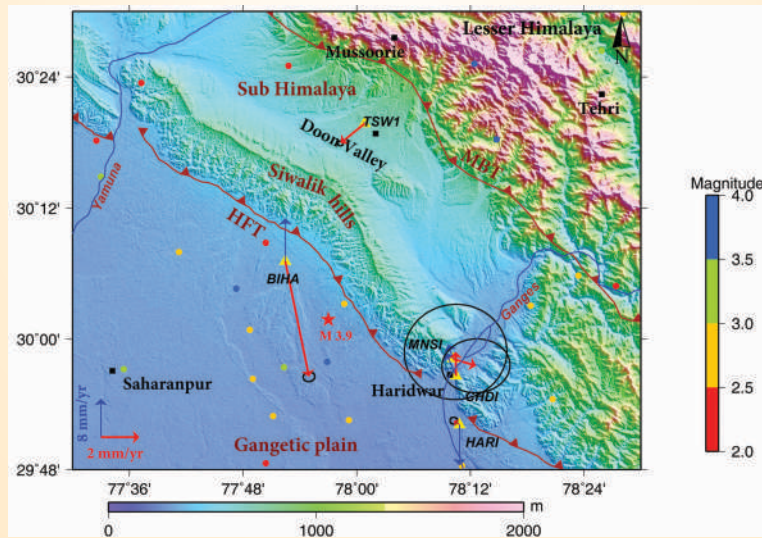


Fig. 54: GPS measured horizontal and vertical deformations of HFT and the adjoining GTF.

southwest direction and it is uplifting at a rate of 0.39 ± 0.2 mm/yr. By analyzing the vertical motion of stations in the north and south of HFT (TSW1 and BIHA), the results indicate that the HFT is uplifting at a geodetic rate of 8.58 ± 0.7 mm/yr and the rate of uplift is in near correlation with the geological uplift rates of the HFT (6.9 ± 1.8 mm/yr). From the study, it is clear that the HFT is active and the recent earthquake (M 3.9) that occurred NW of Haridwar also supports the active nature of the HFT in the study area.

Exhumation Studies in the Central Arunachal Himalaya

Thirty-eight new apatite and zircon fission-track ages from twenty-six bedrock samples vary from 2.0 ± 0.3 to 12.1 ± 1.2 Ma, and 3.3 ± 0.3 and 13.2 ± 0.7 Ma, respectively along three transects of the Kurung, Subansiri, and Siyom Rivers, which flow across the major structures of the Arunachal Himalaya. These cooling ages reveal marked variations in millennial-

scale ($> 10^5$ yr) exhumation rates from 0.6 to 3.0 mm/yr. A distinct positive correlation is visible between local topographic relief, hill slopes, channel steepness, and exhumation rates. The cooling ages are younger in the northern antiformal domains and older within the synformal nappe along the mountain front. Thermal modeling and time-temperature paths suggest that zones of rapid exhumation are controlled by structural windows within the Lesser Himalaya that were

developed between 8 and 6 Ma over blind Main Himalayan thrust (MHT). This time of rapid rock uplift and major topographic change led to a two-fold increase in the exhumation rates in the northern antiformal domains than the southern front of Arunachal Himalaya. Variation in cooling ages does not correlate with the present-day precipitation pattern. Tectonics appears to be the leading factor in driving the exhumation rates and landscape evolution in the Arunachal Himalaya.

SPONSORED PROJECTS

Multi-Parametric Geophysical Observatory (MPGO), Ghuttu Garhwal Himalaya for Earthquake Precursory research

(Naresh Kumar (PI), Gautam Rawat, Devajit Hazarika and P.K.R. Gautam)

Multi-Parametric Geophysical Observatory (MPGO) at Ghuttu, Garhwal Himalaya is established with the main objective of earthquake precursory research in an organized and integrated manner. Temporal variations of different geophysical parameters at a high sampling rate (0.01 s to 15 min) are being collected at two sites Kopardhar and Dhopardhar.

Seismic activity in the vicinity of MPGO Ghuttu

The MPGO Ghuttu site is located near the MCT where the seismic activity is high and mainly focused on the upper crust. Detailed information of the small and moderate magnitude earthquakes ($M \geq 3.0$) that occurred within 300 km distance from the MPGO observatory for the year 2020-2021 (Fig. 55) is used for observation of anomalous pre-seismic variations and assessing its relation with the seismic index. The seismic index is calculated for each selected earthquake to assess the effect of the earthquake by its size and distance. This parameter is proportional to the earthquake seismic energy in the observational point and is computed using formulae (Molchanov *et al.*, 2003):

$$K_s = (1 + R^{-M/2})^{-2.33} \times 10^{0.75M} / 10R \quad (i)$$

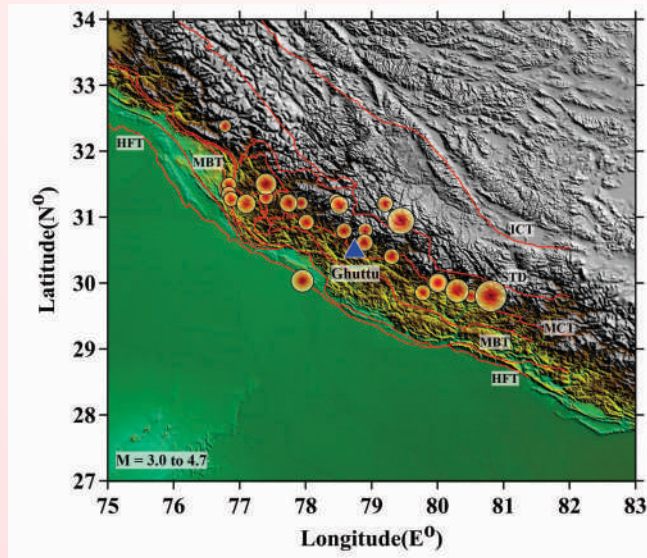


Fig. 55: Epicentres of all earthquakes of magnitude ≥ 3.0 occurred within a 300 km distance from the MPGO, Ghuttu during 2020-2021.

Where R = distance from the observation point and M = Earthquake magnitude.

The information of earthquake epicenter distance, magnitude, and seismic index is also plotted in figure 55. for the local seismic events. These criteria are adopted to search the anomalous behavior before the occurrence of the earthquake.

Assessment of different components of borehole and atmospheric data set

Continuous data of different parameters recorded in two different boreholes of 10 m and 68 m depth at two nearby locations (Kopardhar and Dhopardhar) is plotted in figure 56 as temporal variation observed during 2020 and 2021. The earthquakes ($M \geq 3.0$) that occurred around MPGO Ghuttu are plotted in figures 56(a) and (b). The seismic index measured using a relation based on the epicenter distance and earthquake magnitude is shown in figure 56a. The size of the red star denotes the magnitude of earthquake events (Fig. 56b) while its y-axis scale represents the epicentral distance from MPGO, Ghuttu. The temporal variation of radon emanation in the soil is shown in figure 56(c). The other meteorological and hydrological parameters like level of the water table, rainfall precipitation, subsurface temperature measured at different depths within the borehole, atmospheric temperature, and atmospheric pressure, etc. are also plotted simultaneously in Figure 56. The whole data set indicates a small number of anomalies in the soil radon before the monsoon period which is seen to be the result of rainfall. During the monsoon period, high changes are observed in the radon concentration because of changes in the water level and changes in the pores of the soil which get saturated with water, and therefore other anomalies are suppressed. The sub-surface temperature at 30 m shows declination in the starting months of the year and then increases after the monsoon period to a normal level while at 50 m depth remains almost constant throughout the year. Increasing depth decreases the amount of temporal change in the temperature. Atmospheric temperature and atmospheric pressure have very high daily fluctuations interlinked with each other and influenced by solar radiations. These two parameters also show annual variation suggesting seasonal changes.

The changes are noticed in the radon concentration but the effect seems to be less. During the monsoon period, July to September, there is high rain

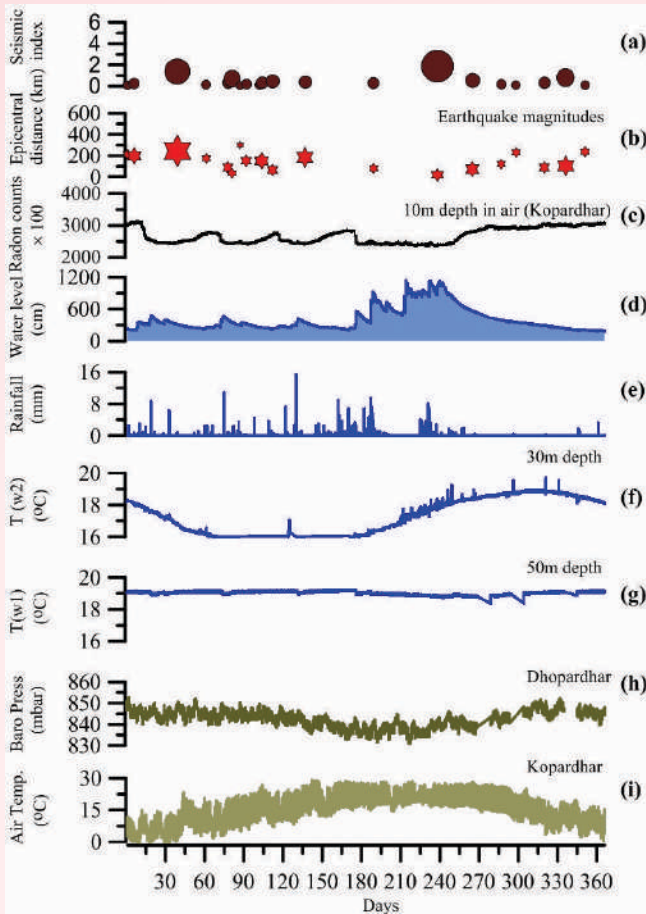


Fig. 56: Plots of the borehole time series of 2020 along with earthquake information. (a) seismic index (b) earthquake epicenter distance and magnitude (c) soil radon (d) water level (e) rainfall (f) temperature 30 m depth (g) temperature 50 m depth (h) atm Pressure (i) atm. Temperature.

precipitation during which changes in the water level measured through 68 m borehole is highest. The soil radon concentration is also highly changed in this period suggesting a drastic change in concentration and also high fluctuations. It indicates that the radon, an inert gas varies due to the hydrological changes. There is a need to recognize these seasonal and short period trends and remove them from the radon data to assess the changes associated with seismic events. Attempts are made in the past to recognize these and separate them from the data.

It can be stated that in the time series of more than six years of data the water radon fluctuation during the Kedarnath disaster is peculiar and on scanning the whole data set the event can be recognized easily. This analysis of anomalous behavior in radon is not only important for the Kedarnath event but it is also important to the earthquake precursory point of view for which this observatory in the Garhwal Himalaya within a high seismicity zone is established.

Our main objective is to extract the anomalous precursory signatures from the continuous-time series of the soil radon. However, the radon also has a variation with other hydrological and environmental parameters (Fig. 56). Our research work reported in many publications of this data set suggests that it has a strong effect on hydrological changes in addition to the effect of atmospheric pressure and temperature along with the temperature difference of outside and inside of the borehole (Chuahan *et al.*, 2021). This recent work (Chuahan *et al.*, 2021) is also reported here. With these effects, the radon also shows semi-diurnal, diurnal, and seasonal variations.

Shukla *et al.*, (2021) utilize these techniques to remove the above-mentioned effect from the radon time series which works well for the period other than monsoon. A new time series generated by removing the effect, the statistical approach is applied to extract the anomalous changes induced by the local seismic events within 300 km which are mostly of moderate and lower magnitude from 2011 to 2017. In this work, the data has experimented with 11 earthquake events. Six earthquakes in the magnitude range 4.5-5.8 show the precursory signatures located close to the recording station. Now we continue this process with this data set to extract these signals on regular basis. We also assess the 27 earthquakes data of 2020-2021 of maximum magnitude 4.5. We got the precursory signatures during the occurrence of two earthquakes. These earthquakes are having magnitudes ≥ 4.0 located within/ 200 km distance from the stations. The anomalous signatures are reported in this data set but also sometimes some changes are not seismic but influenced by other effects.

Multiple linear regression analysis of Radon data

As stated earlier that the radon data is affected by other parameters, therefore to remove their effect, we applied the multiple linear regression analysis. As we know that regression analysis is used to compute the correlation between two or more variables. The regression using one single independent variable is called univariate regression analysis while the analysis using more than one independent variable is called multivariate analysis. The equation of the multivariate regression model is as follows;

$$y = \beta_0 + \beta_1 x_1 + \dots + \beta_n x_n + \epsilon$$

- where y = dependent variable
- x_i = independent variables
- β_i = parameters
- ϵ = error

To calculate the regression model equation, first, we did some pre-analysis steps. Apart from radon data, which is considered as a dependent variable, we have the data of a total of five other parameters including water level, atmospheric pressure, rainfall, air temperature, and temperature at 10m depth. We also calculated the difference of air temperature (T_{out}) and temperature at 10m depth (T_{in}) and used it as one more parameter. To understand the relationship of soil radon with other parameters we applied the regression analysis and calculated the correlation coefficients (Corr. Coeff.) and the results, for the year 2019. The maximum negative correlation (Corr. Coeff. = -0.7) is found between radon and water level. The soil radon is also showing a good negative correlation (Corr. Coeff. = -0.6) with air temperature while a good positive correlation with atmospheric pressure (Corr. Coeff. = 0.5) and difference of inner and outer temperature (Correlation coefficient = 0.6). The temperature at 10m depth and rainfall are not showing any correlation with soil radon. Further, we created the different models by varying training periods and input variables (Fig. 57). The models created using individual parameters show the lowest error and high correlation coefficient in the case of water level while high errors with other individual inputs. Further, the regression equation, generated using six input parameters, is employed to calculate the theoretical values of soil radon for both the training and testing periods (Fig. 58). A large deviation before the rainy season is also observed between 26 February and 27 April 2015, even after removing all effects. It is to be noted here that the devastating

Gorkha-Nepal earthquake (M 7.8) was struck in the central part of the Nepal Himalaya on 25 April 2015. As it can be seen from the above-mentioned observations that the multiple linear regression analysis can minimize different kinds of effects from radon data considerably. However, still, there is a scope for applying more rigorous modeling. Therefore, the work on more elongated modeling techniques like artificial neural networks (ANN) is in process.

Gravity data recorded by Superconducting Gravimeter (SG)

Continuous measurement of gravity is performed at MPMO, Ghuttu through a superconducting gravimeter. Highly sensitive gravimeter records variations to microgal level. The data is processed to evaluate temporal changes in gravity indicating the influence of tidal forces, atmospheric pressure, and hydrological effect. Past data of over seven years has been already used to establish relations to detect the changes inferred due to solid earth tides and atmospheric pressure. It has been used to refine the tidal model for this station. At this site, the tidal forces insert maximum gravity changes to the order of 300 microgal. Changes due to the atmospheric pressure admittance is 3.3 mbar/(Nm/s²). These terms and already adopted methodologies are applied to eliminate these orderly daily, monthly, and seasonal trends of external fields from the recorded gravity data (Fig. 59). De-trend residual gravity data indicates annual variations of the order of 300 Nm/s² and some abrupt changes of low amplitude. These changes are mostly related to the hydrological effect due

SPONSORED PROJECTS

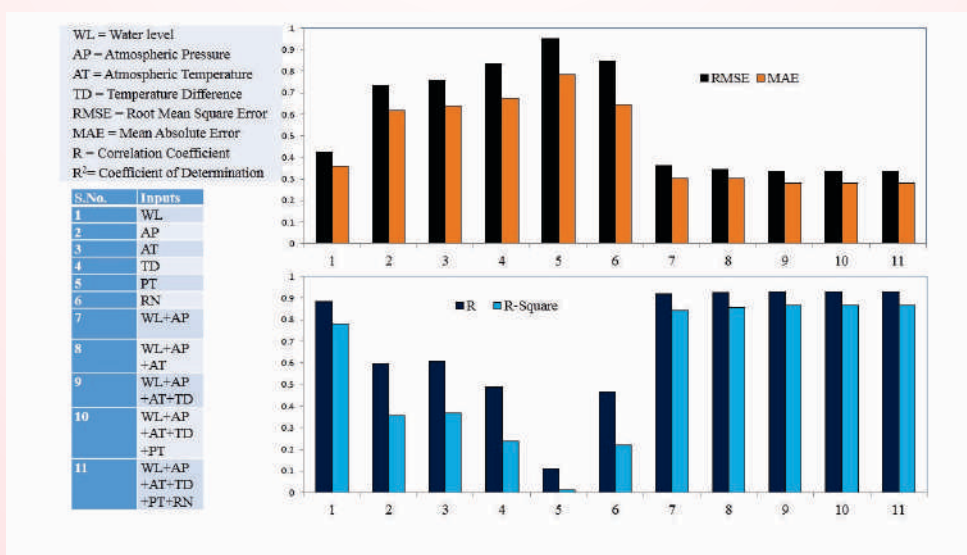


Fig. 57: The estimated errors (upper panel) and correlation coefficients (lower panel) of created models by varying input parameters.

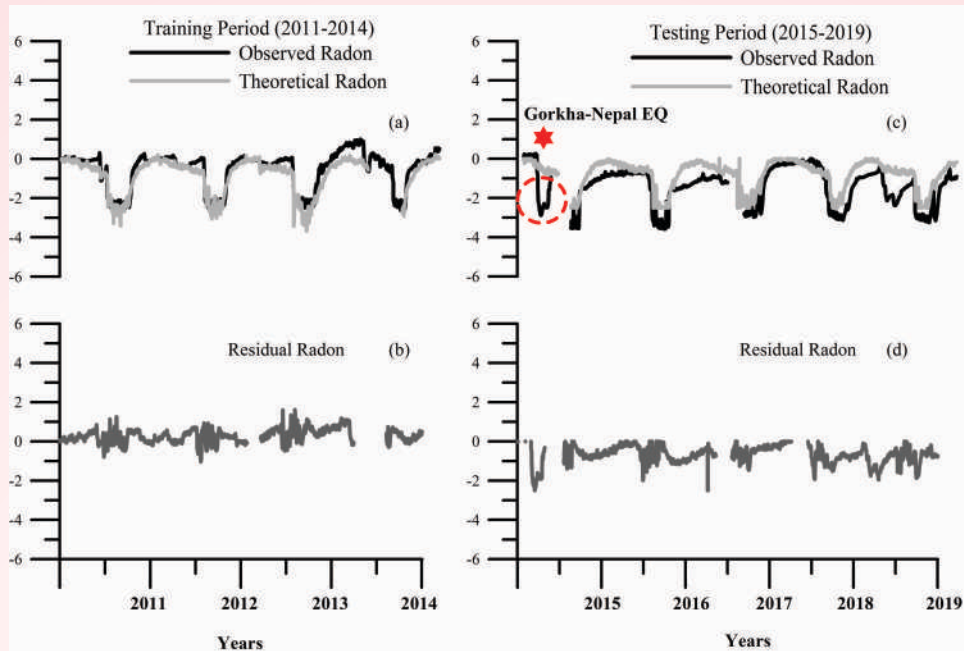


Fig. 58: (a) Plot of observed radon and theoretical radon for the training period (2011 -2014), (b) residual radon for the training period, (c) plot of observed radon and theoretical radon for the testing period (2015 -2019), the star is showing the day of Gorkha-Nepal earthquake (M7.8) of 25 April 2015, (b) residual radon for the testing period.

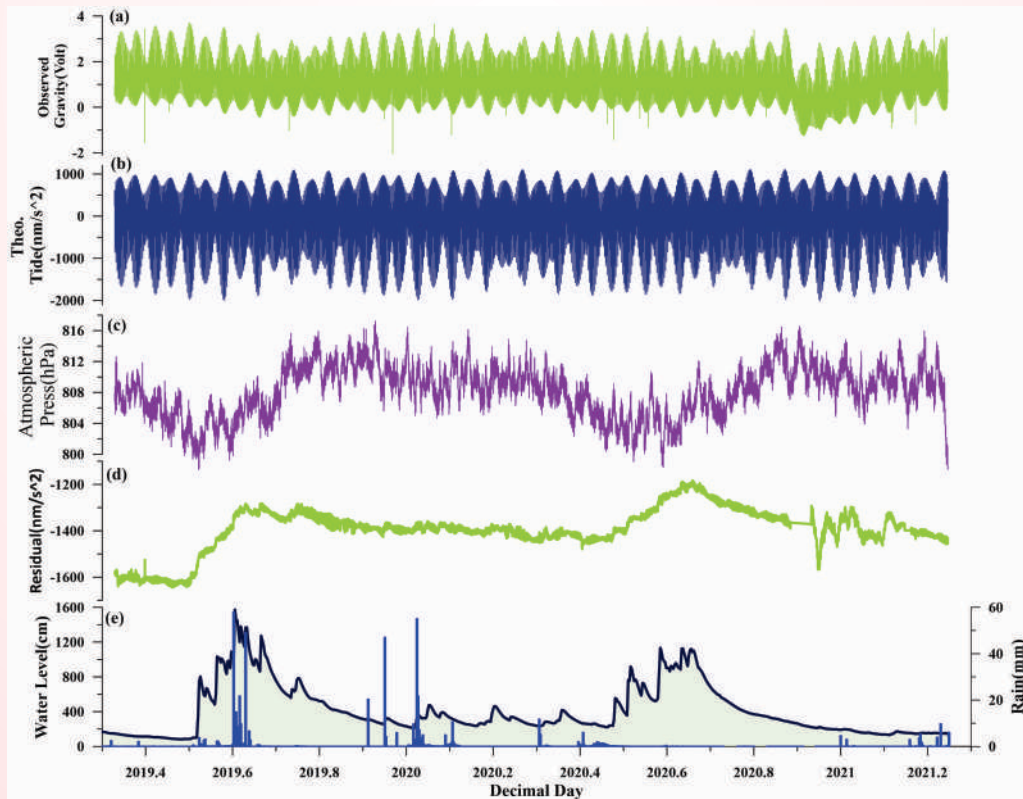


Fig. 59: Annual variation of rainfall and water level in a borehole and its effect on Superconducting gravimeter data observed at MPGO Ghuttu from 2019 to January 2021. (a) observed gravity data (b) Theoretical tides (c) atmospheric pressure (d) residual of gravity after removing the effect of tide and atmospheric pressure, and (e) rainfall and water level.

to the charging and discharging of the groundwater level with the occurrence of rainfall. The annual variations are well correlated with the changes in the water level observed using an underground water level monitoring probe in a 68 m deep borehole. The residual after removing these effects is also used to evaluate Free Earth Oscillation at the time of occurrence of large magnitude earthquakes anywhere in the world. It shows seasonal/annual changes well correlated with the water level and the rain precipitations (Chuah *et al.*, 2016). Loading effects on the Earth's uppermost crust due to the hydrological cycle, as measured from the local water record are advocated for these changes. Our previous work reports that the annual cycle of the gravity variation is in phase with the water level while the vertical crustal motion has an opposite phase.

The occurrence of a large magnitude (~ 8.0) earthquake causes a sudden release of energy to set the entire Earth into vibration. The natural frequencies of these free oscillations are determined by the elastic

properties and the interior structure of the Earth. This vibration produces three-dimensional deformation due to free oscillations of the Earth's spherical shape. These oscillations are categorized into three forms as radial, spheroidal and tangential. In this free oscillation, the shape of the Earth remains "spherical" where all particles vibrate purely radially. The nodal surfaces of higher modes are also spheres internal to the Earth and concentric with the outer surface of the earth. Spheroidal oscillation involves both radial and tangential displacements that can be described by spherical harmonic functions. These functions are referred to as an axis through the Earth at the point of interest, and to a great circle that contains the axis. For this reference frame, they describe the latitudinal and longitudinal variations of the displacement of a surface from a sphere.

The higher-order free oscillations of the Earth are related directly to the two types of surface waves. The similarity between surface waves and higher-order

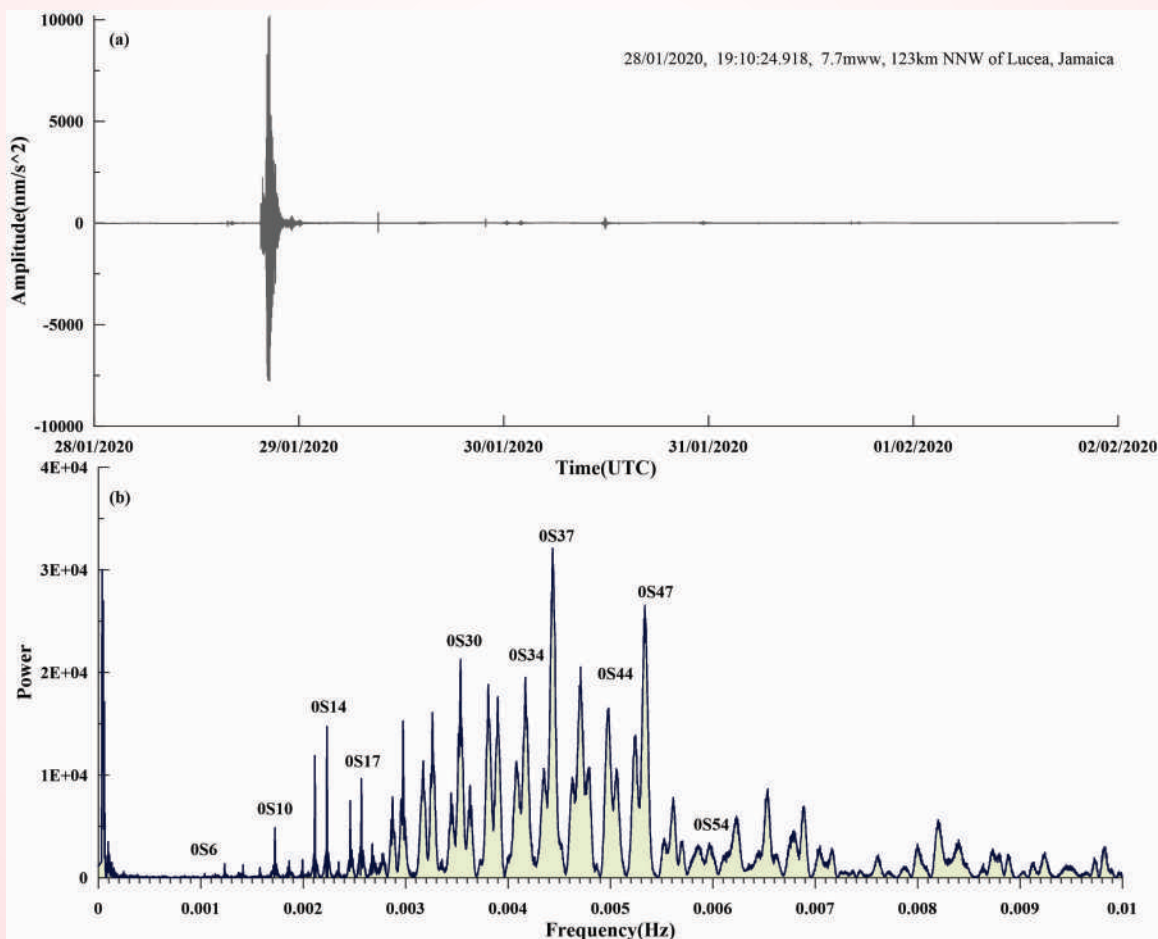


Fig. 60: Free Earth Oscillations (FEO) obtained using the gravity data during Mm7.7 earthquake Lucea Jamaica occurred on 28 January 2020. (a) Observed gravity variation (b) Power spectrum obtained using 120 hours continues time series data and Hann window.

natural oscillations of the Earth is evident in the variations of displacement with depth. The Superconducting Gravimeter records the vertical component of gravity variation and therefore only spherical modes of free oscillations are observed at MPGO Ghuttu. The data is recorded at 1 SPS, the free oscillations obtained for the frequency range 1 to 6 miliHz are shown in figure 60. On 28 January 2020, Mw 7.8 earthquake occurred in Jamaica close to the Lucea. The gravity data of the MPGO station is used to obtain the fundamental spheroidal Free Earth Oscillations from the vibrations initiated due to this earthquake. Continuous data of four days period after the high

oscillations are used for this analysis. The gravity variation for this period is shown in figure 60a where the peak variations are co-seismic vibrations. The power spectra of the post-earthquake data obtained through the Hanning window are plotted in Figure 60b. Many free earth oscillations between 0S6 and 0S45 are evident in the power spectrum. Some other higher-order oscillations are also recorded. High amplitudes are obtained for 0S37, 0S47, and 0S13 free earth oscillations. In the past also we have used more than 10 large magnitude earthquake data to obtain the free earth oscillations.

SPONSORED PROJECTS

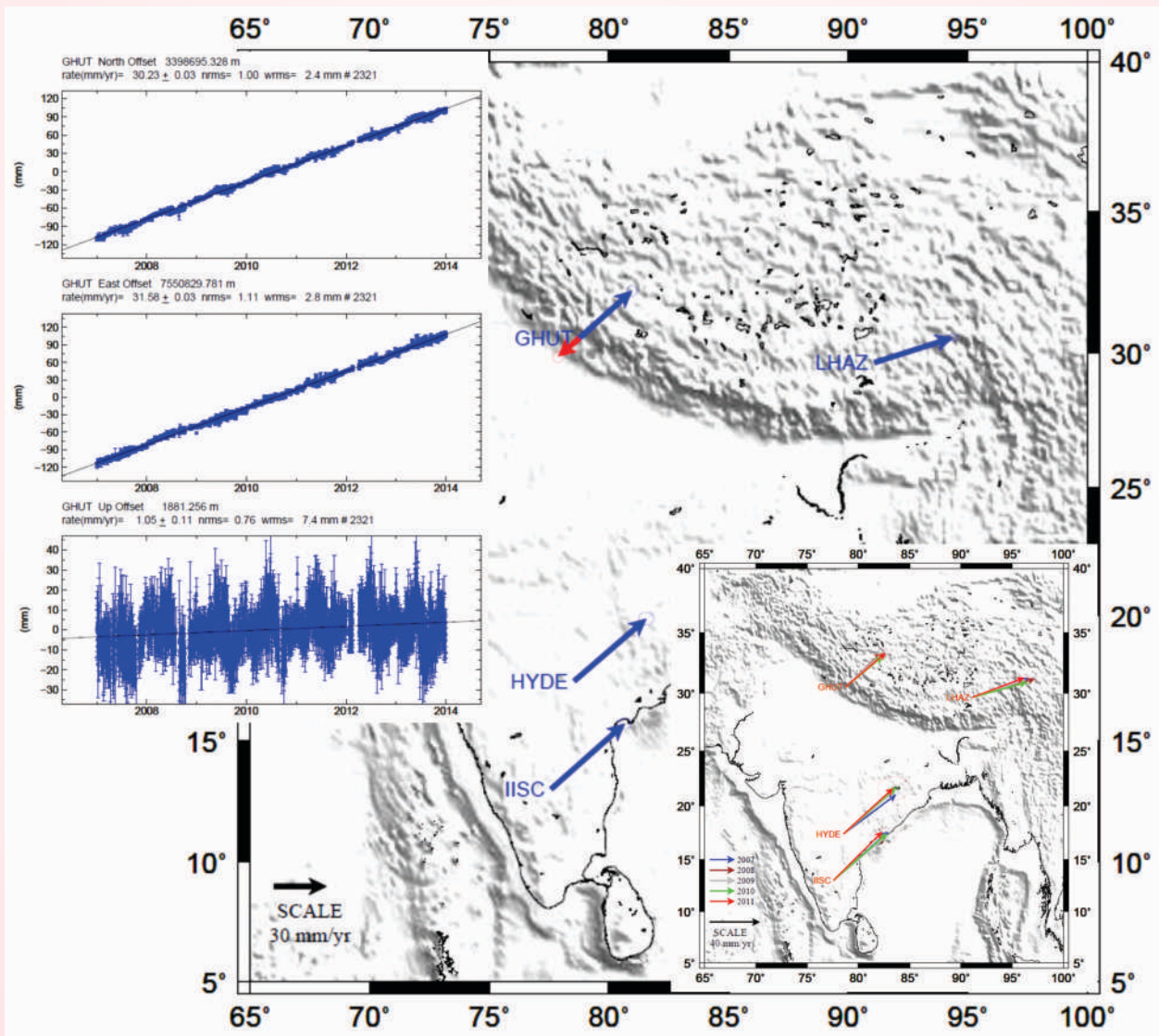


Fig. 61: In the base map (a) blue arrows pointing toward the northeast show the station velocities in ITRF08 Reference Frame and a red arrow pointing towards the southeast is the velocity estimated for GHUT station with reference to IISC. Top-left Inset (b) shows the time series of GHUT and the right-below inset (c) illustrates the yearly motion pattern of GHUT station (in color vectors) along with IGS stations in ITRF08.

Global Positioning System

We investigate the surface deformation pattern using data of the GPS station at M_{PGO} Ghuttu (GHUT) to find out the cause of anomalous behaviors in the continuous GPS time series. Over seven years GPS data has been analyzed using GAMIT/GLOBK software and generated the daily position time series. The horizontal translational motion at GHUT is 43.7 ± 1 mm/yr at an angle of $41 \pm 3^\circ$ towards NE, while for the IGS station at LHAZ, the motion is 49.4 ± 1 mm/yr at $18 \pm 2.5^\circ$ towards NEE. The estimated velocity at the GHUT station to IISC is 12 ± 1 mm/yr towards SW (Fig. 61). Besides, we have also examined anomalous changes in the time series of GHUT before, after, and during the occurrences of local earthquakes by considering the empirical strain radius; such that, a possible relationship between the strain radius and the occurrences of earthquakes have been explored. We considered seven local earthquakes based on the Dobrovolsky strain radius (Eq.1) condition having a magnitude from 4.5 to 5.7, which occurred from 2007 to 2011 (Fig. 62). Results show irrespective of the station strain radius, pre-seismic surface deformational anomalies are observed roughly 70 to 80 days before the occurrence of Moderate or higher magnitude events. This has been

observed for the cases of those events that originated from the Uttarakashi and the Chamoli seismic zones in the Garhwal and Kumaon Himalaya. Occurrences of short (< 100 days) and long (two years) inter-seismic events in the Garhwal region plausibly regulating and diffusing the regional strain accumulation. Dobrovolsky developed the relation for the estimation of surface deformation around the epicenter zone which is given below

$$\rho = 10^{0.43M} \quad (1)$$

where 'ρ' is the strain radius in km and 'M' is the magnitude of the earthquake.

As per Eq. (1), the zone of effective manifestation of the precursor deformation on the surface of the earth is a circle with the center at the epicenter of the earthquake preparation zone.

The investigation of anomalous changes in surface deformation is analyzed from the radius of the circle. In this study data has been analyzed by considering the following aspects: although, the Dobrovolsky equation is valid for a homogeneous isotropic medium; but we attempted to implement it in the Himalayan region, where the geology is complex. We considered relatively bigger earthquake events ($M \geq 4.0$) in this data analysis.

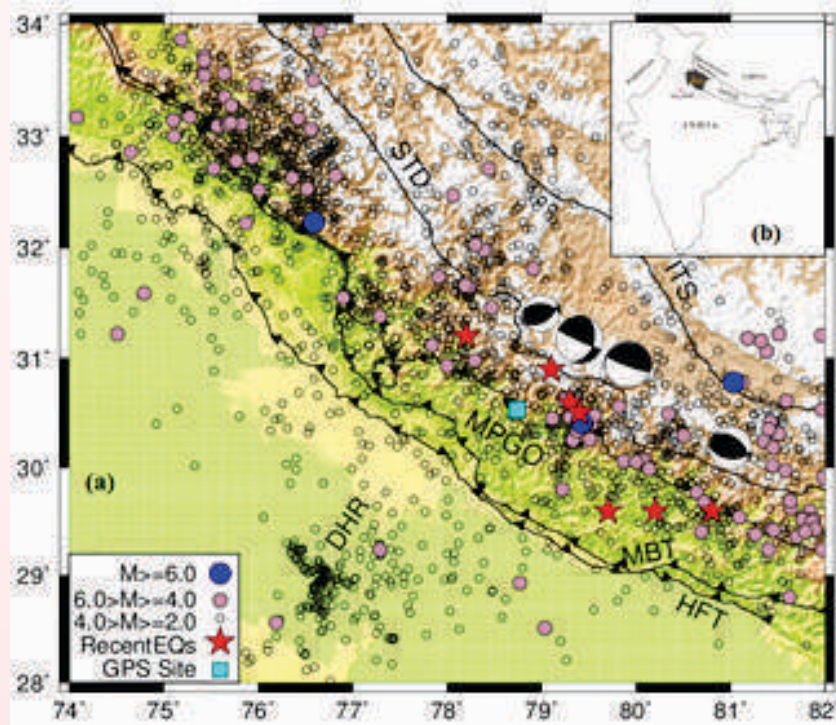


Fig. 62: Base map (a) illustrates the seismotectonic setting of the Ghuttu region with earthquake events of $M > 2.5$ from 1999 to 2010 (Lyubushin et al., 2010; Kumar et al., 2012). Focal mechanisms of recent earthquakes are shown by beach balls and red stars represent the event considered for precursory signature. Inset (b) represents the map of India with International boundaries and the black shaded portion shows the study area Garhwal-Kumaon Himalaya in Uttarakhand, India.

Accordingly, seven earthquake events of magnitude range from 4.5 to 5.7 shown with a red star in figure 62 are selected to identify their precursory signatures.

We assume that if any GPS station lies within the strain radius, then the horizontal positional variation should be affected comparatively more to those stations that lie outside the ambit of the strain radius. Based on the aforementioned criteria five years of continuous time series data has been analyzed to understand the behavior of positional changes, if the earthquake happens within or outside the ambit of the strain radius from the GHUT station. Analysis of daily time series of each year has been plotted individually to identify the precursory signatures in deformation from the anomalous changes in the time series.

A detailed method of analysis is described by Gautam et al., (2020). Estimated earthquake source parameters such as magnitude (M), focal depth (Fd), epicentral distance/distance of GPS station from the earthquake epicenter (Ed), and strain radius (ρ) are also mentioned in the format of (M, Fd, Ed, ρ). Each data consists of three subplots with the top plot represents the N-S positional anomaly components, while the subsequent mid and lower plots represent the E-W and the vertical components respectively. Velocity estimation of GHUT station shows the uncertainty of 1 mm/yr in the horizontal component, whereas large errors are present in the vertical component.

GPS data with earthquake epicenter and strain radius calculated based on Eq. 1 is assessed in the form of two case studies. In the first case study, we considered the GHUT station is within the radius of the earthquake preparation zone (ρ), while in the second case, only those earthquakes that are far from the station, and at a greater distance from the radius of the earthquake preparation zone. Accordingly to the analysis the Uttarkashi (M 5.0) and the Chamoli (M 4.5) had occurred after a relatively long (two years) quiescent or a long inter-seismic period and produced nearly consistent pre-seismic duration of 78 and 75 days of deformational precursory. The shift in the station surface deformational anomalies caused by those far events (events '2' and '5' originated from Pithoragarh) from the strain radius show concurrent variation in the pre-seismic anomaly trend (initiated around 42 days before the events) of north and east component offsets, but with enhanced offset towards the east component. Our observations suggest that in general the MPOG-Guttu is appropriately located to study the deformational precursory characteristics of those moderate or greater magnitude earthquakes that

occurred within or outside the station strain radii in the Garhwal region; especially, from the well-known seismic zones in Uttarkashi and Chamoli in the Garhwal and Kumaun Himalaya.

MoES Sponsored Project

Seismic monitoring and seismological parameters evaluation in the Garhwal-Kumaun region of Himalaya

(Ajay Paul)

The Garhwal-Kumaun region (29°-31.5°N; 77°-81°E) in NW Himalaya lies in the Central Seismic Gap where the accumulated strain energy is sufficient for a future great earthquake. This region lies between the two great earthquakes viz. 1934 Bihar Nepal earthquake and 1905 Kangra earthquake. A seismic network of seven stations is deployed to monitor the seismic activity in the Garhwal-Kumaun region of Northwest Himalaya. The seven-station broad band network is equipped with the Trillium-240 seismometer with a high dynamic range (>138 dB) and Centaur data acquisition system (DAS). The data is recorded in continuous mode at 100 samples per second. High-accuracy GPS synchronizes the DAS clock every minute. The network was initially installed in 2007. The data has been acquired till November 2020 and the detailed earthquake event analysis has been carried out for events till 2018. The total numbers of events recorded are more than seventeen thousand (17,000) which includes local (3634), regional (5282) and teleseismic (8270) events. The well-located local events are plotted on the tectonic map of Garhwal Himalaya justified within the acceptable error bars (ERZ, ERH <5.0). The seismicity plot indicates that the majority of earthquakes are occurring in a narrow zone, south of MCT with focal depth up to 25 km and in the magnitude range between 1.8 to 5.7. We examined the spatial variation of the b-value in the entire region (29°-31.5°N; 77°-81°E) and identified three different zones (Zone A, Zone B and Zone C in figure 63) on the basis of events clustering and b-value characteristics. The obtained b-values for Zone A (Uttarkashi region), Zone B (Rudraprayag-Chamoli region) and Zone C (Kumaun region) are 0.737 ± 0.04 , 0.702 ± 0.03 and 0.97 ± 0.07 , respectively. The results revealed that the proximity of the Rudraprayag-Chamoli region exhibits a significantly low b-value (0.702 ± 0.03) and Dc-value (1.38 ± 0.03) and indicates high-stress accumulation. This region is triggered by the 1999 Chamoli earthquake Mb 6.3 and the 2017 Rudraprayag earthquake M 5.7. We also estimated b- and Dc-value separately for the MCT zone and south of MCT. The inferences based on the spatial and temporal variation indicate that south

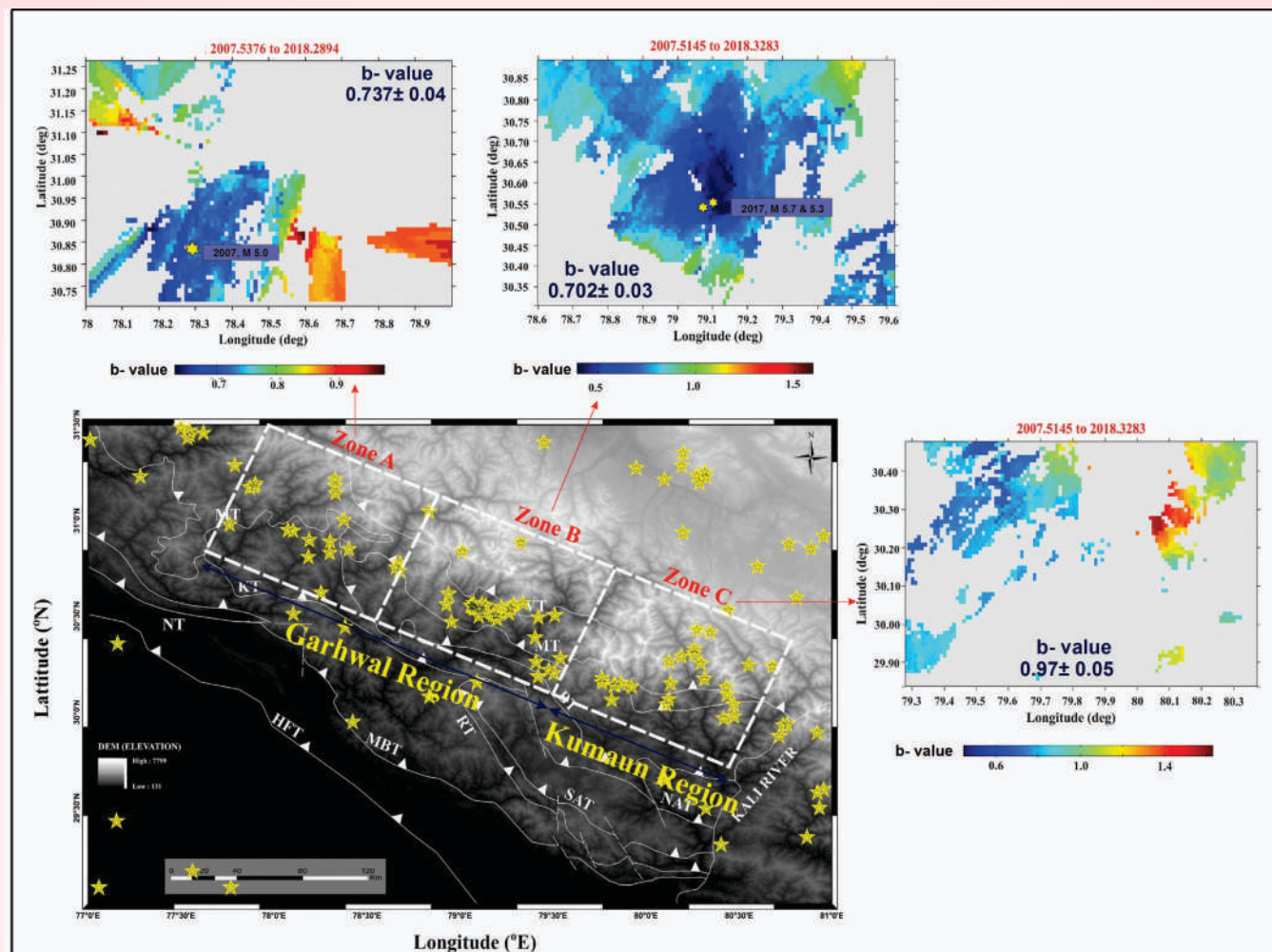


Fig. 63: Figure shows the epicentral locations (2007-2018) of local earthquakes ($M_L > 3.5$). Spatial distribution map of b-value for Zone A, B, and C.

of the MCT (Inner Lesser Himalaya) is more pronounced by homogenous seismic distribution and accumulates high stress than the MCT zone along the strike. The significant changes of b-value with time are observed during the moderate size of the earthquakes in the region. A detailed study of b-value and Dc-value variation as a function of depth is also examined.

In figure 64, depth-wise estimation of b-value suggests that Zone B of Rudraprayag-Chamoli province shows a high degree of variation as compared to Zone A and Zone C. Zone B depicts the minimum b-value < 0.7 at depth $\approx 12-14$ km. In 2017, two moderate size earthquakes of $M_L 5.7$ (6th Feb) and $M_L 5.3$ (6th Dec) magnitudes occurred in this region with focal depths

13.5 km and 14 km, respectively. In addition, the majority of the moderate size of earthquakes occurred in a narrow zone of this region with a depth range of 12-15 km. The trend in a sudden escalation of b-value at the depth of ~ 12 km indicates that the zone is behaving as a transition zone of stress variation and 12-15 km as an asperity zone for significant ruptures composite trend in the abrupt escalation of b-value is observed at depth ~ 12 Km for Garhwal region and ~ 7 km for the Kumaun region. A good demarcation of crustal heterogeneity, high-stress regime, and associated seismogenic asperity is plotted. The low b-value and Dc-value depth ranges are coinciding with the mid-crustal ramp and exhibiting a potential zone (12-15 km) for a future great earthquake in the Garhwal region.

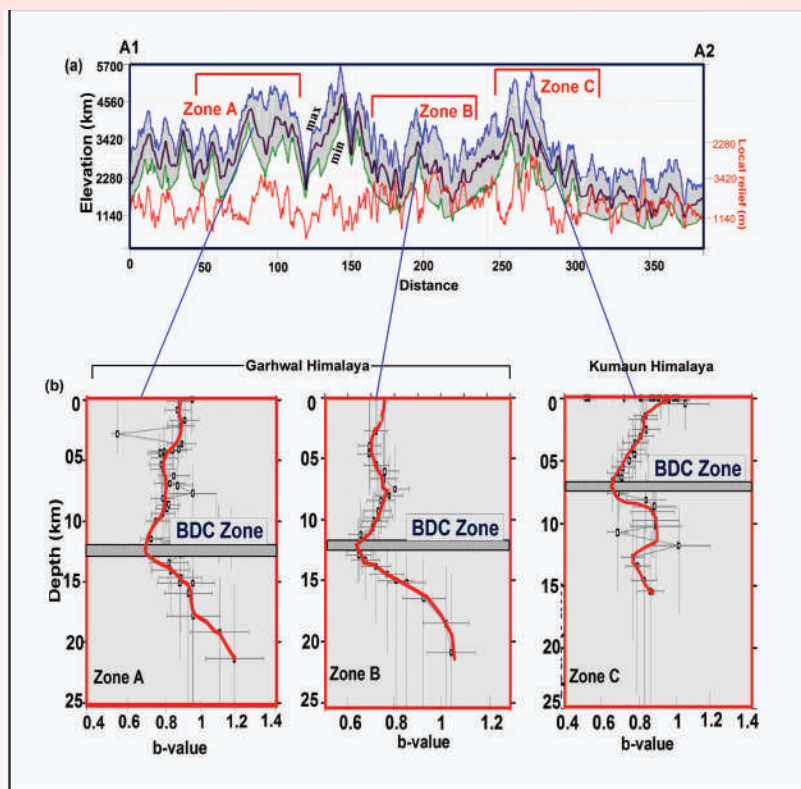


Fig. 64: A well demarcation of crustal heterogeneity, high-stress regime, brittle-ductile transition, and associated subsurface seismogenic asperities for a future great earthquake is plotted in three different zones of the region.

MoES Sponsored Project

Landslide hazard assessment in NE India along the Gangtok-Tsomo/Changu Lake and Gangtok-Chungthang-Lachen corridors

(Vikram Gupta)

This is a joint Indo - Norwegian Project involving Reginald L. Hermanns, John F. Dehls, and Ivanna Penna from Geological Survey of Norway (NGU), Trondheim, Norway, Dr. R.K. Bhasin from Norwegian Geotechnical Institute (NGI), Oslo, Norway, Dr. Aniruddha Sengupta from Indian Institute of Technology, Kharagpur, India and Dr. Vikram Gupta from Wadia Institute of Himalayan Geology, Dehradun, India. The main objective of this project was to (i) Classifying natural rock slopes that can lead to long run-out landslides, with possible river blockage, based on their hazard and risk analysis, and the (ii) the aim is to develop a multi-approach procedure to assess unstable slopes, which will facilitate effective land-use planning

During the reporting year, the inventory of the active landslides in the area was updated and analyzed. More emphasis was given to the spatial distribution of landslides along the Teesta river in a stretch of about 95

km between Lachen and Rangpo. The assessment of landslide distribution in the area was carried out correlating the distribution of landslides with steepness index, valley floor width to valley height ratio, and the rainfall pattern. From this study, it has been observed that (i) In the Higher Himalaya along the Teesta river valley, particularly between Lachen and Chungthang, the landslides owe their origin to the higher tectonic activity. The rainfall in this zone has the least effect on the distribution of landslides as the area is located behind the orographic barriers, (ii) The landslides between Chungthang and Rang Rang are dominantly controlled by the tectonic activity and are also influenced by the higher rainfall, particularly between Mangan and Rangrang, as this area lies to the front of the orographic barrier, therefore some of the bigger landslides in the vicinity of Mangan, owe their origin to the tectonics of the area and are triggered by the high rainfall, (iii) Landslides in the Lesser Himalaya between Rangrang and Rangpo dominantly owe their origin to rainfall and not to the tectonic activities. Therefore this zone accounts for the presence of only the debris landslide.

Besides the distribution of the potential landslides along the Teesta River and its tributary has been mapped

and further classified potential landslides based on their potential for the formation of landslide dams and their stability using different geomorphic indices. These have been identified using high-resolution Tri-stereo Plaiids airbus satellite images, high-resolution satellite images on the google earth platform along with fieldwork. Further, to understand the possibility of the formation of a landslide dam and assess its stability, various geomorphic indices like morphological obstruction index, Blockage Index, Dimension Blockage Index, and Hydromorphological Dam Stability Index were calculated. In the area, 37 such landslide potential zones along the Teesta River and its tributaries that will possibly block the drainages have been identified.

SERB- DST Sponsored Project Hydrological cycle analysis in valleys of Pindari-Kafni glaciers, Kumaun Himalaya (Pankaj Chauhan)

A research project has been implemented in the capacity of a Principle Investigator (PI) titled “Hydrological cycle analysis in valleys of Pindari-Kafni glaciers, Kumaun Himalaya” sponsored by SERB, DST, Government of India (DST No: EEQ/2016/000292). The cost of the project is Rs. 20, 07, 7000/- (Twenty lakh seven thousand only). The project involves the applications of remote sensing as well as field-based real-time monitoring of meteorological data and glacial stream discharge measurement. The objectives involve

are (i) to compute the evapotranspiration at daily to interannual timescale, (ii) Analysis and quantification of discharge from Pindari and Kafni Glaciers, (iii) to calculate the seasonal and interannual water balance, (iv) Delineation and characterization of snow and ice melt, rain from Pindari, Kafni glaciers using stable isotopes, and separation of hydrograph through isotopic methods, (v) Estimation of suspended sediment concentration and suspended sediment load.

The Pindari and Kafni glaciers lie in the Pindar valley, Alaknanda basin, Kumaun Himalaya in the central Himalaya, and located in the Bageshwar district of Uttarakhand state (Fig. 65). The total length of Pindari Glacier is about ~5.9 km and covered an area of approximately 9.6 km² and the Kafni glacier has occupied about ~ 3.3km² with 4.21km of the glacier length. The valley lies between latitudes 30° 12' 15" - 30° 19' 10" N and longitudes 79° 59' 00"- 80° 01' 55" E. The whole Pindar basin occupied about ~173 km², a glacierized area about ~ 9.2 km², elevation range ~2570 to 6183m) located in the central Himalayan region. The outcomes/progress made so far in the research project in the year 2017-19:

Valley-scale meteorology

During an annual cycle, mean atmospheric pressure at the valley-base (2500 m asl, 748 ± 2.6 mb) remained ~100 mb higher than at the glacier snout (3750 m asl,

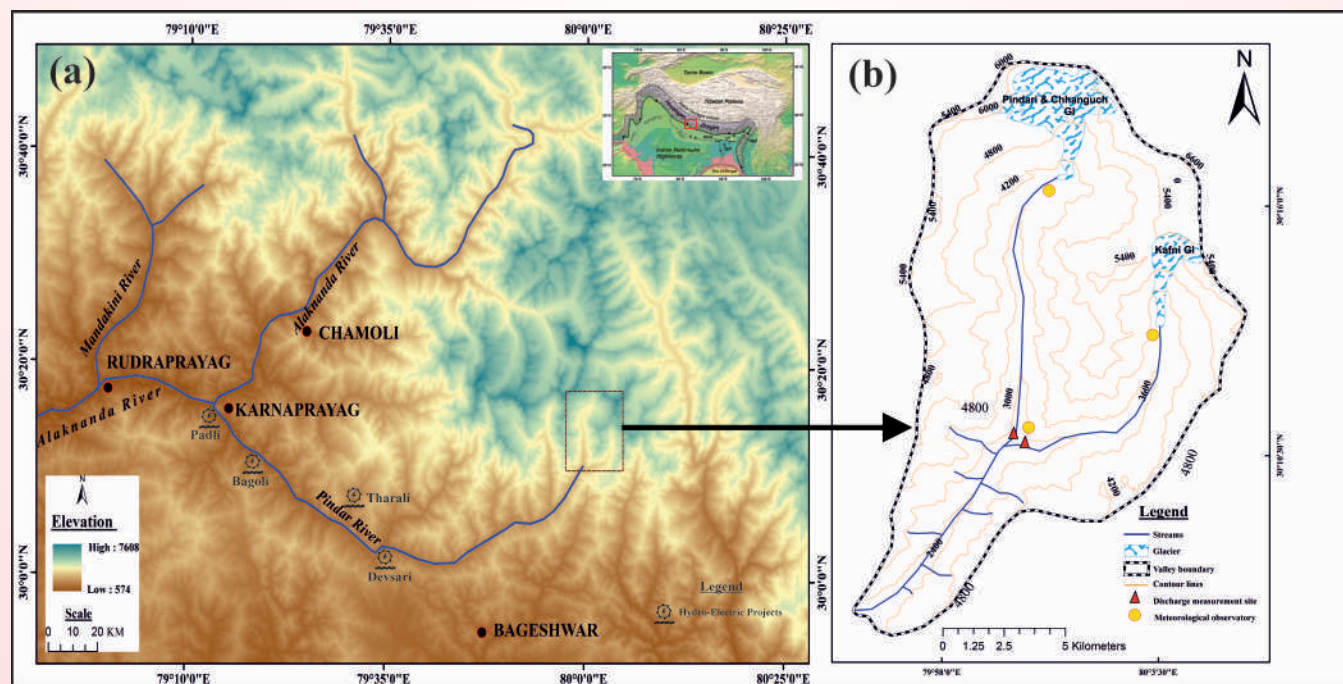


Fig. 65: Map of the study area.

650 ± 2.5 mb). However, seasonal-scale pressure dynamics behaved differentially across altitudinal gradients along the valley. Accordingly, the mean diurnal temperature (11.08 ± 4.99 °C) at the valley-base ranged between 1.4 °C and 19.6 °C. At the glacier snout (Pindari), it (4.05 ± 5.29 °C) varied from -10.0 °C to 12.5 °C. At the Kafni Glacier snout, the mean temperature (3.87 ± 5.03 °C) remained similar but varied in a lower range (-7.4 to 11.6 °C). The temperature remained positive throughout the year at the valley base. While, at the glacier snouts, it remained positive from April to October. Mean wind speed at the snouts remained low during the annual cycle (Pindari snout: 0.81 ± 0.4 ms⁻¹; Kafni snout: 1.12 ± 0.45 ms⁻¹). Wind speed at the glacier snouts did not differ significantly (P > 0.05) across the seasons. During monsoon, the mean wind speed was lowest seasonally, which blew mainly from the south (185 ± 20°). Closed and south-facing glacier valleys could be the reason for low wind speed during monsoon (0.8 ± 0.1 ms⁻¹). As the southwest monsoon retreated, the wind direction changed, which varied between 140 ± 10° (during winter) and 160 ± 10° (during pre-monsoon), with higher mean speed (1.1 to 1.3 ms⁻¹). Radiation sensors are installed only at the Pindari Glacier snout that indicated high variability in incoming shortwave radiation. Daily averaged radiation load varied from 14.5 to 368 W m⁻²; with an annual mean of 170 ± 75 W m⁻². Annually, incoming radiation behaved unimodally, with the lowest levels during winter and highest during summer-monsoon. April to October rainfall data collected from the meteorological observatory at the valley base (Dwali station) show that maximum rainfall occurs in July and a minimum during October. April to October rainfall during the study periods of three years (2017-2019) was 2000, 2800, 1860 mm, respectively. There was heavy rainfall during 2018. Rainfall analyses show considerable inter-annual variations.

Discharge and erosion rate

In this study, the variability in hydrologic components and concurrent biophysical controls were examined in two adjacent central Himalayan valleys (Pindar basin) during three consecutive (2017-2019) growing seasons (April to October). Observations indicate that low flow during pre-monsoon (April-June) increases fivefold during monsoon (July-September). A proportional increase was noticed in sediment transfer behaviour in adjacent glacier valleys in the Pindar basin. Erosion rate (~0.38 ± 0.12 mm yr⁻¹) and sediment yield (1.0 ± 0.3 kt km⁻² yr⁻¹) were found consistent for typical higher central Himalayan valleys. Multiple linear regression analyses suggest

the importance of biophysical factors in determining the magnitude of low flow during pre-monsoon. Analyses of *in-situ* hydro-meteorological datasets coupled with multi-decadal biophysical controls indicate a possible decline in flow during the pre-monsoon period. Sustained multi-year observations and application of machine learning could improve the assessment of regional water resources and management of hydroelectric projects in the region.

Potential Evapotranspiration

For the study period (2017-19) potential evapotranspiration was estimated for each year using the original Penman-Monteith equation and the equations of the aerodynamic and canopy resistance, the FAO Penman-Monteith equation has been given below:

$$\frac{0.408\Delta(R_n - G) + \gamma \frac{900}{T + 273} U_2(e_s - e_a) + \gamma}{\Delta(1 + 0.34u_2)} \quad (1)$$

Where, ETo reference evapotranspiration [mm day⁻¹], R_n net radiation at the crop surface [MJ m⁻² day⁻¹], G soil heat flux density [MJ m⁻² day⁻¹], T air temperature at 2 m height [°C], u₂ wind speed at 2 m height [m s⁻¹], e_s saturation vapour pressure [kPa], e_a actual vapour pressure [kPa], e_s - e_a saturation vapour pressure deficit [kPa], Δ slope vapour pressure curve [kPa °C⁻¹], γ psychrometric constant [kPa °C⁻¹].

Three years ETo based evapotranspiration was quantified for the years (2017-2019) based on in-situ hydro-meteorological observation data. The annual ETo was observed in the Pindari valley 2.49 mm⁻¹day (SD ± 0.39). Further, the results were presented seasons wise. Results show that maximum ETo was computed (3.41 mm⁻¹day ± 0.07) for the summer season and minimum ETo was observed (1.35 ± 0.30 mm⁻¹day) for the winter season. Spring and autumn season ETo was observed (3.04 ± 0.55 mm⁻¹day) and (2.17 ± 0.65 mm⁻¹day) respectively.

MoES Sponsored Project

Geochemistry and Geochronology of the Tethyanophiolites of the Indo-Myanmar Orogenic Belt, Northeast India: Geodynamic and petrogenetic implications and mineralization

(A.K. Singh and Rajesh Sharma)

The Indo-Myanmar Orogenic Belt (IMOB) comprising the Arakan Yoma, Chin Hills, and Naga Hills, pass northeastward into a belt of northwest-trending structures linking them with the Himalayan Arc. West of the Arakan Yoma, turbidites of the Bengal delta fan extend for more than 3,000 km southward across the

floor of the Indian Ocean. The Nagaland-Manipur Ophiolite (NMO) is a remnant of the Neotethyan oceanic lithosphere preserved in a westerly convex linear belt of the IMOB, which represents the suture zone between India and Myanmar plates. It further extends north to the Tuting-Tidding Suture Zone ophiolites and south to the Andaman-Nicobar Island Arc.

The mantle section in ophiolites has a multifaceted tectonic history involving melt-rock reaction, partial melting, and deformation. It has been reported that ophiolites can be originated in various tectonic settings; viz. mid-ocean ridge (MOR) spreading centers, supra-subduction zone (SSZ) environments. Besides, recent studies have also revealed that ophiolites may be originated in other tectonic environments of the continental margin, plume-type, and volcanic arc. Existing theories proposed that the NMO in the IMOB carries signatures of both MOR, SSZ, and plume-type features, which ultimately puzzles us to figure out what had happened in those millions of years ago. Continuous efforts have been made and are still making by various workers to understand this complex

geological phenomenon involved during the process of NMO formation. One of the exciting and challenging topics in NMO and other ophiolite studies globally is to understand the partial melting process of the mantle. Therefore, mantle rocks preserved in ophiolites are often targeted to extract the desired information of mantle melting. Therefore, we study new results of mineral and whole-rock chemistry derived from the rarely occurred dunites from the central part of the NMO, and we discuss its significance in this particular ophiolite section.

Common mantle rocks available in this region are harzburgite and harzburgite, with minor amounts of dunite and chromitite. Sparse ultramafic-mafic cumulate (wehrlite, pyroxenite, gabbro) with minor mafic volcanic rocks (basalt, spilite) and mafic dyke (dolerite) are also encountered. Podiform chromitites are rare in the study area despite their high economic value. Dunites in the study area are often associated with harzburgite (Fig. 66a). They measured ~250 cm in length and ~105 cm in width, as observed in the field. Our sampling site was less than 2 m from the road and

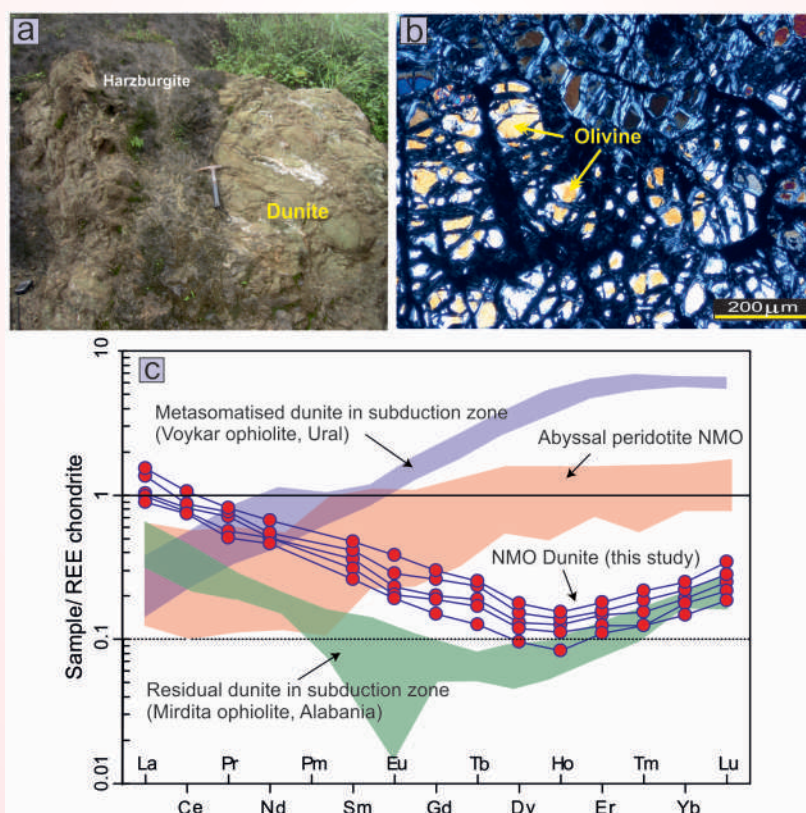


Fig. 66: (a) Field photographs of dunite and associated harzburgite. Representative photomicrograph of (c) olivine grains in dunite (cross-polarized Nicol). (c) Chondrite normalized REE plots for representative dunite samples compared with the abyssal peridotites of the NMO, metasomatized dunite in a subduction zone, Voykar ophiolite, Ural and residual dunite in a subduction zone, Mirdita ophiolite, Albania.

therefore we assume that many parts of the dunites in the area were destroyed due to road construction and other activities. Otherwise, the original size of the dunites must be much larger than that observed. Under the microscope, the dunite samples are moderate to highly serpentinized and composed of olivine and chromian spinel with a small amount of bastite (pseudomorphs after orthopyroxene) (Fig. 66b). The samples contain 94-98 modal % olivine, 1-3 modal % chrome spinels, and 1-2% bastite. The unaltered olivine crystals range from 0.02 to 0.3 mm in size and are free from any signatures of plastic deformation and recrystallization. Chromianspinels are unevenly distributed in the study dunites, but rarely exceed 4 modal% of the rock and have a reddish-brown color.

Olivines in the dunite samples were Mg-rich ($Fo = 92.03-93.34$), significantly higher than the olivine composition of abyssal peridotites ($Fo = 90.1-90.7$) reported from the same study area. These chromian spinels had high $Cr\#$ [$Cr/(Cr + Al)$] ranging from 0.67 to 0.71 and slightly lower $Mg\#$ [$Mg/(Mg + Fe+2)$] values of 0.51-0.54. FeO content ranged from 16.73 to 17.74 wt% and TiO_2 was low (0.10-0.16 wt%). Bulk rock SiO_2 concentration in the dunites ranged between 39.53 and 40.89 wt% and they were rich in MgO (44.46-45.89 wt%). The rocks were also depleted in Al_2O_3 (0.12-0.19 wt%), CaO (0.03-0.04 wt%) and TiO_2 (0.01-0.02 wt%). They had a slightly U-shaped REEs pattern, depleted in middle REEs (MREEs), which is a different pattern from the published data of abyssal peridotites from the NMO11 (Fig. 66). We used REE data from Mirdita ophiolite and Voykar ophiolite for comparison. It shows that the U-shaped REE pattern of NMO dunite is equivalent to the residual dunite of Mirdita ophiolite of subduction origin, but unmatched with metasomatized dunite of Voykar ophiolite (Fig. 66c).

Based on our results of mineral and bulk rock geochemistry, we propose that dunites in NMO are residual mantle sections of extensive partial melting in the mantle wedge of a subduction zone. Low TiO_2 and high $Mg\#$ in chrome spinels suggest the absence of metasomatism, which in other words means no melt-rock interaction has occurred during the process of partial melting and emplacement. The absence of metasomatism is also supported by a depleted MREE pattern similar to non-metasomatic dunites of other ophiolites. Finally, we conclude that although NMO has an ample amount of evidences for MORB-plume interaction, the presence of dunite is key evidence for subduction zone extensive partial melting.

SERB Sponsored project

Geo-Thermochronological Investigation of Lesser Himalayan Crystallines of Garhwal Region, NW Himalaya: Implication to extrusion and duplexing models

(Paramjeet Singh)

In the Kumaun and Garhwal Himalaya, three geologically distinct zones are present which are separated by two major tectonic boundaries the Main Boundary Thrust (MBT) and Main Central Thrust (MCT). The Higher Himalaya has been divided into two groups one is the Vaikrita group and another is the Munsiri formation. The Vaikrita group has been separated by the Vaikrita Thrust (VT)/MCT from the Munsiri formation and the Munsiri Thrust (MT) separates the LHS and Munsiri formation. The LHS has its large exposed width of about 80 KM in the Kumaun and Garhwal region between MBT in the south and the MT in the north. Sub-Himalayan sedimentary sequence is the southern most part and separated by the MBT from the LSMS zone.

Sub Himalaya: The rocks lie in the sub-Himalaya also known as Siwalik sedimentary sequence and separated by the Main Boundary Thrust (MBT) from the LSMS zone. In the section, we travel along the thrust; the contact of MBT is visible between sandstone and Meta sedimentary rocks of the Lesser Himalaya near the village Haripur, Dugadda, and diversion road to Lansdown area.

Lesser Himalaya Sequence: The LHS containing low-grade metamorphic rocks and it is separated from Siwalik by the MBT. The Lesser Himalaya consists of Precambrian and Cambrian sequences which contain the detrital sediments from the passive Indian margin intercalated with some granites and acid volcanic. The LHS is divided into 2 zones (1) Outer and inner Lesser Himalaya meta-sedimentary zone of Proterozoic age to the north of the MBT of para-autochthonous nature. The Outer LHMS consists of the following low grade metamorphic, metapelites rocks of the different formations i.e. (a) Rautgara formation, (b) Chandpur formation, (c) Nagthat formation, (d) Blaini formation, (e) Krol formation and, (f) Tal Formation. Similarly, the Inner LHMS zone also consists of Berinag (well known for massive, compact ortho-quartzite), Deoban and Damta formations, and Ton Thrust (TT) separates the inner and outer LHMS zones. (2) Lesser Himalayan Crystalline Zone (LHC). In the Study area, the two thrust sheet occur: (i) Ramgarh Thrust sheet: the Ramgarh thrust sheet comprises a suite of quartz porphyry, porphyritic gneissose granite, and granitoids. (ii) Lansdown klippe: The overthrust Lansdown klippe

consists of low-medium grade metamorphic such as ganetiferous micaschist, micaceous quartzite, and augen gneiss and granite rocks in the core part. It is very well exposed along the traverse Gumkhal-Jaiharikhal-Lansdown road section.

Higher Himalayan Crystalline (HHC): The HHC is made up of low-medium grade metamorphic rocks of the Munsiri Formation and the high-grade metamorphics of the Vaikrita Group. The Vaikrita Thrust is considered as MCT in this study that separates the higher-grade Vaikrita Group from the low-grade metamorphics of the Munsiri Formation.

Geo-Thermochronological Studies: We have been collected rocks samples for U-Pb (zircon) Geochronology and Fission Track Thermochronology from five traverses in the study area (see Fig. 67). (A) Gaourokund-Tilwara Section (via Agastmuni-Kund-

Phatta-Sersi road section) (B) Ransi-Ukhimath Section (C) Tilwara-Paunthi Section (via Mayali road) (D) Tilwara-Lansdown Section (via Ruderparag-Srinagar-Satpuli-Jaiharikhal-Kotdwar road section) (E) Dadamandi-Dugadda Section.

Table 2: Obtained AFT data sets under project work.

Litho-Units	No. of AFT ages data obtained	AFT age ranges
Vaikrita Group	07	1.5-2.8 Ma
Munsiri Formation	06	1.9-2.9 Ma
Ramgarh Thrust sheet	04	2.4-4.1 Ma
Lesser Himalayan Meta-sedimentary Zone (LHMS)	05	3.4-6.4 Ma
Lansdown Klippe (crystalline klippe)	04	3.6-10.1 Ma

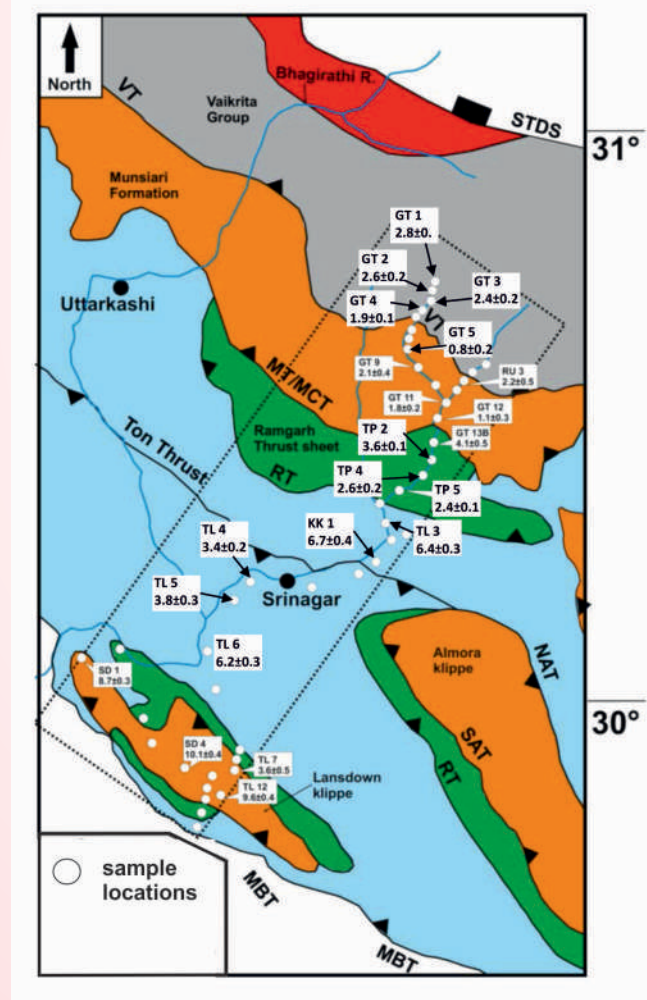


Fig. 67: The AFT ages obtained from the Kotdwar-Gourikund section of the Garhwal-Kumaun region of NW-Himalaya.

Geochemical and U-Pb (zircon) Geochronology data Geochemistry:

- Geochemical analysis using XRF and ICPMS at WIHG of 30 bedrock samples along the Lansdown-Tilwara-Gaourikund section has been completed
- U-Pb (Zircon) Geochronological ages:
- U-Pb (Zircon) Geochronological ages of four samples from Munsiri Formation and Ramgarh thrust sheet give the concordant age with two different events ~1872Ma and 1996Ma.
- Detrital zircon Geochronological ages of Lansdown Klippe indicates the Neoproterozoic (~910Ma) magmatism and indicate roots are connected with the Vaikrita Group of the HHC.
- Based on our initial stage interpretation we suggest that the Lansdown and Ramgarh-Munsiri Formation belongs to two different tectonic units. Additionally, one sample of the Lansdowne sample is in progress.

MoES Sponsored Project

Evaluating conditions of deformation during subduction and exhumation of the north Indian continental margin: A study based on structure and crystallographic features of the Tso Morari Dome of trans-Himalaya, Ladakh, India
(Koushik Sen)

The India-Eurasia collision zone in eastern Ladakh, India is marked by the Tso-Morari Crystallines (TMC) that underwent continental subduction, eclogite grade metamorphism, and exhumation during the Himalayan

orogeny. The TMC is characterized by retrogressed eclogitic enclaves which were extensively studied in the past with surprisingly different results in terms of peak metamorphic conditions and presence/absence of Na-amphiboles and lawsonite from the same outcrop in the core of the complex. We carried out detailed petrography, mineral chemistry, and *P-T* pseudo section of one retrogressed eclogite sample from the western margin of the TMC to assess the differences and discrepancies from previous studies and to understand the transition of omphacite and its subsequent replacement. Our study suggests peak metamorphism at 2.5GPa - 2.6GPa and 540-550 (°C) followed by an isothermal decompression and subsequent retrogression at 0.8GPa - 0.85GPa and 650 - 700 (°C). Various symplectite colonies have been identified. Fine-grained, grain boundary symplectite colonies consisting of omphacite+garnet+amphibole indicate exhumation and probable infiltration of external fluid. We also infer the transition of omphacite into the more calcic variety and subsequent replacement by amphibole. Moreover, the presence of diopside + plagioclase symplectite indicates continued exhumation and fluid infiltration. Our study negates any significant role of lawsonite and/or Na-amphibole in the metamorphic evolution of the TMC.

Electron Back Scatter Diffraction (EBSD) study of six eclogites reveals deformation mechanism and strain regimes during peak metamorphism and subsequent post-peak rapid exhumation of the TMC. Our study shows that the least altered/retrogressed eclogite exhibit strong linear fabric characterized by omphacite, having [001] axes parallel to and (110) poles normal to lineation. A non-coaxial deformation regime can also be inferred from quartz crystallographic fabric. These features concur with constrictional strain during peak metamorphism. A transitional plano-linear fabric is shown by other eclogites that show petrographic omphacite retrogression to amphibole and lower metamorphic grade minerals like actinolite and chlorite. Fabric strengths of omphacite and quartz crystallographic preferred orientation, indicated respectively by the LS and B-indexes, are also compelling for pristine eclogites as compared to their altered counterparts. Based on these results, it is suggested that a constrictional strain regime prevailed during peak metamorphism in the TMC due to buoyant rise of TMC in response to slab break off and reverse slab pull during and after deepest continental subduction. This regime evolved later to plane strain that was superimposed on the UHP rocks at a shallower depth. It is plausibly associated with foliation parallel extension during exhumation at mid-crustal depths.

36th IGC, Sponsored Research Project Paleoseismology along the foothill zone of Central Himalaya, Uttarakhand, India for preparation of excursion guide book

(R. Jayagonda Perumal, V.C. Thakur, Priyanka Singh Rao, Arjun Pandey and Atul Bruce)

Paleoseismological studies have been conducted during the last decade in an attempt to determine the timing, magnitude, rupture extent, return period, and faulting mechanics associated with the occurrence of large surface rupturing earthquakes along the ~2500 km long Himalayan Frontal Thrust Fault (HFT in India) or Main Frontal Thrust Fault (MFT in Nepal).

The 2005 Kashmir earthquake, magnitude Mw 7.6, produced a surface faulting. The mapped surface rupture was 75 km in length and revealed vertical offsets varying 2.7 m to a maximum of 7 m in height. The rupture coincided with bedrock mapped fault indicating activation of the fault. The 1934 Bihar-Nepal earthquake, magnitude Mw 8.1, had its epicentral location in the Lesser Himalayan hinterland, but its surface rupture is recorded in paleoseismology trenches at three locations along the Himalayan Frontal Thrust (HFT). The 1950 Assam-Tibet earthquake (Mw 8.6) produced a surface rupture in the western bank of eastern syntaxis along the eastern Himalayan frontal thrust at Pasigaht, Arunachal Pradesh. Similarly, surfaces ruptures of several historical earthquakes (e.g. C.E 1344; 1505 and 1255) are reported through paleoseismological investigations in the Sub Himalayan frontal zone.

The present field excursion is an attempt to demonstrate the transect across the sub and lesser Himalayan structural framework and paleoseismological studies carried in the Sub Himalayan front of the Kumaun region of Central Himalaya that lies in the western part of Central Seismic Gap (CSG). The HFT demarcates an active fault boundary between the Himalayan front and the Indian alluvium plain. The fault scarps affecting the present geomorphic surface of Quaternary - Holocene are exposed in a discontinuous and linear pattern along the trace of the HFT indicative of reactivation of the fault during a great earthquake.

The field excursion focused on the Ramnagar area of the Kumaun Lesser and Sub Himalaya (Fig. 68). Day 2 includes spots 1 to 7 covers an N-S transect to take an overview of the regional tectonic setting of the Kumaun Lesser and sub-Himalaya. Active faulting along the HFT has been demonstrated, and paleoseismological studies carried earlier explained at two closely spaced

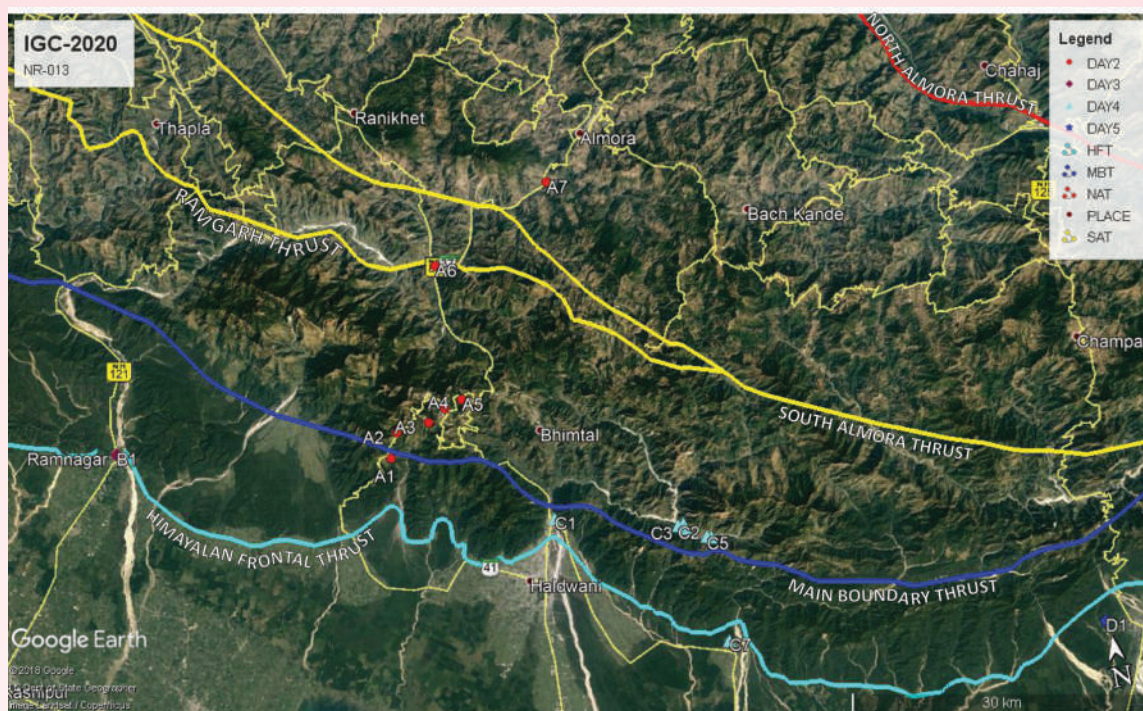


Fig. 68: Regional tectonic framework of conducted pre-congress field trip depicted in the Google Earth image.

sites at localities Belparao and Dol villages on day 3 in the Ramnagar area. In the fourth day, there was fieldwork along the Logar gad Valley, located east of Kathgodam, which displays reactivation of the MBT. Here the MBT marks a boundary between the Lesser Himalayan strata and the Lower Tertiaries, interpreted as Siwaliks by some workers, of the Sub Himalaya. The MBT fault trace between the two formations is covered, overlapped, by late Quaternary - Holocene fan deposits. The fan is dissected by a fault, called Logar fault, aligned - coincides with the MBT trace, very well exposed in the satellite Google image. The Logar fault is characterized by a north-facing linear scarp showing a 15 - 20 m vertical offset. It is a normal fault with some left-lateral relative motion. A series of paleolake depressions in the region represent half grabens developed as a result of strike-slip fault motion step-over to the right. A trench was made across the fault scarp for paleoseismological study. OSL dating of the faulted fan deposits in the trench indicates late Pleistocene (~ 20 - 8 ka) - Holocene reactivation of the MBT. In the afternoon of the 4th day, an active fault scarp between Haldwani and Chougalia were studied. At Tanakpur (Day 5) located near to the western border of Nepal along Kali or called Sarada river, where the trace of active fault deflected a river channel during the 1505 earthquake with coseismic landslide along the mapped fault trace. A trench exposure at Tanakpur shows a forelimb thrust fault with a footwall syncline

displaced the modern surface.

The pre-36th IGC congress field trip guide book was developed through the EMR project grant. This project includes trench excavation across the fault scarp at Chougalia to demonstrate with participants of the IGC, along with NS transects across the Kumaun Himalaya. The pre-conference field workshop was successfully completed (Fig. 68) although the main meeting was suspended due to the COVID-19 pandemic. The project completion report has been submitted to the funding agency, IGC, New Delhi.

MoES sponsored Project

Tectono-thermal evolution of the Lohit Batholith along Dibang and Lohit Valleys, India using Fission Track and (U-Th)/He Thermochronology
(Vikas Adlakha and Koushik Sen)

First (U-Th)/He low-temperature thermochronological record from the Lohit Valley, Eastern Himalaya has been obtained across the major tectonic boundaries. The ZHe cooling ages range from 6.94 ± 1.17 to 12.51 ± 2.84 Ma while AHe ages vary between 1.73 ± 0.15 and 3.56 ± 0.42 Ma. The ZHe cooling ages suggest that the Mishmi Crystallines exposed at the southwestern mountain front are the slowest exhuming domain since ~12 Ma. The ZHe ages are youngest in the Demwe Thrust zone, contact between the frontal low-grade metamorphic rocks of Mishmi Crystalline and high-

grade gneissic rocks of the Mayodia Group. The rapid exhumation in the Demwe Thrust zone as obtained from the ZHe cooling ages suggests an out-of-sequence thrusting at ~ 7 Ma. The QTQt thermal history modeling of the co-genetic pairs of ZHe and AHe cooling ages of the northeasternmost Lohit Plutonic Complex suggests that the exhumation rates in this region were as high as ~ 3.7 mm/yr during the Pliocene-Quaternary. These high rates of exhumation are in good correlation with the local topographic relief, hill slopes, channel steepness which suggests the establishment of the present-day topography of the Lohit Valley region latest by Pliocene-Quaternary. Variation in exhumation rates does not correlate with the present-day precipitation pattern. Tectonics appears to be the prime driver of the exhumation rates of the Lohit Valley region of the easternmost Himalaya.

MoES Sponsored Project

Comparative study of weathered/ soil profiles developed on Granitic and Basaltic rocks of Higher and Lesser Himalaya in Garhwal region: Implication on climate-tectonic interaction.

(Pradeep Srivastava and R. Islam)

Seven weathering profiles in different parts of Garhwal Himalaya are identified and analyzed to understand the weathering behaviour in Himalaya. The in-situ weathering profiles were identified using the criteria in which signatures of fining upward or gradual change in colour progressively change from least altered rock at the base of the profile to regolith towards the top. Gradually the framework fabric of the rock diminishes upwards. Representative samples collected from different zones of the profiles were analyzed using X-ray Fluorescence and Inductive Coupled Plasma-Mass Spectrometry and the major, trace, and rare earth elemental behaviour in different sections of the weathering profiles was studied.

In order to understand the relationship between deformation and weathering processes, detailed structural mapping is also carried out in the areas around the studied weathering profiles. Various geological structures mapped in the Kaliasaur region imply the presence of a normal fault which is also responsible for a chronic landslide in the area. Shear sense indicators including fault striations and en-echelon veins represent the movement of failure oblique to the bedding. Compressive structures from the hanging block of the fault and tensional structures from the foot wall are observed (Fig. 69). Rock mass rating (RMR) is calculated by using various characteristics of the discontinuities to

understand the intensity of deformation of the rock mass. Poor values of RMR are observed near the fault zone and in basaltic weathering profiles. Adjoining quartzite beds are deformed lesser than the basaltic bed, signifying the involvement of the chemistry of the rocks in differential disintegration and alteration in a similar physical environment. The alteration of strata from fresh rock to regolith is analyzed by using Chemical Index of Alteration (CIA) and A-CN-K ternary plots from major oxide data of representative samples.

Ternary diagrams are plotted between A (Al_2O_3), CN ($CaO^* + Na_2O$), and K (K_2O) to evaluate the path of alteration from least altered rock to regolith from identified weathering profiles. Plagioclase feldspar lies on the middle of A-CN tie line and K-feldspar falls on the middle of A-K join. Fresh rock and slightly weathered rocks plot close to the feldspar joining line (line joining plagioclase and K-feldspar compositions). Basic rocks contain comparatively higher plagioclase feldspar and lesser K-feldspar than those of acidic rocks. As a reason being, the fresh rock composition of basic rock falls on the feldspar joining line towards the plagioclase corner while acidic fresh rock composition at the center of the line. Aluminous clay mineral composition lies toward the A-apex. With the intensification of weathering, plagioclase feldspars break down, and Ca and Na leach out the porous sites, and weathering trend moves toward the A-K boundary reflecting the possible K-feldspar composition remaining into the material. Further intensification leads to the removal of remaining K-feldspar and weathering trend shifts toward A-apex. Leaching of all Ca, Na and K from the soil lead to 100% CIA value which lies on the A-apex of the A-CN-K ternary plot. The ternary plot of a representative basaltic profile (PWP) is shown in figure 70a. The fresh basalt of this profile points towards the plagioclase corner on the feldspar joining the line with CIA value of 50. With the progression of weathering the trend follows the universal path parallel to A-CN line and alters up to CIA value 82 in the regolith portion close to A-K join. The basaltic profiles located around the Kaliasaur fault exhibit a weaker trend (from ~ 75 to 81) and where the samples from saprolith tend to cluster. The two profiles developed on granite follow a typical weathering trend.

Following the Goldich stability series, basic rocks containing a higher fraction of ferromagnesian minerals are more susceptible to weathering as compared to acidic rocks, containing silicate minerals. Usually, basalts weather faster than granites. Major elements concentrating in Ca-feldspars, biotites, and amphiboles

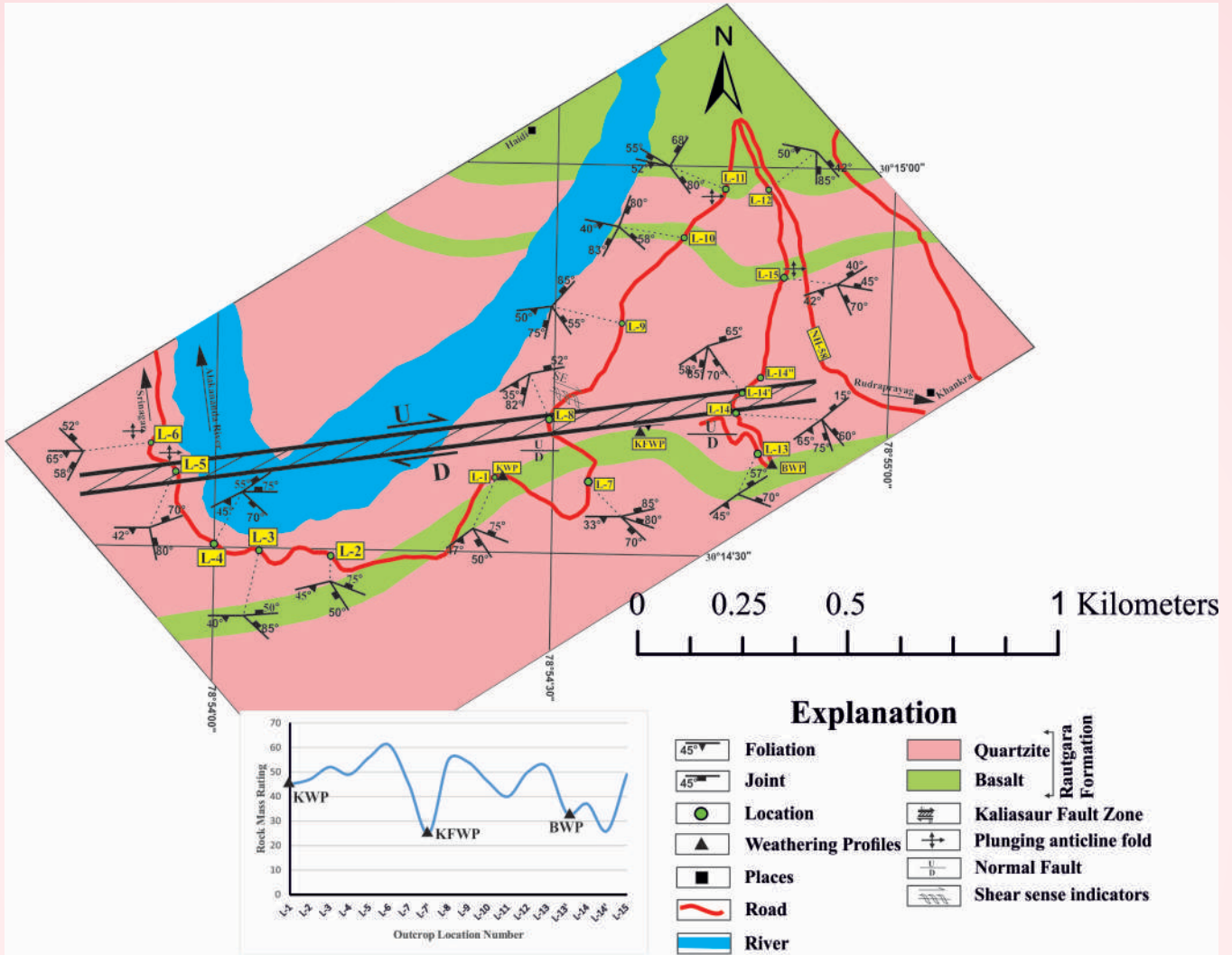


Fig 69: Geological traverse map of Kaliasaur region presenting various discontinuities and a graph representing the variation of RMR at different outcrops.

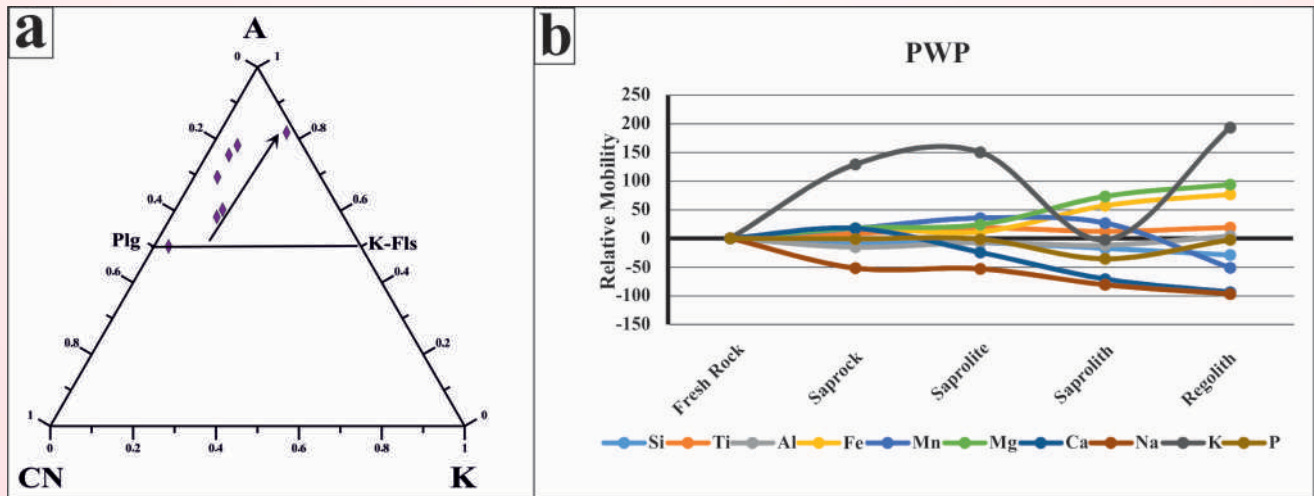


Fig 70: Pailgaon Weathering Profile (PWP); (a) A-CN-K ternary plot; (b) Relative mobility diagram of major element from fresh rock to regolith.

SPONSORED PROJECTS

include Ca, Mg, and Na and deplete more than those concentrating in K-feldspars, quartz which includes K and Si. The mobility diagrams also depict that Na, K, and Ca reflect a progressive decrement trend. K is found to be depleted lesser than Na and Ca. Mg concentration in basaltic profiles decreases from least altered rock to regolith while increment trend can be noticed in granitic and gneissic rocks due to the incrustation of gypsum or other minerals. Si concentration decreases at a higher degree of alteration. Al, Ti, and Fe remain immobile and also make residual deposits. The mobility of Fe is predominantly controlled by the oxidation state. Divalent ferrous ions are highly mobile compared to trivalent ferric ions. P follows a decrement trend because of the alteration of apatite which is highly prone to weathering. The relative movement path of major elements from various zones of a representative basaltic profile (PWP) with respect to the fresh basalt rock is represented in figure 70b. In contrary to the general trend, Mg in this profile increases slightly from fresh rock to regolith, and K increases in saprock and saprolite portion then neutralizes in saprolite and followed by increment in regolith portion. The rest of the three basalt profiles show similar behaviour. The granite follows the normal weathering trend.

SERB, DST Sponsored Project
Glacial chronology, Palaeoclimatic reconstruction and their climatic implications in the Darma Valley, Kumaon Himalaya, India.

(Pinkey Bisht)

The present project is undertaken to understand the geomorphology and chronology of the Darma valley an unstudied region of the Kumaon Himalaya, situated in the Transitional zone of the Indian summer monsoon and Mid-latitude Westerlies. The primary focus in this study is to establish the glacial chronology using Optical Luminescence Dating and to examine the driving factor behind the glaciation in the valley. This study will fill the gap of glacial chronology in the Himalayan region. So far, the literature survey of the glacial study of the Kumaon Himalaya has been done. The Geology and Geomorphological map of the study area has been prepared using Google Earth Image. The relative moraine stratigraphy present in the valley has been demarcated using Google image and DEM. The collection of OSL samples from the mapped moraine is required to establish the absolute glacial chronology for this region which will help to understand the evolutionary history of the landform. The fieldwork was delayed due to Covid 19 Pandemic. Now proper planning has been done for the fieldwork related to this project.

DST Sponsored Project

Status of geo- resources and impact assessment of geological (exogenic) processes in NW Himalayan Ecosystem under National Mission of Sustaining Himalayan Eco-system (NMSHE)

(Director WIHG, Rajesh Sharma and Vikram Gupta)

This National Mission project on Sustaining Himalayan Eco-system mainly pertains to establishing a database and information system about geological resources (Quaternary deposits, groundwater, springs including geothermal springs, mineral resources, and snow cover) and exogenic geological processes (mass - movements including GLOF) along the major valleys, to facilitate policy decision about the sustainable development of the Himalayan Ecosystem taking into account the work of existing knowledge.

During the reporting year, the database for the distribution of active landslides was updated with the induction of the recent landslides of 2020. Thus in the database, we have 3303 active landslides. The area occupied by individual landslides varies between 50 m² and 1.5 km² and the cumulative area coverage of landslides is ~ 64 km² which is ~ 0.12% of the total area of Uttarakhand. Utilizing this data, the regional-scale landslide susceptibility mapping for the state of Uttarakhand has been carried out using two bivariate methods, the weight of evidence (WoE) and information value (IV). Both these methods are relatively simple to use and have been used widely across the globe and in the Himalaya. It has been observed that (i) Around 51% of the area is located in the high and very high landslide susceptible zones, 22-23% in the moderate, and ~26-27% in the low and very low landslide susceptible zones (ii) Most of the high and very high landslide susceptible zones are located in the vicinity of the Main Central Thrust, and in the Higher Himalaya, whereas low and very low landslide susceptible zones are located in the Indo-Gangetic planes, Outer and Lesser Himalaya. (iii) Slopes ranging between 40° and 60°, located at an elevation between 2000 m and 4000 m and facing towards southern sides are more susceptible to failure, and thus falls in the high and very high susceptible zone, (iv) Both the methods used for the preparation of the landslide susceptible maps indicate more or less similar efficacy and accuracy, though, for the present area of study, WoE model is some what better than the IV model.

The distribution of the seismic activities along the vicinity of the MCT is well known, however, to assess the relationship between these seismic events and the landslides, the spatial distribution of landslides and the

earthquake events (magnitudes >1.5) on either side of the MCT zone were evaluated. It has been observed that seismic events of magnitudes <2.1 are clustered around the 1991 Uttarkashi earthquake rupture, the 1999 Chamoli earthquake rupture, and Munsiyari. The zone with 1999 Chamoli earthquake rupture zone indicates the highest earthquake and landslide density of $\sim 75\%$ and 53% , respectively.

The Uttarakhand Himalaya, during the recent past, has witnessed two major earthquakes, the 1991 Uttarkashi earthquake and the 1999 Chamoli earthquake that were triggered in the vicinity of the MCT. Besides, there are numerous smaller earthquakes, ranging in magnitudes from 1.5 to 4.0 that occur almost every day, and the majority of these events are shallow having <25 km depth, and are concentrated in a certain region of the MCT. The causes of the spatial distribution of these earthquakes along the strike length of the MCT are well known. On the contrary, there are numerous and varying causes for the occurrences of landslides in the region. Though most of the landslides are reported during the rainy season and are distributed throughout the Himalayan terrain, still there are certain landslide 'hotspots' in the region where the concentration of these landslides is high and these may be related to the

climate, lithology, and the tectonics of the area. Though micro-earthquake activities in the region do not indicate the presence of instantaneous landslides, however, it is hypothesized that the continuous ground shaking due to earthquakes destabilizes the slopes that may be triggered by various other factors such as rainfall or fractured rock mass. Therefore in the present work, an attempt has been made to understand whether there exists any relation between the spatial distribution of landslides and the epicentral distribution of earthquakes of varying magnitudes in the MCT zone of the Uttarakhand Himalaya.

The study area chosen to meet the objectives as mentioned above is located between latitudes $29^{\circ}33'30''\text{N}$ & $31^{\circ}18'47''\text{N}$ and longitudes $77^{\circ}44'04''\text{E}$ & $80^{\circ}24'13''\text{E}$ (Fig. 71). It extends 10 km to the north of the Vaikrita Thrust and 10 km to the south of the Berinag Thrust within the boundary of the Uttarkhand, thus covering a linear stretch of ~ 278 km along the strike length of MCT, and an area of $\sim 19,000$ km².

The preparation of the inventory depicting the spatial distribution of landslides and the epicentral distribution of earthquakes is a prerequisite for any such kinds of studies that involve the spatial distribution of

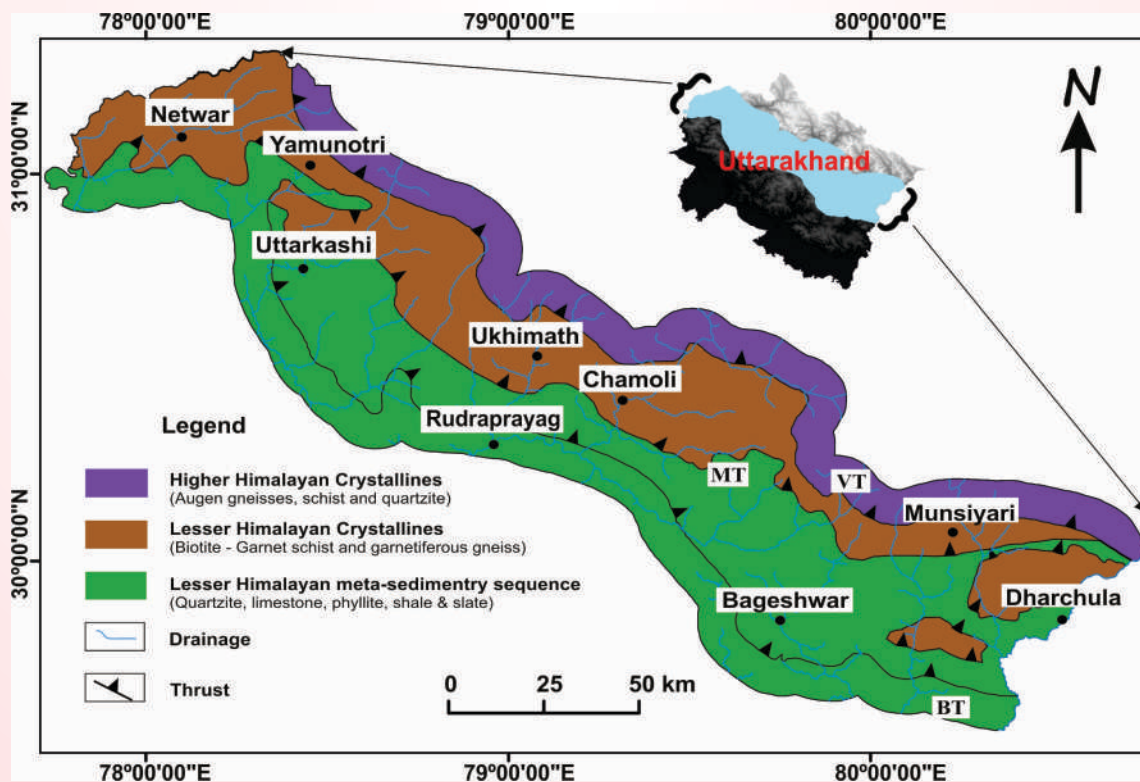


Fig. 71: Location Map of the study area depicting the regional geological setting. BT is Berinag Thrust, MT is Munsiyari Thrust and VT is Vaikrita Thrust.

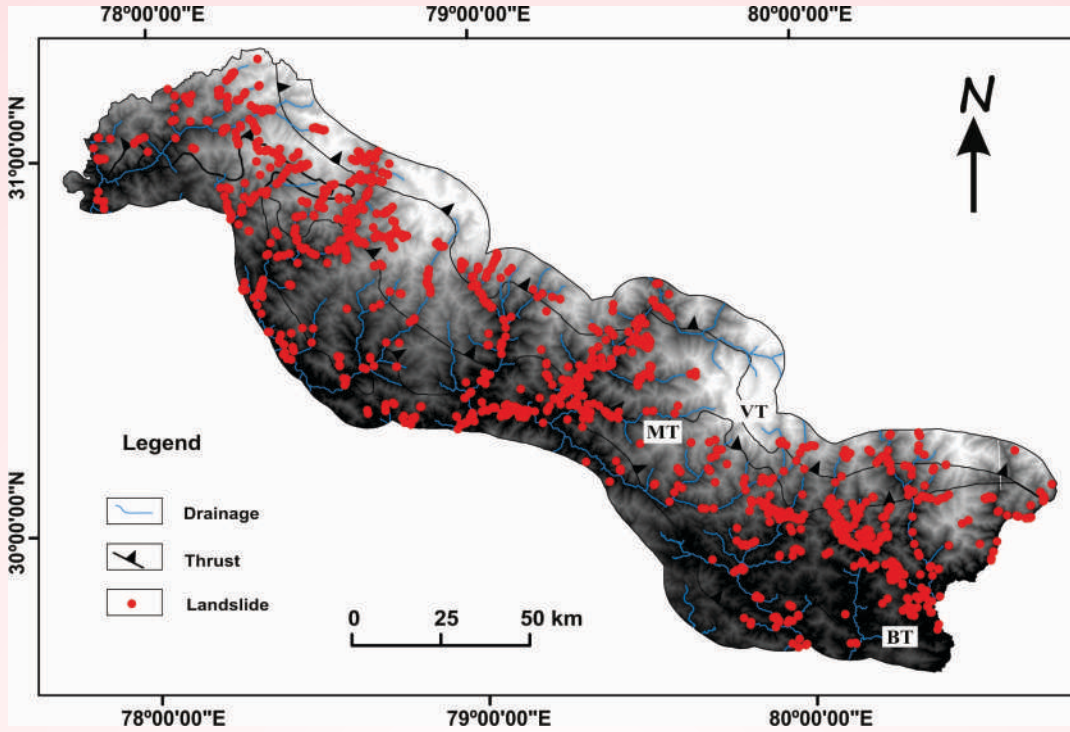


Fig. 72: Inventory of landslides in the study area.

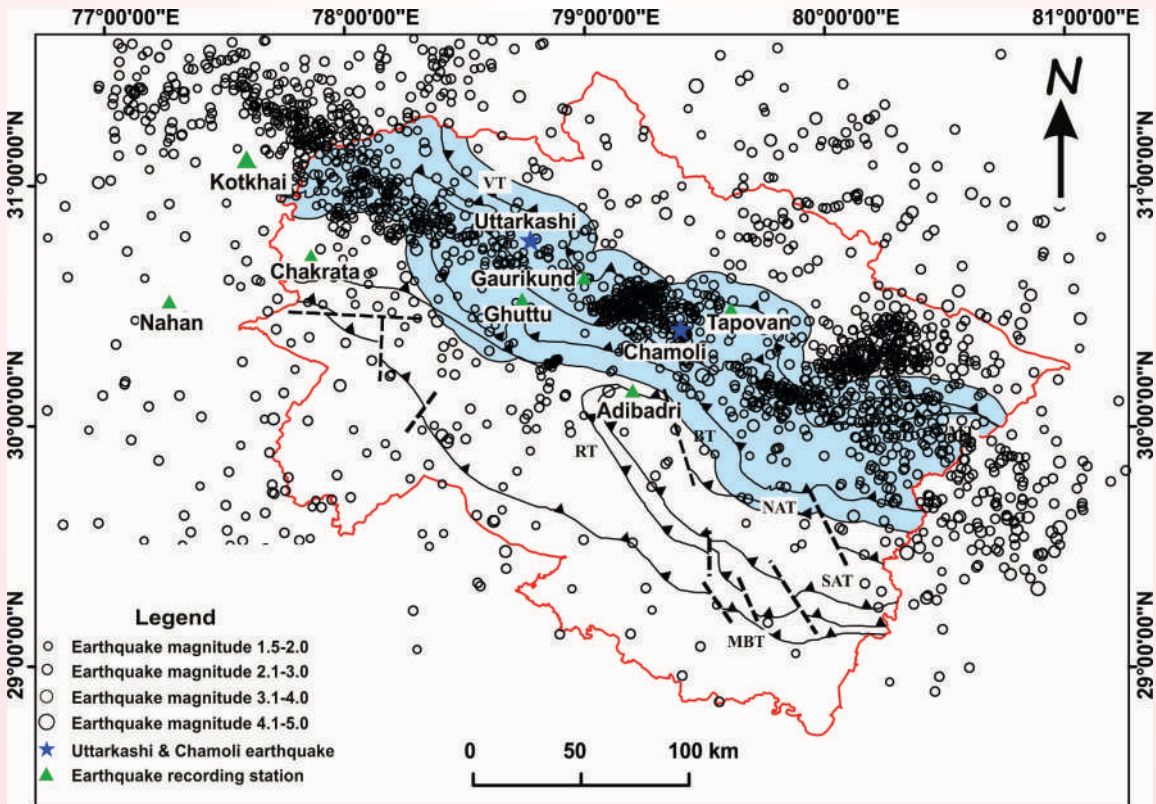


Fig. 73: Inventory of earthquakes of magnitudes ranging between 1.5 and 5.1 recorded during July 2007 - October 2015 on the seismic network of ten broadband seismographs to establish linkage, if any, with the landslide activity (The location of the seismographs for recording earthquake data is presented).

these events. For the present study, an inventory of landslides has been prepared by using high-resolution satellite images, images on the Google Earth platform, and LISS IV images having resolutions of ~ 1 m and 5.8 m, respectively. In addition data from extensive fieldwork have been incorporated. A total of 1342 landslides of different sizes have been mapped in the area (Fig. 72).

The inventory of earthquakes has been acquired from the seismic network of 10 Broadband Seismographs installed in July 2007. Seven of these stations are located in Uttarakhand, two in the adjoining Himachal Pradesh and one in the south of the study area in the Indo Gangetic plains. (Fig. 73). Each station is equipped with a Trillium-240 seismometer of high dynamic range (>138 dB) with a Taurus data acquisition system (DAS) that gives high accuracy of GPS. The catalog of the earthquake compiled for the present study consists of 2,260 earthquake events of magnitude (ML) 1.5 acquired between July 2007 and October 2015.

Several earthquakes have been recorded outside the area of study, and these might have affected the occurrence of landslides in the area of study and the slope instability in the region. It is however reported that smaller magnitude earthquakes, probably < 5.0 magnitude are not good enough for triggering landslides. It is generally observed that landslides are

triggered by earthquakes having magnitudes > 5.0 , as has been widely reported as in the case of the 1991 Uttarkashi earthquake, 1999 Chamoli earthquake, 2005 Kashmir earthquake, 2011 Sikkim earthquake, 2015 Gorkha earthquake. Nevertheless, it is hypothesized that the concentration of the smaller magnitude earthquakes in an area affects the slope instability in the region, leading to subsequent failure possibly by other triggering agents, like rainfall.

There are 2,260 earthquakes of magnitudes ranging between 1.5 and 5.1 in the area of study during July 2007 - October 2015. Of these earthquakes, 769 are of magnitudes ranging between 1.5 and 2.0, 1335 between magnitudes 2.1 and 3.0, 129 between magnitudes 3.1 and 4.0, and 27 between magnitudes 4.1 and 5.0. Data plots indicate that there are no preferential distribution of earthquakes of magnitudes > 3.1 , however smaller earthquakes of magnitude < 3.0 are clustered (Fig. 74). Three clusters are clearly visible, and their boundaries are visually drawn for statistical analysis (Fig. 75).

Cluster - 1 is located in the western part of the study area and its aerial coverage is ~ 3179 km². It covers the 1991 Uttarkashi earthquake rupture zone and the area west of it. The spatial distribution of earthquakes in this cluster is scattered and is mainly located between the Berinag Thrust and the Munsiyari Thrust. The landslides in this cluster are also scattered and mainly

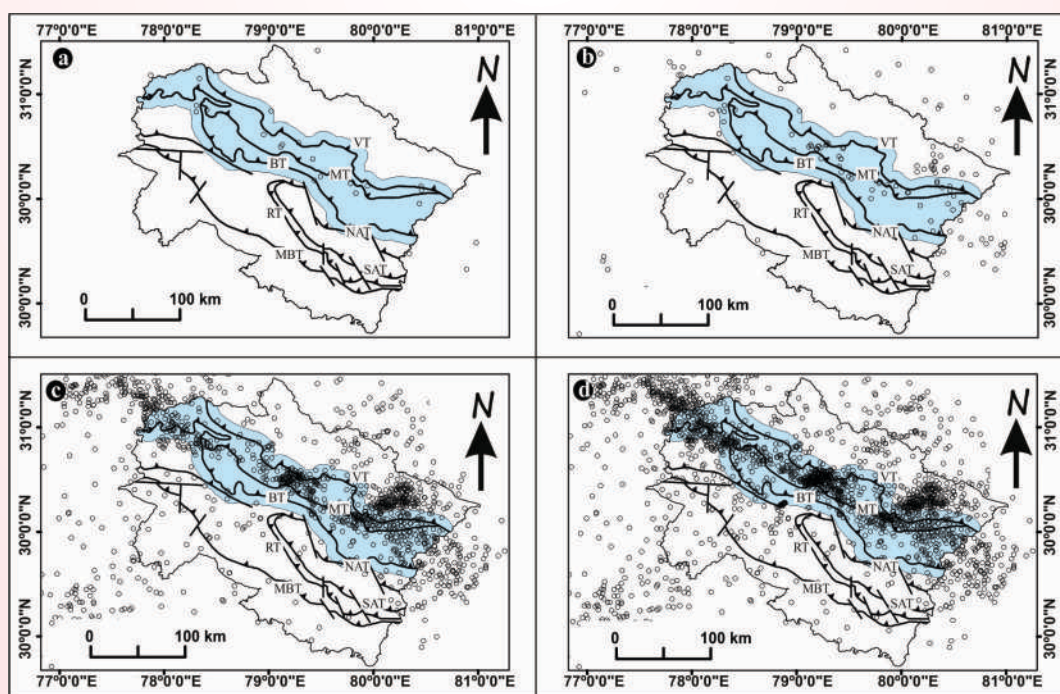


Fig. 74: Data plot of the spatial distribution of earthquakes recorded in the study area and its adjacent of (a) magnitudes ≥ 4.1 (b) magnitudes ≥ 3.1 (c) magnitudes ≥ 2.1 and (d) magnitudes ≥ 1.5

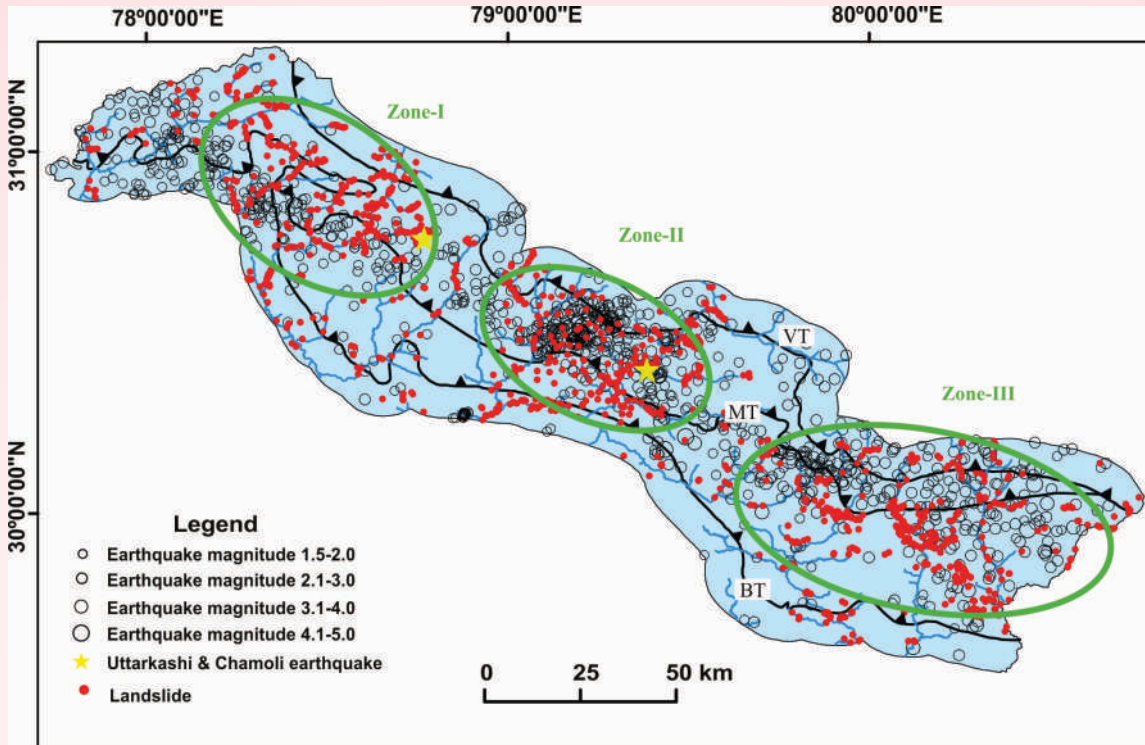


Fig. 75: Data plot indicates the spatial distribution of earthquakes of different magnitudes and landslides. Three prominent clusters of earthquakes and landslides are marked.

located along the drainage. With earthquake and landslide counts of 145 and 300, respectively this zone exhibits earthquake and landslide density of ~24% and 36%. The 1991 Uttarkashi earthquake generated 183 landslides immediately after the earthquake and 360 landslides during the succeeding rainy season of 1992.

Cluster - 2 is located in the central part of the study area and its aerial coverage is ~ 2291 km². It covers the 1999 Chamoli earthquake rupture zone and the area to the west of it. This cluster is pronounced among all three clusters. This cluster includes the highest number (328 earthquakes) of seismic events located between the Munsiyari Thrust and the Vaikrita Thrust. The majority of the earthquakes in this cluster are of magnitude < 3.1. With earthquake and landslide counts of 328 and 313, respectively this cluster exhibits earthquake and landslide density of ~75% and 53%.

Cluster - 3 is located in the eastern part of the study area near Munsiyari and its aerial coverage is ~4220 km². This cluster is scattered in the Uttarakhand Himalaya, though all the earthquakes of magnitude > 2.1 are clustered oblique to the strike of the Himalaya (Fig. 74d) between Munsiyari Thrust and the Vaikrita Thrust and further north of it in the Tibetan part. Most of the landslides in this cluster, particularly in the Kali

valley and its adjoining are because of the active nature of the area. With earthquake and landslide counts of 269 and 401, respectively this cluster indicates earthquake and landslide density of ~34% and 37%, respectively. Though there are few isolated earthquakes of magnitudes 3.1 - 4.0 in the areas between the demarcated clusters, the clustering of the smaller magnitude earthquakes is notably missing.

The mining in the Himalaya is assessed in terms of the size/scale of individual mining activity. Small-scale mining activities are generally adopted in the Himalayan region (Fig. 76a), and large-scale mining is rare. It is because of the size of the ore body, intense tectonics, the topography of the mineralized zones, grade of the ore, and land use. Although large-scale mines are usually more organized with systematic mine plans, only a few mines of limestone and magnesite are relatively large-scale mines in the Himalayan region. Small-scale mining can be carried out on small pockets of ore reserves, and with ease in the hilly topography. It requires less implementation time, less initial investment with fewer infrastructure requirements. But they are commonly unorganized with poor mining skills and low levels of technology involvement. These mines are opencast wherein the general trend of extraction is through an open broad pit created in the center and the



Fig. 76: a) View of small-scale mines in Bageshwar District. b) Mechanization is used in some mines of the region.

mine waste material and mine cover material are stocked/dumped around the pit. They generally do not involve skilled prospecting thereby leads to low recovery, less productivity, and therefore low income. An individual scattered small mine has a lower scale effect on the environment, but a cluster of small mines generally impact adversely on the environment. At places, the mining activity has resulted in damage to the agricultural land because of poor management of mine waste. The development/widening of the motorable road or mule tracks from the road head to the mine site also seen disturbing the flora. Limited use of machines is adopted only in some mines of the region (Fig.76b), and by and large manual operations are underway. The plantation carried out by the mine owners is usually not adequate. An attempt was made to focus the

mineralization near Rangpo in Sikkim. Sikkim in the 60s and 70s was known for only operating Cu-mines in the Himalaya. However, these mines were closed later. The region is considered a potential area for metallic minerals. The central portion of Sikkim Lesser Himalaya consists of the Daling Group of rocks which is overlain by the high-grade gneisses with contact between them demarcated by sheared mylonitic gneisses.

The base metals occur within the Daling Group, which is dominated by a thick sequence of meta-sediments consisting of pelite, psammites, and wackes. The observations on the Cu-mine of Rangpo (Fig. 77) show that mine waste, although not large scale, can be seen around the abandoned mine. The acid mine water is seen flowing from one of the abandoned mine (Fig. 77).



Fig. 77: a) Abandoned mine of Rangpo, Sikkim and b) Acid mine water in the abandoned mine of Rangpo.

The copper mineralization in the study has been studied to understand the ore mineral formation and the host rock evolution. The pyrrhotite, chalcopyrite, sphalerite, galena, arsenopyrite, and pyrite are observed as major primary ore mineral phases (Fig. 78), whereas the covellite, azurite, limonite, and malachite are present as secondary ore minerals. Quartz forms the ubiquitous gangue mineral. Chalcopyrite, pyrrhotite, sphalerite and appear to be coeval indicative of solid solution. The ore mineralization was deposited in two stages. High concentrations of Fe, Co, and Mn point to the magmatically driven hydrothermal system. The mineralization at Dikchu and Rangpo consists of assemblage that points to high-grade ore. The work carried out is expected to add new knowledge on these ore deposits. The present shape of the abandoned mines at Rangpo, which is located near the highway, may be managed to control the acid mine water coming from the mine.

Quaternary deposits mapping in Himachal Pradesh

The Himachal Himalaya is covered by rocks ranging in age from Precambrian to Recent. The normal order of superposition of the rocks in the Lesser Himalaya has been affected by later events of thrusting. Owing to its complex tectonism and geological evolution, establishing a unanimously accepted geology and stratigraphy of Himalaya remained mired with debate and controversy- posing a natural deterrent. The total area of Quaternary deposits is approximately 513 km² delineated from LISS III Satellite Imageries. The thick pile of fluvial, fluvioglacial, glacial, lacustrine, and gravitational sediments exposed in Beas, Banganga, Soan-Sohan, Spiti, Giri -Yamuna, Satluj, and Sunder

Nagar valleys of Kangra, Mandi, Kulu, Spiti, Shimla, and Sirmaur districts represent post-Siwalik Quaternary deposits. A detailed description is given in table 3.

The distribution of Quaternary deposits in Himachal Pradesh has been mapped with the help of remote sensing data (LISS III and Landsat satellite data). The preliminary results reveal that nearly 4481 km² which is only 8% of the total geographical area of the Himachal Himalaya is covered by Quaternary deposits.

The preliminary results reveal that nearly 4481 km² which is only 8% of the total geographical area of the Himachal Himalaya is covered by Quaternary deposits. Valley fill has the highest contribution almost 50% (2440 km²) in Quaternary deposits whereas alluvial fan has the lowest contribution. Furthermore, in the Kangra district, ~ 1103 km² of the area lies under valley fills which is the highest among all the districts followed by Una district (448 km²) and Mandi district (257 km²). Whereas Shimla district (3.69 km²) contributed the lowest among all the districts just next to the Kinnaur district (6.33 km²). In Himachal Pradesh 363 km² area lies under the category of flood plains out of 4481 km² area of Quaternary deposits. Lahaul and Spiti district of the state comprises 110 km² is the highest among other districts whereas Shimla district (4.62 km²) has the lowest.

The quaternary deposits formed by fluvioglacial are moraine complexes, alluvial fan, piedmont moraine, and glacial outwash plains. Moraine complexes are found in higher altitude regions in Chamba Kullu,

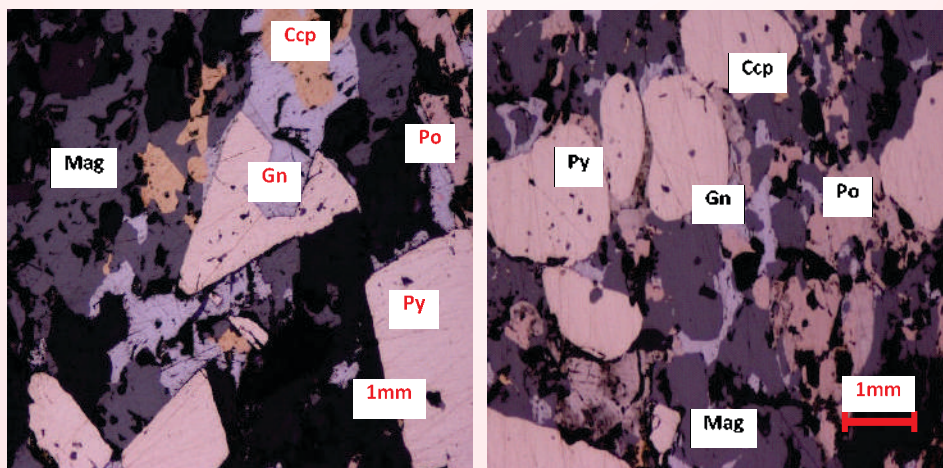


Fig. 78: a) Euhedral and subhedral pyrite, perfect three-set cleavage in form of triangular pits in galena from Rangpo and b) Anhedral and sub-rounded pyrite grains with sphalerite inclusions observed in ore assemblage of Rangpo.

Table 3: Brief Description of Quaternary Deposits.

S.No.	District	Period	Group Formation	Description
1	Una	Quaternary	Alluvium, Terrace & Fluvial deposits	Alluvium, clay, sand, gravel, pebbles, boulders, and cobbles
2	Kangra	Quaternary	Fluvioglacial/glacial/ Interglacial deposits	Sand, silt, clay, gravel, pebble, cobble, and boulders, etc.(Moraine & Fluvial deposits)
3	Chamba	Quaternary	Fluvial/Fluvio-glacial/ Alluvium	Boulder conglomerate, Sandstone, gravel beds, clays, etc.
4	Hamirpur	Quaternary	Alluvium	Sand, Gravel, Pebble & Boulders and clay
5	Bilaspur	Quaternary	Alluvium; fluvial, terrace, piedmont	Sand, silt, clay, gravel, pebble, cobble, and boulders etc.
6	Solan	Quaternary	Alluvium/valley fills/ Older alluvium	Sand with pebble and clay, medium to coarse-grained sand with pebbles of sandstone, and lenses of clay
7	Sirmour	Quaternary	Alluvium/valley fills/ Older	Sand with pebble and clay & multiple cyclic sequences of medium to coarse-grained sand with pebbles of sandstone and lenses of clay
8	Mandi	Quaternary	Alluvium; Terrace & Fluvial deposits	Alluvium, clay, sands, gravels, pebbles, boulders, and cobbles
9	Kullu	Quaternary	Alluvium; fluvial, terrace, piedmont	Sand, silt, clay, boulders, pebble, and cobble, etc.
10	Kinnaur	Quaternary	Alluvium, Terrace & Fluvial deposits	Alluvium, clay, sand, gravel, pebbles, boulders and cobbles
11	Lahaul & Spiti	Quaternary	Fluvial/Fluvio-glacial/ Alluvium	Sand, silt, pebbles, cobbles, boulders
12	Shimla	Quaternary	Alluvium	Sand with pebble and clay, medium to coarse-grained sand with pebbles of sandstone, and lenses of clay

Kinnaur, Lahaul & Spiti, and the Shimla district of the State. The total area of moraine complexes of Quaternary deposits of the state is approximately 718 Km². Alluvial fans a triangle-shaped deposit of gravel, sand, and even smaller pieces of sediment, such as silt. This sediment is called alluvium. Alluvial fans are usually created as flowing water interacts with mountains, hills, or the steep walls of canyons. The total area of Alluvial fan of Quaternary deposits of the state is approximately 113 Km².

DST-SERB Sponsored Project (ECR)
Holocene centennial to millennial-scale changes in Indian Summer Monsoon: a multi-proxy record from high altitude regions of Uttarakhand Himalaya
(Suman Lata Srivastava)

In order to reconstruct a high-resolution record of the Holocene Indian summer monsoon (ISM) variability in the Central Himalaya, inorganic (grain size and environmental magnetism) and organic (total organic

SPONSORED PROJECTS

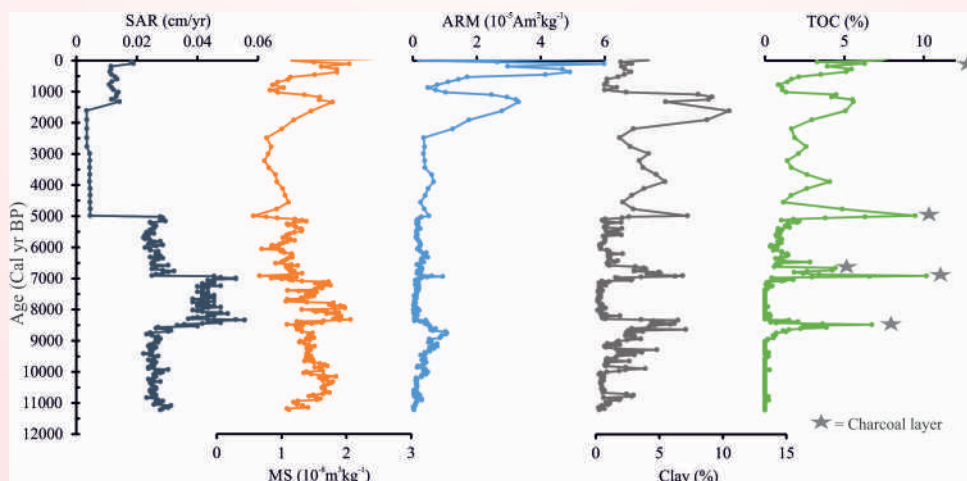


Fig. 79. Results of sediment accumulation, environmental magnetism (MS and ARM), clay, and total organic carbon of the Dayalishera lake plotted against chronology.

carbon) proxy methods were applied on a chronologically well-constrained lake sediment sequence from the high altitude region of Dayalishera Chamoli, Uttarakhand. The sediment accumulation rate varied from ~ 0.003 to 0.055 cm yr^{-1} with maximum sedimentation between ~ 8500 and 7000 cal yr BP , and minimum sedimentation between ~ 5000 and 1500 cal yr BP (Fig. 79). Magnetic susceptibility (MS) showed increased values between $\sim 11,200$ and 9700 cal yr BP indicating a higher supply of magnetic minerals in response to strengthen the ISM precipitation. Increased

anhysteretic remanence magnetization (ARM) and clay percentage between $\sim 11,200$ and 8500 cal yr BP also indicated higher lake level during this period (Fig. 79). The Total Organic Carbon (TOC) showed five big spikes at ~ 8500 , ~ 7000 , ~ 6600 , ~ 5000 , and 0 (i.e. 1950 AD) cal yr BP (Fig. 79). These TOC peaks correspond to black charcoal-rich layers of the lake sediment sequence. Interestingly, these peaks also correspond to increased clay percentage. TOC spikes and increased clay content may indicate events of forest fire leading to abrupt increased carbon burial/charcoal content.

RESEARCH PUBLICATIONS

Papers Published

1. Ali, S.N., Agarwal, S., Quamar, M.F., Dubey, J., Chauhan, N., Bisht, P., Pandey, P., Arif, Md., Shekhar, M. & Morthekai, P. 2020: Climate variability in the Central Himalaya during the last ~15 kyr: Evidence of precipitation variability from multiproxy studies. *Journal of the Palaeontological Society of India*, 65(1), 36-54.
2. Ali, S.N., Quamar, M.F., Dubey, J., Morthekai, P., Bisht, P., Pandey, P., Shekhar, M. & Ghosh, R. 2020: Surface pollen distribution in alpine zone of the higher Himalaya: a case study from the Kalla glacier valley, India. *Botany Letters*, 167, 3, 340-352.
3. Arora, S., Joshi, A., Kumari, P., Kumar, P., Sah, S.K., Lal, S. & Singh, N.P. 2020: Strong ground motion simulation techniques” a review in world context. *Arabian Journal of Geosciences*, 13, 14, 673.
4. Arun, K.P., Sain, K. & Kumar, J. 2020. Application of constrained AVO inversion: 2D modelling of gas hydrates and free gas in Mahanadi basin, India, *Jour. of Natural Gas Sciences & Engineering*, 78, 103287, 1-19.
5. Bali, H., Gupta, A.K., Mohan, K., Thirumalai, K., Tiwari, S.K. & Panigrahi, M.K. 2020: Evolution of the Oligotrophic West Pacific Warm Pool During the Pliocene-Pleistocene Boundary. *Paleoceanography and Paleoclimatology*, 35, 11, e2020PA003875.
6. Barkat, R., Chakraborty, P.P., Saha, S. & Das, K. 2020: Alluvial architecture, paleohydrology and provenance tracking from the Neoproterozoic Banganapalle formation, Kurnool Group, India: An example of continental sedimentation before land plants. *Precambrian Research* 350, 1059302
7. Bhambri, R., Watson, C.S., Hewitt, K., Haritashya, U.K., Kargel, J.S., Pratap, Shahi A., Chand, P., Kumar, A., Verma, A. & Govil, H. 2020: The hazardous 2017-2019 surge and river damming by Shispare Glacier, Karakoram. *Scientific Reports*, 10, 1, 4685.
8. Bhasin, R., Shabanimashcool, M., Hermanns, R.L., Morken, O.A., Dehls, J.F. & Gupta, V. 2020: Back Analysis of Shear Strength Parameters of a Large Rock Slide in Sikkim Himalaya. *Journal of Rock Mechanics and Tunnelling Technology (JRMTT)*, 26(2), 81-92.
9. Bhaskar, Rao, Y.J., Chopra S., Kumar P., Mukherjee, P.K., Singhal, S., Adlakha, V., Vijaya, Kumar, T., Sreenivas, B. & Babu, E.V.S.S.K. 2020: New initiatives to bolster analytical facilities in India for in situ U-Th-Pb geochronology, Hf and O isotope systematics in zircon: A focus on laboratories at the IUAC, WIHG and CSIR-NGRI. *Proceedings of the Indian National Science Academy*, 86, 1, 643-650.
10. Biswal, S., Kumar, S., Roy, S.K., Kumar, M.R., Mohanty, W.K., Parija, M.P. & Paul, A. 2020: Upper mantle anisotropy beneath the western segment, NW Indian Himalaya using shear wave splitting. *Lithosphere*, 2020(1), 1-9.
11. Chahal, P., Kumar, A., Sharma, P.C., Sundriyal, Y.P. & Srivastava, P. 2020: A preliminary assessment of the geological evidence of the mega floods in the upper Zanskar catchment, NW Himalaya. *Journal of Paleontological Society of India*, 65(1), 64-72.
12. Chakraborty, P.P., Tandon, S.K., Roy, S.B., Saha, S. & Paul, P.P. 2020: Proterozoic sedimentary basins of India. *Springer Geology*, 145-177.
13. Chaurasia, C., Madhavan, K., Thakur, S.S., Patel, S.C., Samal, A.K., Nema, S. & Dixit, P.K. 2020: Occurrence and Stability of Allanite and Monazite in the Greater Himalayan Sequence, Dhauliganga Valley, Garhwal Himalaya. *Journal of the Geological Society of India*, 6, 557-564.
14. Coudurier-Curveur, A. Tapponnier, P., Okalc, E., Woerd, J. Van der, Kali, E., Choudhury, S., Baruah, S., Etchebes, M., & Karakaşa, C., 2020: A composite rupture model for the great 1950 Assam earthquake across the cusp of the East Himalayan Syntaxis. *Earth and Planetary Science Letters*, 531, (115928), 1-13.
15. Dailey, S.K, Clift, P.D, Kulhanek, D.K, Blusztajn, J., Routledge, C.M, Calves, G., O'Sullivan, P., Jonell, T.N, Pandey, D.K, Ando, S., Coletti, G., Zhou, P., Li, Y.T, Neubeck, N.E, Bendle, J.A.P, Aharonovich, S., Griffith, E.M, Gurumurthy, G.P, Hahn, A., Iwai, M., Khim, B.K, Kumar, A.,

- Kumar, A.G, Liddy, H.M, Lu, H.Y, Lyle, M.W, Mishra, R., Radhakrishna, T., Saraswat, R., Saxena, R., Scardia, G., Sharma, G.K, Singh, A.D, Steinke, S., Suzuki, K., Tauxe, L, Tiwari, M., Xu, Z.K & Yu, Z.J. 2020: Large-scale Mass Wasting on the Miocene Continental Margin of Western India. *Geological Society of America Bulletin*, 132, 85-112.
16. Das, S., Basu, A.R., Mukherjee, B.K., Marcantonio, F., Sen, K., Bhattacharya, S. & Gregory, R.T. 2020: Origin of Indus ophiolite-hosted ophicarbonates veins: Isotopic evidence of mixing between seawater and continental crust-derived fluid during Neo-Tethys closure. *Chemical Geology*, 551, 119772.
 17. Dhamodharan, S., Rawat, G., Kumar, S. & Bagri, D.S. 2020: Sedimentary thickness of the northern Indo-Gangetic plain inferred from magnetotelluric studies. *Journal of Earth System Science*, 129, 1, 156.
 18. Diwate, P., Meena, N.K. & Pandita, S. 2020: Climate variability from Indian subcontinent in the last 2ka: A Review. *Journal of Critical Review*, 7(5), 2460-2467. doi:10.31838/jcr.07.05.413
 19. Diwate, P., Meena, N.K., Bhushan, R., Pandita, S., Chandana, K.R. & Kumar, P. 2020: Sedimentation rate (210Pb and 137Cs), grain size, organic matter and bathymetric studies in Renuka Lake, Himachal Pradesh, India. *Himalayan Geology*, 41(1), 126-138.
 20. Fareeduddin, Pant, N.C., Gupta, S., Chakraborty, P., Sensarma, S., Jain, A.K., Prasad, G.V.R., Srivastava, P., Rajan S. & Tiwari, V.M. 2020: The Geodynamic Evolution of the Indian Subcontinent- An Introduction. *Episodes*, 43(1), 7-18.
 21. Gautam, P.K., Rajesh, S., Kumar, N. & Dabral, C.P. 2020: GPS measurements on pre-, co- and post-seismic surface deformation at first multiparametric geophysical observatory, Ghuttu in Garhwal Himalaya, India. *Journal of Geodetic Science*, 10, 1, 136-144.
 22. Gupta, A.K., Prakasam, M., Dutt, S., Clift, P.D. & Yadav, R.R. 2020: Evolution and development of the Indian monsoon. *Springer Geology*, 499-535.
 23. Jaglan, S., Gupta, A.K., Cheng, H., Clemens, S.C., Dutt, S. & Balaji, S. 2020: Indian summer monsoon variability during the last millennium as recorded in stalagmite from Baratang Mahadev cave, Andaman Islands. *Palaeogeography, Palaeoclimatology, Palaeoecology*, 109908.
 24. Jain, A.K., Mukherjee, P.K. & Singhal, S. 2020: Terrane characterization in the Himalaya since Paleoproterozoic. *Episodes*, 43, 1, 346-357.
 25. Jain, A.K., Thakur, V.C., Joshi, M., Mukherjee, P.K., Patel, R.C., Bhattacharyya, K., Singhal, S., Agarwal, K.K., Dixit, R., Deshmukh, G. & Mohan, M. 2020: Tectonics of the Western, Sikkim and Arunachal Himalaya. *Proceedings of the Indian National Science Academy*, 189-212.
 26. Jalal, P., Pandey, J.B., Ahmad, S.M., Dutt, S., Shukla, U.K. & Maddodi, B. 2020: Effect of Deccan lava flows on the sedimentological evolution of Gurmatkal intertrappeans Karnataka, Southern India. *Geological Journal*, 55, 6, 4681-4690.
 27. Jamir, I., Gupta, V., Thong, G.T. & Kumar, V. 2020: Litho-tectonic and precipitation implications on landslides, Yamuna valley, NW Himalaya. *Physical Geography (Online)*, org/10.1080/02723646.2019.1672024
 28. Jayangondaperumal, R., Mishra, R.L., Rao, P. Singh, Yadav, R.K., Mohanty, D.P., Pandey, A., Singh, I., Aravind, A. & Dash, S. 2020: Active Tectonics of Himalaya, Rift Basins in Central India and those Related to Crustal Deformation at Different Time Scales (Status report). *Proceedings of Indian National Science Academy*, 86, 445-458.
 29. Kar, A. & Kumar, A. 2020: Evolution of arid landscape in India and likely impact of future climate change. *Episodes*, 43, 1, 511-523.
 30. Khan, Z., Sachan, H.K., Ahmad, A.H.M. & Ghaznavi, A.A. 2020: Microfacies, diagenesis, and stable isotope analysis of the Jurassic Jumara Dome carbonates, Kachchh, Western India: Implications for depositional environments and reservoir quality. *Geological Journal*, 55, 1, 1041-1061.
 31. Khanam, S., Quasim, M.A., Ahmad, A.H.M. & Ghosh, S.K. 2020: Sedimentation in a Rifted Basin: Insights from the Proterozoic Rajgarh Siliciclastics, Delhi Supergroup, Northeastern Rajasthan. *Journal of the Geological Society of India*, 5, 557-564.
 32. Kharya, A., Sachan, H.K. & Rai, S.K. 2020: Fluid evolution of Indus basin, Ladakh North-West Himalaya, India: Constraint from Fluid Inclusion

- and Oxygen Isotope Thermometry. *International Journal of Earth Sciences*, 109, 669-687.
33. Krishnamurthi, R., Sahoo, A.K., Sharma, R. & Sangurmath, P. 2020: Abundance of Carbonic Fluid Inclusions in Hira-Buddini Gold Deposit, Hutti-Maski Greenstone Belt, India: Inferences from Petrography and Volume Ratio Estimation of Fluid Components. *Journal of Earth Science*, 31, 3, 492-499.
 34. Kumar, A., Dutt, S., Saraswat, R., Gupta, A.K., Clift, P.D., Pandey, D.K., Yu, Z. & Kulhanek, D.K. 2020: Late Pleistocene sedimentation in the Indus Fan, Arabian Sea, IODP Site U1457. *Geological Magazine*, 1-9.
 35. Kumar, A., Ray, Y., Ghosh, R., Singh, V. & Srivastava, P. 2020: Late Quaternary sedimentation history of the Himalaya and its foreland. *Episodes*, 43, 498-510.
 36. Kumar, A., Srivastava, P. & Devrani, R. 2020: Using clast geometries to establish paleoriver discharges: Testing records for aggradation and incision from the upper Indus River, Ladakh Himalaya. *Geomorphology*, 362, 107202.
 37. Kumar, A., Srivastava, P., Sen, K., Morell, K. & Hazarika, D. 2020: Evidence for late Quaternary brittle deformation and back thrusting within the Indus Suture Zone, Ladakh Himalaya. *Tectonophysics*, 792, 228597.
 38. Kumar, A.K., Kumar, D., Kumar, V. & Singh, D.S. 2020: Study of temporal response (1976-2019) and associated mass movement event (during 2017) of Meru glacier, Bhagirathi valley, Garhwal Himalaya, India. *Quaternary International*, 565, 12-21.
 39. Kumar, N., Kumar, N., Sharma, R. & Singh, A.K. 2020: Petrogenesis and Tectonic Significance of the Neoproterozoic Magmatism of the Tusham Ring Complex (NW Indian Shield): Insight into Tectonic Evolution of the Malani Igneous Suite and Rodinia Supercontinent. *Geotectonics*, 54, 3, 428-453.
 40. Kumar, Naveen, Sharma, R., Kumar, N. & Singh, A.K. 2020: A Review on Petrology and Geochemistry of the Neoproterozoic Malani Igneous Suite and Related Rocks (Northwestern Peninsular India). *Petrology*, 28, 6, 591-657.
 41. Kumar, P.C. & Sain, K. 2020: A Machine learning tool for interpretation of Mass Transport Deposits from seismic data. *Scientific Reports*, 10,1,14134.
 42. Kumar, P.C. & Sain, K. 2020: Interpretation of magma transport through saucer sills in shallow sedimentary strata using an automated machine learning approach. *Tectonophysics*, 789, 228541.
 43. Kumar, R. 2020: Late Cenozoic Himalayan foreland basin: Sedimentologic attributes. *Episodes*, 43, 1, 417-428.
 44. Kumar, V., Shukla, T., Mishra, A., Kumar, A. & Mehta, M. 2020: Chronology and climate sensitivity of the post-LGM glaciation in the Dunagiri valley, Dhauliganga basin, Central Himalaya, India. *BOREAS: An International Journal of Quaternary research*, 50, 1, 324-329.
 45. Kumari, R., Kumar, P., Kumar, N. & Sandeep 2020: Role of site effect for the evaluation of attenuation characteristics of P, S and coda waves in Kinnaur region, NW Himalaya. *Journal of Earth System Science*, 129, 1, 191.
 46. Kundu, A., Hazarika, D., Hajra, S., Singh, A.K., Ghosh, P. 2020. Crustal thickness and Poisson's ratio variations in the northeast India-Asia collision zone: Insight into the Tuting-Tidding Suture zone, eastern Himalaya. *Journal of Asian Earth Sciences*, 188, 104099.
 47. Lakhan, N., Singh, A.K., Singh, B.P., Premi, K. & Oinam, G. 2020: Evolution of Late Cretaceous to Palaeogene Basalt-andesite-dacite-rhyolite volcanic suites along the northern margin of the Ladakh magmatic arc, NW Himalaya, India. *Journal of Earth System Science*, 129, 1, 108.
 48. Lakhan, N., Singh, A.K., Singh, B.P., Sen, K., Singh, M.R., Khogenkumar, S., Singhal, S. & Oinam, G. 2020: Zircon U-Pb geochronology, mineral and whole-rock geochemistry of the Khardungvolcanics, Ladakh Himalaya, India: Implications for Late Cretaceous to Palaeogene continental arc magmatism. *Geological Journal*, 55, 5, 3297-3320.
 49. Lokho, K., Aitchison, J.C., Whiso, K., Lhoupenyi, D., Zhou, R. & Raju, D.S.N. 2020: Eocene foraminifers of the Naga Hills of Manipur, Indo-Myanmar Range (IMR): Implications on age and basin evolution. *Journal of Asian Earth Sciences*, 191, 105259.
 50. Luirei, K., Bhakuni, S.S., Longkumer, L., Joshi, L.M. & Kothiyari, G.C. 2020: Quaternary

- landform study in Kosi and Dabka river valleys in Kumaun sub-Himalaya: Implication of reactivation of thrusts. *Geological Journal*, 55, 6, 4810-4829.
51. Mahajan, A.K. & Kumar, P. 2020: Subsurface site characterization of Donga Fan, Northwest Himalaya using multichannel analysis of surface waves and response analysis. *Current Science*, 119, 12, 1948-1960.
 52. Mahima, Karakoti, I., Nandan, H. & Pathak, P.P. 2020: An Analytical Study on global radiation and meteorological parameters for India. *International Journal of Ambient Energy*, 10, 1165-1175.
 53. Mal, S., Kumar, A., Bhambri, R., Schickhoff, U. & Singh, R.B. 2020: Inventory and Spatial Distribution of Glacial Lakes in Arunachal Pradesh, Eastern Himalaya, India. *Journal of the Geological Society of India*, 6, 609-615.
 54. Managave, S., Shimla, P., Yadav, R.R., Ramesh, R. & Balakrishnan, S. 2020: Contrasting centennial-scale climate variability in High Mountain Asia revealed by a tree-ring oxygen isotope record from Lahaul-Spiti. *Geophysical Research Letters*, 2020, doi.org/10.1029/2019GL086170.
 55. Matta, G., Kumar, A., Nayak, A., Kumar, P., Kumar, A. & Tiwari, A.K. 2020: Determination of water quality of Ganga River System in Himalayan region, referencing indexing techniques. *Arabian Journal of Geosciences*, 13, 19, 1027.
 56. Matta, G., Nayak, A., Kumar, A., Kumar, P., Kumar, A., Tiwari, A.K. & Naik, P.K. 2020: Evaluation of heavy metals contamination with calculating the pollution index for Ganga River system. *Taiwan Water Conservancy*, 68, 3, 52-65.
 57. Maurya, S. & Rai, S.K. 2020: Geochemical and Isotopic Composition of Gypsum Deposits from Sahastradhara Region of Lesser Himalaya, India. *Journal Geological Society of India*, 95, 205-211.
 58. Mishra, P.K., Chauhan, P.R., Diwate, P., Shah, P. & Ambili, A. 2020: Holocene climate variability and cultural dynamics in the Indian subcontinent. *Episodes*, 43(1), 552-562.
 59. Misra, A., Kumar, A., Haritashya, U.K., Verma, A., Dobhal, D.P., Gupta, Anil K., Gupta, G. & Upadhyay, R. 2020: Topographic and climatic influence on seasonal snow cover: Implications for the hydrology of ungauged Himalayan basins, India. *Journal of Hydrology*, 585, 124716.
 60. Misra, S., Bhattacharya, S., Mishra, P.K., Misra, K.G., Agrawal, S. & Anoop, A. 2020: Vegetational responses to monsoon variability during Late Holocene: Inferences based on carbon isotope and pollen record from the sedimentary sequence in Dzukou valley, NE India. *Catena* 194, 1046972.
 61. Moiya, J.N., Luirei, K., Longkumar, L. Kothiyari, G.C. & Thong, G.T. 2020: Late Quaternary deformation in parts of the schuppen belt of Dimapur and peren districts, Nagaland, India. *Geological Journal*, 55, 457-476.
 62. Monika, Kumar P., Sandeep, Kumar, S., Joshi, A. & Devi, S. 2020: Spatial variability studies of attenuation characteristics of Qa and Qb in Kumaon and Garhwal region of NW Himalaya. *Natural Hazards*, 103, 1, 1219-1237.
 63. Mukherjee, B., Roy, P.N.S. & Sain, K. 2020. Delineation of hydrocarbon and non-hydrocarbon zones using fractal analysis of well-log data from Bhogpara oil field, NE India, *Carbonates and Evaporites*, 35:22, 1-24.
 64. Negi, M., Rai, Santosh, K., Ghosh, S.K., Bhan, U. & Singhal, S. 2020: Characterization of the detrital zircon from the Lesser Himalayan Proterozoic siliciclastics. *Himalayan Geology*, 41(1), 126-138.
 65. Oinam, G., Singh, A.K., Joshi, M., Dutt, A., Singh, M.R., Singh, N.L. & Singh, R.K. Bikramaditya 2020: Continental extension of northern Gondwana margin in the Eastern Himalaya: Constraints from geochemistry and U-Pb zircon ages of mafic intrusives in the Siang window, Arunachal Himalaya, India. *Geoscience Sciences de la Planete*, 352, 1, 19-41.
 66. Panda, S., Kumar, A., Das, S., Devrani, R., Rai, S.K., Prakash, K. & Srivastava, P. 2020: Chronology and sediment provenance of extreme floods of Siang River (Tsangpo-Brahmaputra River valley), northeast Himalaya. *Earth Surface Processes and Landforms*, 11, 2495-2511.
 67. Pandey, C.P., Singh, J., Soni, V.K. & Singh, N. 2020: Yearlong first measurements of black carbon in the western Indian Himalaya: Influences of meteorology and fire emissions. *Atmospheric Pollution Research*, 11, 7, 1199-1210.

68. Patranabis-Deb, S. & Saha, S. 2020: Geochronology, paleomagnetic signature and tectonic models of cratonic basins of India in the backdrop of Supercontinent amalgamation and fragmentation. *Episodes*, 43 (1), 145-163.
69. Prasad, S., Marwan, N., Eroglu, D., Goswami, B., Mishra, P.K., Gaye, B., Anoop, A., Basavaiah, N., Stebich, M. & Jehangir, A. 2020: Holocene climate forcings and lacustrine regime shifts in the Indian summer monsoon realm. *Earth Surface Processes and Landforms*, 15, 3842-3853.
70. Priyamvada, S. & Kumar, S. 2020: Attenuation of seismic coda waves in Sikkim Himalayas, India. *Disaster Advances*, 13, 3, 17-23.
71. Pundir S., Adlakha V., Kumar S. & Singhal S. 2020: Closure of India-Asia collision margin along the Shyok Suture Zone in the eastern Karakoram: new geochemical and zircon U-Pb geochronological observations. *Geological Magazine*, 157, 1451-1472.
72. Pundir S., Adlakha V., Kumar S., Singhal S. & Sen K. 2020: Petrology, geochemistry and geochronology of granites and granite gneisses in the SE Karakoram, India: Record of subduction-related and pre- to syn-kinematic magmatism in the Karakoram Fault Zone. *Mineralogy and Petrology*, 14, 413-434.
73. Quasim, M.A., Ghosh, S.K., Ahmad, A.H.M., Srivastava, V.K. & Albaroot, M. 2020: Integrated approach of lithofacies and granulometric analysis of the sediments of the Proterozoic Upper Kaimur Group of Vindhyan Supergroup, Son Valley, India: Palaeo-environmental implications. *Geological Journal*, 55, 9, 5991-6012.
74. Rai, N., Singha, D.K. Shukla, P.K. & Sain, K. 2020. Delineation of discontinuity using multi-channel seismic attributes: An implication for identifying fractures in gas hydrate sediments in offshore Mahanadi basin, Results in *Geophysical Sciences*, 1-4, 100007, 1-10.
75. Rai, S.K. 2020: Geochemical constituents in hot spring waters in the Third Pole. *Water Quality in the Third Pole* (Elsevier Publication) 211-235.
76. Ram P., Gupta, V., Devi, M. & Vishwakarma, N. 2020: Landslide susceptibility mapping using Bivariate Statistical method for the hilly township of Mussoorie and its surrounding areas, Uttarakhand Himalaya. *Journal of Earth System Science*, 129-167.
77. Rao, Y.J.B., Chopra, S., Kumar, P., Mukherjee, P.K., Singhal, S., Adlakha, V., Kumar, T.V., Sreenivas, B. & Babu, E.V.S.S.K. 2020: New initiatives to bolster analytical facilities in India for in situ U-Th-Pb Geochronology, Hf and O isotope systematics in zircon: a focus on laboratories at the IUAC, WIHG and CSIR-NGRI. *Proceedings of Indian National Science Academy*, 86(1), 643-650.
78. Rawat, G., Bartarya, S.K., Singh, B. & Bhasin, R.K. 2020: Geophysical Characterization of Chumathang (Ladakh) Hot Spring. In: Biswas A. & Sharma S. (eds), *Advances in Modeling and Interpretation in Near Surface Geophysics*. Springer Geophysics. Springer, Cham, doi:10.1007/978-3-030-28909-6_13
79. Sain, K., Sharma, R., Kumar, S., Dobhal, D.P., Gupta, V., Srivastava, P., Perumal, R.J.G. & Lokho, K. 2020. Research status at Wadia Institute of Himalayan Geology (WIHG), Dehradun during 2015-2019, In D.M. Banerjee & Sunil Bajpai (Ed.), *Proceedings of the Indian National Science Academy*, 2015-2019, 86(1), 721-745.
80. Saji, A.P., Sunil, P.S., Sreejith, K.M., Gautam, P.K., Kumar, K.V., Ponraj, M., Amirtharaj, S., Shaju, R.M., Begum, S.K., Reddy, C.D. & Ramesh, D.S. 2020: Surface Deformation and Influence of Hydrological Mass Over Himalaya and North India Revealed from a Decade of Continuous GPS and GRACE Observations. *Journal of Geophysical Research: Earth Surface*, 125, e2018JF004943.
81. Samal, A.K., Mishra, P.K. & Biswas, A. 2020: Assessment of origin and distribution of fluoride contamination in groundwater using an isotopic signature from a part of the Indo-Gangetic Plain (IGP), India. *HydroResearch*, 3, 75-84.
82. Saravanan, P., Gupta, A.K., Panigrahi, M.K., Tiwari, S.K., Rai, S.K. & Prakasam, M. 2020: Response of shallow-sea benthic foraminifera to environmental changes off the coast of Goa, eastern Arabian Sea during the last ~6,100 calyr BP. *Geological Magazine*, 157(3), 497-505.
83. Saravanan, P., Gupta, A.K., Zheng, H., Majumder, J., Panigrahi, M.K. & Kharya, A. 2020: A 23000 year old record of paleoclimatic and environmental changes from the eastern Arabian Sea. *Geological Magazine*, 157, 3, 497-505.

84. Saravanan, P., Gupta, A.K., Zheng, H., Rai, S.K. & Panigrahi, M.K. 2020: Changes in Deep-Sea Oxygenation in the Northeast Pacific Ocean During 32-10 ka. *Geophysical Research Letters*, 47, 11, e2019GL086613.
85. Sharma, A., Kumar, D. & Paul, A. 2020: Estimation of Site response functions for the Kumaun-garhwal region of Himalaya, India. *J. seismology*, 24, 655-678.
86. Sharma, C.P., Rawat, S.L., Srivastava, P., Meena, N.K., Agnihotri, R., Kumar, A., Chahal, P., Gahlaud, S.K.S. & Shukla, U.K. 2020: High-resolution climatic (monsoonal) variability reconstructed from a continuous ~2700-year sediment record from Northwest Himalaya (Ladakh). *Holocene*, 30, 3, 441-457.
87. Shukla, A. & Garg, P.K. 2020: Spatio-temporal trends in the surface ice velocities of the central Himalayan glaciers, India. *Global and Planetary Change*, 190, 103137.
88. Shukla, A., Garg, S., Mehta, M., Kumar, V. & Shukla, U.K. 2020: Temporal inventory of glaciers in the Suru sub-basin, western Himalaya: impacts of regional climate variability. *Earth System Science Data*, 12(2), 1245-1265.
89. Shukla, A.D., Sharma, S., Rana, N., Bisht, P. & Juyal, N. 2020: Optical chronology and climatic implication of glacial advances from the southern Ladakh Range, NW Himalaya, India. *Palaeogeography, Palaeoclimatology, Palaeoecology*, 539, 109505.
90. Shukla, T., Mehta, M., Dobhal, D.P., Bohra, A., Pratap, B. & Kumar, A. 2020: Late-Holocene climate response and glacial fluctuations revealed by the sediment record of the monsoon-dominated Chorabari Lake, Central Himalaya. *Holocene*, 30, 7, 953-965.
91. Shukla, T., Mehta, M., Dobhal, D.P., Bohra, A., Pratap, B. & Kumar, A. 2020: Misinterpreting proxy data for paleoclimate signals: A reply to Srivastava and Jovane. *Holocene*, 30, 12, 1874-1883.
92. Shukla, V., Chauhan, V., Kumar, N. & Hazarika, D. 2020: Assessment of Rn-222 continuous time series for the identification of anomalous changes during moderate earthquakes of the Garhwal Himalaya. *Applied Radiation and Isotopes*, 166, 109327.
93. Singh, A., Ojha, M. & Sain, K. 2020: Predicting lithology using neural network from downhole data of a gas hydrate reservoir in Krishna-Godavari basin, eastern Indian offshore. *Geophysical Journal International*, 220(3), 1813-1837.
94. Singh, J., Yadav, R.R., Negi, P.S. & Rastogi, T. 2020: Sub-alpine trees testify late 20th century rapid retreat of Gangotri glacier, Central Himalaya. *Quaternary International*, 565, 31-40.
95. Singh, M.R., Singh, A.K., Santosh, M., Lingadevaru, M. & Lakhan, N. 2020: Neorchean arc-back arc subduction system in the Indian Peninsula: Evidence from mafic magmatism in the Shimoga greenstone belt, western Dharwar Craton. *Geological Journal*, 55, 7, 5308-5329.
96. Singh, N., Singhal, M., Chhikara, S., Karakoti, I., Chauhan, P. & Dobhal, D.P. 2020. Radiation and energy balance dynamics over a rapidly receding glacier in the central Himalaya. *International Journal of Climatology*, 40(1), 400-420.
97. Singh, P. & 70 others, 2020: Atlas of Structural Geology. *In: S. Mukherjee, (ed.), Atlas of Structural Geology*. Elsevier Publication, 2, 282.
98. Singh, P., Singhal, S. & Das, A.N. 2020: U- Pb (zircon) geochronologic constraint on tectono-magmatic evolution of Chaurgranitoid complex (CGC) of Himachal Himalaya, NW India: implications for the Neoproterozoic magmatism related to Grenvillian orogeny and assembly of the Rodinia supercontinent. *International Journal of earth Sciences*, 109, 1, 373-390.
99. Singh, P.C., Sachan, H.K., Kharya, A., Rolfo, F., Groppo, C., Singhal, S., Tiwari, S.K. & Rai, S.R. 2020: Tectono-metamorphic evolution of the Karakoram Terrane: Constrained from P-T-t fluid history of garnet-bearing amphibolites from trans Himalaya, Ladakh, India. *Journal of Asian Earth Science*, 196, 104293.
100. Singh, S., Gupta, A.K., Dutt, S., Bhaumik, A.K. & Anderson, D.M. 2020: Abrupt shifts in the Indian summer monsoon during the last three millennia. *Quaternary International*, 558, 59-65.
101. Singh, S., Kumar, S., Gupta, P., Singhal, S. & Sahu, A. 2020: The himalayan magmatic events. *Proceeding of the Indian National Science*, 86, 1, 213-216.
102. Solé, Floréal, Bast, Eric De, Legendre, Hélène, Rana, Rajendra S., Kumar, Kishor, Rose, Kenneth

- D. & Smith, Thierry 2020: New Specimens of Frugivastodon (Mammalia: Apatotheria) from the Early Eocene of India Confirm Its Apatemyid Status and Elucidate Dispersal of Apatemyidae. G. Prasad, V.R. & Patnaik, R. (eds.), *Biological Consequences of Plate Tectonics: New Perspectives on Post-Gondwana Break-up—A Tribute to Ashok Sahni Vertebrate Paleobiology and Paleoanthropology Series*, 279-304.
103. Srivastava, P. 2020: Landscape evolution of rivers in the Ganga plain and Himalaya. *Proceeding of the Indian National Science*, 86, 1, 369-377.
104. Srivastava, P., Kumar, A., Singh, R., Deepak, O., Kumar, A.M., Ray, Y., Jayangondaperumal, R., Phartiyal, B., Chahal, P., Sharma, P., Ghosh, R., Kumar, N. & Agnihotri, R. 2020: Rapid lake level fall in Pangong Tso (lake) in Ladakh, NW Himalaya: a response of late Holocene aridity. *Current Science*, 119(2), 219-231.
105. Srivastava, V.K. & Aggarwal, A. 2020: Middle Eocene regressive phase evident in the uppermost part of the Harudi Formation, Kachchh Basin western India. *Carbonates and Evaporites*, 35, 1, 17.
106. Sundriyal, S., Shukla, T., Tripathi, L. & Dobhal, D.P. 2020: Natural Versus anthropogenic influence on trace elemental concentration in precipitation at Dokriani Glacier, central Himalaya, India. *Environmental Science and Pollution Research*, 27(3), 3462-3472.
107. Suresh, N. & Kumar, R. 2020: Late Quaternary Deflections of the Beas-Satluj rivers at the Himalayan mountain front, Kangra re-entrant, India: Response to fold growth and climate. *Journal of Asian Earth Science*, 191, 104248.
108. Thakur, V.C., Joshi, M. & Jayangondaperumal, R. 2020: Active Tectonics of Himalayan Frontal Fault Zone in the Sub-Himalaya, Chapter 12. In: Gupta, N. & Tandon, S.K. (eds.), *Geodynamics of the Indian Plate*. Springer Geology, 439-466, doi.org/10.1007/978-3-030-15989-4_12
109. Thakur, V.C., Joshi, M. & Suresh, N. 2020: Linking the Kangra piggy-back Basin with the reactivation of the Jawalamukhi Thrust and erosion of Dhauladhar Range, Northwest Himalaya. *Episodes*, 43, 335-345.
110. Thewissen, J.G.M., Nanda, A.C. & Bajpai, S. 2020: Indohyus, Endemic Radiation of Raoellid Artiodactyls in the Eocene of India and Pakistan. *Vertebrate Paleobiology and Paleoanthropology*, 337-346.
111. Tiwari, S.K., Gupta, A.K. & Asthana, A.K.L. 2020: Evaluating CO₂ flux and recharge source in geothermal springs, Garhwal Himalaya, India: stable isotope systematics and geochemical proxies. *Environmental Science and Pollution Research*, 27, 14818-14835.
112. Vedanti, N., Vadapalli, U. & Sain, K. 2020: A brief overview of CBM development in India. *Proceeding of the Indian National Science Academy*, 86, 1, 623-629.
113. Yadav, R.K., Gahalaut, V.K., Gautam, P.K., Jayangondaperumal, R., Sreejith, K.M., Singh, I., Kumar, A., Jeevivek, V., Agrawal, R., Catherine, J.K. & Sati, S.P. 2020: Geodetic Monitoring of Landslide Movement at two sites in the Garhwal Himalaya. *Himalayan Geology*, 41(1), 21-30.
114. Yadav, R.R. & Singh, J. 2020: Tree-ring-width chronologies from moisture stressed sites fail to capture volcanic eruption associated extreme low temperature events. *Current Science*, 119, 189-194.
115. Yousuf, B., Shukla, A., Arora, M.K., Bindal, A. & Jasrotia, A.S. 2020: On Drivers of Subpixel Classification Accuracy—An Example from Glacier Facies. *IEEE Journal of Selected Topics in Applied Earth Observations and Remote Sensing*, 13, 601-608.
116. Zhou, R., Aitchison, J.C., Lokho, K., Sobel, E.R., Feng, Y. & Zhao, J.X. 2020: Unroofing the Ladakh batholiths: constraints from autochthonous molasse of the Indus basin, NW Himalaya. *Journal of the Geological Society of London*, 177, 818-825.

SEMINAR/SYMPOSIA/WORKSHOP ORGANIZED

The 4th National Geo-Research Scholars Meet (NGRSM) (June 23-24, 2020)

The Wadia Institute of Himalayan Geology (WIHG), Dehradun has successfully organized the 4th National Geo-research Scholars Meet (NGRSM) through webinars during June 23-24, 2020. The NGRSM started in 2016 as an annual event of WIHG to encourage young researchers and students for improving their research interests, providing them a platform to share their research work, receive feedback from their peers and refine their ideas. The event also provides them an opportunity for interaction with eminent geoscientists and understanding the latest trends in Geoscientific research. This year, due to the global pandemic COVID-19, the 4th NGRSM is being organized through webinars, the first one of this kind from WIHG. The theme of the 4th NGRSM webinar is "Geosciences for Society", which covered presentations of established researchers on the topics such as Natural Resources, Water Management, Earthquake, Monsoon, Climate change, Natural Disaster, River system, etc. The chief guest of this 4th NGRSM was Prof. Ashutosh Sharma, Secretary DST; Patrons Prof Ashok Sahni, Chairman GB, WIHG, and

Prof. Shailesh Nayak, Chairman RAC, WIHG; Chairman Dr. Kalachand Sain, Director WIHG; Co-Chairman Dr. Rajesh Sharma, WIHG and Convenor Dr. Parveen Kumar, WIHG.

- Prof. Ashutosh Sharma, Secretary DST, chief guest, and patron of this event delivered his inaugural address. In his address, he touches on various significant aspects like mapping of spring, geosciences for civil engineers, the study of climate change in respect of crop and water, the convergence of various technologies to get the final goal, use of solar energy in agriculture and sustainable development. Prof. Ashok Sahani, Chairman of Governing Body of WIHG, addressed the webinar; he motivated young scholars to carry out research for the beneficiary of society.
- The two days webinar included 20 invited talks from distinguished eminent speakers from all around the nation. A total of 657 participants have participated in this event from around 82 different Universities/Institutes/Organizations of India. During this event, the young researchers participated actively through discussion with the invited speakers.



Photographs during the 4th National Geo-Research Scholars Meet

International Workshop on “Assessment and Mitigation of Landslides in the Himalaya” (October 28-29, 2020)

International Workshop on “Assessment and Mitigation of Landslides in the Himalaya” was held through Webinar at Wadia Institute of Himalayan Geology, Dehradun during October 28-29, 2020. About 550 participants from across India and from abroad were registered for this Workshop.

In the two days deliberations, there were 29 technical presentations by experts from Indian and Abroad representing the Department of Science and Technology (DST), Govt of India, Geological Survey of India (GSI), Amrita University, Kerala, Indian Institute of Remote Sensing (IIRS), Dehradun, CSIR-Central Building Research Institute (CBRI), Roorkee, Indian Institute of Technology (IIT), Indore, CSIR- Central Road Research Institute (CRRI), New Delhi, HNB Garhwal University, Srinagar, Graphic Era Hill University (GEHU), Dehradun, Indian Institute of Technology (IIT) Kharagpur, Uttarakhand Disaster Management Authority (USDMA) - Dehradun, National Institute of Disaster Management (NIDM), New Delhi, Guru Jambheshwar University (GJU), Hisar, Panjab University (PU), Chandigarh, and Geological Survey of Norway (NGU), Trondheim, Norwegian Geotechnical Institute (NGI), Oslo, NVE, Norway, Liege University, Belgium, NTNU Norway, ITC, Netherland, Durham University, UK, Tribhuvan University, Nepal.

The workshop was inaugurated by Prof. Dr. T.N. Singh, Vice-Chancellor, Mahatma Gandhi Kashi Vidyapeeth (MGKV), Varanasi. In the inaugural address, he stressed the following to mitigate landslides related hazards in the Himalaya: (i) the slope stability should be part and parcel of the road cutting (ii) there must be proper disposal of the muck so that the carrying capacity of the river and drainage channels are not reduced (iii) holistic and integrated approach is required for the landslide stabilization and (iv) the scientific community must demarcate safe and unsafe areas so that the planners know well in advance where to build.

The First Technical Session was devoted to *'Landslide Monitoring and Early Warning'*. In the session, there were four presentations by Dr. Maneesha V Ramesh (Amrita University, Kerala) PK Champati Ray (IIRS, Dehradun), DP Kanungo (CSIR-CBRI, Roorkee), and Prof. Neelima Satlyam (IIT Indore). In this session, different kinds of landslide monitoring systems were discussed along with the various issues and limitations in the implementation of this system. Most of these were based on the rainfall thresholds and the varying time antecedent rainfall, which were presented for the site-specific studies like Chandmari (Sikkim), Chibo-Pashyar, (Kalimpong - Darjeeling), Munnar (Kerala). The development of indigenous low-

cost sensors for the purpose and their reliability were also presented. The efficacy of the Drone-based landslide monitoring system was also presented.

The second Technical Session was on the "Landslide Hazard Assessment". In this session, there were eight presentations by NVE, Norway, NGU, Norway, Leige University, Belgium, NTNU, Norway, ITC, Netherland, Durham University (DU), Durham, UK, IIRS Dehradun, and NGI, Norway. In this session, the Norwegian experience of the implementation of the building codes and guidelines, taking into account the large-scale maps prepared by the experts were discussed, along with the Norwegian policy of monitoring high landslide risk zone, medium landslide risk, and low landslide risk. They also emphasized early warning not less than 72 hours before the event. Identification of unstable slopes and mapping approaches of large landslides including seismic induced, rainfall-induced, erosion induced using varying techniques such as InSAR, Drone, from the Carpathian mountain range, Nepal Himalaya and Norway were also discussed. The importance of the documentation, preparation, and reliability of the inventory of landslides was also discussed to understand the future landslide hazard assessment with an example from various countries. The dissemination of the scientific knowledge to the local community for a safer resilient society was discussed by the researcher representing Durham University, Durham. The use of the high-resolution remote sensing data, modeling of landslides with examples with Indian landslides were also discussed. Finally, the example of implementation of the stabilization measure of a landslide on the slope in the vicinity of the hydropower dam in the Bhutan Himalayan after carrying out an integrated study on rock mass, engineering geology, groundwater condition, modeling, and back analysis was presented in this session.

The second day of the workshop was devoted to three Technical Sessions and the Closing function. There were seven presentations in the third Technical Session *'Large scale mapping'*. In the session, the first special invitee talk was delivered by the Head - NRDMs, Dr. Debapriya Dutta. He discussed various National Geospatial Programs and the DST initiatives for disaster risk reduction and management, particularly in the field of landslides and related hazards. Other presentations included the deliberations on the National Level landslide inventory and susceptibility database for the entire India, and its importance in the Indian context. There was a detailed presentation on the identification and mapping of the 'Deep-seated Gravitational Slope deformation (DGSD)' in the Himalayan terrain including Nepal and Indian Himalaya. The various issues of the development in the Himalayan terrain, including the widening of the Char Dham Yatra route were also discussed, and need for the

sustainable development were stressed despite the various peculiarities along and across the Himalaya. The extreme climate-induced infamous 2013 Kedarnath disaster was also deliberated in view of the increased anthropogenic pressure and interventions on the slopes, along with the preparation of the detailed large scale engineering geological maps between Ruderprayag-Sonprayag, Uttarakhand Himalaya, and along the Mansa Devi Hill Bypass (MDHB) Road in the Haridwar township. These types of maps and studies were deliberated to be useful for any further planning and development of the region.

The fourth technical session was exclusively on the 'Sikkim Himalaya' to disseminate the knowledge generated in the bilateral Indo-Norwegian Project on landslides hazards in the Sikkim Himalaya. In this session, six presentations were made. The overview of landslides in the Sikkim Himalaya and their spatial distribution with respect to geology and geomorphology of the area were discussed. The first record of the airblast from India that caused damage in Yumthang, North Sikkim in 2015 was discussed and the amount of impact energy generated was also assessed. The monitoring of slopes using InSAR depicting the movement of slopes in the Gangtok, Silchey, and Mangan townships were presented and discussed, along with the back analysis of the shear strength parameters of a large rockslide at Dzongu that created a lake and posing threat to the habitations in the area. In addition, a presentation was also made suggestions to adopt a basin-wise approach to landslide hazard assessment.

The fifth and final technical session was '*Education and Training on Landslide Hazards*'. In this session, four presentations were made by experts representing USDMA, NIDM, GJU, and PU. The increased incidences of landslides in the Himalayan region, particularly in Uttarakhand, and the practical constraints in the implementation of recommendations of the technical experts were discussed. The efforts being made by the National Institute of Disaster Management for capacity enhancement on landslide risk reduction and resilience in collaboration with academic institutions and others were also highlighted. The need of having multisectoral and multi-discipline approaches for effectively managing the menace of landslides along with the landslide education focusing on teaching, extension, and research with a focus on gaps in what is taught and what is done, involvement of students, need of extending and intensifying multidisciplinary research, climate change-related hazards, big data analytics, artificial intelligence were also discussed. Finally, Prof. A.D. Ahluwalia of Punjab University, Chandigarh emphasized the need of inculcating landslide education among schools and parents. He highlighted the need for having more geologists across the world and expanding practical knowledge of geosciences. Most problems faced by us,

according to him are attributed to a lack of geotechnical advice to constructing agencies that are busy concealing vast knowledge of geology behind concrete walls. Developing citizen scientists was the key message put forth by him. Poor countries according to him are poor in geosciences and environmental sciences and the key to their prosperity lies in expanding this knowledge informally. Building natural museums at the grassroots level were stressed upon by him. He gave a graphic account of landslides and awareness drives. Warnings are given boldly and out vocally and the need of disseminating the same was stressed upon by him.

The closing ceremony of the Workshop was initiated by Director WIHG, Dr. Kalachand Sain. He thanked all the technical experts for their presentations on the subject and all the participants. He stressed the need for hazard assessment, inculcating the hazard awareness education to the community level, and preparation and the implementation of the guidelines, and building codes for the disaster-free and disaster-resilient society. The Chief Guest of the function was Director-General, Uttarakhand Council for Science & Technology (UCOST), Dehradun Dr. Rajendra Dobhal. Finally, all the technical sessions were summed up by Dr. Vikram Gupta, the convener of the workshop.

e-workshop on “Luminescence dating technique and new applications” (November 25-27, 2020)

The luminescence dating technique has grown substantially and is accepted globally as a prime chronologic method for the estimation of the sediment age (that are a few hundred years to ~500 thousand years) of the Quaternary time. New development in the automated tools and protocols has enlarged the scope of this method and increased the dating limitations and applications. Therefore, to keep in pace with the global scientific trends in luminescence dating technique, the Indian Association of Luminescence Dating (IALD) and WIHG, Dehradun under the umbrella of DST Golden Jubilee celebrations successfully organized 3rd workshop on “Luminescence dating technique and new applications” from 25th-27th November 2020. The workshop was convened by Dr. Anil Kumar and Dr. Pinkey Bisht. More than 300 participants registered and got benefits from this e-workshop.

These three days e-workshop focused on the (i) newer application of Luminescence dating in Earth sciences; (ii) imparting training on the statistical methods/techniques leading to improvement of the age models. The workshop was divided into three sessions that covered 13 lectures from the resource persons from India as well as the internationally renowned laboratories. The workshop was introduced to participants by Dr. Pradeep Srivastava (Scientist, WIHG) and then an address by Prof. Kalachand Sain, Director, WIHG, and an inaugural lecture was delivered

by Prof. Ashok K Singhvi, DST, Vice President, INSA, New Delhi. Prof. Singhvi discussed different new variants of luminescence dating technique and their applicability and he further stressed the need formation of national working groups focusing on the development of new applications of the technique.

Session-1 on 'Applications in luminescence dating' had two lectures from Dr. Mayank Jain (DTU, Denmark) and Dr. Harrison Gray (Luminescence Chronology Lab, USGS, USA). The session-2, 'Development in OSL in India' was dedicated to the new development in OSL dating in India. In this session, 10 lectures were presented by various speakers namely: Dr. Manoj K. Jaiswal (IISER, Kolkata), Dr. Morthekai P. (BSIP, Lucknow), Dr. Naveen Chauhan (PRL, Ahmedabad), Dr. Devender Kumar (NGRI, Hyderabad), Dr. Madhav K Murari (IUAC, New Delhi), Dr. Anil Kumar (WIHG, Dehradun), Sh. Sharat Dutta

(GSI, Faridabad), Dr. Siddharth Prizomwala (ISR, Gandhinagar), Dr. Rabiul H Biswas (Institute of Earth Surface Dynamics, University of Laussane, Switzerland) and Dr. Nathan D Brown (U.C., Berkeley, USA). Session-3' Student interaction and Panel Discussion' had two sections: (1) a student interaction session, where three research scholars Dr. Biraj Borgohain (IIT-Bombay), Dr. Poonam Chahal (WIHG), and Ms. Kartika Goswami (IISER-Kolkata) shared their experiences while they completed their Ph.Ds involving the technique; (2) a Panel discussion session, which was dedicated to discussing the issues in luminescence chronology, global, development and gaps in Indian laboratory. This session was moderated by Dr. Pradeep Srivastava with a summary given by Prof. Singhvi. The meeting ended with a vote of thanks proposed by Dr. Suresh N. and the next workshop decided to be held at IISER-Kolkata.

AWARDS AND HONOURS

- Dr. Kalachand Sain & Dr. P.C. Kumar received Best Paper Award (ONGC Bulletin) from KDMIPE-ONGC, Dehradun.
- Dr. Kalachand Sain was revered as Corona Warrior title by the Uttarakhand State Government.
- Dr. Kalachand Sain was elected as Vice President of the Indian Geophysical Union (2020-2023).
- Dr. Kalachand Sain was elected as Congress Director of the Federation of Indian Geosciences Association.
- Dr. Kalachand Sain was elected as the Fellow, Indian National Science Academy, New Delhi.
- Dr. Kalachand Sain was elected as the Fellow, Indian Academy of Sciences, Bangalore.
- Dr. Kalachand Sain was recognized as the Honorary Outstanding Professor by AcSIR-CSIR.
- Dr. H. K. Sachan received MR Srinivas Rao Award - 2020 by the Geological Society of India for excellent contribution in the field of Petrology.
- Dr. R.J. Perumal was conferred Anni Talwani Memorial Prize by the Indian Geophysical Union.
- Dr. Sushil Kumar has been chosen as 'Guest editors' of Quaternary International (Elsevier Journal) 2021 volume on the theme titled “Dynamic Terranes: Surface Deformation, Seismicity, and Climate Change”.
- Dr. A.K. Singh has been chosen as Guest Editor of Geological Journal (Special issue: Geodynamic evolution of Eastern Himalayan and Indo-Myanmar Orogenic belts: Advances through interdisciplinary studies).
- Dr. A.K. Singh has been chosen as Associate Editor of the Indian Journal of Geosciences (published by the Geological Survey of India).

PH.D. THESES

Sl. No.	Name of Student	Supervisor	Title of the Theses	University	Awarded/ Submitted With date
1.	S. Khogenkumar Singh	Dr. A.K. Singh Prof. Santosh Kumar	Petrology and Geochemistry of mafic and ultramafic rocks of Central Part of Nagaland-Manipur Ophiolite Complex, Northeast India	Kumaun University, Nainital	Awarded June 17, 2020
2.	Simran Singh Kotla	Dr. R.K. Sehgal Prof. Rajeev Patnaik	Reconstruction of palaeoecology and palaeoclimatology using stable carbon and oxygen isotopes of pedogenic clays, molluscan shells and mammalian dental enamel from siwalik sequences exposed between Ghaggar and Markanda river valleys (Haryana, India).	Panjab University, Chandigarh	Awarded- June, 17 2020
3.	Soumya Jana	Dr. Maheswar Ojha Dr. Kalachand Sain Prof. Shalivahan	Stochastic modeling of gas hydrates reservoirs	IIT-ISM, Dhanbad	Awarded July 07, 2020
4.	Purbajyoti Phukon	Dr Koushik Sen Prof. HB Srivastava	Deformation, magmatism and exhumation history of the crystalline rocks of the Kumaun Higher Himalaya along the Kali River, Uttarakhand: an integrated structural and geochronological approach	Banaras Hindu University	Awarded July 29, 2020
5.	Arpita Paul	Dr. Devajit Hazarika Prof. Charu C. Pant	Seismic anisotropy and lithospheric configuration across the north-west India-Asia collision zone with special emphasis on the eastern Ladakh-Karakoram zone	Kumaun University, Nainital, Uttarakhand	Awarded August 26, 2020
6.	Jai Ram Yadav	Prof RBS Yadav Dr. D.P. Dobhal	Glacier Mass Fluctuations and Meteorological Parameters: Implications for Regional Climate	Kurukshetra University Kurukshetra	Awarded August 27, 2020
7.	Somenath Ganguly	Dr. Santosh K. Rai Dr. Udai Bhan, Dr. Saurabh Mittal	Estimation of absolute ground water temperature by Oxygen-18 fractionation.	UPES, Dehradun	Awarded September 24, 2020
8.	Thandan Babu Naik	Dr. Kalachand Sain Prof. K. Satya Prasad	Sub-surface image enhancement and feature extraction of oil and gas reserves using Eigen-based Kernels and principal component analysis	JNTU, Kakinada, Visakhapatnam	Awarded September, 26, 2020
9.	Jitender Kumar	Dr. Kalachand Sain Prof. P. Rama Rao	Delineation of gas-hydrates using advanced seismic tools: example from offshore Mahanadi basin, India	Andhra University, Visakhapatnam	Awarded October 21, 2020
10.	Neeraj Ramola	Dr.Y.P. Sundriyal Dr.Vikram Gupta	Large scale Engineering Geological & Geotechnical mapping of Kali Ganga and Mandakini valley	HNB Garhwal University, Srinagar	Awarded January 05, 2021
11.	Shubhasmita Biswal	Dr. Sushil Kumar Dr. William K. Mohanty	Seismic velocity structure, Anisotropy and Attenuation characteristics of NW Himalaya (India) region: Tectonic Implications from the Wadia Institute and Indian Institute of Technology Kharagpur (IITKgp)	Indian Institute of Technology, Kharagpur	Awarded February 23, 2021

Sl. No.	Name of Student	Supervisor	Title of the Theses	University	Awarded/ Submitted With date
12.	Pranaya R. Diwate	Dr. Narendra K. Meena Prof. Sandeep Pandeeta	Holocene paleoclimate records from Renuka lake, Himachal Pradesh, India	Jammu University, Jammu	Awarded February 23, 2021
13.	Gambhir Chauhan	Dr. H.C. Nainwal Dr. Vikram Gupta	Study of Landslides between Ichhari Dam Site and Atal along Tons River Valley, Uttarakhand Himalaya	HNB Garhwal University, Srinagar	Awarded March 05, 2021
14.	Shailendra Pundir	Dr. Vikas Adlakha Prof. Santosh Kumar	"Magmatism, Deformation and Exhumation History of the Southern Margin of Karakoram, Northern Ladakh, India"	Kumaun University, Nainital	Submitted August 17, 2020
15.	Harshita Joshi	Dr. Meera Tiwari Prof. Rajeev Upadhyay India	Paleobiological investigations in the Neoproterozoic-Cambrian deposits of Kumaun and Garhwal Lesser Himalaya,	Kumaun University, Nainital	Submitted October 15, 2020
16.	Aranya Sen	Dr. Koushik Sen Prof. H.B. Srivastava	Characterizing Metamorphism, deformation and magmatism in the crystallines of Bhagirathi Valley of Garhwal Himalaya	Baranas Hindu University, Varanasi	Submitted December 26, 2020
17.	N. Lakhan Singh	Dr. A.K. Singh Prof. B.P. Singh	Geochemical and geochronological studies of magmatic rocks of the Khardung-Shyok valley, western Himalaya, India	BHU, Varanasi	Submitted February 22, 2021
18.	Arjun Pandey	Dr. R. Jayangondaperumal Prof. H.B.Srivastava	Active tectonics and pattern of strain release along the north-eastern Himalayan Frontal Thrust between Saralbhanga and Subhansiri valleys	Banaras Hindu University, Varanasi	Submitted February 20, 2021
19.	Amrita Dutt	Dr. A.K.Singh Prof. Rajesh K. Srivastava	Geochemical and Isotopic studies of the Tethyan Ophiolitic Sequences in the Eastern Himalaya	Banaras Hindu University, Varanasi	Submitted March 04, 2020
20.	Dhamodharan S.	Dr. Gautam Rawat Dr. R S Bagri	Imaging Geo-Electrical Structures Along The Satluj Valley, North Western Himalaya, India using Magnetotelluric Method	HNB Garhwal University, Srinagar	Submitted January 01, 2021
21.	Somak Hajra	Dr. Devajit Hazarika Dr. Sanjit Kumar Pal	Structure of crust and upper mantle beneath the Kumaon Himalaya	IIT (ISM), Dhanbad	Submitted July 12, 2021

PARTICIPATIONS IN SEMINARS / SYMPOSIA / MEETINGS

- The 4th National Geo-Research Scholar Meet (NGRSM-2020), held during June 23-24, at WIHG, Dehradun.
Participants: All Scientists & Research Scholars of WIHG, Dehradun
- The e-Training on “Refresher Course on Marine Geoscience”, conducted by Geological Survey of India Training Institute, Hyderabad during June 24-29, 2020.
Participant: Kapesa Lokho
- International Conference on “Paleoclimate Changes (ICPC-2020)”, held at Vellore Institute of Technology (VIT), Chennai during July 09-10, 2020
Participant: Prakasam M.
- The e-training on “Fundamental of analytical chemistry training course” organized by the Geological Society of India, Hyderabad, during July 15-17, 2020.
Participant: Prakasam M.
- The e-Training on “Micropalaentology and C14 dating” organized by Geological Survey of India, Regional Training Division, Northern Region, Lucknow during July 21-31, 2020.
Participant: Kapesa Lokho, Sudipta Sarkar & Prakasam M.
- Online conference on “Approaching the contagious diseases from a Geospatial perspective” conducted by the University of Allahabad and other organizations during August 26-27, 2020.
Participant: Sudipta Sarkar
- 2nd International virtual Workshop on “Global Seismology and Tectonics” organized by the Geoscience and Technology Division, North-east Institute of Science and Technology (NEIST-CSIR) Jorhat Assam, India, during September 14-25, 2020.
Participants: Sushil Kumar, Dilip Yadav, Devajit Hazarika
- International Virtual Workshop on “Advanced Seismic Hazards and Earthquake Engineering: Theory Simulation and Observations (ASSHEE-2020)” organized by the National Institute of Technology, Agartala. During the period December 12-16, 2020.
Participants: Sushil Kumar, Dilip Yadav, Devajit Hazarika
- The 44th Annual Winter Meeting, Geol. Soc. London (Online) held during 14-16 December 2020
Participant: Manas M.
- Young Scientist Conference organized by the Ministry of Science and Technology, Ministry of Earth Science, and Ministry of Health and Family Welfare, Govt. of India during December, 22-24, 2020.
Participant: Rouf A. Shah
- The 58th Annual General Meeting of Tectonics Studies Group (Virtual meeting) of Geological Society, London, held during January, 5-8, 2021.
Participant: Arun Prasath, R.
- The 57th annual convention of the *Indian Geophysical Union* on “Sustainable Geosciences & Blue Economy”, organized by CSIR-National Institute of Oceanography (virtual mode) during February 2-4, 2021.
Participant: Richa Kumari
- Online workshop on “Research, academic institutions, and user departments in the field of water”, organized by Indian Institute of Technology Roorkee (IIT-R), Roorkee on February 11, 2021.
Participant: Santosh K. Rai
- Webinar on "Future Earth South Asia Webinar Series" organized by: Future Earth (FE) South Asia, Divecha Centre for Climate Change (DCCC), Indian Institute of Science(IISc), Bangalore & FE National Committee-India during March 11-12, 2021.
Participant: Pankaj Chauhan
- Online review meeting of the 'Indo-Norwegian Project' on behalf of Indian and Norwegian project partners on March 23, 2021.
Participant: Vikram Gupta
- Emergent meeting of council of the Palaeontological Society of India on March 23, 2021.
Participant: Kapesa Lokho

LECTURES DELIVERED/ INVITED TALK BY INSTITUTE SCIENTISTS

Name of Institute Scientist	Venue/Organizer	Date	Topic
Kalachand Sain	WIHG	May 11, 2020	Address on National Technology Day
Kalachand Sain	Dept. of Geography faculty of Earth, Environment and space Sciences, Chaudhary Bansi Lal University, Bhiwani	May 21, 2020	Delivered an online talk on faculty development programme
Vikram Gupta	WIHG	June 24, 2020	Landslides research- the recent trends in the National Geo-Research Scholars Meet
Rajesh Sharma	4th NGRSM-2020, WIHG	June 23-24, 2020	Applications of Raman spectroscopy in Geoscience
Devajit Hazarika	4th NGRSM-2020, WIHG	June 23-24, 2020	Role of the Main Himalayan Thrust in understanding seismogenesis: Kumaon Himalaya
Pradeep Srivastava	ICPC-2020, Vellore Institute of Technology (VIT), Chennai	July 09-10, 2020	Geology of Past and Present Floods in Himalaya
Vinit Kumar	SPC, College, Ajmer	July 24, 2020	Climate Change-Natural and Anthropogenic"
Sushil Kumar	Women Institute of Technology, Dehradun (online)	August 06, 2020	Earthquake Engineering: Role of Site Effect
Pankaj Chauhan	Gaya College of Engineering, Gaya	August 19, 2020	Himalayan Glaciology: Challenges,
Kalachand Sain	National Institute of Disaster Management, New Delhi	August 25, 2020	Distinguished Expert Panelist in the three day conference on science & Technology Research Policy Practice Interface for climate risk management Special panel discussion session-103: path breaking research needs
Kalachand Sain	Centre of Atmospheric and Ocean Studies, University of Allahabad, Allahabad	August 26, 2020	Delivered a talk in the online conference, Approaching the contagious diseases from a geospatial perspective
Pradeep Srivastava	Training program on Quaternary Geology, Geological Survey of India, NR	August 26, 2020	Himalaya as a critical taper: a Quaternary perspective
Pradeep Srivastava	Training program, Geological Survey of India	August 27, 2020	Floods and Geology of Himalaya
Kalachand Sain	Petroleum Engineering Indian Institute of Petroleum & Energy, Visakhapatnam	August 28, 2020	Delivered a lecture to Petroleum Engineering students
Kalachand Sain	HT Media Group's Hindustan Newspaper	September 5, 2020	Participated as an expert in e-Samvad on the occasion of Himalaya
Rajesh Sharma	WIHG Himalayan Divas	September 9, 2020	An introductory talk on Himalaya Diwas
Chhavi P. Pandey	WIHG Himalayan Divas	September 09, 2020	Journey of black carbon towards Himalayan Cryosphere
Vikram Gupta	WIHG Himalayan Divas	September 09, 2020	Landslide Disaster Risk Reduction (L-DRR) Strategy: Some fundamental concepts on the 'Himalayan Day'
S.K. Tiwari	WIHG Himalayan Divas	September 09, 2020	Use of Geothermal resources for heat utilization: An assessment for the Uttarakhand Himalaya
Kalachand Sain	G.B. Pant National Institute of Himalayan Environment, Almora	September 10, 2020	Graced the occasion of Annual Day Function of the Institute

Annual Report 2020-21

Pradeep Srivastava	JNU, New Delhi	September 16, 2020	Flood Disaster in Himalaya". 4th Refresher Online Course in Environmental Studies,
Kalachand Sain	National Institute of Disaster Management, New Delhi	September 21, 2020	Delivered a talk at Partner in Faculty Development Programme for Teachers' Training on Disaster Management
Chhavi P. Pandey	WIHG Hindi Pakhwara	September 21, 2020.	"Hamari prithvi ka jeevandayi aanchal: vegyanik drishti se"
Kalachand Sain	National Institute of Disaster Management, New Delhi	September 25, 2020	Delivered special address through online on Disaster Management
Vinit Kumar	University of Mumbai	September 26, 2020	Resource Person on short term online course on "Disaster Mangment: An integrated Approach
Sushil Kumar	Kendriya Vidyalay, ITBP, Dehradun	October 20, 2020	Earthquake, its origin and the mock drill for earthquake preparedness and hazard mitigation
Kalachand Sain	Lucknow University	October 26, 2020	Delivered a talk on refresher courses and faculty induction programme (FIP) for the teachers of Indian Universities and Colleges
Kalachand Sain	WIHG	October 28-29, 2020	International Workshop on "Assessment and Mitigation of Landslides in the Himalaya
Vikram Gupta	NIDM, New Delhi Webinar on 'Climate Resilient Development with special reference to Landslide'	November 09, 2020	Recent Examples of Landslides in the Himalaya and impact on climate change
Vikram Gupta	International Webinar on 'Natural Hazard and Management'	November 20, 2020	Landslides in the Himalaya and impact of climate change in the
Anil Kumar	WIHG	November 25-27, 2020	Luminescence dating technique and new applications'
Kalachand Sain	Uttarakhand State Council for Science & Technology (UCOST)	December 5, 2020	NASI webinar entitled "Science & Technology based solution to combat the Covid-19 Pandemic" (Jagrukta Abhiyan)
Pradeep Srivastava	Department of Earth Sciences, Assam University	December 10, 2020	"Flood History of Himalaya: a Geologist's perspective" International Conference Geoscientific Research during COVID-19: Challenges & Advances
Vikram Gupta	Kurukshetra University, Kurukshetra	December 10, 2020	Landslide Hazards:-Landslide Disaster Risk Reduction (L-DRR) Strategy and Impact of climate change in the Himalaya in the Refresher Course on 'Earth System Sciences for Mitigating Disaster and climate Change'
Kalachand Sain	Integrated Mountain Initiative, Sikkim	December 12, 2020	Panelist & Session Co-chair for "Disaster Risk Reduction and Climate resilient future for IHR" at the 9th Sustainable Mountain Development Summit (SMDS-IX)
Devajit Hazarika	National Institute of Technology (NIT), Agartala	December 12, 2020	Receiver function analysis and its application for imaging subsurface structure of the earth
Kalachand Sain	KV ITBP D.Dun	December 14, 2020	Valedictory programme of Online In-service Course-2020
Sushil Kumar	Eklavaya Adarsh Vidyalaya, Kasli Chakrata	December 16, 2020	Earthquake, its origin and the mock drill for earthquake preparedness and hazard mitigation
Kalachand Sain	India Meteorological Department, New Delhi	December 17, 2020	Plenary Talks during TROPMET-2020 "Climate Change Impact on Himalayan Glaciers
Vikram Gupta	National Institute of Disaster Management, New Delhi	December 18, 2020	Landslide Hazards Assessment and Mitigation' in the training program on Training Program on 'Landslides Risks Reduction and Resilience'

Sushil Kumar	Kendriya Vidyalaya, ITBP, Dehradun	January 11, 2021	Earthquake education, awareness and preparedness for earthquake hazard.
Sushil Kumar	University of Petroleum and Energy Studies	January 23-24, 2021	Awareness of cause of recent Natural hazards in INDIA
Narendra K. Meena	WIHG	January 28, 2021	संस्थान स्तरीय आपदा न्यूनीकरण एवं इस के प्रति कर्मचारियों की प्रतिक्रिया: विशेष सन्दर्भ अग्नि आपदा
Pankaj Chauhan	WIHG	February 05, 2021	Characterization of hydrologic behaviour and sediment budget in central Himalayan glacier valleys
Chhavi P. Pandey	Vigyan Prasar, Department of Science and Technology, Govt. of India	February 09, 2021	Black carbon air pollutants in our environment: causes, effects, and mitigation strategies
Kalachand Sain	IIT Roorkee	February 11, 2021	Online workshop of Research, Academic Institutions and User Departments in the field of water
Sushil Kumar	Department of Geology, Jammu University	February 17, 2021	Refresher course in Disaster Management: Earthquake Science and Earthquake Awareness (Online)
Kapesa Lokho	WIHG	February 18, 2021	The Geologic Time Scale
Suman Lata Srivastava	WIHG	February 22, 2021	Palaeobiology of Precambrian to Early Cambrian
Kapesa Lokho	WIHG	February 24, 2021	Mesozoic time scale and its strata in the Himalaya
Sushil Kumar	Webinar on Prakritik Aapada evam Bachaav: Ministry of Information and broadcasting	February 26, 2021	Earthquake in Himalayas and awareness to mitigate earthquake hazard
S.K. Tiwari	Geological Society of India, Bengaluru, India	March 10, 2021	Isotopic, aquatic geochemistry of geothermal springs of northwest Himalaya, India: implications for their source of origin and orogenic CO ₂ degassing
Sushil Kumar	IRDE (DRDO) Dehradun	March 10, 2021	Earthquake science and preparedness to mitigate earthquake hazard
Kalachand Sain	Department of Earth and Climate Science, IISER Pune	March 13, 2021	Delivered a talk at SAMEEKSHA 2021
Subhojit Saha	WIHG	March 19, 2021	Enigmatic molar-tooth structures (MTS) From Mesoproterozoic Deoban limestone, NW-lesser Himalaya: evidence for microbial decay and in-situ precipitation
Pradeep Srivastava	Staff Training College, Lucknow University, Lucknow	March 19, 2021	Flood disaster in Himalaya: past and present"
Vineet Kumar	GIC School, Jonpur, Tehri, Garhwal	March 22, 2021.	Science awareness program and science education to school children, focus on Disaster and its mitigation,
Sushil Kumar	GIC Garikhet, Tehri Garhwal	March 22, 2021	Earthquake, its origin and the mock drill for earthquake preparedness and hazard mitigation
Kalachand Sain	CSIR-NGRI, Hyderabad	March 24, 2021	Delivered a talk at virtual training Program on "Inversion and Machine Learning applications for geoscience data analysis
Kalachand Sain	Integrated Mountain Initiative Former MP (Lok Sabha), Sikkim	March 27, 2021	Chair a session as "Panelist" to the 9th Meet of the Mountain States
Kalachand Sain	Prime Minister's Science, Technology & Innovation Advisory Council (PM-STIAC)	March 31, 2021	Trans-Himalayan Research for Informed Decision making to predict and mitigate disasters

MEMBERSHIP

- Kapesa Lokho : Member - Executive Council of the Palaeontological Society of India, Lucknow
- Santosh K. Rai : Member - Geochemical Society, America
- Narendra K. Meena : Member - Editorial Board, Journal of Geosciences Research, published by Gondwana Geological Society, Nagpur, India
- Narendra K. Meena : Chairman - Research Assessment and Advisory committee at Suresh Gyan Vihar University, Jaipur
- Amit Kumar : Member - European Geosciences Union (EGU)
- Pankaj Chauhan : Member - International Association for Water, Environment, Energy, and Society
- Sushil Kumar : Member - Bureau of Indian Standards technical committee 'Earthquake Engineering Sectional Committee-CED 39', New Delhi, India (2020-21)
- : Member - Asia Oceania Geosciences Society (AOGS) (2020-21)
- : Member - Seismological Society of America (SSA)
- : Member - American Geophysical Union (AGU)
- : Member - RAC Working Group of the National Institute of Hydrology Roorkee

PUBLICATION AND DOCUMENTATION

The Publication & Documentation section brought out the (i) 'Himalayan Geology' volumes 41(2) 2020, and 42(1) 2021 (ii) Annual Report' of the Institute for the year 2019-20 in Hindi and English (iii) Hindi magazine 'Ashmika' volume 26 and (iv) Abstract volume for the International Workshop on "Assessment and Mitigation of Landslides in the Himalaya" during the reporting year.

The section was also involved in the dissemination of the publications to individuals, institutions, lifetime subscribers, book agencies, national libraries, indexing agencies, under exchange program, and maintaining the sale & accounts of publications. Apart from this, works pertaining to the printing of publicity brochures and certificates, etc., are also taken up.

Himalayan Geology (journal) website <http://www.himgeology.com> is functioning along with

an online manuscript submission facility under this section. All information regarding the journal including contents and abstracts is updated from time to time on the website. Online access of current volume to the Life Time Subscribers (those who have given the choice to obtain the volumes in soft copy through online access/email) also has been provided. Out of 485, 150 Life Time Subscribers receive the journal through online access. Journal is indexing in the Thomson Reuters (US), Elsevier (Netherlands), and Indian Citation Index (India) regularly. The impact factor for 2020 was 0.53.

The section also provides the facility & technical support services of printing and scanning to the scientists, research scholars, and other staff of the Institute.

LIBRARY

The Library of WIHG, Dehradun has a special status owing to its best collection of books, monographs, journals, and e-books, etc. on the mountain building process, geological and geophysical phenomenon with special reference to Himalaya. Also, the collection and services offered make it one of the best libraries in the country in the field of earth sciences. The scientists, researchers, project staff, and students make full utilization of the Library while publishing their research work in the reputed peer-reviewed journals. Specialists and professionals across the country also visit our Library to consult thematic and rare collections available at the Library.

The Library has more than 4000 selected e-books from different publishers and learned societies on the thrust areas of the research in the Institute.

Institutional Repository (IR): For the easy access and exclusive publications of the research work by WIHG, further digitization of research publications was carried out by incorporating them into the Institutional Repository (IR). The IR is essentially developed using DSpace (OSS) for organizing and disseminating the research output of the Institute. The articles published by our scientists in various journals have also been digitized. The repository consists of 100 full PDF texts of Prof D.N. Wadia's publications and 2375 PDFs of WIHG Scientist's publications and placed on the intranet within the Institute.



WIHG Library

Acquisition of Documents: The Library has paid and subscribed to 62 International and 27 Indian Journals. 01 more reference books are added. In addition to this, a total number of 95 books have been purchased to the Hindi Collections.

National Knowledge Resource Consortium (NKRC): The Library is a member of NKRC and continues to receive the support of Consortia towards online access to Elsevier's "Earth and Planetary Science collection", Wiley's "Earth, Space & Environmental Sciences"; Springer "Earth and Environmental Science and Chemistry" collections. In addition to this, WIHG Library has access to the publications of American Institute of Physics, American Physical Society, Derwent Innovation Index (with Web of Knowledge), Emerald Group Publishing, IEEE, NPG: Nature -Main

Journal, NPG: Nature Geoscience, Royal Society of Chemistry, Science magazine, Springer Journals, Taylor & Francis, Web of Science, Elsevier-Scopus, Wiley & Blackwell. All these publishers contribute online access to more than four hundred journals' titles, apart from our own subscription.

Binding of Journals: The binding work of loose issues of journals was undertaken by the Library. A total number of 285 volumes of journals also are bound during 2020-21. All the volumes have been accessioned and their bibliographic data entry and has been incorporated into the digital database.

Inter-Library Loan: The WIHG scientists were provided books/journals on inter-library loans from the Libraries of other organizations situated at Dehra Dun as per the requirement of the users.

Reprography facility: The Library serves as the central facility for the reprography demand of the Institute. This facility is being extended to scientific and administrative sections of the Institute. The facility was also extended on a payment basis to the external users of the Library and a total of 60000 pages were copied during the reporting year.

Computer Facility: The Library has the hub of computers for the users for accessing the e-books and e-journals and other e-resources available, either subscribed by WIHG Library or available through NKRC. This facility was also extended to the students and summer trainees. The hub is also being used for conducting several tests towards the recruitment of administrative and technical staff of the Institute.

S.P. NAUTIYAL MUSEUM

The year 2020-2021 was onerous and challenging. The museum closed its door for the visitors due to measures introduced by the government to curb the coronavirus pandemic. This year important days such as National Technology Day, Foundation Day, Founder's Day, and National Science Day were celebrated in virtual mode through live sessions, webinars, Facebook live, etc. During the period under report, the shooting of a documentary film on WIHG was undertaken on behalf of DST.

This year Museum participated in an outdoor exhibition to celebrate Basantoutsav from 13th -14th March 2021 at Raj Bhavan, Dehradun. Welcomed more than two thousand visitors which reflects a successful exhibition. The exhibition was inaugurated by the Hon'ble Governor of Uttarakhand and visited by many cabinet ministers of the Uttarakhand Government.



Smt. Baby Rani Maurya, Governor of Uttarakhand, visiting WIHG stall on the occasion of Spring Festival, at Raj Bhavan on 13th March 2021.



Shri Satpal Maharaj, Hon'ble Cabinet Minister, at exhibition stall arranged by the WIHG at Raj Bhavan, Dehradun.

In addition, Museum added two important exhibits i.e. drifting continents and dial-based geological clock which are widely appreciated. Replica of the geological clock, in a smaller version, was prepared from the market in bulk for commercial purposes and as a memento.



Geological Clock

TECHNICAL SERVICES

Analytical Services

The number of samples analyzed by various instruments is listed in the following table:

Laboratory/Instruments	Number of samples analysed		
	WIHG Users	Outside Users	Total
ICP-MS Lab	528	435	963
LA MC ICPMS	Liquid mode (Sr and Nd isotopes): ~990 Solid mode (U-Pb Zircon dating): ~18 samples	NIL	Liquid mode (Sr and Nd isotopes): ~990 Solid mode (U-Pb Zircon dating): ~18 samples
Stable Isotope Lab	1438 analyses	0	1438 analyses
Luminescence Dating (TL/OSL) Lab	110	29	139
Fission Track Lab & Mineral Separation Lab (includes samples for Fission Track Analysis and Zircon U-Pb Geochronology)	49 (including 17 samples of Fission Track Counting)	18	Mineral Separation: 67 samples Fission Track Counting: 17 samples
XRF lab	334	305	639
SEM Lab	1953	12	1965
Laser Micro Raman Spectrometer (LMRS) & Fluid inclusion and Raman Spectroscopy Lab	14	2	16
Rock magnetic & Paleomagnetism Lab Dendrochronology Lab	1978 18 tree cores (Remeasurement)	0 NIL	1978 18 tree cores (Remeasurement)
Micropaleontology Lab	130	NIL	130
Laser Particle Size Analyzer (LPSA)	126	0	126
Sedimentology Lab			
Vibratory Sieve Shaker	45	0	45
Clay Slide Preparation	0	5	5
Palyonology Lab	83	0	83
Laser Water Isotope Analyzer (LWIA)	600	90	690
Water Chemistry Lab (Ion-Chromatograph)	400	10	410
Total Organic Carbon Lab	655	--	655

Photography Section

The Photography section provides high-Quality images of various functions and activities organized by the institute. These high-quality digital images of important events are useful for the institute web pages as well for the preparation of different reports by the institute. During the reporting year 2020-2021, approximately

2000 photographs were taken using a high-resolution DSLR camera to cover the various functions organized in the Institute including Foundation Day, Founders Day, National Science Day, National Technology Day, New Year's Day, Republic Day, Independence Day, Seminars/Symposia, culture program, and superannuation parties for institute events,

Approximately 510 snaps were taken for rocks and fossils in the museum. The colour printing of around 250 digital images was arranged from the market. The majority of scientists have cameras issued permanently to them for use in the field and laboratory, while the remaining scientists form projects and research scholars are provided cameras from a pool as and when they require it.

Drawing Section

The Drawing Section catered to the cartographic needs of the Scientists of the Institute including the sponsored projects. During the Year, the section has provided thirty-seven geological maps/structural maps/geomorphological maps/seismicity diagrams for the scientists and research scholars of the Institute. Besides, the tracing of five topographic sheets/aerial photo maps was carried out along with the preparation of the three geological columns. The section has also provided name Labels, thematic captions during different activities and functions of the Institute including written work on the photo Identity cards of the employees of the Institute.

Sample Preparation Laboratory

The sample preparation laboratory provided thin/microprobe/polished sections to the requirements of the Institute Scientists, Research Scholars, and Outside users. During the year 2020-21, the laboratory provided 678 thin rock wafers and polished sections to various users for carrying out microscopic, fluid inclusion, and Electron Probe Micro Analysis studies. The laboratory also processed crushing/grinding of 937 rock samples for carrying out major, trace, and REE analysis by Inductively Coupled Plasma Mass Spectrometer, X-ray fluorescence, and X-ray Diffraction methods

Computer and Networking Section

WIHG Computer Section takes care of all the computational requirements of the Institute to facilitate important research work free of any IT-related worries. The role and responsibilities of the Computer section have increased manifold during the ongoing challenges posed due to the spread of Covid-19. The employees of the Computer Section have been working tirelessly to provide all the uninterrupted IT services to the whole Institute. During this period, not only have all the meetings been conducted online but important Seminars, Conferences, Workshops, Interviews have also been organized and conducted successfully. Moreover, this has resulted in the saving of a handsome amount to the Institute.

The Computer Section caters to the computational requirements of the whole Institute i.e., scientists and all the other employees of the Institute. It manages various servers which have been installed and configured in-house by the Computer Section. All the servers are working on a secure Linux environment and using the latest Open Source Technology. The different types of servers being used are DNS, Mail, Web, Application, etc. The Institute is connected with the National Knowledge Network through a high-speed 1 Gbps link. For uninterrupted internet connectivity, a standby internet bandwidth leased line connectivity has also been taken. The section has not only maintained a virus and spyware-free environment by adopting centralized anti-virus and anti-spyware solution but also adopting the prevailing preventive security measures in this regard.

Apart from the above, WIHG Computer Section also:

- Caters to the hardware troubleshooting and maintenance requirement of the whole Institute and along with the same, support is also being provided for the different software being used in the Institute and also for other facilities like data backup, data retrieval, etc.
- Uses the latest networking technologies for excellent speed and reliability of all the network-related services which are the need of the hour.
- Maintains and upgrade the network as per the requirement. The network is not limited to the office but the same has been extended to the WIHG residential colony and the Institute Guest House also.
- Provides VPN facility to facilitate the access of Institute resources securely over the public network.
- Maintains the different web portals hosted by the Institute viz., Institute website, Institute publication portal, WAICS (Wadia Analytical Laboratory Instrument Facility, and Consultancy Advisory Services) portal.

For the optimum utilization of the hardware resources, Virtualization has been used. Apart from this, extensive use of open-source software has been done by the section on different computers, workstations, and servers thereby saving considerable financial resources that may have been spent in purchasing other commercial paid software and solutions.

CELEBRATIONS

National Women Day

The Institute organized International Women's Day on March 09, 2020. Mrs. Renu Lohani, SP Vigilance Dehradun was invited to deliver a motivational speech. The program was attended by the Director and all the institute female employees and research scholars. Some of the cultural activities were performed by the institute employees and research scholars. They shared their respective experiences in life and celebrated the event with enthusiasm.



Group photograph during women day celebration

National Technology Day

On the occasion of National Technology Day on May 11, 2020, Director, WIHG addressed all the Institute employees, students & project staff and delivered a lecture on the topic "Impact of lockdown due to COVID-19 on Earth System and Society". The lecture was delivered in virtual mode.

6th International Yoga Day

6th International Yoga Day on June 21, 2020, was celebrated in the Institute through online mode. On this occasion, more than 100 employees and research students participated in Yoga from 6:30 to 7:30 AM under the directive and guidance of Yoga Instructors.

Foundation Day

The Institute celebrated its 53rd Foundation Day on June 29, 2020. On this occasion, Prof. Mrinal Sen, Institute for Geophysics, DGS, John A. and Katherine G. Jackson Chair in Applied Seismology, Texas was the Chief Guest, and Dr. Kalachand Sain, Director WIHG chaired the function. The chief guest delivered the Foundation Day Lecture on "Machine Learning and Data Analytics: A new technology in Geosciences" in virtual mode from Texas. The occasion was also marked by the distribution of awards. Prof. R. C. Misra award for the year 2020 was awarded to Dr. Tribid Kumar of



Jadavpur University, for his outstanding contribution in the field of Geosciences. The best research paper award was given to Dr. Rakesh Bhambri and his co-authors for the research paper entitled "Ice-dams, outburst floods, and movement heterogeneity of glaciers, Karakoram" published in the journal "Global and Planetary Change"

Independence Day

Independence Day was celebrated in the Institute on August 15, 2020, and Dr. Kalachand Sain, Director unfurled the National flag. To mark the occasion, a painting competition, and various sport events were organized for the staff and children of the Institute's employees. Director Wadia Institute distributed the prize to the winners.



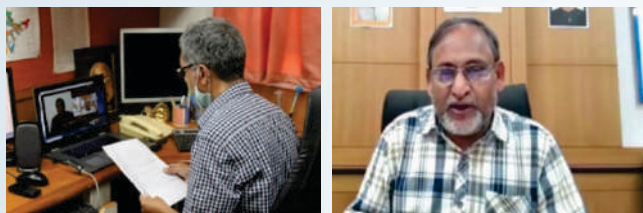
Swachchata Pakhwara

Observation of “Swachhta Hi Seva” Campaign

The “SWACHHTA HI SEVA” campaign was observed in the Institute under Swachch Bharat Mission in October 2020. This event is celebrated every year. During October 2020 various activities were carried out regarding swachchta. This year special precautions were taken due to COVID 19 pandemic.

At the outset, Dr. Kalachand Sain, Director WIHG addressed the institute employees (in virtual mode) on October 01, 2020 regarding the importance of the swachchta in our daily life, and a pledge was taken by the institute employees. It was followed by a lecture on “Disposal of E-waste” by Sh. Tajender Ahuja.

A cleanliness drive was conducted by sanitization and cleaning of rooms and laboratories by the employees on October 02, 2020, 9:30 to 11:30 AM. All the employees were involved in contributing towards



Swachchta Pledge

Director's address on 2nd October



Distributions of sanitizers and hand gloves



Institute employees cleaning rooms and labs followed by Director's visit

making Garbage-free, clean and green campus. They were given sanitizers, hand gloves by the institute. The cleanliness performed by the institute employees was meticulously observed by Director, WIHG. The above work was in addition to the daily cleanliness work of corridors, the whole of the premise, the encompassing lawns and ground, and the sanitization.

Founder's Day

The Institute celebrated its Founder's Day, the 137th birth anniversary of Prof. D. N. Wadia, on October 23, 2020. On this occasion, Prof. Rajender Singh Sangwan, Director, CSIR-Academy of Scientific and Innovative Research, Ghaziabad, was the Chief Guest and he delivered the Founder's Day Lecture. The Guests of Honor of this event were Prof. Neelam Singh Sangwan, HOD Biochemistry, Central University of Haryana, Mahendragarh, and Dr. Anjan Ray, Director, CSIR - Indian Institute of Petroleum, Dehradun.

On this occasion, an MoU was also signed between WIHG and CSIR- AcSIR for recognizing WIHG as one of the Centre of AcSIR for pursuing Ph.D. work by research scholars of the Institute.



CELEBRATIONS

Vigilance Week

The Vigilance Awareness Week-2020 was observed this year from October 27 to November 02, 2020, on the theme “Satark Bharat, Samriddh Bharat (Vigilant India, Prosperous India)”. Towards this scientists and other staff of the institute took the pledge on November 02, 2020.



Photograph of scientists and staff of the Institute during the pledge on November 02, 2020

Annual Sports Event- Badminton Tournament

In the annual sports event, Wadia Institute`s Badminton Tournament took place at open court on January 20-22, 2021 on the premises. In this tournament 73 matches were played with 56 entries in the 4 categories, which was inaugurated by Dr. Kalachand Sain, Director, Wadia Institute. Medals were distributed to the winners of various categories.

Republic Day

Dr. Kalachand Sain, Director hoisted the National Flag on Republic Day, January 26, 2021. As a mark of Republic Day celebrations various sports and cultural activities were organized at the Institute lawn under the banner “Manoranjan Mela” for the employees and their family members, which was inaugurated by Ms. Tumpa Sain. Prizes were distributed to the winners of various events.



Few moments of the “Manoranjan Mela” on the Republic Day

National Science Day

National Science Day was celebrated on February 28, 2021. Padma Shri Prof. K. Vijay Raghavan, Principal Scientific Adviser to the Government of India delivered "National Science Day Lecture-2021" in virtual mode. In



his lecture, he emphasized that increased opportunity of knowledge generation and decreasing the gap between knowledge and the society as well as increased usage of Artificial Intelligence in analyzing the large data can make India a world leader in Science, Innovation, and Technology.

Outreach program

Under this program, we reached to common people for providing education and training on disaster mitigation from earthquakes under a project entitled “भूकंप के लिए तैयारी करने और खतरे की कमी के लिए शिक्षा और जागरूकता कार्यक्रम: (“Education and awareness program for



Installation and inauguration of school seismograph system at Kendriya Vidyalaya ITBP, Dehradun



Students performing mock drill



A lecture on earthquake education



Mock drill...self protection at the time of an earthquake



Earthquake preparedness talk at IRDE, DRDO Dehradun



Explaining steps for earthquake mock drill GIC Garikhet



Explaining ...how to mitigate the hazard



GIC Garikhet



Lecture to Teachers at Kendria Vidyalay, ITBP



Lecture on lanslides avalanche and floods



earthquake preparedness and hazard mitigation”). The objectives of this program are to educate and aware school children, villagers, and the general public towards earthquake disaster and hazard mitigation.

In 2020-21 the following activities were performed in this outreach program and lectures/training were provided to nearly 1200 people.

A team of WIHG, visited Kendriya Vidyalaya, ITBP Dehradun and (i) interacted with teachers and staff for earthquake education and awareness lecture and

performed mock drill and (ii) installed school seismograph. The equipment would help to educate and aware students more effectively.

Lectures on earthquake education were delivered through three webinars organized by (i) The Department of Geology, Jammu University on the topic: “Refresher course in Disaster management” (ii) Ministry of Information and broadcasting and coordinated by ADG, IOB/PIB Dehradun on the topic “Prakritik Aapada evam Bachaav” (iii) WIHG Rajbhaashasamiti on the topic: “Bhukamp se bachaav ke sujhaav”. One lecture on earthquake awareness and education was also delivered at Instruments Research & Development Establishment (IRDE-DRDO), Dehradun. A one-day workshop at Government Inter College (GIC), Garikhet was attended by four scientists wherein lectures on different aspects of hazard were covered which includes earthquakes, landslides, avalanche, and cloud bursts. Mock drill was also performed.

STATUS OF IMPLEMENTATION OF HINDI

The Institute follows the policy and guidelines of Rajbhasha Vibhag and regularly submitting its quarterly and half-yearly progress report to Rajbhasha Vibhag, Department of Science and Technology. Institute also sent the reports to NARAKAS, Dehradun. Implementation of Hindi in the institute is being monitored by Rajbhasha Implementation Committee. Director of the institute chair the committee. The committee monitors and plans for progressive increment in the implementation of Hindi. The committee takes cognizance of the progress in the Hindi implementation through its regularly organized quarterly meetings.

This year under the banner of the Rajbhasha Implementation committee, Institute celebrates Hindi Pakhwara during September 14-28, 2020 in the institute. Following the COVID-19 pandemic guidelines, Committee organizes all the programs in online mode. Prof. S.K. Joshi, Vice-Chancellor Ayurved Vishwavidyalaya inaugurated the pakhwara. In his opening remark, he described the role of the Ayurveda and the Marm Chikitsa for medical treatment and their importance in the corona pandemic.

Dr. D.R. Shilpa delivered the first invited lecture on a healthy and happy lifestyle. In her lecture, she elaborated on the ways of overcoming stress in life and suggest following a disciplined routine that must include regular yoga-asana. She has answered the questions and queries of the audience patiently.

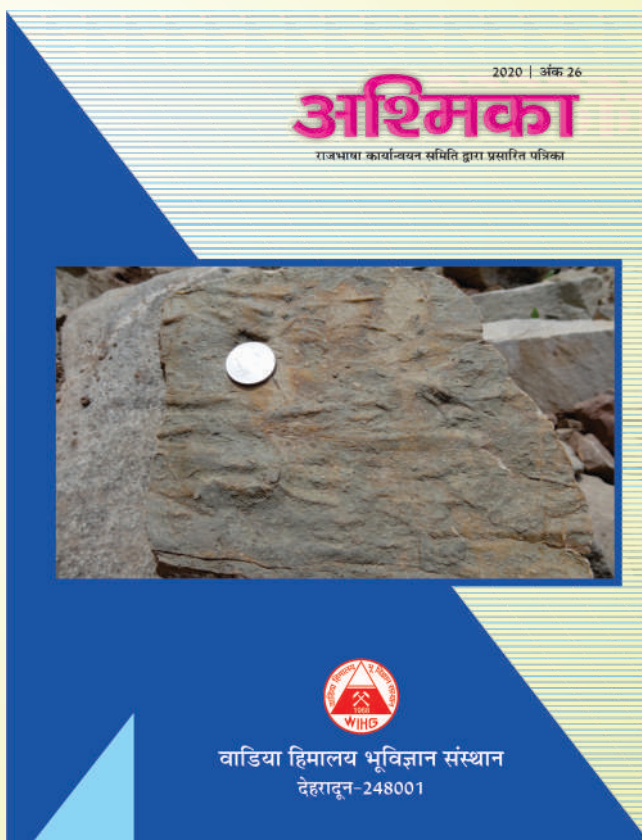
Dr. Subhrata Mishra delivered the second invited lecture. She spoke about the popular face of science in India. She presented interesting facts which increased the interest of the audience. She answered, queries raised by the listeners.

Dr. M.R. Saklani, in his invited talk, told about the Rajbhasha and Unity of the Nation. He described various rules pertaining to the use of Rajbhasha in office and emphasizes its role in uniting the entire country as one nation.

In the Pakhwara, institute employees also delivered talks on various science topics pertaining to their

research. Celebration of Pakhwara observed various competitions like essay writing, photography competition, etc. In the closing ceremony of the Pakhwara, Mr. Ram Singh Meena, former IPS and presently Member of the State Human Rights Commission was the chief guest, and Dr. Uday Singh Rawat, Vice-Chancellor, Shri Guru Ram Rai University, Dehradun was the special guest. Both the guest expresses requirement of science awareness to society in the language of the common man as the need of the hour.

This year we published the 26th issue of Annual Hindi Magazine "Ashmika". Authors from various organizations and employees of the institute contributed articles to the magazine. The articles of the magazines are informative and well appreciated by the readers. The attempt is to get more and more popular science articles in Hindi.



MISCELLANEOUS ITEMS

1. Reservation/Concessions for SC/ST employees

The government's orders on reservations for SC/ST/ OBCs are followed in recruitment to posts in various categories.

2. Monitoring of personnel matters

Monitoring of personnel matters relating to employees of the Institute is done through various Committees appointed by the Director/Governing Body from time to time.

3. Mechanism for redressal of employee's grievances

The Grievance Redressal Committee (GRC) consisting of five senior scientists/officers, is operational in this institute. During the reporting period, a total of nine grievances were received. Five of them were from the applicants of vacancies advertised, two were from ex-contractual employees and the remaining two were of suggestive nature from the general public. Of these six were received through the Prime Minister's Office (PMO), New Delhi, and three through the Department of Science and Technology (DST). The grievances of the applicants against the posts advertised were related to their disqualified applications. All the grievances were replied citing advertisements and rules. Two grievances from ex-contractual employees were replied with reference to their project posts. One grievance was regarding the continuation of glaciology studies in the institute and one related to maintenance of instruments and logbook. Both these suggestions have already been adhered to in the institute

4. Welfare measures

The Institute has various welfare measures for the benefit of its employees. Various advances like House Building Advance, Conveyance Advance, Festival Advance, etc. are given to the employees. There is a salary Earner's Cooperative Society run by the Institute employees that provide loans to its members as and when required. The Institute also runs a canteen for the welfare of the employees. As a welfare measure, the Institute is providing recreational facilities to its employees.

5. Mechanism for redressal of complaints of sexual harassment of women employees at work places

To inquire into the complaints of sexual harassment of women employees at workplaces in the Institute, a separate Committee has been constituted. The Committee consists of seven members. The Chairman and three other members of the Committee are female officers, which includes a female officer from the Department of Food and Civil Supplies, Govt. of Uttarakhand. No complaint of sexual harassment of women employees at workplaces was received by the Committee during the year 2020-21.

6. Status of Vigilance Cases

No vigilance case is pending in the year 2020-21

7. Information on the RTI cases

The details of information on the RTI cases during the year 2020-21 are as under:

Details	Opening balance as on 01.04.2020	Received during the year 2020-2021	Number of cases transferred to other public authorities	Decisions where requests/ appeals were rejected	Decisions where requests/ appeals accepted
1	2	3	4	5	6
Requests for information	0	44	0	0	44
First appeals	0	13	0	0	13

8. Sanctioned Staff strength (category wise)

Group/ Category	Scientific	Technical	Administrative	Ancillary	Total
A	63	0	2	0	65
B	0	4	14	0	18
C	0	63	22	40	125
Total	63	67	38	40	208

9. Sanctioned and released budget grant for the year 2020-21

Plan : 4089.00 Lakhs
 Non-Plan :
 Total : 4089.00 Lakhs

STAFF OF THE INSTITUTE

Scientific Staff

1.	Dr. Kalachand Sain	Director
2.	Dr. Rajesh Sharma	Scientist 'G'
3.	Dr. H.K. Sachan	Scientist 'G'
4.	Dr. Sushil Kumar	Scientist 'G'
5.	Dr. D.P. Dobhal	Scientist 'F' (Retired on 30.06.2020)
6.	Dr. Vikram Gupta	Scientist 'F'
7.	Dr. Suresh N.	Scientist 'F' (Retired on 28.02.2021)
8.	Dr. Pradeep Srivastava	Scientist 'F'
9.	Dr. Ajay Paul	Scientist 'E'
10.	Dr. R. Jayangonda Perumal	Scientist 'E'
11.	Dr. A.K. Singh	Scientist 'E'
12.	Dr. (Mrs.) Kapesa Lokho	Scientist 'E'
13.	Dr. K.S. Luirei	Scientist 'E'
14.	Dr. P.S. Negi	Scientist 'E'
15.	Dr.A.K.L Asthana	Scientist 'E' (Retired on 28.02.2021)
16.	Dr R.K. Sehgal	Scientist 'E'
17.	Dr. Santosh Kumar Rai	Scientist 'E'
18.	Dr. Jayendra Singh	Scientist 'E'
19.	Dr. B.K. Mukherjee	Scientist 'E'
20.	Dr. Gautam Rawat	Scientist 'D'
21.	Dr. Naresh Kumar	Scientist 'D'
22.	Dr. Devajit Hazarika	Scientist 'D'
23.	Dr. Dilip Kumar Yadav	Scientist 'D'
24.	Dr. Kaushik Sen	Scientist 'D'
25.	Dr. Satyajeet Singh Thakur	Scientist 'D'
26.	Dr. (Mrs.) Swapnamita Choudhuri	Scientist 'D'
27.	Dr. Narendra Kumar Meena	Scientist 'D'
28.	Dr. Param Kirti Rao Gautam	Scientist 'D'
29.	Dr. Manish Mehta	Scientist 'D'
30.	Dr. (Ms.) Aparna Shukla	Scientist 'D' (On lien MoES)
31.	Dr. Rajesh S.	Scientist 'D'
32.	Dr. Vikas	Scientist 'C'
33.	Dr. Som Dutt	Scientist 'C'
34.	Dr. Anil Kumar	Scientist 'C'
35.	Sh. Saurabh Singhal	Scientist 'C'
36.	Dr. Narendra Kumar	Scientist 'C'
37.	Dr. Vinit Kumar	Scientist 'C'
38.	Dr. Aditya Kharya	Scientist 'C'
39.	Dr. (Ms) Suman Lata Rawat	Scientist 'C'
40.	Dr. (Mrs.) Chhavi Pant Pandey	Scientist 'C'
41.	Dr. Parveen Kumar	Scientist 'C'

42.	Dr. Paramjeet Singh	Scientist 'C'
43.	Dr. Sudipta Sarkar	Scientist 'B'
44.	Dr. M. Prakasam	Scientist 'B'
45.	Dr. Sameer Kumar Tiwari	Scientist 'B'
46.	Dr. Pinkey Bisht	Scientist 'B'
47.	Dr. C. Perumalsamy	Scientist 'B'
48.	Dr. Pratap Chandra Sethy	Scientist 'B'
49.	Dr. Mutum Rajnikanta Singh	Scientist 'B'
50.	Dr. Rouf Ahmad Sah	Scientist 'B'
51.	Dr. Chinmay Haldar	Scientist 'B'
52.	Dr. Subhojit Saha	Scientist 'B'
53.	Dr. Priyadarshi Chinmoy Kumar	Scientist 'B'
54.	Dr. Pankaj Chauhan	Scientist 'B'

Technical Staff

1.	Shri Sanjeev Kumar Dabral	Sr. Technical Officer
2.	Shri Samay Singh	Sr. Technical Officer
3.	Shri Rakesh Kumar	Sr. Technical Officer
4.	Shri H.C. Pandey	Sr. Technical Officer
5.	Shri N.K. Juyal	Sr. Technical Officer
6.	Shri T.K. Ahuja	Technical Officer
7.	Shri C.B. Sharma	Assistant Engineer
8.	Shri Gyan Prakash	Asstt. Pub. & Doc. Officer
9.	Shri S.S. Bhandari	Technical Officer
10.	Shri Rambir Kaushik	Technical Officer
11.	Dr. Balram	Librarian
12.	Shri Bharat Singh Rana	Librarian
13.	Dr. Pankaj Chauhan	Junior Technical Officer (Resigned & joined as Sci. 'B')
14.	Shri Lokeshwar Vashistha	Sr. Lab. Technician
15.	Dr. S.K. Chabak	Sr. Lab. Technician
16.	Shri R.M. Sharma	Sr. Lab. Technician
17.	Shri C.P. Dabral	Sr. Lab. Technician
18.	Shri Rajendra Prakash	Sr. Lab. Assistant (Retired on 28.02.2021)
19.	Shri Nand Ram	Elect. cum Pump. Optr.
20.	Smt. Sarita	Senior Technical Assistant
21.	Shri Rakesh Kumar	Senior Technical Assistant
22.	Ms. Sakshi Maurya	Technical Assistant
23.	Ms. Disha Vishnoi	Technical Assistant
24.	Shri Prateek Negi	Artist cum Modeller
25.	Shri Vipin Chauhan	Technical Assistant
26.	Shri Rahul Lodh	Lab Assistant
27.	Shri Nain Das	Lab Assistant
28.	Shri Tarun Jain	Draftsman

29. Shri Pankaj Semwal	Draftsman
30. Shri Santu Das	Section Cutter
31. Shri Puneet Kumar	Section Cutter
32. Shri Amit Bhandari	Junior Photographer
33. Shri Hari Singh Chauhan	Field-cum-Lab-Attendant
34. Shri Ravi Lal	Field-cum-Lab-Attendant
35. Shri Preetam Singh	Field-cum-Lab-Attendant
36. Mrs. Rama Pant	Field Attendant (Retired on 31.07.2020)
37. Shri Ramesh Chandra	Field Attendant
38. Shri B.B.Panthri	Field Attendant
39. Shri M.S.Rawat	Field Attendant
40. Shri Sanjeev Kumar	Field-cum-Lab-Attendant
41. Shri Deepak Tiwari	Field-cum-Lab-Attendant
42. Shri Ajay Kumar Upadhaya	Field-cum-Lab-Attendant
43. Km. Sangeeta Bora	Field-cum-Lab-Attendant
44. Sh. Deepak Kumar	Field-cum-Lab-Attendant
45. Km. Anjali	Field-cum-Lab-Attendant

Administrative Staff

1. Shri Pankaj Kumar	Registrar
2. Mrs. Manju Pant	Asstt. Fin. & Acc. Officer (Retired on 30.04.2020)
3. Shri Manas Kumar Biswas	Store & Purchase Officer
4. Shri S.K.Chhetri	Accountant (Retired on 31.05.2020)
5. Shri Rahul Sharma	Asstt. Fin. & Acc. Officer
6. Smt. Rajvinder Kaur Nagpal	Stenographer
7. Km. Shalini Negi	Stenographer
8. Shri S.K.Srivastava	Office Superintendent
9. Mrs. Prabha Kharbanda	Accountant
10. Mrs. Kalpana Chandel	Assistant
11. Mrs. Anita Chaudhary	Assistant
12. Shri Shiv Singh Negi	Assistant
13. Mrs. Neelam Chabak	Assistant
14. Mrs. Seema Juyal	Assistant
15. Sh. Yashpal Singh Bisht	Jr. Hindi Translator
16. Km. Richa Kukreja	Stenographer
17. Mrs. Suman Nanda	Upper Division Clerk
18. Shri Kulwant Singh Manral	Upper Division Clerk
19. Sh. Vijai Ram Bhatt	Upper Division Clerk
20. Shri Girish Chander Singh	Upper Division Clerk

21. Sh. Rajeev Yadav	Upper Division Clerk
22. Sh. Deepak Jakhmola	Lower Division Clerk
23. Sh. Dinesh Kumar Singh	Lower Division Clerk
24. Km. Rachna	Lower Division Clerk
25. Smt. Pushpa Barthwal	Lower Division Clerk

Ancillary Staff

1. Mrs. Kamla Devi	Bearer
2. Mrs. Deveshawari Rawat	Bearer
3. Shri S.K. Gupta	Bearer
4. Mrs. Omwati	Bearer
5. Shri Jeevan Lal	Bearer
6. Shri Surendra Singh	Bearer
7. Shri Pritam	Bearer
8. Shri Ramesh Chand Rana	M.T.S.
9. Shri Pankaj Kumar	M.T.S. (Died on 19.11.2020)
10. Shri Ashish Rana	M.T.S.
11. Shri Harish Kumar Verma	M.T.S.
12. Sh. Dinesh Parsad Saklani	Guest House Attendant cum Cook
13. Sh. Sunil Kumar	Guest House Attendant cum Cook
14. Shri Rohlu Ram	Chowkidar
15. Shri H.S. Manral	Chowkidar
16. Shri G.D. Sharma	Chowkidar
17. Shri Satya Narayan	Mali

Contractual Staff

1. Sh. Dhanveer Singh Shah	Lower Division Clerk
2. Smt. Megha Sharma	Lower Division Clerk
3. Shri Rezaw Uddin Chaudhary	Driver
4. Shri Rajesh Yadav	Driver
5. Shri Bhupendra Kumar	Driver
6. Shri Manmohan	Driver
7. Sh. Vijay Singh	Driver
8. Shri Rudra Chettri	Bearer
9. Shri Laxman Singh Bhandari	Chowkidar
10. Shri Pradeep Kumar	Chowkidar (Retired on 30.09.2020)
11. Shri Kalidas	Chowkidar
12. Shri Ummed Singh	Chowkidar

MEMBERS OF THE GOVERNING BODY/RESEARCH ADVISORY COMMITTEE /FINANCE COMMITTEE / BUILDING COMMITTEE

Governing Body

(w.e.f. Nov. 13, 2018)

Sl.	Name	Address	Status
1.	Prof. Ashok Sahni	Emeritus Professor, Lucknow University 98, Mahatma Gandhi Marg, Lucknow -226001,UP (India)	Chairman
2.	Secretary to the Government of India or his/her nominee	Dept. of Science & Technology, Technology Bhawan, New Mehrauli Road, New Delhi - 110016 (India)	Member
3.	Prof. Talat Ahmad	Vice Chancellor, Jamia Millia Islamia Jamia Nagar, New Delhi-110025 (India)	Member
4.	Dr V.M. Tiwari	Director, CSIR-NGRI (Council of Scientific & Industrial Research) Uppal Road, Hyderabad-500007, Telangana (India)	Member
5.	Prof. Harilal B. Menon	Department of Marine Sciences Goa University, Taleigoa Plateau Goa-403206 (India)	Member
6.	Prof. G.V.R. Prasad	Department of Geology, Center for Advance Studies University of Delhi, Delhi-110007 (India)	Member
7.	Dr. Rasik Ravindra	Former Director, National Center for Antarctic and Ocean Research (NCAOR) Headland Sada, Vasco-da-Gama-403804, Goa (India)	Member
8.	Prof. Deepak Srivastava	Head, Department of Earth Sciences Indian Institute of Technology Roorkee (IITR), Roorkee-247667, Uttarakhand (India)	Member
9.	Prof. Pramod K. Verma	Department of Applied Geology Vikram University, University Road, Madhav Bhavan (Near Vikram Vatik), Ujjain-456010, MP (India)	Member
10.	Prof. S.K. Dubey	Former Director, Indian Institute of Technology Khargapur	Member
11.	Financial Adviser or his/her nominee	Dept. of Science & Technology, Technology Bhawan, New Mehrauli Road, New Delhi-110016 (India)	Member
12.	Director, WIHG	Director, Wadia Institute of Himalayan Geology, 33, GMS Road, Dehra Dun-248001, Uttarakhand (India)	Member Secretary
13.	Sh. Pankaj Kumar	Registrar, Wadia Institute of Himalayan Geology, 33, GMS Road, Dehradun-248001, Uttarakhand (India)	Non-Member Asstt. Secretary

Research Advisory Committee

(w.e.f. Feb 13, 2019)

Sl.	Name	Address	Status
1.	Dr. Shailesh Nayak	Director National Institute of Advanced Studies Indian Institute of Science campus, Bengaluru -560012	Chairman
2.	Prof. Talat Ahmad	Vice Chancellor University of Kashmir, Hazratbal, Srinagar Jammu & Kashmir - 190006	Member
3.	Prof. D.C. Srivastava	Department of Earth Sciences Indian Institute of Technology Roorkee, Roorkee - 247667	Member
4.	Prof. O.N. Bhargava	(Ex-Director, GSI) 103, Sector-7, Panchkula - 134109	Member
5.	Dr. K.J. Ramesh	D.G., IMD Mausam Bhavan, Lodi Road, New Delhi - 110 003	Member
6.	Dr. P.P. Chakraborty	Professor, Department of Geology, University of Delhi, Delhi - 110007	Member
7.	Prof. N.V. Chalapathi Rao	Department of Geology, Banaras Hindu University(BHU) Varanasi(U.P.) - 221 005	Member
8.	Dr. Thamban Meloth	Scientist 'F', & Group Director (Polar Sciences) National Centre for Polar and Ocean Research, Ministry of Earth Sciences, Govt. of India, Headland Sada, Vasco-da-Gama, Goa-403 804	Member
9.	Dr. O.P. Mishra	Scientist 'F', Ministry of Earth Sciences, Government of India, Prithvi Bhavan, Opp. India Habitat Centre, Lodhi Road, New Delhi- 110 003	Member
10.	Dr. Prakash Chauhan	Director, Indian Institute of Remote Sensing, 4, Kalidas Road, Dehradun - 248001	Member
11.	Prof. Biswajit Mishra	Geology and Geophysics Indian Institute of Technology, Kharagpur, 721302	Member
12.	Prof. Avinash Chandra Pandey	Director Inter- University Accelerator Centre Aruna Asaf Ali Marg, Near Vasant Kunj, New Delhi - 110067	Member
13.	Prof. Ajoy Bhowmik	Associate Professor Department of Applied Geology Indian Institute of Technology (Indian School of Mines), Dhanbad - 826004, Jharkhand	Member
14.	Dr. Vandana Prasad	Director Birbal Sahni Institute of Paleoscience 53, University Road, Lucknow-226 007	Member
15.	Dr. Prantik Mandal	Chief Scientist, Co-ordinator & Professor at AcSIR-NGRI, Theoretical & Computational Geophysics Group, CSIR-NGRI, Uppal Road, Hyderabad - 500 007, Telangana	Member
16.	Prof. Anil V. Kulkarni	Distinguished Visiting Scientists Divecha Centre for Climate Change, Indian Institute of Science, Bengaluru- 560012, Karnataka	Member

Research Advisory Committee

(w.e.f. Feb 13, 2019)

Sl. Name	Address	Status
17. Dr. Kalachand Sain	Director Wadia Institute of Himalayan Geology, Dehradun - 248001	Member
18. Dr Rajesh Sharma	Scientist 'G' Wadia Institute of Himalayan Geology, Dehradun - 248001	Member Secretary

Finance Committee

(w.e.f. Feb 13, 2019)

Sl. Name	Address	Status
1. Sh. B. Anand	Financial Advisor Department of Science & Technology, Technology Bhavan, New Mehrauli Road, New Delhi- 110016	Chairman
2. Dr. Rasik Ravindra	608, Lalleshwari Apart Sector 21 D, Faridabad- 121 001	Member
3. Dr. Kalachand Sain	Director, Wadia Institute of Himalayan Geology, Dehradun - 248001	Member
4. Sh. Pankaj Kumar	Registrar, Wadia Institute of Himalayan Geology, Dehradun - 248001	Member
5. Shri Rahul Sharma	AF&AO, Wadia Institute of Himalayan Geology, 33, GMS Road, Dehradun-248001 (UK)	Member Secretary

Building Committee

(w.e.f. Feb 13, 2019)

Sl. Name	Address	Status
1. Dr. Kalachand Sain	Director, Wadia Institute of Himalayan Geology, Dehradun - 248 001	Chairman
2. Sh. B. Anand or his/her nominee	Financial Advisor Department of Science & Technology Technology Bhavan, New Mehrauli Road, New Delhi - 110016	Member
3. Dr. H.K. Sachan	Scientist-'G', Wadia Institute of Himalayan Geology, Dehradun 248001	Member
4. Representative of Survey of India	Hathibarkala, Dehradun	Member
5. Sh. D. K. Tyagi	General Manager (Civil) Infrastructure Development, Oil & Natural Gas Corporation, Dehradun - 248 001	Member
6. Sh. Prashant Singh	Executive Engineer, CPWD, 20, Subhash Road, Dehradun - 248 001	Member
7. Mrs. Poonam Gupta	Sr. Principal Scientist CSIR-Indian Institute of Petroleum, Haridwar Road, Dehradun - 248 005	Member
8. Sh. Pankaj Kumar	Registrar, Wadia Institute of Himalayan Geology, Dehradun - 248001	Member
9. Sh. C.B. Sharma	Assistant Engineer, Wadia Institute of Himalayan Geology, Dehradun - 248001	Member Secretary

STATEMENT OF ACCOUNTS

BHATIA SUBHASH & CO. **CHARTERED ACCOUNTANTS**



Dehradun Off: 17 Pankaj Vihar, Pitthuwalla, Shimla By Pass, Po Mehuwala, Dehradun (U.K)

Sre Off: 11nd Floor, Narayan Tower, Opp. Narayan Mandir, Gill Colony, Saharanpur (U.P)

Yamunanagar Off: H.No 1140, Sector 17 Huda, Jagadhri Yamunanagar – 135001 (H.R)

Tel.No. 9528173229, 9897226991

Email: rkgupta091@gmail.com, rkguptarke@yahoo.com

AUDITOR'S REPORT ON CONSOLIDATED FINANCIAL STATEMENTS

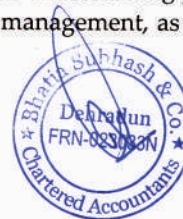
**The Members of Governing Body,
Wadia Institute of Himalayan Geology,
33, GMS Road, Dehradun
Uttarakhand**

We have audited the accompanying Consolidated Financial Statements of **WADIA INSTITUTE OF HIMALAYAN GEOLOGY, 33, GMS Road, Dehradun** for the year ended March 31st, 2021 which comprises Balance Sheet, Income and Expenditure Account, Receipt and Payment Account and summary of significant accounting policies.

Society's management is responsible for the preparation of these Financial Statements in accordance with law. This responsibility includes the design, implementation and maintenance of internal control relevant to the preparation and presentation of the financial statements that give a true and fair view and are free from material misstatement, whether due to fraud or error.

Our responsibility is to express an opinion on these financial statements based on our audit. We conducted our audit in accordance with the Standards on Auditing issued by the Institute of Chartered Accountants of India. Those Standards require that we comply with ethical requirements and plan and perform the audit to obtain reasonable assurance about whether the financial statements are free from material misstatement.

An audit involves performing procedures to obtain audit evidence about the amounts and disclosures in the financial statements. The procedures selected depend on the auditor's judgment, including the assessment of the risks of material misstatement of the financial statements, whether due to fraud or error. In making those risk assessments, the auditor considers internal control relevant to the Society's preparation and fair presentation of the financial statements in order to design audit procedures that are appropriate in the circumstances. An audit also includes evaluating the appropriateness of accounting policies used and the reasonableness of the accounting estimates made by management, as well as evaluating the overall presentation of the financial statements.



We believe that the audit evidence we have obtained is sufficient and appropriate to provide a basis for our audit opinion.

In our opinion and to the best of our information and according to the explanations given to us, the financial statements give the information required by the Act in all material respects and give a true and fair view in conformity with the accounting principles generally accepted in India subject to our comments given in Annexure-“1”:

- a) in the case of the Balance Sheet, of the state of affairs of the Society as at March 31st, 2021;
- b) in the case of the Income and Expenditure Account of the deficit for the year ended on that date; and
- c) in the case of the Receipt and Payment Account, of the cash flows for the year ended on that date.

**FOR BHATIA SUBHASH & CO
CHARTERED ACCOUNTANTS**


CA RAHUL GUPTA
FCA, DISA (ICAI), PARTNER

FRN: 023033N

M.NO: 425249

UDIN : 21425249AAAAHA2798

Date: 31st August, 2021

Place: Dehradun

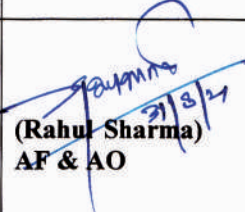
Action Taken Report on observations of the Chartered Accountant- Annexure-1 to the Consolidated Financial Statement of Audit Report (F.Y. 2020-21)

Sl. No.	Comments/Observations by Chartered Accountants	Replies and Action taken by the Institute
1	The Institute is maintaining accounts on cash basis except interest accrued on investments, which is not conformity with the generally accepted accounting policy adopted in India and as per the accounting standard-1 "Disclosure of Accounting Policies" issued by the Institute of Chartered Accountants of India. The "Uniform Accounting Format" of financial statements of the central autonomous bodies as has been made compulsory by the Ministry of finance w. e. f. 01.04.2001 and adopted by the Institute also, recommends accrual method of accounting.	The Institute is receiving Grants-in-aid from Govt. of India on the basis of projection of expenditure submitted by the Institute. However sufficient funds as against the projected amount are not being received. Hence the accounts are maintained on cash basis for the actual transaction during the year reported. Interest on investment out of the fund for GPF/Pension etc, is taken on accrual basis. Audit observations are noted for future compliance and best efforts will be made to the effect and progress will be reported to next audit.
2	The Institute has not booked the current liability for the retirement benefit of the employees as per Accounting Standard-15 "Employee Benefits" as issued by the Institute of Chartered Accountants of India.	Noted
3	<p>The internal control regarding fixed assets needs to be strengthened. The following observation are made:</p> <p>(a) The physical verification of fixed assets for the financial year 2020-21 has not been undertaken.</p> <p>While auditing the accounts in the store section it was observed following Assets Register were maintained by the store section: -</p> <div style="border: 1px solid black; padding: 5px;"> <p>[Details]</p> <p>A.</p> <p>1. Assets-1</p> <p>2. Assets-2</p> <p>3. Assets-3</p> <p>4. Assets-4</p> <p>5. Assets-5</p> <p>B. General Equipment</p> <p>C. Field Equipment</p> <p>D. Vehicle register</p> <p>E. Engineering Section</p> <p>F. Fixed Assets buildings.</p> <p>Physical verification of the above-mentioned Assets has not been carried out by the verifying officer till date. Reason of not doing the needful may be specified.</p> </div>	Action with regard to the physical verification for the year 2020-2021 onwards is in progress and report will be submitted to the audit shortly.



	<p>Physical verification of library not conducted.</p> <p>While auditing the accounts pertaining to the Library located inside WIHG it was observed that physical verification of the books/journals and magazines available in the library have not been physically verified till the date of completion of audit report. The reason for not complying with the rule laid down in GFR regarding physical verification of Assets may be specified.</p>	
4.	<p>The contribution towards medical scheme for pensioners is accounted for in pension fund account whereas the payment of actual expenditure is met from the institute account. it is recommended that the expenses should be met from the specific fund only.</p>	<p>The matter has already been submitted to DST for seeking of sufficient grant in pension fund account. Finance Committee of the Institute was decided that till a decision is taken by the MoF/DST on this matter, the status-quo be maintained. The payment of medical reimbursement was made only one time during the year 2020-21 from the institute account which will be refunded after receiving the grant in the pension fund account.</p>
5.	<p>It was observed that Institute is maintaining its financial accounting in the software developed in FOXPRO Database with clipper compilation which is based on the huge codification process and not has the window base verification system. This software is obsolete in the present scenario comparing with the recent available Accounting software in use. To maintain the accounts of institute it is suggested that a software which is more user friendly to all the staff working in the account section and that to customized as per the need of the institute be developed. The management of the Institute needs to take urgent action. The institute has purchased "Tally Software" for maintaining records of the financial transactions/ledgers etc. The shifting of all records/ledgers to Tally Software is under process.</p>	<p>The process of development of customized accounting system has been completed. This software is being build on windows environment and user friendly, which is easily available to all the members of staff of the section through terminals provided to them. All the accounting reports will be generated through the software.</p> <p>During the year 2020-21, all the financial entries have been made in the new software. On fully conversion to FAS (Windows) system of accounting, work of maintaining of financial accounting on FOXPRO database, which is obsolete software, will not be required.</p> <p>Action in this regards will be shown in the next audit.</p>
6.	<p>During the audit it was observed that the Mr. Uttam Singh has been suspended in November, 2013 but there is CPF balance of Rs.34658/- outstanding in the books of institute.</p>	<p>The outstanding amount of CPF balance can only be paid finally to the ex-subscriber or his family member(s) . Either of them has not submitted any claim.</p>
7.	<p>Non Adjustment of Advances against the staff Debtors: Some advances against staff debtors and Party Debtors are pending for recovery since long time. The Party Debtors amounting to Rs.845791.00 and staff debtors amounting to Rs.1067161.00. The advance which could not be realized in due course should be written off with the approval of the competent authority.</p>	<p>This is being recurring process, the advances which are allowed during last quarter of financial year are normally not settled at the end of that particular financial year is a continuous process. In regard to long pending advances which are irrecoverable, the same have already been intimated to DST for writing off.</p>



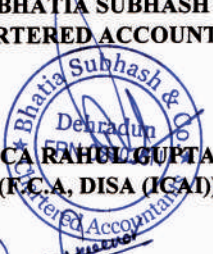
	Please clarify, if they are irrecoverable nature, initiative for write off is required.	
8.	TDS not deducted on Fellowship paid Amount Institute is not deducting TDS on fellowship paid during the period under audit.	As per Sec.10(16) of the Act, the full amount of scholarship granted to meet the cost of education is exempted. The fellowship of the students are covered under the above section. Although, we have deducted TDS on post doctorate fellowship.
9.	Bank reconciliation In bank Reconciliation provided to us showing unadjusted entries since long period. It is suggested to clear/adjusted the same.	Noted.
	For Bhatia Subhash & Co. Chartered Accountants  CA Rahul Gupta (FCA, DISA (ICAI))	 (Rahul Sharma) AF & AO  (Pankaj Kumar) Registrar  (Dr. Kalachand Sain) Director

WADIA INSTITUTE OF HIMALAYAN GEOLOGY, DEHRADUN**BALANCE SHEET
(AS AT 31st MARCH 2021)**

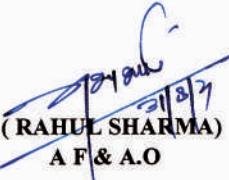
PARTICULARS	SCHEDULE	(Amt in Rs...)	
		CURRENT YEAR	PREVIOUS YEAR
LIABILITIES			
Corpus/ Capital Fund	1	698,961,057	694,146,273
Reserves and Surplus	2	-	-
Earmarked/ Endowment Fund	3	2,348,394	1,253,319
Secured Loans & Borrowings	4	-	-
Unsecured Loans & Borrowings	5	-	-
Deferred Credit Liabilities	6	-	-
Current Liabilities & Provisions	7	18,107,322	12,886,938
TOTAL		719,416,773	708,286,530
ASSETS			
Fixed Assets	8	326,429,121	344,943,451
Investments from Earmarked/ Endowment Funds	9	98,532	-
Investment- Others	10	-	-
Current Assets, Loans & Advances	11	392,889,120	363,343,079
TOTAL		719,416,773	708,286,530
Significant Accounting Policies	37		
Contingent Liabilities and Notes on Accounts	38		

AUDITOR'S REPORT

"As per our separate report of even date"

**FOR BHATIA SUBHASH & CO
CHARTERED ACCOUNTANTS**


CA RAHUL GUPTA
(F.C.A. DISA (ICAI))


(RAHUL SHARMA)
A F & A.O


(PANKAJ KUMAR)
Registrar


(DR. KALACHAND SAIN)
Director

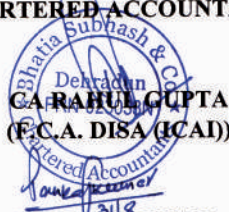
Date : 31st Aug, 2021
Place : Dehradun

WADIA INSTITUTE OF HIMALAYAN GEOLOGY, DEHRADUN**INCOME & EXPENDITURE ACCOUNT**
FOR THE PERIOD ENDED 31st MARCH 2021

S.NO.	PARTICULARS	SCH.	(Amt in Rs...)	
			CURRENT YEAR	PREVIOUS YEAR
A	<u>INCOME</u>			
	Income from sales/ services	12	-	-
	Grants/ Subsidies	13	374,726,411	371,115,482
	Fees/Subscription	14	134,830	55,153
	Income from Investments	15	663,675	1,263,625
	Income from Royalty, Publication etc.	16	104,255	125,401
	Interest earned	17	10,775,008	14,358,819
	Other Income	18	6,311,413	12,002,502
	Increase/ Decrease in Stock (Goods & WIP)	19	-	-
	TOTAL (A)		392,715,592	398,920,982
B	<u>EXPENDITURE</u>			
	Establishment Expenses	20	330,592,478	332,558,820
	Other Research & Administrative Expenses	21	63,604,050	70,325,274
	Expenditure on Grant/ Subsidies etc.	22	-	-
	Interest/ Bank Charges	23	6,084,662	8,181,281
	Depreciation Account	8	52,187,173	54,912,834
	Increase/ Decrease in stock of			
	Finished goods, WIP& Stock of Publication	A-2	(80,222)	(10,308)
	Loss / (Profit) on sale of Assets	A-19	-	-
	TOTAL (B)		452,388,141	465,967,901
	Surplus/ (Deficit) being excess of Income over Expenditure (A - B)		(59,672,549)	(67,046,919)
	Transfer to Special Reserve (Specify each)		-	-
	Transfer to / from General Reserve		-	-
	SURPLUS / (DEFICIT) CARRIED TO CAPITAL FUND		(59,672,549)	(67,046,919)

AUDITOR'S REPORT

"As per our separate report of even date"

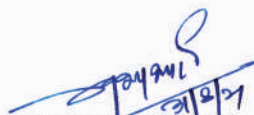
FOR BHATIA SUBHASH & CO
CHARTERED ACCOUNTANTSDehradun
CA RAHUL GUPTA
(F.C.A. DISA (ICAI))
(PANKAJ KUMAR)
Registrar
(DR. KALACHAND SAIN)
Director
(RAHUL SHARMA)
A F & A.ODate : 31st Aug, 2021
Place: Dehradun

WADIA INSTITUTE OF HIMALAYAN GEOLOGY, DEHRA DUN**RECEIPTS & PAYMENTS ACCOUNT
(FOR THE YEAR ENDED 31st MARCH 2021)**

PARTICULARS	SCH.	(Amt in Rs...)	
		CURRENT YEAR	PREVIOUS YEAR
RECEIPTS			
Opening Balance	24	169,665,588	223,750,227
Grants - in - Aids	26	432,173,411	408,553,482
Grants - in - Aids/Other Receipts (Ear Marked)	27	1,273,226	20,995,716
Loan & Advances	28	262,297,046	255,685,961
Loan & Advances (Ear Marked)	31	360,369	400,000
Fees/Subscription	14	134,830	55,153
Income from Investments	15	663,675	1,263,625
Income from Royalty, Publication etc.	16	104,255	125,401
Interest earned	17	16,291,998	8,528,129
Other Income	18	6,311,413	12,002,502
Investment (L/C Margin Money)	34	-	5,000,000
		889,275,811	936,360,196
PAYMENTS			
Establishment Expenses	20	330,592,478	332,558,820
Other Administrative Expenses	21	63,604,050	70,325,274
Expenditure on Grant/Subsidies Etc.	22	-	-
Interest/ Bank Charges	23	6,084,662	8,181,281
Loans & Advances	29	252,956,082	247,506,189
Loans & Advances (Ear Marked)	32	563,826	853,365
Investment (L/C Margin Money)	35	39,623,765	-
Fixed Assets	36	34,491,475	29,240,689
Ear Marked Fund Expenses	33	73,226	21,795,941
Grant - in - Aid (Ear Marked) Refunded	30	-	-
Closing Balance	25	161,286,247	225,898,636
		889,275,811	936,360,196

AUDITOR'S REPORT

"As per our separate report of even date"

FOR BHATIA SUBHASH & CO.
CHARTERED ACCOUNTANTSCA RAHUL GUPTA
(F.C.A, DISA (ICAI))


(RAHUL SHARMA)
A F & A.O



(PANKAJ KUMAR)
Registrar



(DR. KALACHAND SAIN)
Director

Date : 31st Aug, 2021
Place: Dehradun

WADIA INSTITUTE OF HIMALAYAN GEOLOGY,
33, GMS ROAD DEHRADUN

SCHEDULE FORMING PART OF ACCOUNTS FOR THE YEAR ENDED 31ST MARCH, 2021

SCHEDULE – 37: SIGNIFICANT ACCOUNTING POLICIES

1. ACCOUNTING CONVENTION

The financial statements are prepared on the basis of historical cost convention, unless otherwise stated and on the cash method of accounting except interest accrued on fixed deposit.

2. INVESTMENTS

Investments classified as “long term investments” are carried at cost.

3. FIXED ASSETS

- a) Fixed Assets are stated at net book value as recommended in the “Uniform Accounting Format” of financial statements for the Central Autonomous Bodies as made compulsory by the Ministry of Finance w.e.f. 01.04.2001.
- b) Additions to fixed assets are taken at cost of acquisition, inclusive of freight, duties and taxes, incidental and direct expenses related to acquisition.

4. DEPRECIATION

- a) Depreciation is provided on Written down Value method as per rates specified in the Income Tax Act, 1961.
- b) When an asset is discarded or sold or deleted, the original cost is deducted from the gross block, the W.D.V. is deducted from the W.D.V. block and accumulated depreciation on the asset upto the date of deletion is deducted from accumulated depreciation of the respective block.
- c) In respect of addition to/ deduction from fixed assets during the year, depreciation is considered on full yearly basis.



WADIA INSTITUTE OF HIMALAYAN GEOLOGY,
33, GMS ROAD DEHRADUN

5. MISCELLANEOUS EXPENDITURE

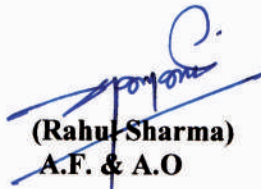
Deferred revenue expenditure, if any, will be written off over a period of 5 years from the year it is incurred.

6. ACCOUNTING FOR SALES & SERVICES

The consultancy services provided by the institute is accounted for on net service basis.

7. GOVERNMENT GRANTS / SUBSIDIES

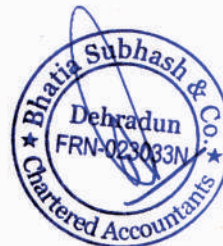
- a) Government grants of the nature of contribution towards Capital Cost are directly credited to Corpus Fund and Other Revenue cost are transferred to Income & Expenditure account and the surplus or deficit after deducting all the expenses is transferred to Capital / Corpus fund.
- b) Grants towards Earmarked / Endowment Funds are directly transferred to the respective fund account.
- c) Government grants / subsidy are accounted on realization basis.


(Rahu Sharma)
A.F. & A.O


(Pankaj Kumar)
Registrar


(Dr. Kalachand Sain)
Director

Date : 31st August, 2021
Place: Dehradun



WADIA INSTITUTE OF HIMALAYAN GEOLOGY,
33 GMS ROAD, DEHRADUN

SCHEDULE FORMING PART OF ACCOUNTS FOR THE YEAR ENDED 31ST MARCH, 2021

SCHEDULE – 38: CONTINGENT LIABILITIES AND NOTES ON ACCOUNTS

1. CONTINGENT LIABILITIES

(Amount in Rs.)

a)	Claims against the Entity not acknowledged as debts	- Nil -
b)	In respect of	
	i) Bank Guarantees given by /on behalf of the Entity	- Nil -
	ii) Letter of credit opened by Bank on behalf of the entity	-Nil-
	iii) Bills discounted with banks	- Nil -
c)	Disputed demands in respect of	
	i) Income –tax (TDS)	- Nil -
	ii) Sales tax	- Nil -
	iii) Municipal Taxes	- Nil -
d)	In respect of claims from parties for non-execution of orders, but contested by the Entity	- Nil -

2. CAPITAL COMMITMENTS

Estimated Value of contracts remaining to be executed on capital account and not provided for (net of advances)		
a)	Construction of Building	- Nil -
b)	Other Assets	-Nil -

3. LEASE OBLIGATIONS

Future obligations for rentals under finance lease arrangements for plant and machinery amount to Rs. Nil	- Nil -
---	---------

4. CURRENTS ASSETS, LOANS AND ADVANCES

In the opinion of the Institute, the current assets, loans and advances have a value on realization in the ordinary course of business, equal at least to the aggregate amount shown in the Balance Sheet.

5. TAXATION

In view of there being no taxable income of the Institute under income tax Act, 1961, no provision for Income Tax has been considered necessary



WADIA INSTITUTE OF HIMALAYAN GEOLOGY,
33 GMS ROAD, DEHRADUN

6. FOREIGN CURRENCY TRANSACTIONS

a)	Value of Imports Calculated on C.I.F basis:	
i)	Purchase of finished goods	- Nil -
ii)	Raw Materials & Components (including in transit)	- Nil -
iii)	Capital goods	- Nil -
iv)	Stores, Spares and Consumables	- Nil -
b)	Expenditure in foreign currency	
i)	Travel (for attending Seminar/Conference abroad)	- Nil -
ii)	Remittances and Interest payment to Financial Institutions / Banks in Foreign Currency	- Nil -
iii)	Other expenditure	
	Commission on Sales	- Nil -
	Legal and Professional Expenses	- Nil -
	Miscellaneous Expenses	- Nil -
c)	Earnings	
i)	Value of Exports on FOB basis	- Nil -
ii)	Grants for Projects	- Nil -

7. The payments to auditors during the F.Y. 2020 -21 is as follows:

Remuneration to auditors		
i)	As Auditors	47,200/-
	Taxation matters	- Nil -
	For Management Services	- Nil -
	For Certification	- Nil -
ii)	Others	- Nil -

8. Separate Financial Statements have been prepared for:

- a) Wadia Institute of Himalayan Geology.
- b) Contributory/ General Provident Fund.
- c) Pension Fund.
- d) Consolidated financial statement of projects sponsored by other Agencies.
- e) Individual financial statements of Projects sponsored by other agencies.

9. Corresponding figures for the previous year have been regrouped / rearranged, wherever necessary.

10. Annexed Schedules & Annexures are an integral part of the Balance Sheet as on 31st March, 2021, Income and Expenditure Account and Receipt & Payment for the year ended on 31st March, 2021.


(Rahul Sharma)
A.F. & A.O


(Pankaj Kumar)
Registrar

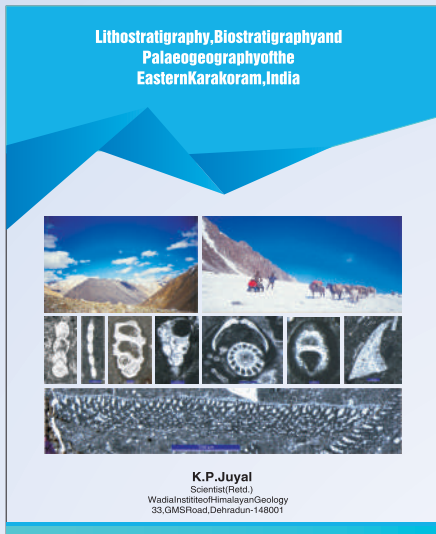

(Dr. Kalachand Sain)
Director

Date : 31st August, 2021
Place: Dehradun



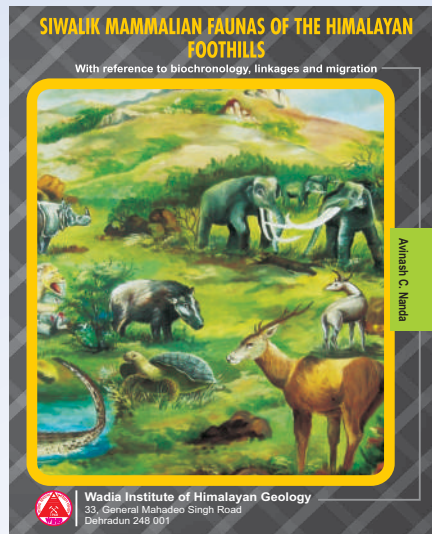
Latest Publications

2018

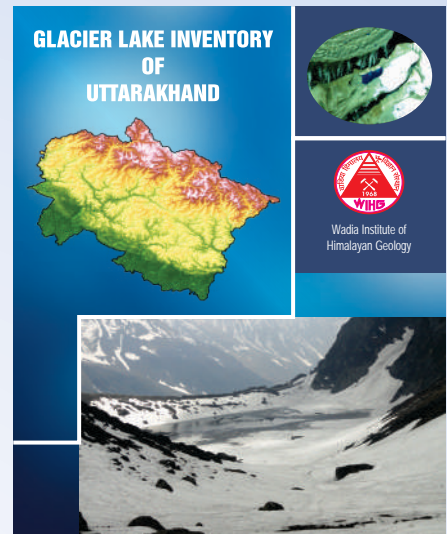


Rs.600/- (India), US\$ 50/- (Abroad)

2015

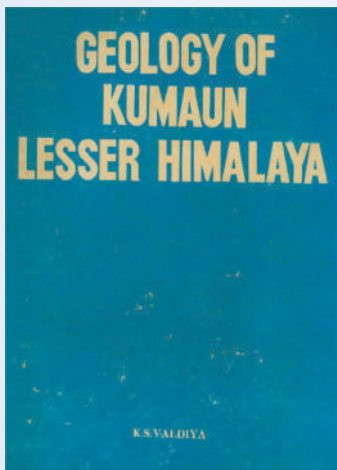


Rs.1200/- (India), US\$ 100/- (Abroad)

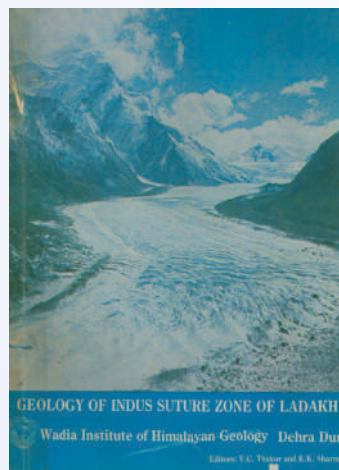


Price: Rs. 500/- (India), US\$ 50/- (Abroad)

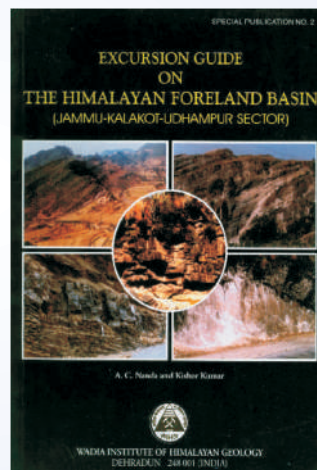
Previous Publications



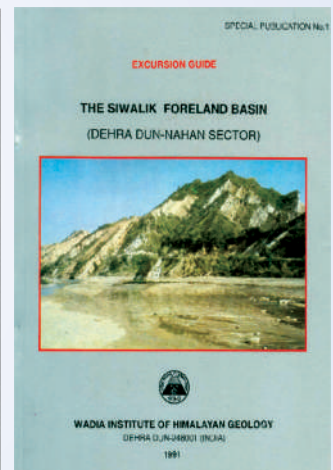
Rs.180/- (India), US\$ 50/- (Abroad)



Rs.205/- (India), US\$ 40/- (Abroad)



Rs.180/- (India), US\$ 15/- (Abroad)



Rs.45/- (India), US\$ 8/- (Abroad)



Rs.200/- (India), US\$ 15/- (Abroad)

Procurement details:
 Corresponding address:
The Director
 Wadia Institute of Himalayan Geology,
 33, GMS Road, Dehradun 248001, India
 or
Asstt. Publication & Doc. Officer
 Wadia Institute of Himalayan Geology,
 33, GMS Road, Dehradun 248001, India
 Phone: +91-0135-2525430, Fax: 0135-2625212
 Email: himgeol@wihg.res.in,
 Web: <http://www.himgeology.com>
Cheque/Bank Draft:
 Should be in favour of the
 'Director, WIHG, Dehradun, India'



Wadia Institute of Himalayan Geology

(An Autonomous Institute of Dept. of Science & Technology, Govt. of India)

33, General Mahadeo Singh Road, Dehradun-248001 (INDIA)